
THE UNIVERSITY *of* EDINBURGH

# Synthesis of f-block Complexes in a Polypyrrolic Macrocyclic Environment

Natalie Alison Potter (neé Jones)

MSci, AMRSC

This thesis is submitted for the degree of

Doctor of Philosophy of the

University of Edinburgh

5th April 2011

Nothing in life is to be feared, it is only to be understood. Now is the time to understand more, so that we may fear less.

**Marie Curie**

## *Declaration*

Except where specific reference has been made to other sources, the work presented in this thesis is the original work of the author. It has not been submitted, in whole or in part, for any other degree.

Natalie A. Potter

5th April 2010

## *Abstract*

In this thesis, the chemistry of lanthanide and actinide complexes of Schiff-base, polypyrrolic macrocyclic ligands has been evaluated.

Chapter one introduces some general chemistry of uranium before focussing on uranium(III) and (IV) coordination complexes of nitrogen donor ligands. The surface chemistry of uranium metal is also briefly discussed along with the synthesis of uranium borohydride, hydride and alkyl complexes.

Chapter two describes the synthesis and characterisation of the monometallic complexes [M(L)] or [M(HL)], where M = Y, Ce, and U, of the octadentate Schiff-base pyrrole macrocycle $H_4L$. In particular, these complexes display a new binding mode of the macrocycle which leads to the formation of the unique trinuclear supramolecular complexes $[M(HL)]_3$, (M = Ce, Y). Reactions of these materials towards hydrolysis, oxygen sources and other metal reagents are also exemplified.

Chapter three details the synthesis and characterisation of the bimetallic complexes, $[(MX)_2(L)]$, where M = Ce, U, and Np and X = I or Cl, and $[(MX_2)_2(L)]$, where M = U, and the attempts to transform these complexes into metal hydrides *via* their borohydrides. The solid state variable temperature magnetism of the binuclear U(III) and Np(III) complexes was recorded and was found to be consistent with the formation of iodide-bridged, polymeric structures.

Chapter four explores the synthesis and reactions of adducts between $UI_3$ and neutral macrocyclic ligands that incorporate either oxygen or nitrogen donors such as crown ethers and cyclam, respectively. The new synthesis of the key starting material, unsolvated $UI_3$ is also outlined, along with the full characterisation of $UI_4(OEt)_2$.

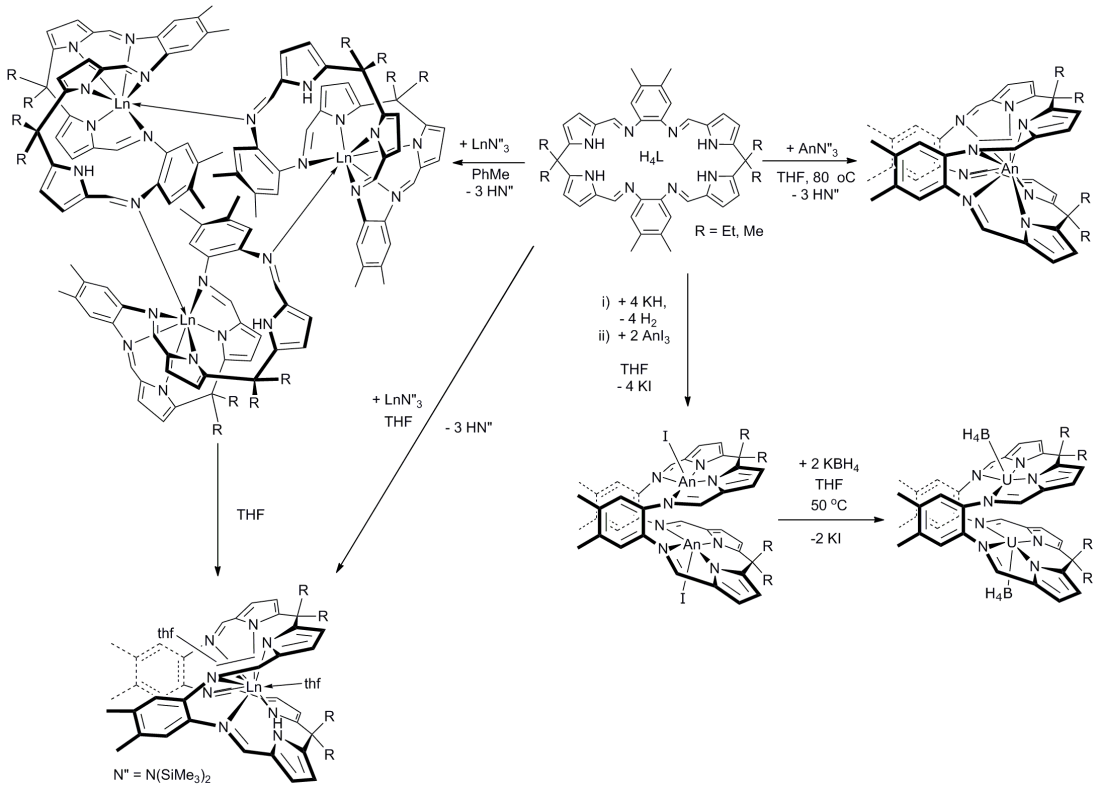
+ LnN"3
PhMe
- 3 HN"
H4L
R = Et, Me
+ AnN"3
THF, 80 oC
- 3 HN"
i) + 4 KH,
- 4 H2
ii) + 2 AnI3
THF
- 4 KI
+ LnN"3
THF
- 3 HN"
THF
+ 2 KBH4
THF
50 oC
-2 KI
thf
N" = N(SiMe3)2

## Acknowledgements

I would like to thank my supervisors Jason and Polly for their continued support, advice and their endless enthusiasm for chemistry and to Paul my industrial supervisor for funding.

Also I would like to thank the sponsors of this project; The University of Nottingham, The University of Edinburgh and the Atomic Weapons Establishment (AWE).

I would like to thank the support staff at the University of Edinburgh; Mr Juraj Bella and Dr. Marika McCremoux for NMR support, Prof. Simon Parsons, Dr. Anna Collins and Dr. Fraser White for help with X-ray crystallography.

Thanks go to all in lab 34 past and present, the post-docs; Steve, Chris. Manuel, Sergey, Lorena, Emmalina, Bernabe and Stephen and my fellow students; Ian, Dipti, J.-C., Mo, Stephen, James, Aline, Zoë, Anne-Fred, John, Anne, Guy, Aáron, Chloe, Isobel, Rebecca and Colin. Also I would like to thank everyone in the department, for helping us to settle in so well, especially to Jill and Phil.

I would also like to thank my family for their love, and support and my sister, Michelle, for being a great chemistry role model. I would also like to thank Craig's family who have been very supportive during my PhD.

Special thanks to my husband, Craig, for his endless encouragement, and support.

## *Abbreviations*

| | |
|---|---|
| Å | Angstrom |
| Ad | Adamantyl |
| atm | Atmosphere |
| bar | Bar, unit of pressure |
| *n*-Bu | *n*-butyl |
| *t*-Bu | *tert*-butyl |
| Bn | Benzyl |
| *ca.* | *circa*, about |
| COT | Cyclooctatetraene |
| Cp | Cyclopentadiene |
| Cp* | Pentamethylcyclopentadiene |
| $Cp^{‡}$ | Monoethyltetramethylcyclopentadiene |
| Cyclam | 1,4,8,11-tetraazacyclotetradecane |
| DABCO | 1,4-diazabicyclo[2.2.2]octane |
| DMF | Dimethylformamide |
| dme | Dimethylether |
| dmpe | Bis(1,2-dimethylphosphino)ethane |
| fc | ferrocene |
| *i*-Pr | Isopropyl |
| Me | Methyl |
| N″ | Hexamethyldisilyl amide |
| $NN'_3$ | $[N(CH_2CH_2NSiMe_2t\text{-}Bu)_3]^{3-}$ |
| NON | $[N(^tBu)Si(Me_2)OSi(Me_2)N(^tBu)]$ |
| Ph | Phenyl |
| Py | Pyridine |
| RT | Room temperature |
| R | Generic alkyl group |
| T | tesla |
| THF | Tetrahydrofuran |
| TMS | Trimethylsilyl |
| tpy | 2,2′:6′,2″-terpyridine |
| Tren | Tris(2-aminoethyl)amine |

### Nuclear Magnetic Resonance spectroscopic data (NMR)

| | |
|---|---|
| δ | chemical shift in ppm |
| J | coupling constant |
| m | multiplet |
| ppm | parts per million |
| $^{13}C\{^{1}H\}$ | proton decoupled $^{13}C$ NMR |
| q | quaternary carbon |
| s | singlet |
| t | triplet |

### Mass spectroscopic data

| | |
|---|---|
| EI | Electron Impact |
| *m/z* | mass to charge ratio |
| $M^+$ | molecular ion |

### Infrared spectroscopic data (IR)

| | |
|---|---|
| br | broad |
| $cm^{-1}$ | wavenumber |
| m | medium |
| s | strong |
| w | weak |

### SQUID data

| | |
|---|---|
| SQUID | Superconducting QUantum Interference Device |
| χ | Magnetic susceptibility |
| μ | Effective magnetic moment |

**For Mum, Dad, Michelle**

**and Craig**

**In Memory of**

**John Clark Potter**

**(1946 – 2010)**

# Table of Contents

Chapter 1: Introduction ..... 1

1.1 Uranium……1

1.2 Surface Chemistry…….5

1.3 Uranium(III) and Uranium(IV) Chemistry……..…….6

1.4 Uranium Hydrides……..……6

1.4.1 $UH_3$…….6

1.4.2 Uranium Hydride Complexes…….8

1.5 Uranium Borohydrides…….…..11

1.5.1 Uranium Alkyls..... …..15

1.6 Uranium Amides…….....……17

1.7 Uranium Aryloxides…….……...……27

1.8 Uranium Cp and COT complexes……...28

1.9 Uranium Alkyls……..……..……...29

1.10 Uranium Polypyrrolic Complexes……..32

1.10.1 Macrocyclic Uranium Complexes ..... 36

1.10.2 Actinide/Lanthanide Separation.....44

1.10.3 Uranium Schiff Base Complexes..... 46

1.10.4 Schiff Base Pyrrole Macrocycles..... 47

1.11 References……...51

Chapter 2: Monometallic Complexes ..... 60

2.1 Synthesis of Schiff-base Macrocycles……60

2.1.1 Synthesis of $H_4L^{Me}$ ..... 60

2.1.2 Synthesis of $H_4L^{Et}$ ..... 61

2.2 Synthesis of Uranium Complexes……..65

2.2.1 Synthesis of $[U(L^{Et})]$ ..... 65

2.2.2 Synthesis of $[UO_2(Opy)(H_2L^{Et})]$ ..... 71

2.3 Synthesis of Cerium Complexes……74

2.3.1 Synthesis of $[Ce(HL^{Et})]_3$ ..... 74

2.3.2 Synthesis of $[Ce(THF)_2(HL^{Et})]$ ..... 86

2.3.3 Synthesis of $[Ce(L^{Et})]$ ..... 90

2.3.4 Synthesis of $[\{Ce(L^{Et})\}_2Zn]$ ..... 92

2.4 Synthesis of Yttrium Complexes……95

2.4.1 Synthesis of $[Y(HL^{Et})]_3$ ..... 95

2.4.2 Synthesis of $[Y(THF)_2(HL)]$ ..... 97

2.4.3 Synthesis of $[\{Y(OH_2)(H_2L^{Et})\}_2(\mu\text{-}OH)_2]$ ..... 102

2.5 Conclusions……..…….106

2.6 References……106

Chapter 3: Bimetallic Complexes……111

3.1 Direct uranium–metal bonds……111

3.2 Multinuclear uranium complexes……113

3.3 Synthesis of Starting Materials……118

3.3.1 Preparation of $[K_4L^{Et}]$ ..... 118

3.3.2 Preparation of $UI_3(THF)_4$ ..... 119

3.4 Synthesis of Bimetallic Complexes……..119

3.4.1 Synthesis of $[(UI)_2(L^{Me})]$ and $[(UI)_2(L^{Et})]$ ..... 119

3.4.2 Preparation of $[(UBH_4)_2(L^{Et})]$ ..... 125

3.4.3 Preparation of $[(UH)_2(L^{Et})]$ ..... 128

3.4.4 Preparation of $[(UCl_2)_2(L^{Et})]$ ..... 129

3.4.5 Synthesis of $[(CeI)_2(L^{Et})]$ ..... 130

3.5 Neptunium Chemistry……...130

3.5.1 Synthesis of $[(NpI)_2(L^{Et})]$ ..... 133

3.6 Conclusions……...139

3.7 References……139

Chapter 4: Adducts of Uranium Halides ..... 142

4.1 Uranium halides……..……..……142

4.1.1 Uranium trihalide ..... 142

4.1.2 Uranium tetrahalide ..... 144

4.2 New Preparation of $UI_3$ and $UI_4(OEt_2)_2$……145

4.2.1 Synthesis of $UI_3$ ..... 145

4.2.2 Synthesis of $UI_4(OEt_2)_2$ ..... 147

4.2.3 Synthesis of $UI_4(OBu_2)$ ..... 151

4.3 Preparation of $UI_3$ adducts..... 151

4.3.1 Synthesis of $[U(OPPh_3)_2(THF)_2I_3]$ ..... 151

4.3.2 Synthesis of $[U(18\text{-crown-}6)I_3]$ ..... 154

4.3.3 Synthesis of $[U(OAr)_4][Na(py)_2(18\text{-crown-}6)]$ ..... 156

4.3.4 Synthesis of $U(BH_4)_3(THF)_x$ ..... 161

4.3.5 Synthesis of $[U(Cyclam)I_3]$ ..... 162

4.3.6 Synthesis of $^{TMS}$Cyclam ..... 164

4.3.7 Attempted Synthesis of $[U(^{TMS}Cyclam)I_3]$ ..... 165

4.3.8 Synthesis of $[U(^{Bn}Cyclam)I_3]$ ..... 165

4.4 Conclusions..... 166

4.5 References..... 166

Chapter 5: Conclusions and Experimental details..... 171

5.1 Chapter 2: Preparation of $H_4L^{Et}$ and $H_4L^{Me}$ Macrocycle..... 174

5.1.1 Preparation of 5,5'-diformyl-2,2'-diethyldipyrromethane..... 174

5.1.2 Preparation of $H_4L^{Et}$ ..... 175

5.2 Chapter 2: Preparation of Monometallic Complexes..... 176

5.2.1 Synthesis of $[U(L^{Et})]$ ..... 176

5.2.2 Synthesis of $[UO_2(OPy)(L^{Et})]$ ..... 177

5.2.3 Synthesis of $[UN_3(L^{Et})]$ ..... 177

5.2.4 Synthesis of $[\{(Ce(HL^{Et})\}_3]$ ..... 178

5.2.5 Synthesis of $[Ce(THF)_2(HL^{Et})]$ ..... 179

5.2.6 Synthesis of $[Ce(L^{Et})]$ ..... 181

5.2.7 Synthesis of $[\{Ce(L^{Et})\}_2Zn]$ ..... 181

5.2.8 Synthesis of $[\{(Y(HL^{Et})\}_3]$ ..... 182

5.2.9 Synthesis of $[(Y(THF)_2(HL^{Et})]$ ..... 182

5.2.10 Synthesis of $[\{Y(OH_2)(H_2L^{Et})\}_2(\mu\text{-}OH)_2]$ ..... 184

5.3 Chapter 3: Preparation of Bimetallic Complexes……..……184

5.3.1 Preparation of tetrapotassium salt, $[K_4(L^{Et})]$..... 184

5.3.2 Preparation of $[(UI)_2(L^{Me})]$ ..... 184

5.3.3 Preparation of $[(UI)_2L^{Et}]$ ..... 185

5.3.4 Substitution reactions of $[(UI)_2L]$ ..... 186

5.3.5 Preparation of $[(UBH_4)_2(L^{Et})]$ ..... 187

5.3.6 Substitution reactions of $[(UI)_2(L)]$ by Boron groups..... 188

5.3.7 Attempted Preparation of $[(UH)_2(L)]$ ..... 188

5.3.8 Preparation of $[(UCl_2)_2(L^{Et})]$..... 189

5.3.9 Preparation of $[(CeI)_2(L^{Et})]$..... 189

5.3.10 Preparation of $[(NpI)_2(L^{Et})]$ ..... 190

5.4 Chapter 4: Adducts of Uranium Halides……...190

5.4.1 Uranium Turnings ..... 190

5.4.2 Synthesis of $UI_3$ ..... 191

5.4.3 Synthesis of $UI_4(OEt_2)_2$,..... 191

5.4.4 Reaction of $UI_4(OEt_2)_2$ with uranium turnings to give $UI_3$..... 192

5.4.5 Synthesis of $UI_4(OBu_2)$..... 192

5.4.6 Synthesis of $[U\{N(SiMe_3)_2\}_3]$ from $UI_3$ ..... 192

5.4.7 Synthesis of $U(Cp)_3I$ from $UI_4(OEt_2)$ ..... 192

5.4.8 Synthesis of $[U(OC_6H_2{}^tBu_3)_3]$ ..... 193

5.4.9 Synthesis of $UI_3(Ph_3PO)_2(THF)_2$ ..... 193

5.4.10 Synthesis of $U(BH_4)_3(THF)_x$..... 193

5.4.11 Synthesis of $[U(18\text{-crown-}6)I_3]$ ..... 194

5.4.12 Synthesis of $[Na(18\text{-crown-}6)(py)][U(OC_6H_2\text{-}t\text{-}Bu_3)_4]$ ..... 194

5.4.13 Synthesis of $[^{TMS}Cyclam]$ ..... 194

5.4.14 Synthesis of $[U(Cyclam)I_3]$..... 195

5.4.15 Attempted Synthesis of $[U(^{TMS}Cyclam)I_3]$ ..... 195

5.4.16 Attempted Synthesis of $[U(^{Bn}Cyclam)I_3]$..... 195

5.5 SQUID magnetic studies……..……...195

5.5.1 Ligand field analysis .. ……196

5.6 References……196

5.7 Appendixes……...198

5.7.1 X-ray details..... 198

# Chapter 1: Introduction

At the outset of the work described in this thesis the aim was to increase our understanding of the chemistry of molecular hydrides of uranium. This topic is of considerable interest, because it is relevant to the corrosion processes which occur on uranium surfaces when they are exposed to proton-sources. The systems studied (section 1.10.5) were chosen because they used multidentate ligands of the types developed in the Love group at Edinburgh University which had already been shown to form stable complexes with f-block and d-block metal ions in which the ligands control the disposition of most of the donor atoms in the coordination sphere and consequently the properties of the complexes.

## 1.1 Uranium

The f-elements consist of the lanthanides (lanthanum to lutetium), and the actinides (actinium to lawrencium). Uranium is one of the actinides, and was first observed in 1789 by Klaproth in a sample of pitchblende which mainly consists of $UO_2$.[1] It is the heaviest naturally occurring element and has an abundance of 2.4 ppm in the Earth's crust. In natural sources, uranium exists as three major isotopes; $^{238}U$, $^{235}U$ and $^{234}U$ with abundances of 99.28 %, 0.71 % and 0.0054 % respectively. All isotopes are radioactive, with $^{238}U$ having the longest half-life of $4.468 \times 10^9$ years, decaying via α-particles emission, Table 1.1.

| Isotope | Natural Abundance | Half life (billions of years) | Decay mode | Decay energy |
|---|---|---|---|---|
| $^{234}U$ | 0.0054 % | 0.000245 | α | 4.8 MeV |
| $^{235}U$ | 0.71 % | 0.704 | α, γ | 4.4, 0.21 MeV |
| $^{238}U$ | 99.28 % | 4.468 | α | 4.2 MeV |

**Table 1.1 – Decay data for uranium.**

Aside from its long standing small-scale use as an agent for colouring glass and ceramics, uranium's only other significant industrial use is as a nuclear fuel. $^{235}U$ is one of two fissile isotopes that can absorb a neutron and sustain a fission chain reaction (the other being $^{239}Pu$).

Uranium metal can be isolated in a variety of ways: reduction of uranium oxide with strongly electropositive elements (e.g. Ca), electrodeposition from molten salt baths, thermal decomposition of uranium halides and reduction of uranium halides with electropositive metals. The latter technique is the most commonly used today and is the last step in the extraction process from ore.[2]

The extraction of uranium from its ore is usually performed via leaching with $H_2SO_4$ in the presence of an oxidising agent such as $MnO_2$ or $NaClO_3$. The resulting uranyl ($UO_2^{2+}$) complexes of sulfate and chloride are then neutralised with $NH_3$ to give a yellow precipitate known as 'yellowcake', typically compromised of 70-90% of $U_3O_8$. This is then heated to 300 °C to give uranium salts of approximate composition $(NH_4)_2U_2O_7.UO_3$, which are reduced to $UO_2$ by heating at 700 °C under an atmosphere of $H_2$. Finally, conversion to $UF_4$ is carried out using hydrofluoric acid before reduction with magnesium to give pure uranium metal.[1]

Uranium compounds are difficult to reduce due to the strongly electropositive nature of the metal. Uranium metal is also highly reactive, being known to react with almost all of the elements of the periodic table (with the exception of the noble gases). When exposed to oxygen or water, the metal reacts rapidly to form a black oxide layer at room temperature.[2]

The ground state electronic configuration of uranium is $[Rn]5f^36d^17s^2$, with a variety of stable oxidation states from II to VI available upon successive removal of the s, d and f valence electrons. The early actinides, thorium to curium, share similar characteristics with early transition metals. For example, both are sensitive to water and oxygen, and can adopt variable oxidation states. Unlike transition metals however, the 18 electron rule cannot be applied for actinide complexes as steric effects of saturating the coordination sphere around the metal cation are the predominate factors and it is this which determines the structure of these complexes.

The later actinides are more like the lanthanides with their marked tendency to favour trivalent oxidation states. The coordination number of actinide complexes is typically higher than transition metals due to their larger size. Coordination numbers of up to 12 for the lanthanides, in $[Pr(NO_3)_3(18\text{-crown-6})]$, and 15 for the actinides, in $[Th(H_3BNMe_2BH_3)_4]$, have been observed, with the spatial arrangement of the ligands dominated by steric factors.[3, 4]

Across the actinide period there is a gradual reduction in the ionic radii as a result of the limited radial extension of the 5f-orbitals and the poor screening ability of the f-electrons. This is known as the actinide contraction. As the number of f-electrons increases across the group, the effective nuclear charge experienced by the f-electrons increases and due to the poor screening, leads to the contraction across the series. In the lanthanides, the 4f-orbitals are radially contracted and 'core-like' and do not interact significantly with ligands. Bonding in lanthanide complexes is therefore strongly ionic in character. Actinides 5f-orbitals are comparatively diffuse, allowing greater orbital overlap and increased interactions with ligands allowing more covalent character in bonding.

The electronic properties of the weak crystal field imposed by f-orbitals means that the crystal field splitting is lower in f-orbital complexes than those of transition metals. The result is that all f-orbital complexes have high spin conformations. Relativistic effects on the d- and f-electrons in uranium means that they are more expanded, giving a lower binding energy to the uranium valence electrons thus making the f-elements chemically active.

A major breakthrough during the 1950s at the University of California, Berkeley, showed that trivalent actinides and lanthanides could be separated using ion-exchange chromatography with chloride anions, see Table 1.2.[5] This has lead to a plethora of research into ligands to be used to separate low valent f-block elements.

The chemistry of cerium(III) and uranium(III) are comparable as they have very similar ionic radii, 1.01 Å and 1.025 Å respectively.[6] Cerium(III) and uranium(III) compounds have been compared to calculate the difference the f-electrons in either 4f- or 5f-orbitals, make to the chemistry shown by these systems.[7]

| | | | |
|---|---|---|---|
| La | 1.032 | Ac | 1.120 |
| Ce | 1.010 | Th (+4) | 0.940 |
| Pr | 0.990 | Pa | 1.040 |
| Nd | 0.983 | U | 1.025 |
| Pm | 0.970 | Np | 1.010 |
| Sm | 0.950 | Pu | 1.000 |
| Eu | 0.947 | Am | 0.975 |
| Gd | 1.000 | Cm | 0.970 |
| Tb | 0.923 | Bk | 0.960 |
| Dy | 0.912 | Cf | 0.950 |
| Ho | 0.901 | Es | - |
| Er | 0.890 | Fm | - |
| Tm | 0.880 | Md | - |
| Yb | 0.868 | No | - |
| Lu | 0.861 | Lr | - |

**Table 1.2 – Ionic radii of f-block elements in the +3 oxidation state[6]**

Uranium has become a focus of much research over the past 50 years. Research that began in the Manhattan Project has continued with more peaceful goals in mind, including the recent explosion in organometallic chemistry of low oxidation state uranium compounds.

## 1.2 Surface Chemistry

Corrosion of f-block metals is problematic, both in terms of cost and unwanted by-products. The study of the surface corrosion of uranium and plutonium is currently of great interest in relation to their storage for the nuclear power industry.[8]

The surface oxidation rate of both uranium and plutonium is accelerated in moist air and, in the presence of pure water vapour. Corrosion produces large amounts of hydrogen gas and results in the formation of an oxide surface layer, although hydrides can also be formed during the process. Hydride intermediates can then interact with more water vapour to form an oxide and liberate hydrogen gas, Scheme 1.1.[8]

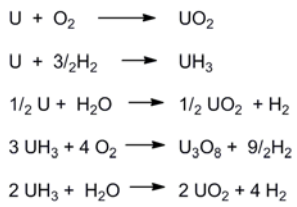


**Scheme 1.1 – Reactions occurring at the surface of uranium in a $H_2$ atmosphere (containing traces of $H_2O$ and $O_2$).**

The corrosion rate of the metals with hydrogen is much greater than in oxygen at 100 °C and 0.2 atm with rates of $10^{-1}$ mgcm$^{-2}$s$^{-1}$ and $10^{-5}$ mgcm$^{-2}$s$^{-1}$ respectively. The hydride layer that is formed on the surface is non-protective meaning the hydride product continually flakes away from the metal surface.[8]

It has been shown computationally that hydrogen could travel through a layer of $UH_3$ to react with the uranium metal residing underneath.[9] The activation energy for this process was calculated as 21 kcal mol$^{-1}$, however it was also found that the presence of $UH_3$ catalyses the reaction.

Impurities present in the surface can also affect the rate of the formation of uranium hydride, for example, the presence of around 100 ppm of silicon increases the rate of

hydriding rapidly.[10] Research by Scott and co-workers, has shown that $UD_3$ is formed preferentially at the metal grain boundaries on the uranium surface.[11]

## 1.3 Uranium(III) and Uranium(IV) Chemistry

All uranium ions are hard Lewis acids, and their size results in large coordination spheres in their complexes. Uranium(III) is unstable with respect to oxidation to uranium(IV) in the presence of trace oxygen. Unsolvated uranium trichloride $(UCl_3)_n$ is polymeric and insoluble in all organic solvents, limiting its usefulness as a reagent. The organometallic and coordination chemistry of trivalent uranium was made accessible by the synthesis of the soluble and monomeric $UI_3(THF)_4$ by Clark and co-workers, Scheme 1.2.[12]

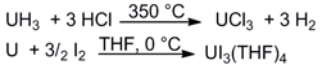


**Scheme 1.2 – Preparation of uranium halides.**

This research led to a more convenient synthesis of $[U\{N(SiMe_3)_2\}_3]$, allowing protonolysis methodology to be used in synthesising new compounds avoiding the reduction of $UCl_4$ with sodium, which is problematic.[13, 14] Despite this progress in trivalent uranium chemistry, more stable tetravalent uranium complexes are more predominate in the literature.

## 1.4 Uranium Hydrides

### 1.4.1 $UH_3$

Uranium hydride is a pyrophoric dark grey powder, formed by the reaction of oxygen-free hydrogen on oxide-free uranium at 250 °C at 1 atm. It is the only stable molecular uranium hydride and acts as a useful starting material for uranium compounds, as its decomposition leaves the uranium finely divided and in a highly reactive state, Equation 1.1.[15]

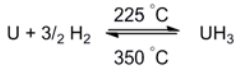


**Equation 1.1**

The ability of uranium to react directly with hydrogen is shared with the other actinides up to americium. Analogous reactions with deuterium or tritium can also be performed to form $AnD_3$ or $AnT_3$.[15]

Hydrogen reacts rapidly with a block of uranium once the reaction is initiated, by removal of surface oxide. The uranium hydride formed is a voluminous finely divided powder (density 3.4 $gcm^{-3}$) with the metallic structure having been completely destroyed during the reaction (density 19.05 $gcm^{-3}$). The rate of reaction is greatest at 225 °C under 1 atm pressure of $H_2$ and sharply falls above 250 °C, as hydrogen is evolved to produce very finely divided uranium metal. Uranium metal in this form re-reacts rapidly with hydrogen even at 0 °C.[2]

Uranium hydride can exist in two polymorphs, α and β, with the latter being the more prevalent at room temperature, although at -80 °C approximately 50 % of the mixture is the α-$UH_3$ form. At 100 °C α-$UH_3$ becomes more stable with respect to β-$UH_3$, with complete conversion taking place at 250 °C. The reverse transformation upon cooling has, however, eluded measurement.[2]

The structure of $UH_3$ was first presented by Rundle in 1947. It was observed that, unlike many other metal hydrides, uranium hydride did not fall into one of the classes of volatile, salt-like, or interstitial hydrides previously observed but was a new class of metal-like hydride. The X-ray powder diffraction analysis showed no metal to metal bonds with uranium atom being surrounded by twelve hydrogen atoms in the X-ray crystal structure.[16, 17]

### 1.4.2 Uranium Hydride Complexes

Uranium hydride complexes can be formed in a variety of ways including: β-H elimination reactions of alkyl compounds, substitution reactions of halide complexes, formation of anionic hydrides by NaH addition, and hydrolysis of alkyl complexes.

The first stable organouranium(IV) hydride complex was synthesised by Ephritikhine and co-workers in 1991.[18] The complex, [($\eta^5$-$C_5H_4SiMe_3$)$_3$UH], was synthesised by a reaction of [($\eta^5$-$C_5H_4SiMe_3$)$_3$UCl] with an excess of $KBEt_3H$ in THF, Figure 1.1. Cyclopentadienyl ligands are one of the classic co-ligands used in the organometallic chemistry of electropositive metals.

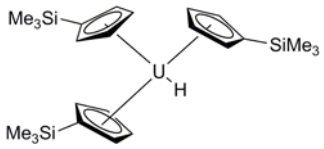


**Figure 1.1 – [(η$^5$-$C_5H_4SiMe_3$)$_3$UH]**

Reduction of [($\eta^5$-$C_5H_4SiMe_3$)$_3$UH], to form the anionic uranium(III) complex [Na(18-crown-6)][($\eta^5$-$C_5H_4SiMe_3$)$_3$UH] was later achieved using a Na/Hg amalgam in the presence of 18-crown-6, Scheme 1.3. Direct reduction of [($\eta^5$-$C_5H_4SiMe_3$)$_3$UCl] also yielded the same product with NaH and 18-crown-6, for 3 days at 20 °C in THF.

The hydride proton was identified by $^1$H NMR spectroscopy in THF-d8 at + 547.1 ppm and the U-H stretch by infrared spectroscopy at 1405 cm$^{-1}$ in nujol.

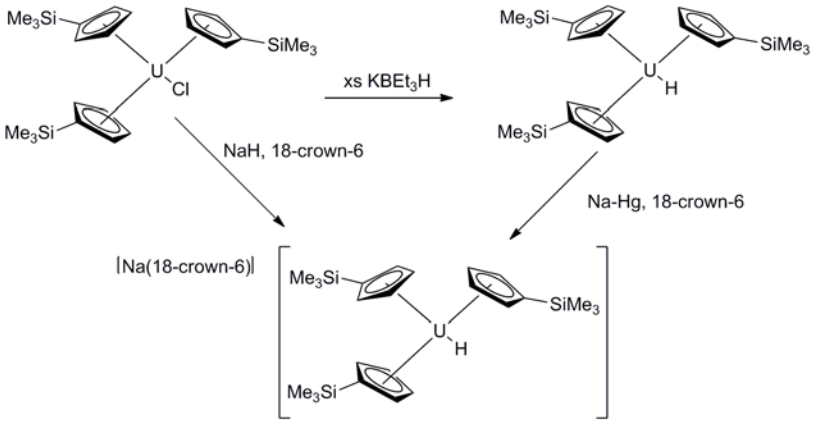


**Scheme 1.3 – [(η$^5$-$C_5H_4SiMe_3$)$_3$UH] formation**

Anionic tris(cyclopentadienyl)uranium(III) hydrides were first prepared by Ephritikhine and co-workers by several different routes. In one example,

$[Cp_3U(THF)]$ was reacted with NaH under sonication, affording the complex $[Na(THF)_2][(Cp_3UHUCp_3]$, Figure 1.2.[19]

A range of other uranium(III) cyclopentadiene hydride complexes has since been synthesised, and, although the U-H infrared frequencies were not observed, $^1$H NMR spectroscopy (THF-$d_8$) was used to characterise the compounds, Table 1.3.

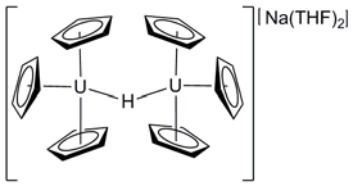


**Figure 1.2 - $[Na(THF)_2][Cp_3UHUCp_3]$**

| Compound | Hydride (ppm) |
|---|---|
| $[Na(THF)_2][Cp_3UHUCp_3]$ | 293.1 |
| $[Na(THF)_2][(C_5H_4Me)_3UHU(C_5H_4Me)_3]$ | 302.2 |
| $[Na(18\text{-crown-}6)][(C_5H_5)_3UHU(C_5H_5)_3]$ | 293.1 |
| $[Na(18\text{-crown-}6)][(C_5H_4SiMe_3)_3UH]$ | 547.1 |
| $[Na(18\text{-crown-}6)][(C_5H_4{}^tBu)_3UH]$, | 521.3 |
| $[Na(18\text{-crown-}6)][(C_5H_4SiMe_3)_3UHU(C_5H_4SiMe_3)_3]$ | 319.2 |

**Table 1.3 - $^1$H NMR data (THF-d8) of a range of anionic uranium hydrides.**

The dimethyl uranium (IV) complex , Figure 1.4, was synthesised from $[(Cp^*)_2UCl_2]$ and two equivalents of MeLi at -78 °C in diethyl ether.

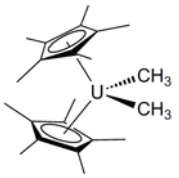


**Figure 1.4 – $[U(Cp^*)_2(CH_3)_2]$**

Hydrogenolysis of the uranium(IV) dialkyl, $[U(Cp^*)_2(CH_3)_2]$, in toluene at room temperature with 1 atm of $H_2$ resulted in the formation of the doubled-bridged uranium hydride complex $[(Cp^*)_2U(\mu\text{-}H)H]_2$.[20]

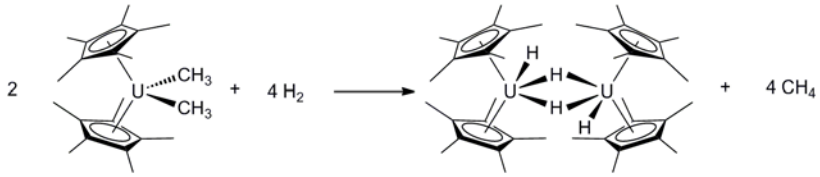


**Equation 1.2**

Gas experiments showed that two equivalents of methane were produced per uranium for two equivalent of hydrogen. The infrared spectrum of the species showed absorptions indicative of terminal U-H stretching mode at 1335 $cm^{-1}$ and the bridging U-H-U stretching mode at 1180 $cm^{-1}$. $^1H$ NMR spectroscopy showed a singlet for the hydrides at + 316.8 ppm down to -85 °C. The complex is unstable, if left at room temperature and under reduced pressure it loses hydrogen over 3 hours. The process can be reversed if a hydrogen atmosphere is reintroduced.

To investigate the nature of the hydride in this complex the reaction with chloromethane was undertaken, resulting in the formation of a mixture of the dichloride and chloromethyl uranium complexes in a ratio of 5:1.

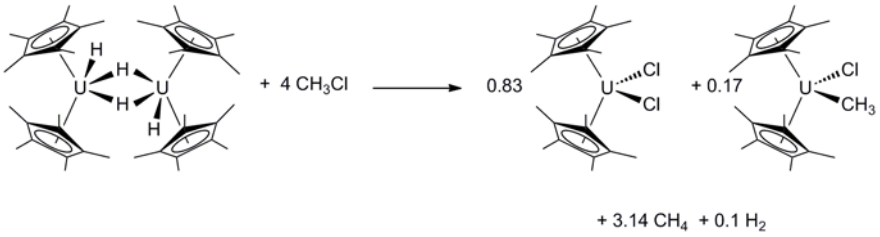


**Equation 1.3**

The first trivalent uranium monohydride compound was synthesised in 1982 by Marks and co-workers. The uranium(III) diphosphine hydride, $[(Cp^*)_2U(dmpe)H]$, was synthesised via the reaction of $[(Cp^*)_2U(CH_3)_2]$ with 1.5 equivalents of 1 atm $H_2$ and 1 equivalent of dmpe in toluene.[21]

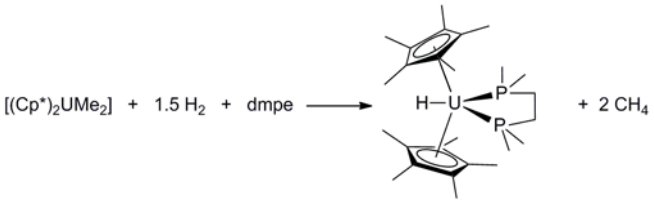


**Equation 1.4**

The presence of the hydride was indicated by a strong, broad absorption at 1219 $cm^{-1}$ in the infrared spectrum, attributed to the U-H stretching mode. The hydride resonance could not be located in the room temperature $^1H$ NMR spectrum. The solution magnetic moment detected by Evans' method confirmed that the compound was U(III) with an effective magnetic moment of 3.47 $\mu_B$. Single crystals suitable for single crystal diffraction were grown but structural analysis could not locate the hydride. From the position of the other ligands a reasonable hydride location was inferred however, it was also noted that the complex readily reacts with THF, CO or $N_2$ to give free dmpe and a mixture of U(III) and U(IV) compounds.[21]

## 1.5 Uranium Borohydrides

Simple and tractable models for uranium hydride are provided by uranium borohydride complexes.[21, 22] $U(BH_4)_4$ is very volatile and this was one of the key reasons that so much research has been undertaken into this class of compound.[22]

$BH_4$ can bind to uranium in a variety of ways, Figure 1.5, with each mode displaying different IR stretching frequencies, Chart 1.1.[23]

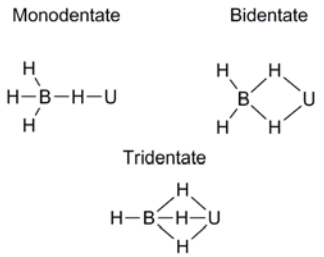


**Figure 1.5 – $BH_4$ binding modes**

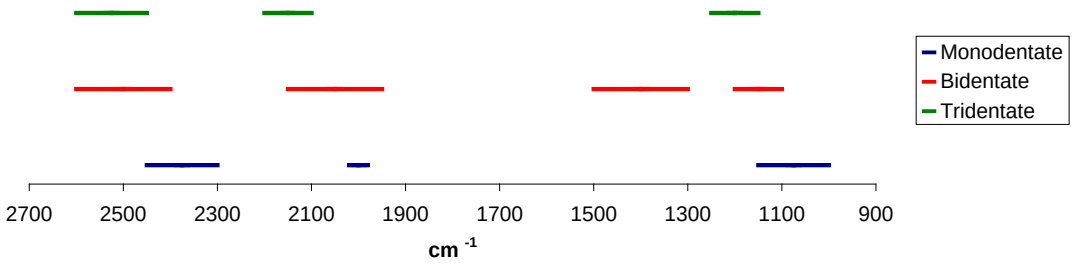


**Chart 1.1 – IR frequencies for different binding modes of $BH_4$**

Much work has been done on uranium(IV) borohydride complexes starting from $U(BH_4)_4$, however the only published method for this, not involving uranium tetrafluoride, is a solid phase reaction of uranium tetrachloride and lithium borohydride. The reaction takes place in a vibrating ball mill.[24] The X-ray crystal structure of $U(BH_4)_4$ showed polymeric interlocking helical chains with each uranium atom associated with six borohydride groups, of which four are bridging and two are terminal. The bridging borohydrides lie equidistant between two uranium atoms.[25]

In the vapour phase IR spectrum of the molecular $U(BH_4)_4$ complex one band is observed for terminal triple bridged, B–H and two for double bridged B-H, at 2570, 2155 and 2090 $cm^{-1}$ respectively. There is also a very strong band at 1230 $cm^{-1}$ possibly resulting from a U-H stretch in a U-H-B bridge. Solid state IR spectroscopy shows a much lower symmetry; with two stretching modes assigned to terminal

tridentate B-H at 2552 and 2538 $cm^{-1}$ and three bands in the bidentate region at 2262, 2182 and 2087 $cm^{-1}$. Four bands are observed in the U-H region at 1240, 1163, 1132 and 1100 $cm^{-1}$.[26, 27]

Uranium(IV) tetraborohydride is stable at temperature below 70 °C but at higher temperature begins to decompose, undergoing rapid decomposition at 100 °C to yield uranium(III) triborohydride, Equation 1.5.[28]


**Equation 1.5**

Ephritikhine and co-workers described the treatment of $U(BH_4)_4$ with TlCp in toluene to give $[CpU(BH_4)_3]$, Equation 1.6.[29]


**Equation 1.6**

Only a few borohydride complexes have been made in situ from mixed ligand complexes. $[Cp_3U(BH_4)]$ could be produced in excellent yield from the treatment of $[Cp_3UCl]$ with $NaBH_4$ in THF at room temperature for 16h, Equation 1.7.[30]

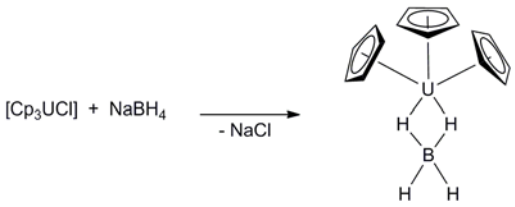


**Equation 1.7**

The solution was then filtered from the excess $NaBH_4$ and NaCl and all volatiles removed. The pure product was then obtained by sublimation at 170 °C at $10^{-4}$ mmHg. The IR spectrum of this compound suggests that the $BH_4^-$ group is binding in a bidentate mode as there is a band observed at 2142 $cm^{-1}$.

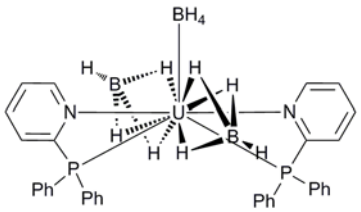


**Figure 1.6 - Trivalent borohydride complex, $[U(BH_4)_3(Ph_2Ppy)_2]$**

Trivalent uranium borohydrides have been reported but not in a macrocyclic manifold.[31, 32] From the reaction of uranium(III)tris(borohydride) with an excess of $Ph_2Ppy$, $[U(BH_4)_3(Ph_2Ppy)_2]$ was synthesised, Figure 1.6. The IR spectrum and X-ray analysis showed that the borohydride was bound in a tridentate manner, with bands in the IR spectrum at 2420, 2300 and 2200 $cm^{-1}$.[31] The starting material $U(BH_4)_3(THF)_x$, was synthesised by the reaction shown in Scheme 1.7 in THF at room temperature.[33] This is of particular synthetic interest as $UCl_3$ has poor solubility in THF.

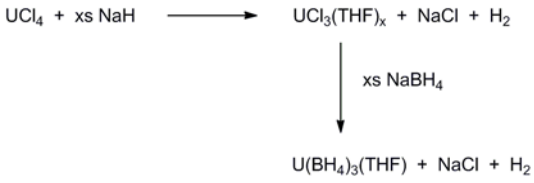


**Scheme 1.7 - Synthesis of $UCl_3(THF)_x$ as an intermediate in the synthesis of $U(BH_4)_3$**

$U(BH_4)_4$ can also be used as a starting material in the synthesis of uranium(III) borohydrides. For example, treatment of $U(BH_4)_4$ with mesitylene affords ($\eta$-mesitylene)$U(BH_4)_3$, Equation 1.8.[34] The $^1H$ NMR spectrum of this complex, in toluene-$d_8$, contained a resonance at 150 ppm due to the borohydride ligand, and the IR spectrum showed bands at 2486, 2198 and 2128 $cm^{-1}$. The mesitylene can be replaced with hexamethylbenzene to form the analogous uranium(III) tris(borohydride) complex.

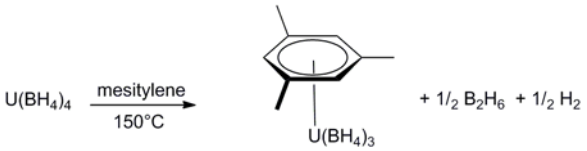


**Equation 1.8**

Uranium borohydrides can be used as starting materials to synthesise uranium hydrides by the elimination of $BH_3$. An example of this is the reaction where $(dme)U(BH_4)_4$, (dme = $MeOCH_2CH_2OMe$), was heated in toluene at 110 °C for 1.5 hours, to give the diuranium, bridged hydride complex $[(dme)(BH_4)_3UHU(BH_4)_3(dme)]$.[35]

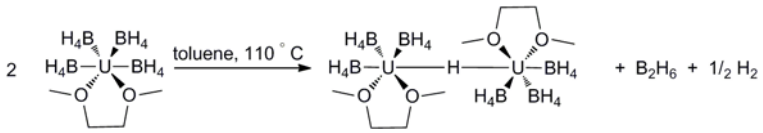


**Equation 1.9**

This hydride-bridged species was characterised by X-ray crystallography and IR spectroscopy (nujol mull) which showed a U-H stretching mode at 1195 $cm^{-1}$, but the hydride was not identified by $^1H$ NMR spectroscopy.

### 1.5.1 Uranium Alkyls

The decomposition of f- and d-element alkyl complexes via β-elimination is a well known pathway yielding metal hydrides. The f-elements do not form strong bonds with π-ligands such as alkenes due to limited orbital overlap of the f-orbitals on the metal and the π-orbitals on the ligand, therefore, the intermediate formed by β-elimination will rapidly dissociate to give a hydride species. This is particularly favoured for f-elements as there are a large number of orbitals in various orientations, increasing the probability that an orbital will be of suitable energy and orientation to bond to the β hydrogen.[1]

Alkyl metal complexes have been used as a precursor to hydride complexes. The uranium alkyl complex shown in Scheme 1.8, was synthesised via the reaction of

[$Cp_3U(THF)$] with RLi.[36] The reaction yields a number of products which are in equilibrium with the Li[$Cp_3UR$] complexes.

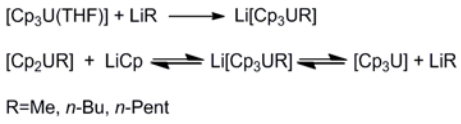


**Scheme 1.8 – Li[$Cp_3UR$] Synthesis**

Another example of such a reaction, is shown in Scheme 1.9, whereby a uranium(IV) halide complex is reacted with $CH_3MgBr$ in toluene, followed up by the addition of an excess of dioxane.[37]

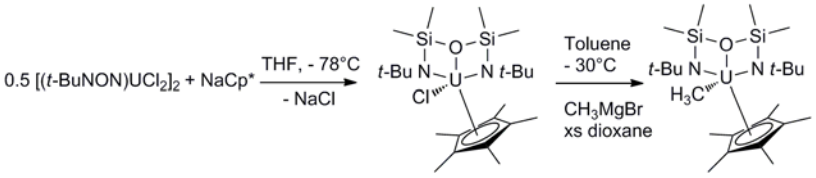


**Scheme 1.9 - Example of chloride substitution**

As well as solid state characterisation, the uranium-methyl proton resonance in the $^1H$ NMR spectrum was shown to be located was paramagnetically shifted to -146.3 ppm.

As discussed in section 1.4.2, the complex, [$(Cp^*)_2U(Me)_2$], reacted with hydrogen to give the dimeric complex [$(Cp^*)_2U(\mu\text{-}H)H]_2$.

The uranium(III) alkyl shown in Figure 1.10, was synthesised by Arnaudet and co-workers in 1986.[38]

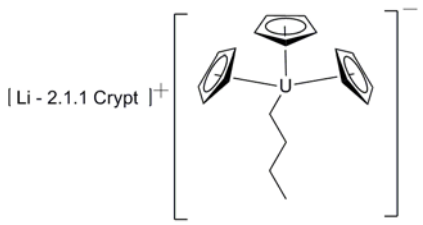


**Figure 1.10 - [$Cp_3UC_4H_9$][Li(2.1.1)]**

The complex was synthesised via the reduction of $[Cp_3UC_4H_9]$ by $LiC_4H_9$. Butane was the only observed by-product, the reaction product crystallised in the presence of the cryptand (2.1.1) as $[Cp_3UC_4H_9][Li(2.1.1)]$ by slow diffusion of a solution of $[Cp_3UC_4H_9]Li$ and a solution of the 2.1.1 cryptand ($C_{14}H_{28}N_2O_4$).

Tetra(allyl)uranium $[(C_3H_5)_4U]$ was synthesised by reaction of $UCl_4$ with 4 equivalents of $C_3H_5MgBr$ in diethyl ether at -30 °C. The complex is highly pyrophoric and is only thermally stable up to -20 °C.[39] The compound was characterised by IR spectroscopy and magnetic susceptibility analysis, and decomposition studies were also in agreement with the other data.

Marks and co-workers showed that in the complex $UR_4$, when R has a β-hydrogen, β-hydrogen elimination occurs at room temperature, producing alkanes, alkenes and dimers. When no β-hydrogen is present the major product is the corresponding alkane.[40] The pathways that produce this mixture of alkanes, alkenes and dimers are shown in Scheme 1.11.

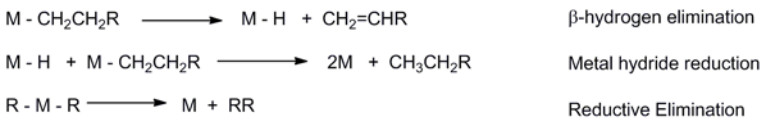


**Scheme 1.11 - Decomposition pathways of metal-alkyls**

## 1.6 Uranium amides

Uranium-amide complexes have been well studied in the literature as they can provide useful insights into the fundamental chemistry of the metal in terms of reactivity and coordination behaviour as well as the bonding interactions present.[41, 42] They are a relatively stable species, although synthetically useful due to the relative stability of the strongly polarised uranium–nitrogen bond.

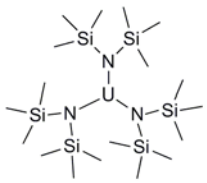

**Figure 1.12 - Tris((hexamethyldisilyl)amido) uranium**

Tris{(hexamethyldisilyl)amido}uranium is a monomeric, volatile uranium(III) complex, first synthesised by Andersen in 1979, Figure 1.12.[13] Along with $Cp_3U$, it was the first readily organic solvent-soluble uranium(III) complex. $[U\{N(SiMe_3)_2\}_3]$ was originally synthesised from $UCl_4$ with a in situ reduction with sodium naphthalene and the subsequent reaction with sodium (hexamethyldisilyl)amide. The molecule is pyramidal, comparable to the tris(hexamethyldisilyl)amides of the 4f-elements in the solid state, with average U-N distances of 2.320 Å. The ease of preparation of this complex has led to it being utilised extensively in protonolysis reactions.

Oxidation of $[U\{N(SiMe_3)_2\}_3]$ has been employed to give a range of uranium(IV) products. The hydride complex $[U(H)\{N(SiMe_3)_2\}_3]$ was synthesised from four equivalents of $Na\{N(SiMe_3)_2\}$ and $UCl_4$. The solid state structure did not allow direct localisation of the hydride ion but its location was inferred via the U-N bond lengths, confirming that the metal centre was in the tetravalent oxidation state.[43, 44]

The four-membered uranium(IV) metallocycle, $[\{N(SiMe_3)_2\}_2U\{N(SiMe_3)SiMe_2CH_2\}]$, was isolated via the pyrolysis of either $[U(H)\{N(SiMe_3)_2\}_3]$ or the methyl uranium complex $[(Me)U\{N(SiMe_3)_2\}_3]$.[45] The reaction with 2,6-disubstituted arenethiols and phenols can then be used to afford the mono substituted uranium(IV) products.[46-48]

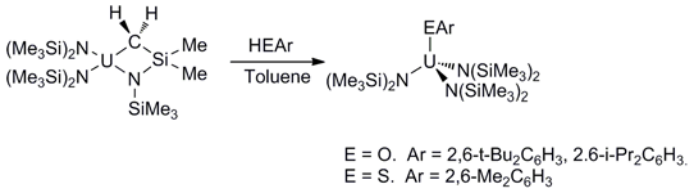


**Equation 1.10**

The polymeric uranium(IV) azide complex $[Na(THF)_4][U\{N(SiMe_3)_2\}_3(N_3)_2]_x$, was synthesised via the reaction of $[U(Cl)\{N(SiMe_3)_2\}_3]$ and $NaN_3$ in THF, Equation 1.11.[49] Each uranium atom has a trigonal bipyramidal geometry and is coordinated by three equatorial amido ligands and two axial azide ligands. The repeating units are linked by sodium cations which bridge between the azide ligands

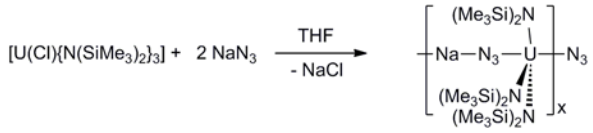


**Equation 1.11**

The anionic uranium complex $[U\{N(SiMe_3)_2\}_4][K(THF)_6]$ was isolated from the reaction of $[U\{N(SiMe_3)_2\}_3]$ with potassium sand in THF.[50] The U-N bond lengths in the complex are longer than those of its parent complex due to the higher coordination number. It is the only solid state example of a tetrakis{bis(trimethylsilyl)amide} uranium complex.

The use of the strong uranium(III) reductant, $[U\{N(SiMe_3)_2\}_3]$ and sodium azide resulted in the formation of the bridged uranium(IV) nitrido compound, $[Na(DME)_2(TMEDA)][\{N(SiMe_3)_2\}_2U(\mu\text{-}N)(CH_2SiMe_2\{N(SiMe_3)_2\}_2]$, Equation 1.12.[51]

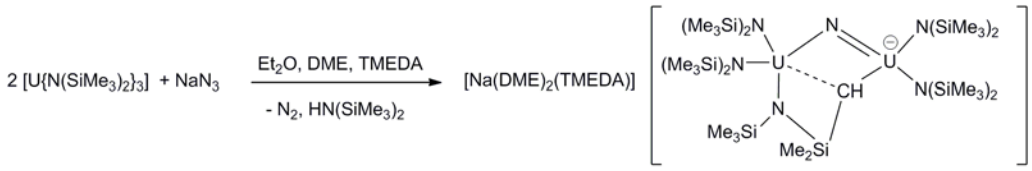


**Equation 1.12**

The reaction proceeds via the two electron reduction of azide coupled with the deprotonation of a silylmethyl group to give bridging $\mu$-$CH_2$ and nitrido groups across two uranium(IV) centres. The uranium–nitrogen bond distances in the U–N=U moiety are inequivalent (1.95(1) and 2.12(1) Å) confirming the localised bond orders.

Uranium tetrakis(diethylamide) was first reported in 1956, by Gilman and co-workers and was the subject of much research due to its volatility.[52] The thermal instability and extreme air- and moisture-sensitivity of uranium tetra(amides) meaning that handling must be performed with great care.

The green uranium(IV) amide was prepared by the treatment of uranium tetrachloride with lithium diethylamide in diethyl ether. Purifying the product by distillation lead to considerable decomposition and an isolated yield of only 30 %, however, it has been reported that isolation via solvent extraction could increase the yield. Gilman also showed that $[U\{N(C_2H_5)_2\}_4]_2$ could be used to access other complexes by protonolysis and isolated the first uranium(IV) alkoxide and thiolate compounds, Figure 1.13.

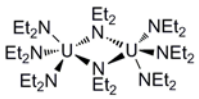


**Figure 1.13 – $[U\{N(C_2H_5)_2\}_4]_2$**

In 1976 the solid state structure of $[U\{N(C_2H_5)_2\}_4]_2$ was ascertained by Templeton, displaying a dimeric complex with two bridging amides connecting the uranium centres, 4.004(1) Å apart. $^1$H NMR spectroscopy studies and freezing point depression analysis show that the dimeric structure is not maintained in solution.[53]

In 1977, Templeton and co-workers produced further results using other amide ligands with increased steric bulk.[54-56]

$[U(NPh_2)_4]$ was characterised along with the by-product $[UO\{N(C_6H_5)_2\}_3LiO(C_2H_5)]_2$ from the reaction of $UCl_4$ and four equivalents of $LiNPh_2$. The formation of the latter was attributed to a reaction of $[U(NPh_2)_4]$ with adventitious air,. In contrast to the smaller ethyl-substituted analogue, the phenyl complex exists as a monomer in the solid state.

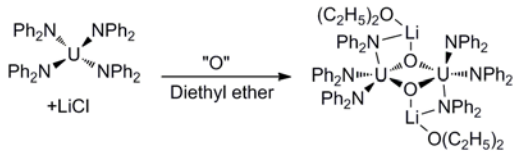


**Equation 1.13**

In the solid state $[U(NPh_2)_4]$ has a distorted tetrahedral geometry with an average U-N bond lengths of 2.27(2) Å. The uranium centre in $[UO\{N(C_6H_5)_2\}_3LiO(C_2H_5)]_2$ has a five coordinate geometry with dimerisation through oxygen bridges. One U-N bond is considerably lengthened in comparison to the other two, 2.44(1) Å compared to 2.33(1) Å and 2.34(1) Å, due to the nitrogen binding to the incorporated lithium atom. $[U(NPh_2)_4]$ is less thermally stable than $[U(NC_2H_5)_4]_2$, preventing the use of sublimation as a means of purification.

The reaction of $UI_3(THF)_4$ with the potassium salt of a primary amides was investigated by Sattleberger and co-workers.[57] The reaction of 3 equivalents of potassium 2,6-diisopropylaniline with $UI_3(THF)_4$ resulted in intractable products, however the reaction employing an excess of potassium 2,6-diisopropylaniline produced the uranium(III) complex $[\{K(THF)_2\}_2U(NH\text{-}2,6\text{-}i\text{-}Pr_2C_6H_3)_5]$, Figure 1.14, from THF as a brown crystalline solid. The formation of 'ate' complexes is a common problem in both actinide and lanthanide chemistry.[58]

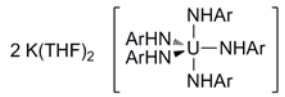


**Figure 1.14 - $[\{K(THF)_2\}_2U(NHAr)_5]$, where Ar = 2,6-i-$Pr_2C_6H_3$**

In the solid state structure, the uranium centre was shown to adopt a five coordinate, with a distorted trigonal-bipyramidal geometry, with an average U-N bond length of 2.34(2) Å. The potassium cations were shown to interact with the two arene rings of the amide ligand in an $\eta^6$ and $\eta^4$ mode in addition to coordination by two THF molecules. The UV absorption spectrum is consistent with that of a uranium(III) complex, containing maxima with weak intensities between 1600 and 600 nm, assigned to the Laporte forbidden f-f transitions.

Ephritikhine and co-workers synthesised the uranium(IV) complex $[U(NMe_2)_4]$ from $UCl_4$ and four equivalents of $LiNMe_2$ in toluene followed by extraction with diethyl ether gave the neutral complex.[59] Initially the 'ate' complex $Li[U(NMe_2)_4Cl]$ was isolated from the reaction and so extraction was necessary to isolate $[U(NMe_2)_4]$. The complex was crystallised and its solid-state structure showed that it is trimeric with the uranium atoms bridged by three amide groups, Figure 1.15.

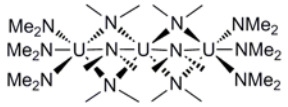


**Figure 1.15 - $[U(NMe_2)_4]_3$**

There are two different environments for the uranium atoms in the trimer. The central uranium atom has octahedral coordination with the other two uranium atoms having a trigonal prismatic environment. The average U-N bond distances for the bridging amides from the central uranium is 2.39 Å, while the bridging bond lengths from the outer uranium atoms are longer at 2.67 Å, whilst the terminal amides have shorter bond lengths (average 2.25 Å). The authors note an interesting trend in that the analogous complexes for metals with smaller radii; $[Mo(NMe_2)_4]$ is a monomer, $[Zr(NMe_2)_4]_2$ a dimer and $[U(NMe_2)_4]_3$ a trimer. Coordinating Lewis bases can break up the trimeric structure in $[U(NMe_2)_4]_3$ to give a monomeric complex.

Anionic uranium(IV) complexes with lithium counter ions have been synthesised by the addition of $LiNR_2$, where R = Me, Et, to the corresponding $[U(NR_2)_4]$ complex, or from $UCl_4$ with $LiNR_2$.[60] $[Li(THF)][U(NEt_2)_5]$ and $[Li(THF)]_2[U(NMe_2)_6]$ were isolated from pentane solutions.

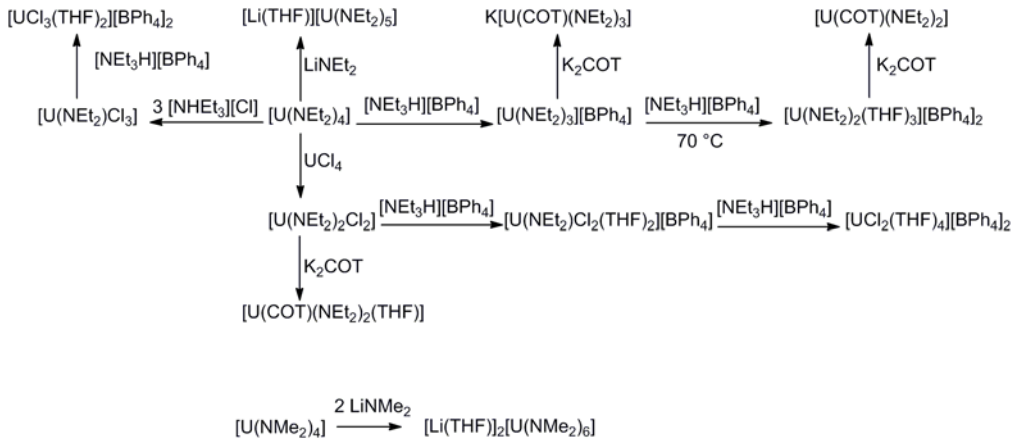


**Scheme 1.16 – Reactivity of $[U(NEt_2)_4]$**

Cationic complexes can be synthesised from the treatment of $[U(NEt_2)_4]$ with $[NEt_3H][BPh_4]$ to yield the complex $[U(NEt_2)_3][BPh_4]$, Scheme 1.16. This then can be reacted with a further equivalent of $[NEt_3H][BPh_4]$ to give $[U(NEt_2)_2(THF)_3][BPh_4]_2$. These cationic complexes can be further reacted with the potassium salt of cyclooctatetraene ($K_2COT$) to yield $[K][U(COT)(NEt_2)_3]$ and $[U(COT)(NEt_2)_2]$ respectively. The protonation of the diethylamide ligand with $[NEt_3H][BPh_4]$, yields the appropriate uranium cationic complex with the elimination of $NEt_3$ and $NHEt_2$. The complex $[U(NEt_2)_3][BPh_4]$ was crystallised from THF/pentane giving the structure $[U(NEt_2)_3(THF)_3][BPh_4]$, Figure 1.17. The coordinated THF molecules are labile, and can be removed under reduced pressure.

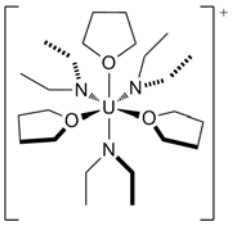


**Figure 1.17 – $[U(NEt_2)_3(THF)_3]+$**

The molecule crystallises with the uranium in a distorted facial octahedral geometry with each amide group positioned trans to a THF molecule. The U-N bond lengths average 2.18(1) Å which are short for terminal amides. If $[U(NEt_2)_2(THF)_3][BPh_4]_2$ is crystallised from pyridine the pyridine adduct, $[U(NEt_2)_2(py)_5][BPh_4]_2$, is formed

with five pyridine molecules coordinated to the uranium centre making it seven coordinate with a pentagonal-bipyramidal arrangement, and an average U-$N_{Et}$ bond distances of 2.202(9) Å.

Reactions between $UCl_4$ and $[U(NEt_2)_4]$, or from reactions between $[U(NEt_2)_4]$ and $[NHEt_3][Cl]$ can be used to synthesise the heteroleptic complexes $[U(NEt_2)_2Cl_2]$ and $[U(NEt_2)Cl_3]$.[61] Synthesis via the reaction of between $UCl_4$ and two equivalents of $LiNEt_2$ yielded only an anionic complex, $[Li][U(NEt_2)_2Cl_3]$. The monochloride trisamide complex $[U(NEt_2)_3Cl]$ was only observed by $^1H$ NMR spectroscopy and was in equilibrium with $[U(NEt_2)_4]$ and $[U(NEt_2)_2Cl_2]$ in a ratio of 1:1:3 in THF. The authors suggested that all the uranium chloroamide complexes have an extended structure whether polymeric or oligomeric, as evidenced by the complexes insolubility in aromatic solvents and the formation of monomeric complexes in the presence of $(Me_2N)_3PO$, (HMPA), which were characterised by single crystal X-ray diffraction studies. $[U(NMe_2)_3Cl(HMPA)_2]$ was prepared from the reaction of $[U(NMe_2)_4(HMPA)_2]$ with $[NHEt_3][Cl]$ or LiCl, Figure 1.18.

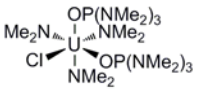


**Figure 1.18 - $[U(NMe_2)_3Cl(HMPA)_2]$**

These heteroleptic uranium(IV) complexes have proven to be very useful starting materials for organometallic complexes.[62]

Recently Cummins has reported the isolation of a bis(uranium) $\mu$-nitrido anion, Scheme 1.19, and then studied its redox chemistry.[63]

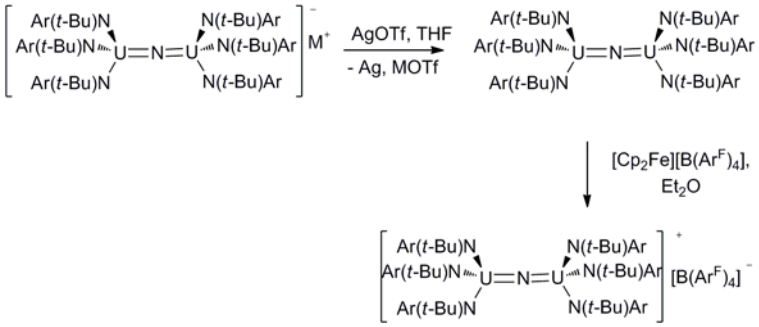


**Scheme 1.19 – Reactivity of M[($\mu$-N){U[N(*t*-Bu)Ar]$_3$}$_2$] where Ar = 3,5-Me$_2$C$_6$H$_3$, and M = Na or N(*n*-Bu)$_4$**

The diuranium(IV) complex was synthesised from the treatment of the uranium(III) complex [(THF){U[N(t-Bu)Ar]$_3$}$_2$] with either sodium or tetra-n-butyl ammonium azide, in THF, in high yields. The solid-state structure of [N(n-Bu)$_4$][($\mu$-N){U[N(t-Bu)Ar]$_3$}$_2$]was determined and the U=N bond lengths were asymmetric (2.080(4) and 2.007(4) Å), and shorter than the terminal U-N amide bond average (2.323(4) Å). The bisuranium(IV) complex was then oxidised with AgOTf to a mixed valence bisuranium(V/IV) complex, [($\mu$-N){U[N(t-Bu)Ar]$_3$}$_2$], with the elimination of Ag and MOTf. After the oxidation there is little change in the U=N bond length, now symmetric (2.0625(2) Å), and the U-N bond lengths have shortened slightly to 2.243 Å. This neutral bisuranium complex was then oxidised further to a ($U^V/U^V$) cationic complex, [($\mu$-N){U[N(t-Bu)Ar]$_3$}$_2$][B(Ar$^F$)$_4$] with [Cp$_2$Fe][B(Ar$^F$)$_4$].

Bagnall and co-workers reported insertion chemistry into the U-N bond, in [U(NR$_2$)$_4$] (R = Me, Et, by $CO_2$, $CS_2$, $CSe_2$ and COS), showing the exciting chemistry possible with these compounds, Figure 1.20.[64, 65] The structure of these complexes was determined to be isomorphous by IR spectroscopy and X-ray powder diffraction analysis.

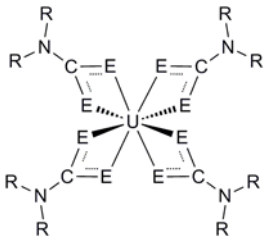

**Figure 1.20 – $[U(S_2CNR_2)_4]$, where S = O, S, Se and R = Me, Et**

The first organometallic uranium amide complex, $[Cp_2U(NMe_2)_2]$, was synthesised by Jamerson and co-workers and is the first in a vast number of complexes using both cyclopentadienyl-type and amide ligands to stabilise low oxidation state uranium, Figure 1.21.[66]

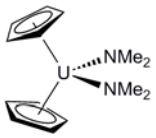

**Figure 1.21 – $[Cp_2U(NMe_2)_2]$**

They reacted in-situ prepared $[U(NMe)_4]$ with two equivalents of $C_5H_6$ to give the bis(cyclopentadienyl) complex in high yield. Care must be taken with the stoichiometery as the tris(cyclopentadienyl) complex was also synthesised.

Replacement of the amide groups were then investigated with a range of ligands, Equation 1.14.

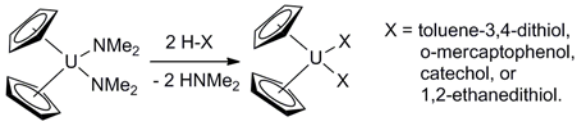


**Equation 1.14**

Possibly inspired by the research of Bagnall and co-workers, Marks and co-workers have reported the insertion of CO into the U-N bond of $[Cp^*_2U(NR_2)_2]$, where R = Me, Et, Scheme 1.22.[67]

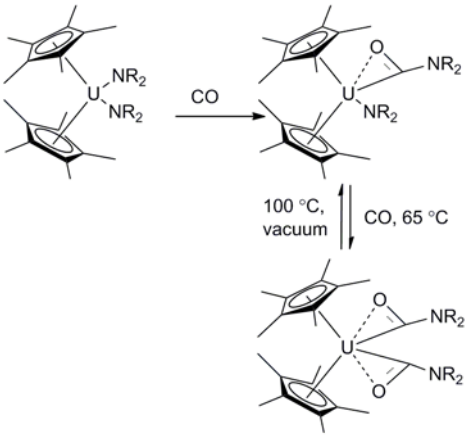


**Scheme 1.22 – CO insertion into the U-$NR_2$ bond**

It was shown that the bis(amide) complex was reactive towards CO despite the steric bulk. Interestingly, the CO can be added in steps and the second equivalent of CO can only be added with increased temperature. However, this addition is reversible upon heating under reduced pressure.

The mixed ligand complex [{$(Me_3Si)_2N$}$_2$$UCl_2$(DME)] was first synthesised by Templeton and co-workers, Figure 1.23.[68] It was isolated from the reaction of two equivalents of sodium bis(trimethylsilyl)amide and uranium tetrachloride in DME.

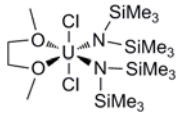


**Figure 1.23 - [{$(Me_3Si)_2N$}$_2$$UCl_2$(DME)]**

The reaction of three equivalents of lithium bis(trimethylsilyl)amide and uranium tetrachloride in THF affords the trisamide derivative [{$(Me_3Si)_2N$}$_3$UCl].[69] Subsequent reactions can give the mono(methyl) and mono(borohydride) complexes using salt elimination methodology.

## 1.7 Uranium Aryloxides

The mixed ligand uranium amide, aryloxide complexes, [$U(NEt_2)(OAr)_3$] and [$U(NEt_2)_2(OAr)_2$] where Ar = 2,6- t-$Bu_2C_6H_4$, were synthesised by Lappert and co-workers in the early 1980s from the tetraamide precursor [$U(NEt_2)_4$], Figure 1.24.[70]

The reaction between $[U(NEt_2)_4]$ with HOAr in pentane gave the desired complexes in high yield, with no observation of the tetraaryloxide uranium complex even when an excess is used. The complexes were monomeric and four coordinate which is low for uranium complexes. The uranium–nitrogen bond length is very short at just 2.162(5) Å.

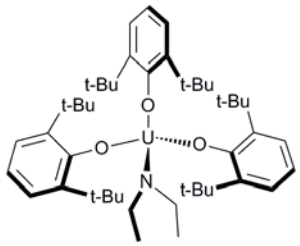


**Figure 1.24 - $[U(NEt_2)(OAr)_3]$**

In the same publication, Lappert and co-workers also reported the formation of other uranium-amide compounds via salt elimination with the use of the stabilising ligand Cp", $\{\eta^5\text{-}C_5H_3(SiMe_3)_2\}$, to yield the complexes $[UCp"_2(NMe_2)_2]$ and $[UCp"_2Cl(NMe_2)]$ from $[UCp"_2Cl_2]$.[70]

## 1.8 Uranium Cp and COT complexes

The complex $[U(THF)(COT)(NEt_2)_2]$ has been used in a vast array of substitution reactions since its first isolation by Ephritikhine in 1996.[59, 71]

As with many other metals the use of the cyclopentadienyl ligand to stabilise low-oxidation state uranium chemistry is vast. The use of both COT and Cp ligands in uranium(III) and (IV) chemistry is summarised up until 1998 in a review by Ephritikhine.[59]

$[U(COT)\{N(SiMe_3)_2\}_2]$ was used as a precursor to the dimeric complex, $[\{U(COT)\}_2\{\mu\text{-}\eta^4\text{:}\eta^4\text{-}HN(CH_2)_3\text{-}N(CH_2)_2N(CH_2)_3NH\}]$.[72] Tetraazadodecane was added in excess and the product was formed immediately and precipitated out of solution. Due to its insoluble nature the complex has only be characterised by X-ray diffraction analysis and elemental analysis. Interestingly, Ephritikhine observed no

reaction between $[U(COT)\{N(SiMe_3)_2\}_2]$ and cyclam (1,4,8,11-tetraazacyclotetradecane).

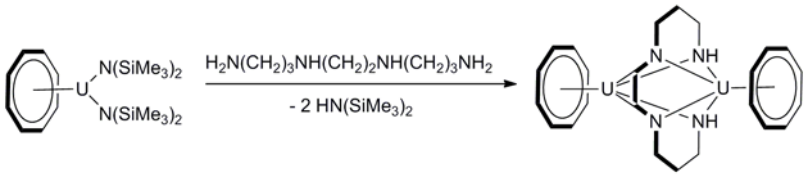


**Equation 1.15**

The crystal structure showed that each uranium atom is five coordinate with average U-N bond distances of 2.46(7) Å. At the time it had the shortest example of a U-U distance at 3.3057(9) Å, with a U-U single bonded interaction calculated to be 2.84 Å.[73]

## 1.9 Uranium Alkyls

The reactivity of $[\{(Me_3Si)_2N\}_2UCl_2(DME)]$ with lithium alkyls and $KC_8$ has been studied.[74] Unusual reactivity for uranium(IV) was observed when this complex was treated with MeLi. The product, $[U\{(\mu\text{-}CH_2\text{-}SiMe_2)N(SiMe_3)\}_2]_2\{\mu\text{-}Li(DME)\}]_2$, is a dimeric uranium(III) complex where one ligand on each uranium had been deprotonated at the γ position and forms a uranium-carbon bond, Figure 1.25.

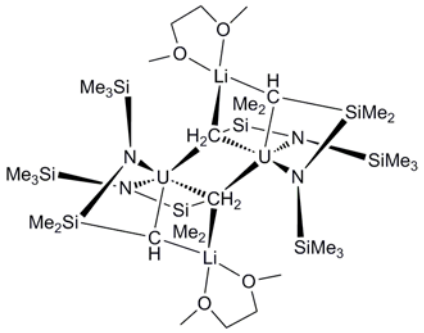


**Figure 1.25 – $[U\{(\mu\text{-}CH_2\text{-}SiMe_2)N(SiMe_3)\}_2]_2\{\mu\text{-}Li(DME)\}]_2$**

The authors of the publication propose that the product is formed by two C-H σ-bond metathesis reactions of two of the silazanate methyl groups by two methyl groups from the methyl lithium reagent. The third equivalent of methyl lithium is then free

to act as a reducing agent. Attempts to isolate a uranium(IV) product with two equivalents of MeLi, yielded only a uranium(III) complex in a lower yield.

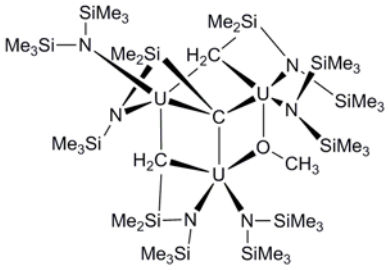

**Figure 1.26 - $[U\{(\mu\text{-}CH_2\text{-}SiMe_2)N(SiMe_3)\}\{N(SiMe_3)_2\}]_2[U\{(\mu_3\text{-}C\text{-}SiMe_2)N(SiMe_3)\}\{N(SiMe_3)_2\}\{\mu\text{-}OMe\}]$**

When $LiCH_2(SiMe_3)$ was used instead a trimeric uranium(IV) complex was isolated. The cluster, $[U\{(\mu\text{-}CH_2\text{-}SiMe_2)N(SiMe_3)\}\{N(SiMe_3)_2\}]_2[U\{(\mu_3\text{-}C\text{-}SiMe_2)N(SiMe_3)\}\{N(SiMe_3)_2\}\text{-}\{\mu\text{-}OMe\}]$, showed cleavage of DME, single deprotonation of two $SiMe_3$ unit and a triple deprotonation to give a carbyne, Figure 1.26. Each uranium centre has a silylamide ligand as well as one that has been deprotonated and all coordinate to the capping carbon atom.

To avoid DME (to prevent its cleavage), the reaction was carried out in hexane which gave a similar trimeric structure, Figure 1.27.

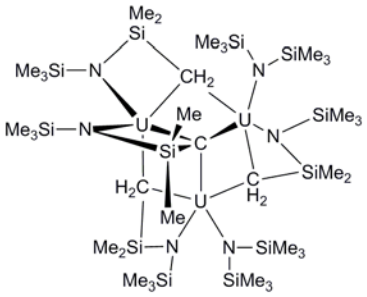

**Figure 1.27 - $[U\{(\mu\text{-}CH_2\text{-}SiMe_2)N(SiMe_3)\}\{N(SiMe_3)_2\}]_2[U\{(\mu_3\text{-}C\text{-}SiMe_2)N(SiMe_3)\}]\{(\mu\text{-}CH_2\text{-}SiMe_2)N(SiMe_3)\}]$**

In this structure it can be seem that the methyoxy bridge from the DME has been replaced by another deprotonation of a $SiMe_3$ fragment and the triply deprotonated carbon, capping three uranium atoms, remains. This highlights the high reactivity of tetravalent uranium centres in conjunction with organolithium reagents.

Noting the reduction of the uranium centres with MeLi, the reduction of $[\{(Me_3Si)_2N\}_2UC1_2(DME)]$ was studied with $KC_8$. In DME this led to the formation of $[U\{N(SiMe_3)_2\}_3]$ and a trimeric chloride bridged complex, Figure 1.28.

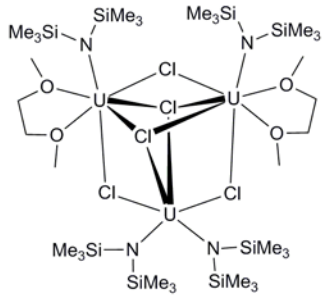

**Figure 1.28 - $[U\text{-}\mu\text{-}Cl\{N(SiMe_3)_2\}(DME)]_2[U\text{-}\mu\text{-}Cl\{N(SiMe_3)_2\}_2]\text{-}(\mu^3\text{-}Cl)_2$**

The X-ray crystal structure shows that the uranium atoms are bridged by three $\mu_2$ and two $\mu_3$ chloride atoms bridging all three uranium atoms. Two of the three uranium(III) centres have one silylamide group whereas the remaining uranium atom has two attached.

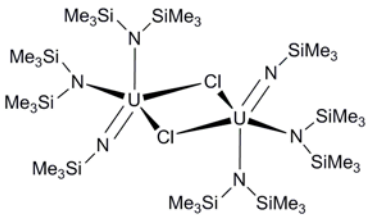

**Figure 1.29 – $[U\text{-}\mu\text{-}Cl\{N(SiMe_3)_2\}_2\{N(SiMe_3)\}]_2$**

In the absence of coordinating solvent the reduction of $[\{(Me_3Si)_2N\}_2UCl_2(DME)]$ with $KC_8$ resulted in a dimeric uranium(V) imido complex, Figure 1.29. The

observation of the imido group was confirmed by IR and the solid-state structure, as determined by X-ray crystallography, showed a U=N bond length of 2.081(5) Å much shorter compared to the other U-N bond lengths (average at 2.243(5) Å).

## 1.10 Uranium Polypyrrolic Complexes

In work published in 2001, Gambarotta and co-workers highlighted the difference in reactivity in uranium(III) chemistry depending on the reaction conditions with the stabilising ligand $(Cy)_4$-calix[4]tetrapyrrole, Figure 1.30.[75]

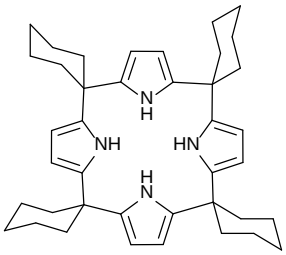


**Figure 1.30 – $(Cy)_4$-calix[4]tetrapyrrole**

The reaction of the potassium salt of the tetraanion polypyrrolic ligand, $(Cy)_4$-calix[4]tetrapyrrole, with $UI_3(THF)_4$ in THF afforded a dinuclear oxygen bridged uranium(IV) complex in a 45% yield, Figure 1.31.

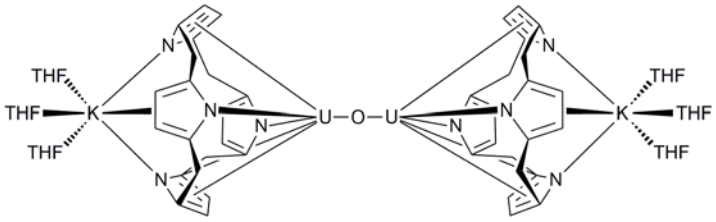


**Figure 1.31 – [{$(Cy)_4$-calix[4]tetrapyrrole}UK$(THF)_3]_2(\mu_2$-O)**

The U-O-U moiety is nearly linear with an angle of 171.3(2)° and U-O bond lengths of 2.0861(5) Å. The origin of the oxygen was determined as arising from oxygen abstraction from a THF molecule. The ligand binds in two different modes, with the uranium atom bonding to two pyrrole units via σ-bonds to the nitrogen atom whilst the other pyrrole units are bound in a $\eta^5$-fashion, in a similar geometry to uranocene.

The pyrrole units bound in a $\eta^5$-geometry are also bound via the nitrogen atom to a potassium atom and vice versa with the U-N bond pyrrole rings also bound $\eta^5$ to the potassium atom.

When the lithium salt of the ligand is used in a ratio of 2:1 with the same uranium starting material a different dinuclear tetravalent uranium complex is formed, without the incorporation of bridging oxygen in a moderate 38% yield, Figure 1.32.

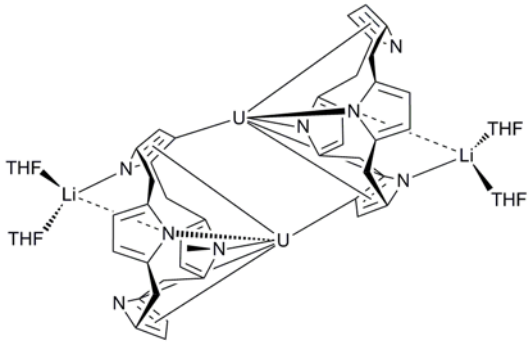


**Figure 1.32 - [{(Cy)$_4$-calix[4]tetrapyrrole}ULi(THF)$_2$]$_2$**

This complex contains a U-C bond, which is formed between the β-C atom of one of the pyrroles and the uranium of another molecule, thus forming a dimer. The authors suggest that the C-H bond activation is facilitated by the lithium salt of the ligand.[75]

Interestingly, the reaction between $UCl_3$ and two equivalents of the lithium salt of the same ligand results in another binding motif giving, [{(Cy)$_4$-calix[4]tetrapyrrole(N-confused)}ULi(OC$_2$H$_5$)(THF)$_2$]$_2$, Figure 1.33. The 'N-confused ligand', where the chain has shifted from the α position to the β position, binds to one uranium and one lithium and THF cleavage has again occurred to form an ethoxide group.

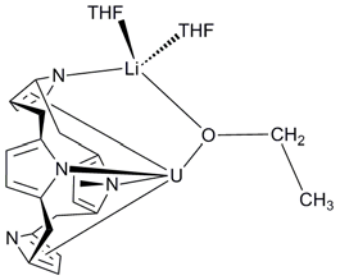


**Figure 1.33 -[{(Cy)$_4$-calix[4]tetrapyrrole(N-confused)}ULi(OC$_2$H$_5$)(THF)$_2$]$_2$**

The analogous reaction of $UI_3(DME)_2$ with the tetrapotassium salt of the polypyrrolic ligand in DME resulted in a trivalent uranium complex, [{$(Cy)_4$-calix[4]tetrapyrrole}U(DME)]-[K(DME)], and no ligand isomerisation or solvent incorporation was observed in this reaction, Figure 1.34.

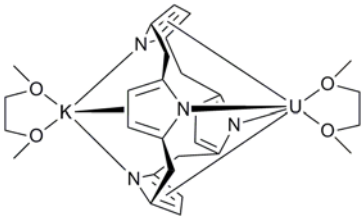

**Figure 1.34 - [{$(Cy)_4$-calix[4]tetrapyrrole}U(DME)]-[K(DME)]**

Reactions to reduce a slightly modified analogue of this complex in which the cyclohexane groups were replaced with two ethyl groups, with potassium naphthalide yields the isolation of three different complexes, Scheme 1.35.[76]

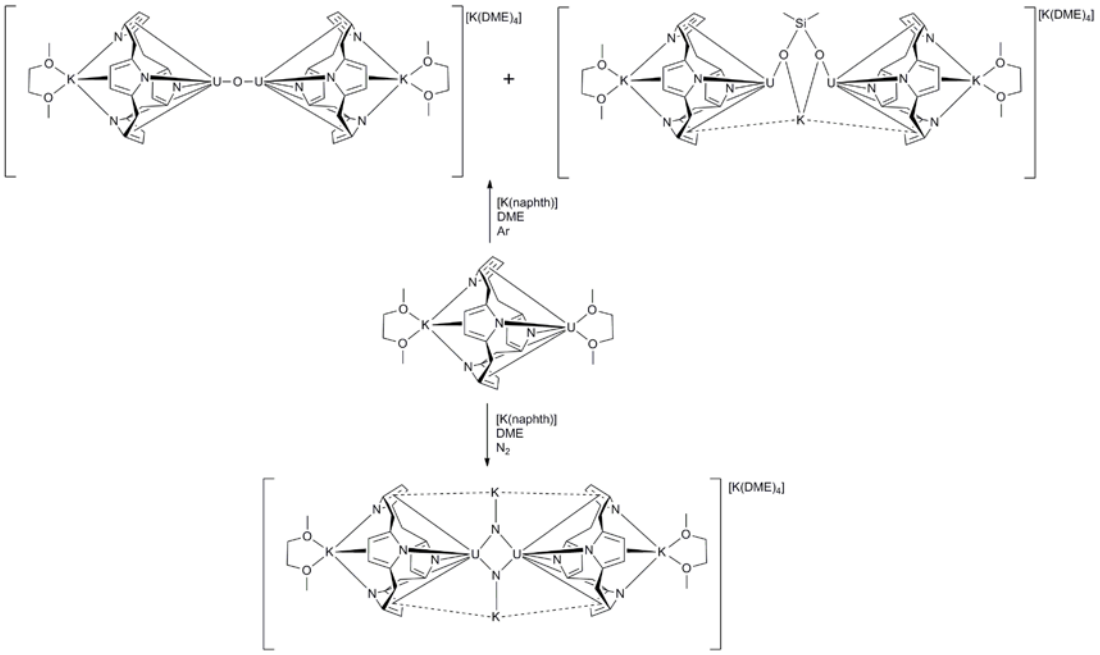


**Scheme 1.35 – Reactivity of [{$(Cy)_4$-calix[4]tetrapyrrole}U(DME)]-[K(DME)]**

Under $N_2$, dinitrogen cleavage is observed to give an anionic, dinuclear mixed valence uranium(IV/V) complex, [{K(DME)(calix[4]tetrapyrrole)U]$_2$($\mu$-NK)$_2$][K(DME)$_4$]. The cleavage of dinitrogen was confirmed by $^{15}N$ labelling studies.

When the reaction is performed under Ar, two complexes are isolated, in an unreported ratio of products with only the total yield stated. The first is an anionic binuclear mixed valence (III/IV) uranium bridged-oxo complex, [{K(DME)-(calix[4]tetrapyrrole)U]$_2$($\mu$-O)][K(DME)$_4$] and the second complex is an anionic binuclear trivalent complex formed from the activation of silicon grease, [{K(DME)-(calix[4]tetrapyrrole)U}($\mu$-Me$_2$SiO$_2$)($\mu$-K){U-(calix[4] tetrapyrrole)K][K(DME)$_4$]. There are a few examples reported of grease activation, but none with uranium(III), again highlighting the high reactivity of this system.[77-79]

The first dinitrogen complex of an actinide was isolated by the group of Scott in 1998, using a triamidoamine ligand, [N(CH$_2$CH$_2$NSiMe$_2$t-Bu)$_3$]$^{3-}$, (NN′$_3$), Scheme 1.36.[80] The solid-state structure showed that a molecule of $N_2$ binds side-on between two uranium atoms. The uranium centres remain in the trivalent state, confirmed by Evans' method magnetic susceptibility measurement and UV-vis spectroscopy. The N-N bond length (1.109(7) Å) is the same as in free dinitrogen gas (1.0975 Å) with the experimental error. The U-N bond lengths fall in the longer end of the usual uranium amido distances.

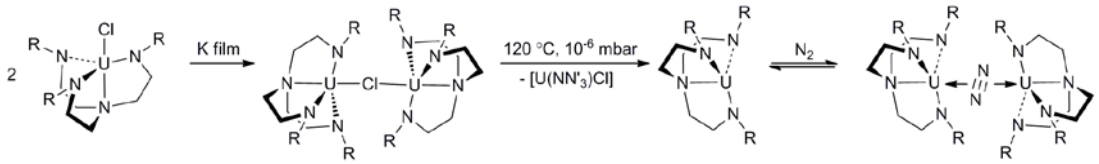


**Scheme 1.36 – Preparation of [{U(NN′$_3$)}$_2$($\mu^2$-$\eta$:$^2\eta^2$-N$_2$)] where R= SiMe$_2$-*t*-Bu**

The authors suggest that the dinitrogen uranium interaction is a $N_2$–U $\sigma$ bond, with [U(NN′$_3$)] acting as a Lewis acid. The dinitrogen $\pi_p$ orbital was thought to be a better $\sigma$-donor than the $\sigma_p$ orbital with trivalent uranium, leading to side-on bonding over an end-on interaction. However, DFT calculations performed on this complex showed that the only significant interaction was covalent uranium 5f to $N_2$ $\pi_p$ backbonding and no dative interaction was observed.[81, 82] The study also addresses why the N-N bond is so short, which they propose is a competition between strong electronic forces to lengthen the bond against the steric effects of the interlocking ligands which are greater resulting in the short N-N distance.

The mixed valence uranium(III/IV) dimer, [{(NN′$_3$)U}$_2$($\mu$-Cl)], with a bridging chloride is a convenient source of a trivalent uranium complex for further reactions. The uranium atom has been drawn out of the ligand cavity in this complex to bound to the chloride bridge leading to longer U-N bond lengths. The cerium mixed valent analogue has also been isolated.[83]

### 1.10.1 Macrocyclic Uranium Complexes

The uranium(IV) porphyrin complex shown in Figure 1.37 was synthesised by Girolami and co-workers in 1987. Due to the small binding pocket the metal centre sits above the plane of the macrocycle.[84]

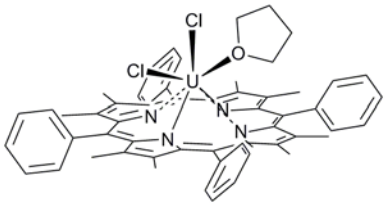


**Figure 1.37 – [U(TPP)Cl$_2$(THF)]**

The ligand 5,10,15,20-tetraphenylporphyrin, (H$_2$TPP), was treated with five equivalents of UCl$_4$ and an excess of 2,6-lutidine in benzonitrile at 150 °C for 4 hours. A constant flow of argon was passed over the reaction to remove the HCl produced. Recrystallisation from THF/1,2-dichloroethane/heptane produced single crystals of U(TPP)Cl$_2$(THF) suitable for X-ray diffraction. The uranium centre sits 1.29 Å out of the plane of the porphyrin, which would obviously be destabilising for the complex, however, the dianionic charge on the porphyrin ring is sufficient to stabilise the metal complex. The U-N bond distances average to 2.41(1) Å which are longer than expected for uranium(IV).

Bisporphyrin uranium(IV) complexes, e.g. [(TPP)$_2$U], have been reported, but have not been characterised by single crystal X-ray diffraction. In the thorium analogue, [(TPP)$_2$Th], the metal centre sits out of the plane of the porphyrin rings, forming a sandwich complex.[85] The photophysics of these complexes were also studied in detail.[86]

The Kadish group have studied the redox chemistry of a range of metal bis(porphyrin) complexes. The results of the uranium and thorium complexes, $[(TTP)_2M]$, were compared to complexes containing two different macrocycles e.g. [(TPP)U(OEP)] where OEP is octaethylporphyrin. It was found that all of the neutral complexes undergo two reversible ligand-centred oxidations and two reversible ligand-centred reductions, however, the half-wave oxidation potential varies with metal ion size (i.e. the smaller U(IV) complexes are more difficult to reduce but easier to oxidise) where as the reduction potential is invariant.[87]

Sessler and co-workers have made key progress in the area of f-element porphyrin complexes. Lanthanide(III) complexes were synthesised with a larger macrocyclic ligand, texaphyrin, $[(texaphyrin)Ln(OH)_2]$.[88] However a uranium(VI) $UO_2^{2+}$ (uranyl) cation was not able to bind to the ligand. The macrocycle binding pocket can be enlarged to encapsulate larger metal centres like uranium(III) by using expanded porphyrins and Schiff-base calixpyrroles. This research opened the door to a wide variety of Schiff base macrocycles, which have been used in a range of chemistry including magnetic resonance imaging, anion recognition, and transition metal complexes used in catalysis, including the macrocycle that has been used extensively in the work described in this thesis, Figure 1.38.[41, 89]

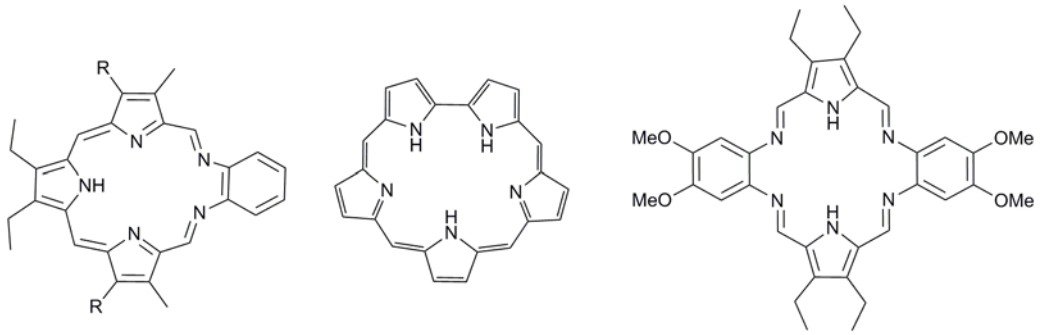


**Figure 1.38 – Texaphyrin, sapphyrin and monoxasapphyrin ligands**

The group of Meyer have been very successful in stabilising uranium(III) in a macrocyclic ligand environment. Reactions between $UN"_3$ and the proligand, 1,4,7-tris(3,5-di-tert-butyl-2-hydroxybenzyl)-1,4,7-triazacyclonane, $\{O(Ar)\}_3tacn$, gave the complex $[U\{O(Ar)\}_3tacn]$, Scheme 1.39.[90] This has proven to be a very reactive

species.[91-102] The structure of [U{O(Ar)}$_3$tacn] has only been determined with one molecule coordinated (e.g. THF, acetonitrile), giving a seven coordinate complex.

The high reactivity of [U{O(Ar)}$_3$tacn] is demonstrated by the numerous by-products isolated in attempts to recrystallise this compound from ethers, which show incorporation of oxygen, ligand reactivity and metal centre oxidation in both diethyl ether and THF, Scheme 1.39.[90] The complex [{O(Ar)}$_3$tacnU(OAr)] was initially isolated from bond cleavage of the (ArO)tacn ligand, and later synthesised via the reaction of [U{O(Ar)}$_3$tacn] and 2,4-di-t-butylphenol. The other products in the reaction mixture were not identified.

The dinuclear complex [({O(Ar)}$_3$tacnU)$_2$($\mu$-O)], was isolated from a solution of [U{O(Ar)}$_3$tacn] in THF left for 2 weeks. The origin of the oxygen atom is unclear, it could have derived from cleavage of THF, or from adventitious atmospheric dioxygen.

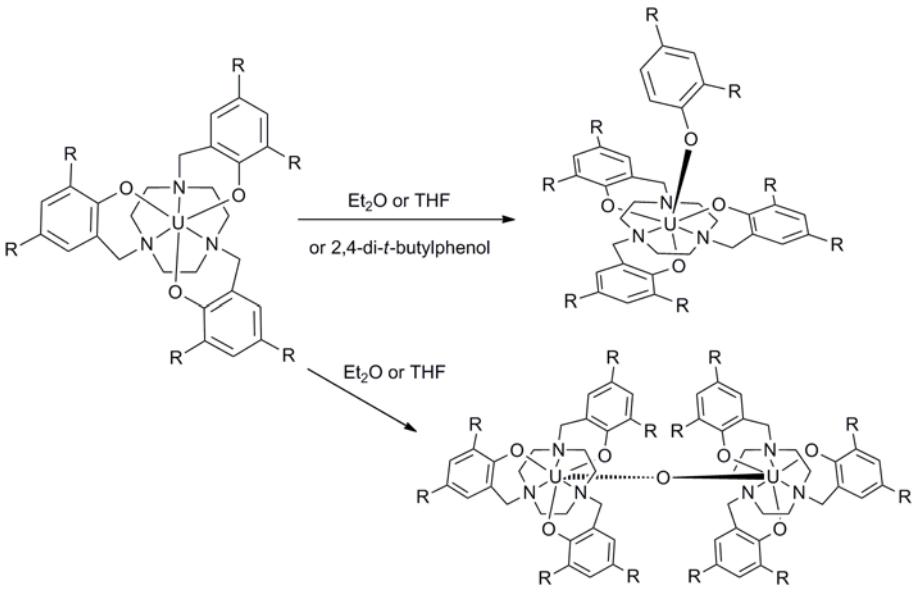


**Scheme 1.39 – Reactivity of [U{O(Ar)}$_3$tacn]with Et$_2$O or THF, where R = *t*-butyl**

The reaction between [U{O(Ar)}$_3$tacn] and $Me_3SiN_3$ gave the tetravalent complex [U(N$_3$)({O(Ar)}$_3$tacn)], as well as a pentavalent imido complex, Equation 1.16.[102]

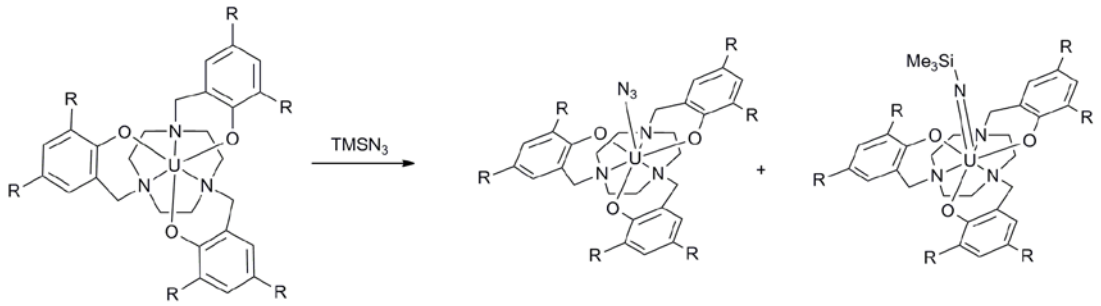


**Equation 1.16**

Terminal azide complexes of low valent uranium centres are very rare with only one other uranium(III) example described.[103] The U-$N_{azide}$ bond distance is 2.562(12) Å and binding to the azide ligand has resulted in the lengthening of the other uranium-ligand bonds. DFT studies indicated that there is little covalent bonding between the uranium atom and the azide group and magnetic studies show a purely ionic species.

Increasing the steric bulk of the ligand by replacement of the tert-butyl groups with adamantyl groups on the ligand has resulted in different reactivity due to the increased protection of the metal centre.[96] The analogous imido complex was synthesised and showed reactivity with CO and methyl isocyanide, forming uranium(IV) isocyanate, [U(NCO)({O($^{Ad}$Ar)}$_3$tacn)], and cyanamide, [U(NCNCH$_3$)({O($^{Ad}$Ar)}$_3$tacn)], complexes respectively, whereas [U(N$_3$)({O(Ar)}$_3$tacn)] showed no reactivity. The cyanamide group can be transferred to organic molecules via successive one electron steps. For example, [U(NCNCH$_3$)({O($^{Ad}$Ar)}$_3$tacn)] reacts with $CH_3I$ to yield $CH_3NCNCH_3$ and [U(I)({O($^{Ad}$Ar)}$_3$tacn)]. The cycle can be closed and the starting complex recovered by reduction with sodium amalgam to give [U{O($^{Ad}$Ar)}$_3$tacn].

Meyer has also observed alkane coordination to the uranium(III) complex, [U{O(Ar)}$_3$tacn], to yield complexes with the general formula, [(C$_n$)U{O(Ar)}$_3$tacn], where C$_n$ is cyclohexane, cyclopentane, methyl cyclohexane, methyl cyclopentane and neohexane, Equation 1.17.[101]

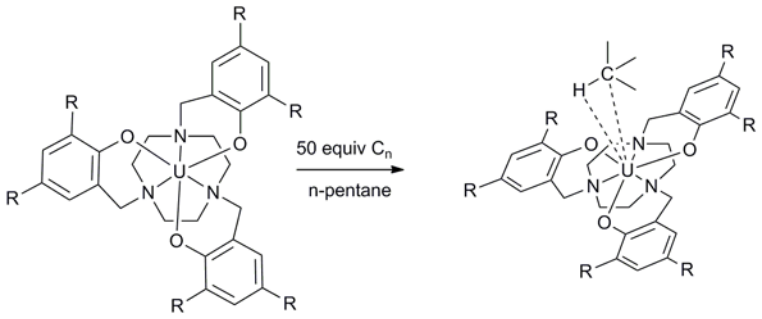


**Equation 1.17**

The interaction between the uranium centre and the carbon atom on the alkane was confirmed by solid-state X-ray crystallography structures as well as DFT calculations. No $^{1}$H NMR spectroscopy studies were reported, despite the promise of a diagnostic spectrum with coordination to the highly paramagnetic centre. The interaction shown by the X-ray crystallography structure ranged between 3.864(7) Å and 3.731(8) Å where as the sum of van der Waals radii was determined at 3.9 Å.

The complex [U{O($^{Ad}$Ar)}$_3$tacn] has also been shown to bind to an N-heterocyclic carbene (NHC), tetramethylimidazol-2-ylidene, $Me_4$IMC, to yield the uranium(III) complex [($Me_4$IMC)U{O($^{Ad}$Ar)}$_3$tacn].[100]

The unprecedented $\eta^1$ complexation of $CO_2$ through the oxygen atom has been seen from the reaction of $CO_2$ with [U{O($^{Ad}$Ar)}$_3$tacn] to yield the uranium(IV) complex [($CO_2$)U{O($^{Ad}$Ar)}$_3$tacn], Scheme 1.40.[99] In the solid-state structure the C-O bond lengths of the $CO_2$ molecule are inequivalent (UO-C 1.122(4) Å, C-O 1.277(4) Å and U-O 2.351(3) Å) and this is consistent with the theory that the $CO_2$ ligand has been reduced by one electron to give the molecular structure as $U^{IV}$=O=C$^{\bullet}$-O$^-$ ↔ $U^{IV}$-O≡ C-O$^-$. Magnetism studies, and electronic and vibrational spectra are all consistent with the proposed model.

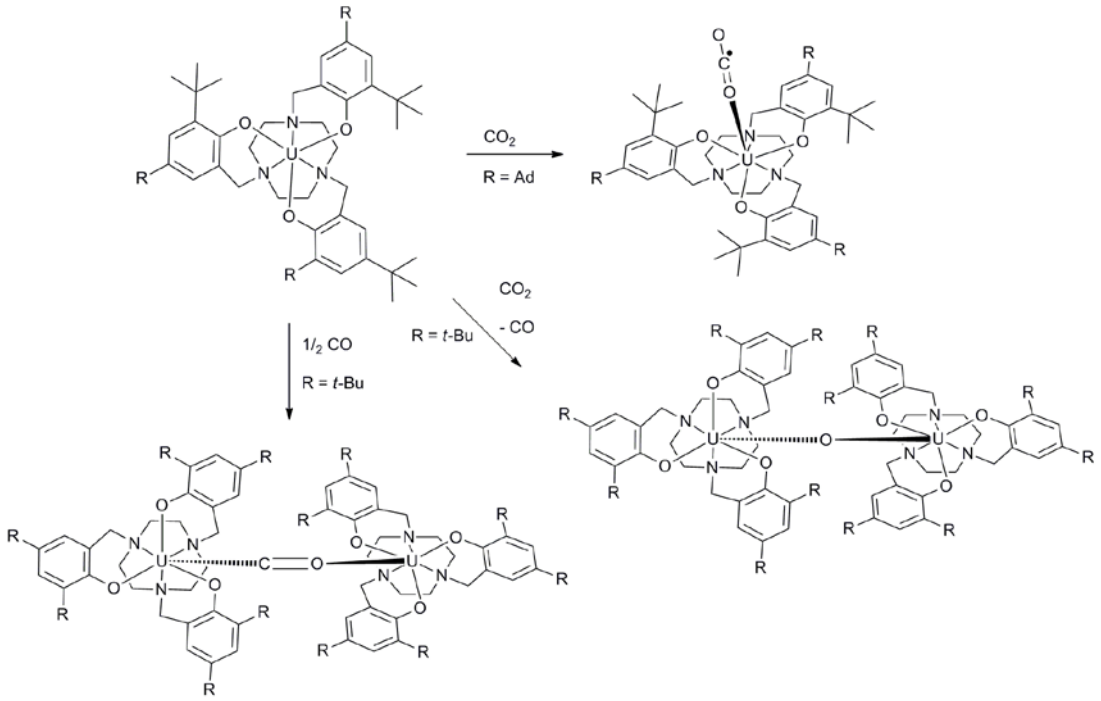


**Scheme 1.40 - $CO_2$ and CO reactivity**

However, when the large adamantyl groups are replaced by t-butyl groups there is no steric bulk to prevent dimerisation, and the reaction proceeds with complete cleavage of $CO_2$ forming the oxo bridged species [{({O(Ar)}$_3$tacnU}$_2$($\mu$-O)] with the loss of CO as confirmed by IR spectroscopy. The carbon dioxide in this reaction has been reduced by two electrons, and the uranium centres oxidised.[98]

When the reaction between CO and [U{O(Ar)}$_3$tacn] was studied, another dimer was formed, [U{O($^{Ad}$Ar)}$_3$tacn]$_2$($\mu$-CO). From X-ray crystallography data and by comparison of uranium(III) and uranium(IV) complexes, the oxidation states of the uranium atoms is given as a mixed valent (III/IV) complex. It is the first uranium complex which contains CO as a bridging ligand with the $\mu$:$\eta^1$,$\eta^1$ binding mode.

The uranium(IV) amido complex [(NHMes)U{O(Ar)}$_3$tacn] has shown interesting reactivity with $CO_2$, Scheme 1.41, with insertion of $CO_2$ into the U-N bond resulting in a uranium(IV) carbamate complex, [($CO_2$NHMes)U{O(Ar)}$_3$tacn].[93]

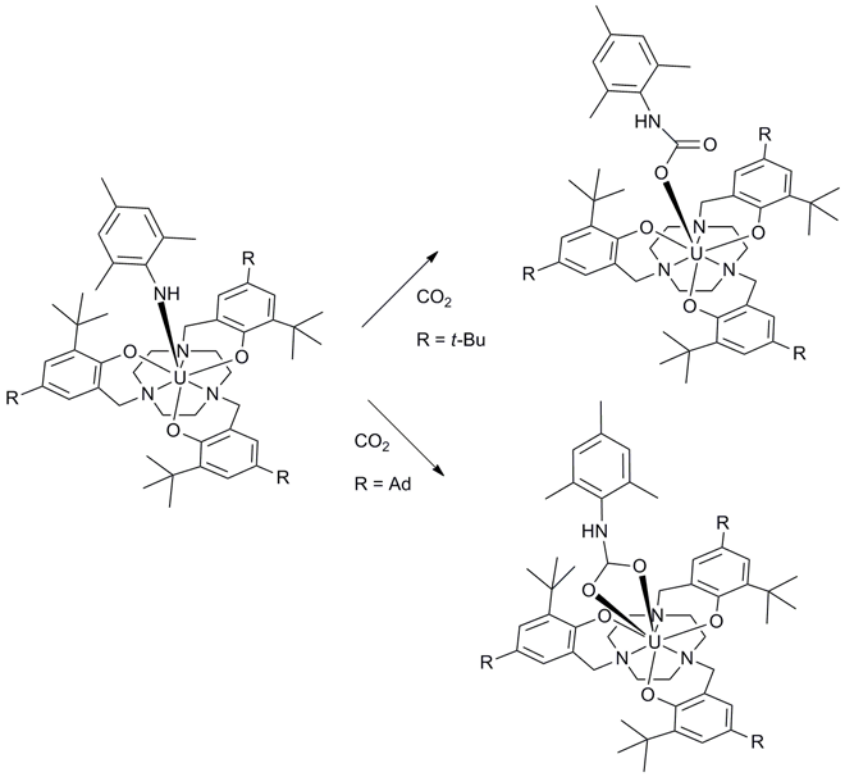


**Scheme 1.41 - $CO_2$ reactivity with [(NHMes)U{O(Ar)}$_3$tacn]**

The carbamate binds in different modes depending on the ligand, in the t-butyl case the carbamate binds via one oxygen atom in a $\eta^1$ mode, whereas in the adamantyl ligand the carbamate binds via two oxygen atoms in a $\kappa^2$ mode. Due to the $CO_2$ ligand's inability to approach closly the metal centre as a result of its increased steric bulk in [($CO_2$NHMes)U{O($^{Ad}$Ar)}$_3$tacn], the U-O bonds are longer (2.434(4) Å and 2.527(4) Å) whereas in [($CO_2$NHMes)U{O(Ar)}$_3$tacn] the U-O bond is a short (2.227(3) Å).

A charge-separated species with a radical anionic ligand [($\eta^2$-NNCPh$_2$)U{O(Ar)}$_3$tacn] was isolated from the reaction of diphenyldiazomethane and [U{{O(Ar)}$_3$tacn}], Scheme 1.42.[95] The uranium is eight coordinate with the diphenyldiazomethane bound via the two nitrogen atoms. Single crystal X-ray crystallography studies showed bond lengths in the C-N-N moiety in line with bond orders being between one and two, one electron being delocalised, and SQUID measurements confirmed this with identification of a uranium(IV) centre.

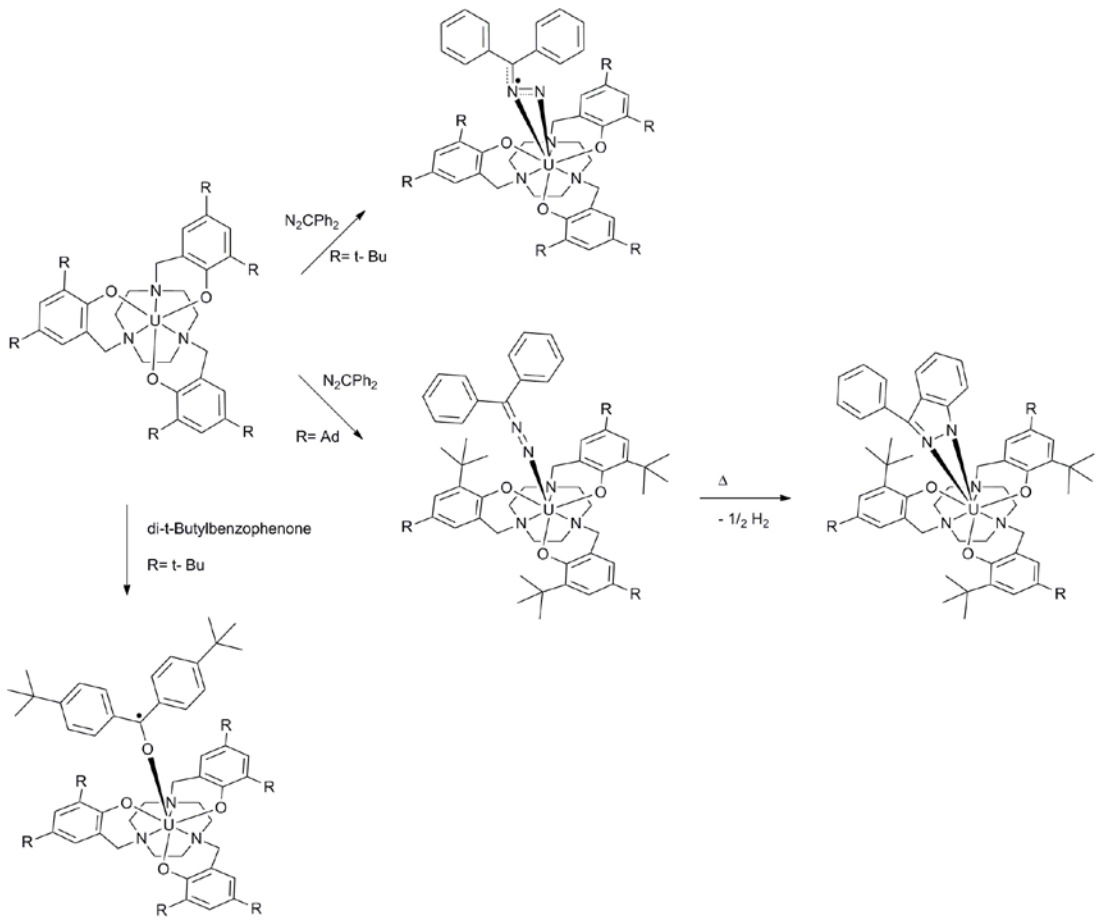


**Scheme 1.42 – Reactivity of [U{O(Ar)}$_3$tacn]with diphenyldiazomethane and 4,4'-di-*t*-butylbenzophenone**

When the steric bulk of the ligand increases to adamantyl, different reactivity with diphenyldiazomethane is shown. Whilst no structural data was obtained, other characterising methods imply that the reaction product is [($\eta^1$-NNCPh$_2$)U{O($^{Ad}$Ar)}$_3$tacn] with the diphenyldiazomethane unit binding via one nitrogen atom, maintaining a uranium(III) centre. Further reactivity is seen upon heating, with the formation of an indazole which then binds in a $\eta^2$-fashion via the two nitrogen atoms, accompanied by the evolution of half an equivalent of dihydrogen to give [($\eta^2$-3-phen(Ind))U{O($^{Ad}$Ar)}$_3$tacn]. This is an example of C-H activation with uranium resulting in cyclisation.

A uranium(IV) ketyl radical complex, [(OC$^{\bullet}$t$^{-Bu}$Ph$_2$)U{O(Ar)}$_3$tacn], has been isolated using disubstituted 4,4'-di-t-butylbenzophenone to help stabilise the reaction products, Scheme 1.42.[94] The structure of [(OC$^{\bullet}$t$^{-Bu}$Ph$_2$)U{O(Ar)}$_3$tacn] can be drawn

with four resonance structures, three of which are uranium(IV) and one uranium(III). This is reflected in the characterisation data for this complex as the data deviates from that expected for a uranium(IV) complex. H-abstraction products were also isolated including the uranium(IV) diphenylmethoxide complex, [(OCHt$^{Bu}$Ph$_2$)U({O(Ar)}$_3$tacn)] and [(OCHPh$_2$)U{O($^{Ad}$Ar)}$_3$tacn], and the dinuclear complex [({O($^{Ad}$Ar)}$_3$tacn)U(OCPh$_2$-CPh$_2$O)U({O($^{Ad}$Ar)}$_3$tacn)].

### 1.10.2 Actinide / Lanthanide Separation

Separation of actinide(III) ions from lanthanide(III) ions has been a guiding principle behind much uranium(III) chemistry. The PUREX (Plutonium-Uranium Extraction) process is the main process used in the separation of spent nuclear fuel.[104] The process uses the continuous liquid-liquid extraction of U(VI) and Pu(IV) from nitric acid solutions by tributyl phosphate in kerosene, Figure 1.43.

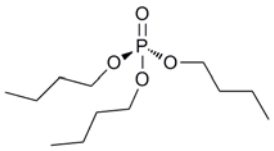

**Figure 1.43 –Tributylphosphate**

Although sulfur donor ligands have been studied, the nuclear industry prefer nitrogen donors as they can be incinerated to produce only gaseous products (if they contain only C, H, O and N) whereas the phosphorous containing S-donors leaves a solid residue.[105]

Ephritikhine and others have utilised bidentate and tridentate N-donor ligands in binding to metal triiodides, Figure 1.44.[106-109] The bidentate ligands didn't show higher binding affinity for uranium compared to the lanthanides. However, when the ligand was changed to the functionalised terpyridine, R-btp, a vast improvement was observed and the uranium(III)/cerium(III) separation factor was > 20.

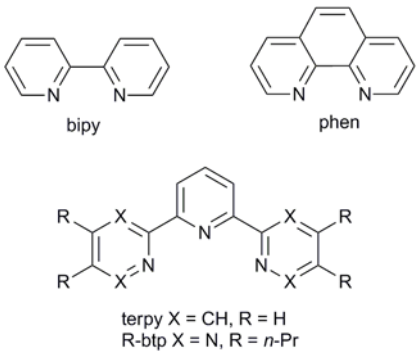


**Figure 1.44 – Ligands used by Ephritikhine**

Mazzanti has used tetradentate, tripodal N-donor ligands, in the quest for better lanthanide/actinide separation, Figure 1.45.[110, 111] By synthesising isostructural complexes it was hoped to observe differences in the metal ligand bonds due to the difference in covalent character of the metals.

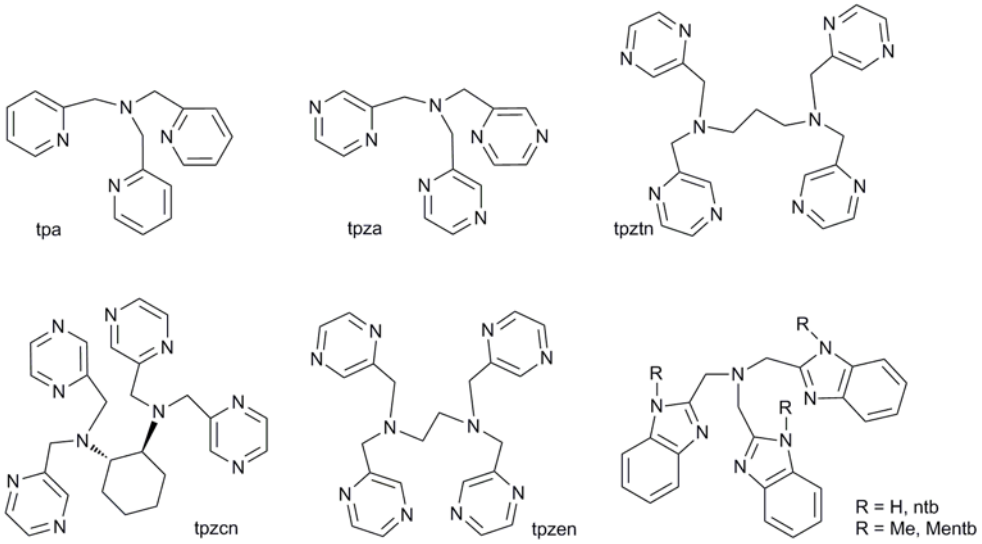


**Figure 1.45 – Ligands used by Mazzanti**

Only minimal differences were reported for the tris[(2-pyridyl)methyl]amine (tpa) ligand, whereas the tris[(2-pyrazinyl)methyl]amine (tpza) ligand showed better selectivity (the formation constant of $[M(tpza)I_3]$, $K_U/K_{La}$, was 3.3 in favour of uranium). This behaviour was explained by the authors as due to the softer character of tpza, which is expected to give rise to a stronger interaction with the actinides.

The hexadentate ligand, N, N, N, N,-tetrakis(2-pyrazinylmethyl)ethylenediamine, tpzen, in competition studies with europium(III) and americium(III) was shown to give higher separation than the more rigid tpza ligand.[112, 113]

### 1.10.3 Uranium Schiff Base Complexes

Schiff bases were discovered by Hugo Schiff in 1866. Since then much research has been performed using Schiff bases as ligands.

Ephritikhine has synthesised a series of salen uranium(IV) complexes, Figure 1.46.

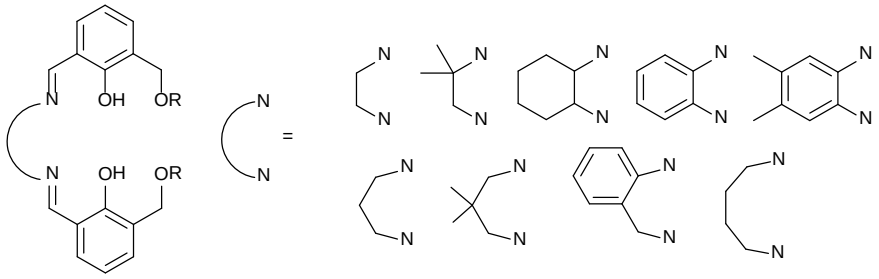


**Figure 1.46 – Salen Ligands used by Ephritikhine**

When R ≠ H, the ligand has only two hydroxide groups and when treated with $[U(acac)_4]$, complexes with the formula $[U(L)_2]$ are formed.[114] Interestingly, the complexes $[U(L)(acac)_2]$ were not isolated as they readily disproportionated into $[U(L)_2]$ and $[U(acac)_4]$.

When R = H, the ligand can be tetraanionic and when the diamine backbone is 2-methyl-1,2-propanediamine, the only uranium complex formed is $[U(H_2L)(acac)_2]$. However, when the diamine part of the ligand is 1,2-phenylenediamine or 2-aminobenzylamine, polynuclear clusters are isolated.

When complexes were synthesised from $UCl_4$, the monoligand complexes were favoured with the formula $[U(L)Cl_2]$, and when the reaction was performed in pyridine, polynuclear structures were again observed.[115]

A trinuclear species with one uranium(IV) and two copper ions has been synthesised, Figure 1.47.[116] The $[U(CuL)_2]$ complex showed an antiferromagnetic interaction between copper ions at 2 K.

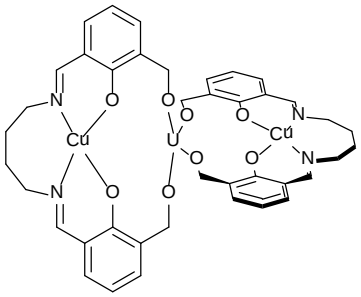

**Figure 1.47 -[U(CuL)$_2$]**

### 1.10.4 Schiff Base Pyrrole Macrocycles

Porphyrins are a group of compounds containing four pyrrole rings connected by hydrocarbon bridges in a macrocycle. Porphyrins are the building blocks of both haem and chlorophyll, Figure 1.48.

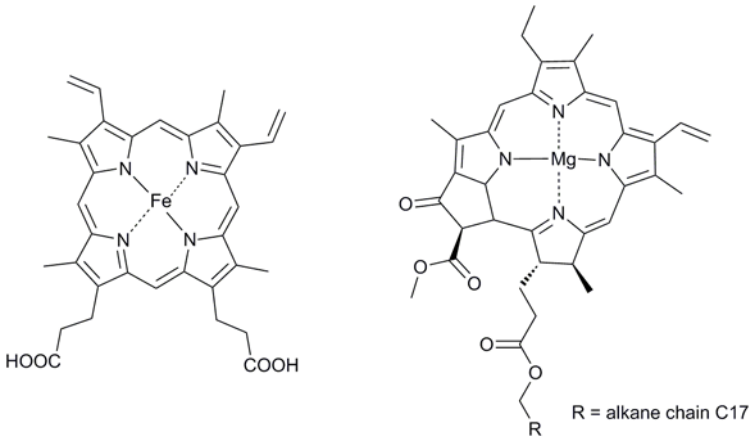


**Figure 1.48 - Haem B and Chlorophyll A**

Cofacial-diporphyrins have been studied in relation to the catalytic production of water.[117, 118] As a replacement for these expensive, hard to synthesise ligands, extended polypyrrolic ligands were developed. Accordion porphyrins contain two iminopolypyrrolic moieties connected by hydrocarbon chains, Figure 1.49.

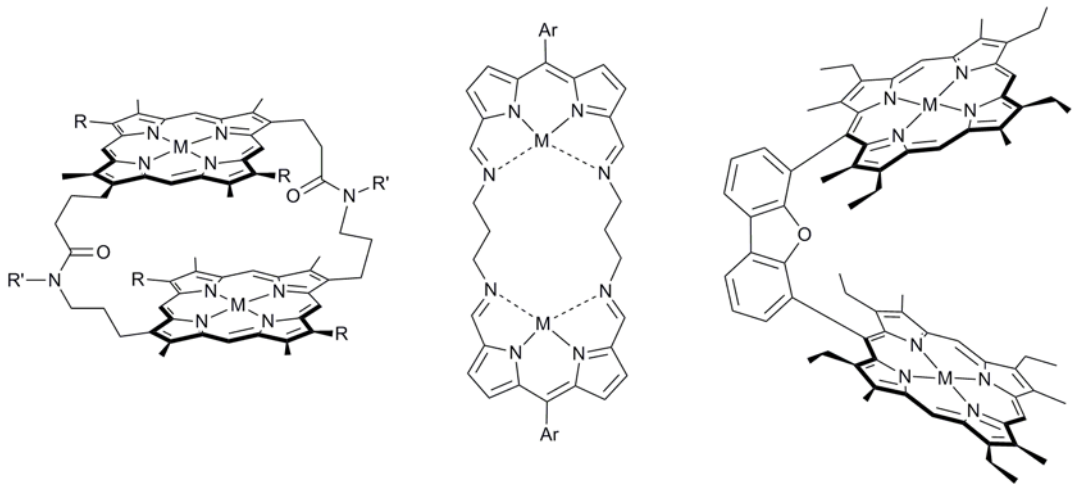

**Figure 1.49 – Examples of cofacial, accordion and Pacman porphyrin complexes**

The polypyrrolic Schiff base macrocycle, $H_4L$, Figure 1.50, was developed independently and simultaneously by the Love and Sessler research groups.[119] The macrocycle is synthesised in relatively few steps and is high yielding, Table 1.3.

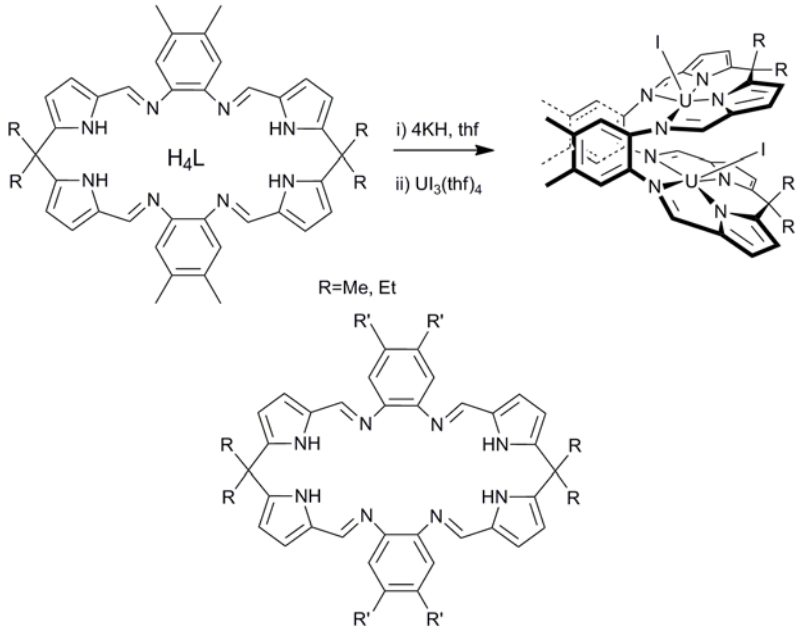


**Figure 1.50 – Example reaction and Macrocycle**

| R group | R′ group | Overall Yield % | Number of steps |
|---|---|---|---|
| Me | H | 61 | 3 |
| Ph | H | 31 | 3 |
| c-$C_6H_6$-2,4-$Me_4$ | H | 27 | 4 |
| Me | Me | 42 | 3 |
| Et | Me | 21 | 3 |
| Ph | Me | 35 | 3 |
| c-$C_4H_4$ | Me | 60 | 3 |
| Fluorenyl | Me | 32 | 3 |

**Table 1.3 – Overall yields for differently substituted Pacman ligands**

The macrocycle has been coordinated to a variety of metals including Ni, Cu, Mn, Cd, Pd, V, Ti, as well as uranyl and mixed-metal uranyl-transition metal, and Sn-(Fe or Zn), Figure 1.51.[120-124] The same ligand has been used by the Sessler group to investigate Fe, Cu, Zn and Cd complexes.[125-127]

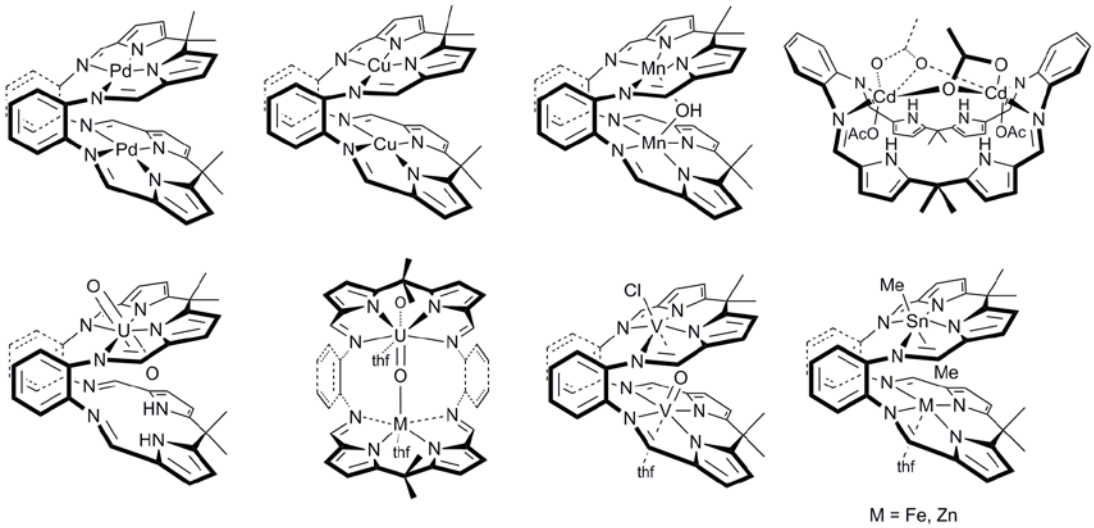


**Figure 1.51 - Examples of metal complexes of $H_4L$.**

The ligand is affectionately known as Pacman, due to its likeness to the character from a 1980s computer game, Figure 1.52.

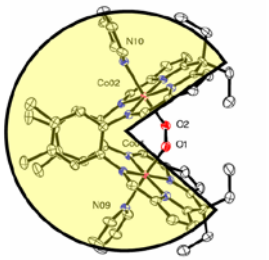


**Figure 1.52 - Pacman resemblance to complexes.**

Dicolbalt Pacman complexes synthesised in the Love group have shown great promise for the four electron reduction of oxygen to water. [$Co_2$(L)] was synthesised from [Co(THF)N"$_2$] and $H_4$L, in a high-yielding reaction. The reaction with oxygen is spontaneous and forms, [$Co_2(O_2)$(L)] the peroxide complex with both cobalt centres oxidised as the major product, Figure 1.53.

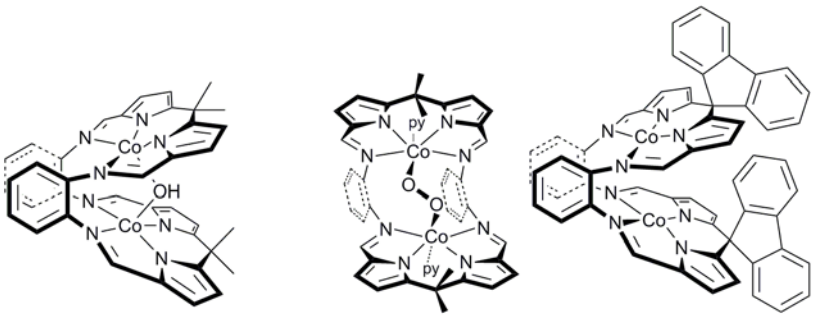


**Figure 1.53 –Cobalt Pacman complexes**

The catalytic cycle can be hindered by the formation of the bridging hydroxyl complex, [$Co_2(\mu$-OH)(L)]$^+$, which is a very stable complex. The use of bulky fluorenyl groups at the meso position modifies the geometry of the bimetallic complexes in an attempt to hinder the formation of the hydroxyl product.[128, 129] In the manifold of this ligand the two Co atoms form a mixed-valent complex with a bridging hydroxyl and a superoxo complex. The hydroxyl complex can go on to react with oxygen to form the superoxo complex, which is a very active catalyst for oxygen reduction.

Arnold, Love and co-workers have carried out research on the manipulation of the uranyl cation in this well defined macrocycle.[123] When the macrocycle is treated with $[(UO_2)\{N(SiMe_3)_2\}_2]$, only one uranyl moiety fits in one of the binding pockets available to the metal cation and this has allowed the manipulation of the U-O bonds and desymmetrisation of the uranyl moiety, Equation 1.18.[122, 130]

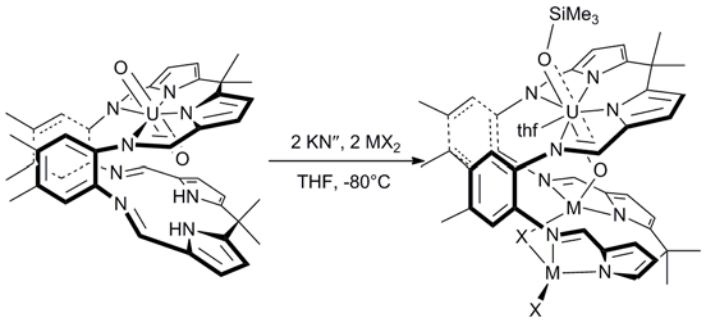


**Equation 1.18**

The complex $[UO(OSiMe_3)(THF)M_2X_2(L)]$, where M = Fe, X = I or M = Zn, X = Cl, I, was isolated in high yield and a single crystal X-ray diffraction study showed that the pentavalent complex has longer U-O bonds than those in its +6 oxidation state. The complex showed the first uranyl oxo covalent bond of a uranyl oxo group with the isolation of this silylation reaction as well as the breaking of a N-Si bond. The mechanism of this reaction has been studied computationally, and these results correlate very well with the experimental results.[131-133]

### 1.10.5 Aims

Chapter 2 describes the reactions of f-block amides with the 'Pac-man' ligand, $H_4L$. It was considered that binary metal complexes of the type $[(MX)_2L]$ would result and that hydride derivatives of these could be prepared and characterised.

A salt elimination methodology is discussed in Chapter 3 in which the potassium salt of the 'Pac-man' ligand, $K_4L$, was reacted with various f-block metal salts to generate the binary metal complexes, $[(MX)_2L]$. A number of techniques have been used to assign structures to these complexes in the absence of single crystals of the quality which would allow X-ray structure determination.

In the final experimental chapter, Chapter 4, we describe attempts to make soluble "carriers" for uranium hydride which could transfer this moiety into the 'Pac-man' ligand, or allow the study of uranium hydride chemistry alone. This work requires the development of high yielding routes $UI_3$ and $UI_4(OEt)_2$.

In the context of the initial aims of the thesis it would be of great interest to define whether polynucleating organic ligands could be developed as corrosion inhibitors for uranium by forming thermodynamically and kinetically stable complexes at the hydridic surface.

## 1.11 References


1. N. Kaltsoyannis and P. Scott, *The f elements*, Oxford University Press, Oxford, 1999.
2. J. J. Katz and G. T. Seaborg, *The Chemistry of the Actinide Elements.*, John Wiley & Sons New York, 1957.
3. S. R. Daly, P. M. B. Piccoli, A. J. Schultz, T. K. Todorova, L. Gagliardi and G. S. Girolami., *Angew. Chem., Int. Ed. Engl.*, 2010, **49**, 3379-3381.
4. R. D. Rogers and A. N. Rollins, *J. Chem. Crystallogr.*, 1994, **24**, 321-329.
5. R. M. Diamond, K. Street, Jr. and G. T. Seaborg, *J. Am. Chem. Soc.*, 1954, **76**, 1461-1469.
6. R. D. Shannon, *Acta Crystallogr., Sect. A* 1976, **A32**, 751-767.
7. I. J. Casely, S. T. Liddle, A. J. Blake, C. Wilson and P. L. Arnold, *Chem. Commun.*, 2007, 5037-5039.
8. J. Glascott, in Discovery - Sci. Technol. J. At. Weapons Establ, 2003, p. 16.
9. K. Balasubramanian, W. J. Siekhaus and W. McLean, *J. Chem. Phys.*, 2003, **119**, 5889-5900.
10. A. L. DeMint and J. H. Leckey, *J. Nucl. Mater.*, 2000, **281**, 208-212.
11. T. B. Scott, G. C. Allen, I. Findlay and J. Glascott, *Philosophical Magazine*, 2007, **87**, 177 - 187.
12. L. R. Avens, S. G. Bott, D. L. Clark, A. P. Sattelberger, J. G. Watkin and B. D. Zwick, *Inorg. Chem.*, 1994, **33**, 2248-2256.
13. R. A. Andersen, *Inorg. Chem.*, 1979, **18**, 1507-1509.
14. J. L. Stewart and R. A. Andersen, *Polyhedron*, 1998, **17**, 953-958.

15. C. J. Rodden, *Analytical Chemistry of the Manhatten Project*, McGraw-Hill Book Company Inc., 1950.

16. R. E. Rundle, *J. Am. Chem. Soc.*, 1947, **69**, 1719-1723.

17. R. E. Rundle, *J. Am. Chem. Soc.*, 1951, **73**, 4172-4174.

18. J. C. Berthet, J. F. Le Marechal and M. Ephritikhine, *J. Chem. Soc., Chem. Commun.*, 1991, **6**, 360-361.

19. J.-C. Berthet, C. Villiers, J.-F. Le Marechal, B. Delavaux-Nicot, M. Lance, M. Nierlich, J. Vigner and M. Ephritikhine, *J. Organomet. Chem.*, 1992, **440**, 53-65.

20. P. J. Fagan, J. M. Manriquez, E. A. Maatta, A. M. Seyam and T. J. Marks, *J. Am. Chem. Soc.*, 1981, **103**, 6650-6667.

21. J. W. K. Bruno, G. Dale, E. A. Mintz and T. J. Marks, *J. Am. Chem. Soc.*, 1982, **104**, 1860-1869.

22. M. Ephritikhine, *Chem. Rev.*, 1997, **97**, 2193-2242.

23. T. J. Marks, W. J. Kennelly, J. R. Kolb and L. A. Shimp, *Inorg. Chem.*, 1972, **11**, 2540-2546.

24. V. V. Volkov and K. G. Myakishev, *Radiokhimiya*, 1980, 745-749.

25. E. R. Bernstein, T. A. Keiderling, S. J. Lippard and J. J. Mayerle, *J. Am. Chem. Soc.*, 1972, **94**, 2552-2553.

26. B. D. James, B. E. Smith and M. G. H. Wallbridge, *J. Mol. Struct.*, 1972, **14**, 327-329.

27. R. T. Paine, *Inorg. Chem.*, 1977, **16**, 2996-3000.

28. H. I. Schlesinger and H. C. Brown, *J. Am. Chem. Soc.*, 1953, **75**, 219-221.

29. D. Baudry, E. Bulot and M. Ephritikhine, *Chem. Commun.*, 1988, 1369-1370.

30. M. L. Anderson and L. R. Crisler, *J. Organomet. Chem.*, 1969, **17**, 345-348.

31. H. J. Wasserman, D. C. Moody, R. T. Paine, R. R. Ryan and K. V. Salazar, *J. Chem. Soc., Chem. Commun.*, 1984, **8**.

32. L. Maria, A. Domingos and I. Santos, *Inorg. Chem.*, 2003, **42**, 3323-3330.

33. D. C. Moody and J. D. Odom, *J. Inorg. Nucl. Chem.* , 1979, **41**, 533-535.

34. D. Baudry, E. Bulot, P. Charpin, M. Ephritikhine, M. Lance, M. Nierlich and J. Vigner, *J. Organomet. Chem.*, 1989, **371**, 155-162.

35. D. Baudry, P. Charpin, M. Ephritikhine, M. Lance, M. Nierlich and J. Vigner, *Chem. Commun.*, 1987, 739-740.

36. M. Foyentin, G. Folcher and M. Ephritikhine, *J. Organomet. Chem.*, 1987, **335**, 201-206.

37. K. C. Jantunen, R. J. Batchelor and D. B. Leznoff, *Organometallics*, 2004, **23**, 2186-2193.

38. L. Arnaudet, P. Charpin, G. Folcher, M. Lance, M. Nierlich and D. Vigner, *Organometallics*, 1986, **5**, 270-274.

39. G. Lugli, W. Marconi, A. Mazzei, N. Palladino and U. Pedretti, *Inorg. Chim. Acta*, 1969, **3**, 253-254.

40. T. J. Marks and M. Seyam Afif, *J. Organometal. Chem.* , 1974, **67**, 61-66.

41. J. L. Sessler, P. J. Melfi and G. D. Pantos, *Coord. Chem. Rev.*, 2006, **250**, 816-843.

42. J. L. Sessler, A. E. Vivian, D. Seidel, A. K. Burrell, M. Hoehner, T. D. Mody, A. Gebauer, S. J. Weghorn and V. Lynch, *Coord. Chem. Rev.*, 2001, **216-217**, 411.

43. R. A. Andersen, A. Zalkin and D. H. Templeton, *Inorg. Chem.*, 1981, **20**, 622-623.

44. S. J. Simpson, H. W. Turner and R. A. Andersen, *Inorg. Chem.*, 1981, **20**, 2991-2995.

45. S. J. Simpson, H. W. Turner and R. A. Andersen, *J. Am. Chem. Soc.*, 1979, **101**, 7728-7729.

46. M. Roger, N. Barros, T. Arliguie, P. Thuery, L. Maron and M. Ephritikhine, *J. Am. Chem. Soc.*, 2006, **128**, 8790-8802.

47. J. M. Berg, D. L. Clark, J. C. Huffman, D. E. Morris, A. P. Sattelberger, W. E. Streib, W. G. Van der Sluys and J. G. Watkin, *J. Am. Chem. Soc.*, 1992, **114**, 10811-10821.

48. D. L. Clark, M. M. Miller and J. G. Watkin, *Inorg. Chem.*, 1993, **32**, 772-774.

49. S. Fortier, G. Wu and T. W. Hayton, *Dalton Trans.*, 2010, **39**, 352-354.

50. W. J. Evans, D. S. Lee, D. B. Rego, J. M. Perotti, S. A. Kozimor, E. K. Moore and J. W. Ziller, *J. Am. Chem. Soc.*, 2004, **126**, 14574-14582.

51. S. Fortier, G. Wu and T. W. Hayton, *J. Am. Chem. Soc.*, 2010, ASAP.

52. R. G. Jones, G. Karmas, G. A. Martin, Jr. and H. Gilman, *J. Am. Chem. Soc.*, 1956, **78**, 4285-4286.

53. J. G. Reynolds, A. Zalkin, D. H. Templeton, N. M. Edelstein and L. K. Templeton, *Inorg. Chem.*, 1976, **15**, 2498-2502.

54. J. G. Reynolds, A. Zalkin, D. H. Templeton and N. M. Edelstein, *Inorg. Chem.*, 1977, **16**, 1858-1861.

55. J. G. Reynolds, A. Zalkin, D. H. Templeton and N. M. Edelstein, *Inorg. Chem.*, 1977, **16**, 1090-1096.

56. J. G. Reynolds, A. Zalkin, D. H. Templeton and N. M. Edelstein, *Inorg. Chem.*, 1977, **16**, 599-603.

57. J. E. Nelson, D. L. Clark, C. J. Burns and A. P. Sattelberger, *Inorg. Chem.*, 1992, **31**, 1973-1976.

58. H. Schumann, J. A. Meese-Marktscheffel and L. Esser, *Chem. Rev.* , 1995, **95**, 865-986.

59. J. C. Berthet and M. Ephritikhine, *Coord. Chem. Rev.*, 1998, **178-180**, 83-116.

60. J. C. Berthet and M. Ephritikhine, *Chem. Commun.*, 1993, 1566-1567.

61. J.-C. Berthet, C. Boisson, M. Lance, J. Vigner, M. Nierlich and M. Ephritikhine, *J. Chem. Soc., Dalton Trans.*, 1995, 3019-3025.

62. M. Ephritikhine, J. C. Berthet, C. Boisson, M. Lance and M. Nierlich, *J. Alloys Compd.*, 1998, **271-273**, 144-149.

63. A. R. Fox, P. L. Arnold and C. C. Cummins, *J. Am. Chem. Soc.*, 2010, **132**, 3250-3251.

64. K. W. Bagnall, D. Brown and D. G. Holah, *J. Chem. Soc. A*, 1968, 1149-1153.

65. K. W. Bagnall and E. Yanir, *J. Inorg. Nucl. Chem.* , 1974, **36**, 777-779.

66. J. D. Jamerson and J. Takats, *J. Organomet. Chem.*, 1974, **78**, C23-C25.

67. P. J. Fagan, J. M. Manriquez, S. H. Vollmer, C. S. Day, V. W. Day and T. J. Marks, *J. Am. Chem. Soc.*, 1981, **103**, 2206-2220.

68. L. G. McCullough, H. W. Turner, R. A. Andersen, A. Zalkin and D. H. Templeton, *Inorg. Chem.*, 1981, **20**, 2869-2871.

69. H. W. Turner, R. A. Andersen, A. Zalkin and D. H. Templeton, *Inorg. Chem.*, 1979, **18**, 1221-1224.

70. P. B. Hitchcock, M. F. Lappert, A. Singh, R. G. Taylor and D. Brown, *Chem. Commun.*, 1983, 561-563.

71. C. Boisson, J.-C. Berthet, M. Lance, J. Vigner, M. Nierlich and M. Ephritikhine, *J. Chem. Soc., Dalton Trans.*, 1996, 947-953.

72. T. Le Borgne, M. Lance, M. Nierlich and M. Ephritikhine, *J. Organomet. Chem.*, 2000, **598**, 313-317.

73. R. H. Cayton, K. J. Novo-Gradac and B. E. Bursten, *Inorg. Chem.*, 1991, **30**, 2265-2272.

74. I. Korobkov and S. Gambarotta, *Inorg. Chem.*, 2010, **49** 3409-3418.

75. I. Korobkov, S. Gambarotta and G. P. A. Yap, *Organometallics*, 2001, **20**, 2552-2559.

76. I. Korobkov, S. Gambarotta and G. P. A. Yap, *Angew. Chem., Int. Ed.*, 2002, **41**, 3433-3436.

77. I. Haiduc, *Organometallics*, 2004, **23**, 3-8.

78. S. Caddick, F. G. N. Cloke, P. B. Hitchcock and A. K. d. K. Lewis, *Angew. Chem., Int. Ed.*, 2004, **43**, 5824-5827.

79. P. L. Arnold, S. Zlatogorsky, N. A. Jones, C. D. Carmichael, S. T. Liddle, A. J. Blake and C. Wilson, *Inorg. Chem.*, 2008, **47**, 9042-9049.

80. P. Roussel and P. Scott, *J. Am. Chem. Soc.*, 1998, **120**, 1070-1071.

81. P. Roussel, W. Errington, N. Kaltsoyannis and P. Scott, *J. Organomet. Chem.*, 2001, **635**, 69-74.

82. N. Kaltsoyannis and P. Scott, *Chem. Commun.*, 1998, 1665-1666.

83. C. Morton, N. W. Alcock, M. R. Lees, I. J. Munslow, C. J. Sanders and P. Scott, *J. Am. Chem. Soc.*, 1999, **121**, 11255-11256.

84. G. S. Girolami, S. N. Milam and K. S. Suslick, *Inorg. Chem.*, 1987, **26**, 343-344.

85. G. S. Girolami, P. A. Gorlin, S. N. Milam, K. S. Suslick and S. R. Wilson, *J. Coord. Chem.*, 1994, **32**, 173 - 212.

86. O. Bilsel, S. N. Milam, G. S. Girolami, K. S. Suslick and D. Holten, *J. Phys. Chem.*, 1993, **97**, 7216-7221.

87. K. M. Kadish, G. Moninot, Y. Hu, D. Dubois, A. Ibnlfassi, J. M. Barbe and R. Guilard, *J. Am. Chem. Soc.*, 1993, **115**, 8153-8166.

88. J. L. Sessler, T. Murai and G. Hemmi, *Inorg. Chem.*, 1989, **28**, 3390-3393.

89. J. L. Sessler, A. E. Vivian, D. Seidel, A. K. Burrell, M. Hoehner, T. D. Mody, A. Gebauer, S. J. Weghorn and V. Lynch, *Coord. Chem. Rev.*, 2001, **216-217**, 411-434.

90. I. Castro-Rodriguez, K. Olsen, P. Gantzel and K. Meyer, *Chem. Commun.*, 2002, 2764-2765.

91. O. P. Lam, C. Anthon and K. Meyer, *Dalton Trans.*, 2009, 9677-9691.

92. S. C. Bart, F. W. Heinemann, C. Anthon, C. Hauser and K. Meyer, *Inorg. Chem.*, 2009, **48**, 9419-9426.

93. S. C. Bart, C. Anthon, F. W. Heinemann, E. Bill, N. M. Edelstein and K. Meyer, *J. Am. Chem. Soc.*, 2008, **130**, 12536-12546.

94. O. P. Lam, C. Anthon, F. W. Heinemann, J. M. O'Connor and K. Meyer, *J. Am. Chem. Soc.*, 2008, **130**, 6567-6576.

95. O. P. Lam, P. L. Feng, F. W. Heinemann, J. M. O'Connor and K. Meyer, *J. Am. Chem. Soc.*, 2008, **130**, 2806-2816.

96. I. Castro-Rodriguez, H. Nakai and K. Meyer, *Angew. Chem., Int. Ed.*, 2006, **45**, 2389-2392.

97. I. Castro-Rodriguez and K. Meyer, *Chem. Commun.*, 2006, 1353-1368.

98. I. Castro-Rodriguez and K. Meyer, *J. Am. Chem. Soc.*, 2005, **127**, 11242-11243.

99. I. Castro-Rodriguez, H. Nakai, L. N. Zakharov, A. L. Rheingold and K. Meyer, *Science*, 2004, **305**, 1757-1760.

100. H. Nakai, X. Hu, L. N. Zakharov, A. L. Rheingold and K. Meyer, *Inorg. Chem.*, 2004, **43**, 855-857.

101. I. Castro-Rodriguez, H. Nakai, P. Gantzel, L. N. Zakharov, A. L. Rheingold and K. Meyer, *J. Am. Chem. Soc.*, 2003, **125**, 15734-15735.

102. I. Castro-Rodriguez, K. Olsen, P. Gantzel and K. Meyer, *J. Am. Chem. Soc.*, 2003, **125**, 4565-4571.

103. J. C. Berthet, M. Lance, M. Nierlich, J. Vigner and M. Ephritikhine, *J. Organomet. Chem.*, 1991, **420**, C9-C11.

104. H. H. Anderson; and L. B. Asprey., ed. U. S. P. Office, 1960.

105. Z. Kolarik, *Chem. Rev.* , 2008, **108**, 4208-4252.

106. P. B. Iveson, C. Riviere, M. Nierlich, P. Thuery, M. Ephritikhine, D. Guillaneux and C. Madic, *Chem. Commun.*, 2001, 1512-1513.

107. C. Riviere, M. Nierlich, M. Ephritikhine and C. Madic, *Inorg. Chem.*, 2001, **40**, 4428-4435.

108. J.-C. Berthet, Y. Miquel, P. B. Iveson, M. Nierlich, P. Thuery, C. Madic and M. Ephritikhine, *J. Chem. Soc., Dalton Trans.*, 2002, 3265-3272.

109. M. J. Hudson, M. G. B. Drew, M. R. S. Foreman, C. Hill, N. Huet, C. Madic and T. G. A. Youngs, *Dalton Trans.*, 2003, 1675-1685.

110. R. Wietzke, M. Mazzanti, J.-M. Latour and J. Pecaut, *Dalton Trans.*, 2000, 4167-4173.

111. M. Mazzanti, R. Wietzke, J. Pecaut, J.-M. Latour, P. Maldivi and M. Remy, *Inorg. Chem.*, 2002, **41**, 2389-2399.

112. L. Karmazin, M. Mazzanti, J.-P. Bezombes, C. Gateau and J. Pecaut, *Inorg. Chem.*, 2004, **43**, 5147-5158.

113. L. Karmazin, M. Mazzanti, C. Gateau, C. Hill and J. Pecaut, *Chem. Commun.*, 2002, 2892-2893.

114. L. Salmon, P. Thuery and M. Ephritikhine, *Dalton Trans.*, 2004, 4139-4145.

115. L. Salmon, P. Thuery and M. Ephritikhine, *Dalton Trans.*, 2004, 1635-1643.

116. L. Salmon, P. Thuery, E. Riviere and M. Ephritikhine, *Inorg. Chem.*, 2006, **45**, 83-93.

117. J. Rosenthal and D. G. Nocera, in *Prog. Inorg. Chem.*, 2007, pp. 483-544.

118. P. D. Harvey, C. Stern, C. P. Gros and R. Guilard, *Coord. Chem. Rev.*, 2007, **251**, 401-428.

119. J. B. Love, *Chem. Commun.*, 2009, 3154-3165.

120. G. Givaja, M. Volpe, J. W. Leeland, M. A. Edwards, T. K. Young, S. B. Darby, S. D. Reid, A. J. Blake, C. Wilson, J. Wolowska, E. J. L. McInnes, M. Schroder and J. B. Love, *Chem. Eur. J.* , 2007, **13**, 3707-3723.

121. G. Givaja, A. J. Blake, C. Wilson, M. Schroder and J. B. Love, *Chem. Commun.*, 2005, 4423-4425.

122. P. L. Arnold, D. Patel, A. J. Blake, C. Wilson and J. B. Love, *J. Am. Chem. Soc.*, 2006, **128**, 9610.

123. P. L. Arnold, A. J. Blake, C. Wilson and J. B. Love, *Inorg. Chem.*, 2004, **43**, 8206-8208.

124. G. Givaja, A. J. Blake, C. Wilson, M. Schroder and J. B. Love, *Chem. Commun.*, 2003, 2508-2509.

125. E. Tomat, L. Cuesta, V. M. Lynch and J. L. Sessler, *Inorg. Chem.*, 2007, **46**, 6224-6226.

126. J. M. Veauthier, W. S. Cho, V. M. Lynch and J. L. Sessler, *Inorg. Chem.*, 2004, **43**, 1220-1228.

127. W. B. Callaway, J. M. Veauthier and J. L. Sessler, *J. Porphyrins Phthalocyanines* 2004, **8**, 1-25.

128. E. Askarizadeh, S. B. Yaghoob, D. M. Boghaei, A. M. Z. Slawin and J. B. Love, *Chem. Commun.*, 2010, **46**, 710-712.

129. E. Askarizadeh, A. M. J. Devoille, D. M. Boghaei, A. M. Z. Slawin and J. B. Love, *Inorg. Chem.*, 2009, **48**, 7491-7500.

130. P. L. Arnold, D. Patel, C. Wilson and J. B. Love, *Nature*, 2008, **451**, 315-317.

131. A. Yahia, P. L. Arnold, J. B. Love and L. Maron, *Chem. Commun.*, 2009, 2402-2404.

132. A. Yahia, P. L. Arnold, J. B. Love and L. Maron, *Chem.-Eur. J.* , 2010, **16**, 4881-4888.

133. J. J. Berard, G. Schreckenbach, P. L. Arnold, D. Patel and J. B. Love, *Inorg. Chem.*, 2008, **47**, 11583-11592.

# Chapter 2: Monometallic Complexes

Transamination reactions between lanthanide and actinide amides and the free ligands $H_4L$ have been investigated as a facile method of synthesising macrocyclic complexes. These complexes could then be used to investigate the difference between the f-elements within the polypyrrolic macrocyclic environment. The metals principally researched were uranium, cerium and yttrium, which displayed different reactivity. Further reactivity of these complexes was also studied.

## 2.1 Synthesis of Schiff-base Macrocycles

The Schiff-base polypyrrolic macrocycles, $H_4L$ was synthesised independently by both the Love and Sessler groups, with the general route shown in Scheme 2.1.[1, 2]

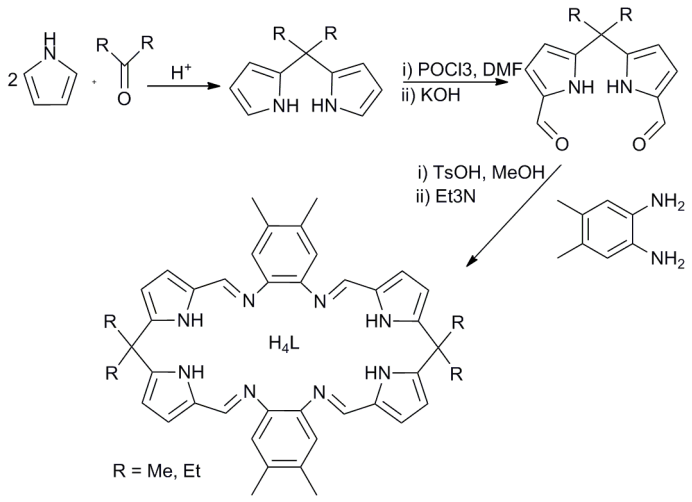


**Scheme 2.1 – Synthesis of $H_4L$.**

### 2.1.1 Synthesis of $H_4L^{Me}$

The synthesis of the octamethyl substituted ligand, $H_4L^{Me}$ where R=Me, involves the preparation of 5,5′-dimethyldipyrromethane,[3] in which excess pyrrole, distilled under reduced pressure, was combined with acetone in acidic conditions to afford 2,2′-dimethyldipyrromethane as a colourless solid, in a good yield. 2,2′-dimethyldipyrromethane was then reacted with $POCl_3$ and DMF in a Vilsmeier

Haack reaction which carbonylates at the 5 position, to afford 5,5′–diformyl–2,2′–dimethyldipyrromethane, once quenched, in a excellent yield as a white solid.[4]

Schiff base condensation between 5,5′–diformyl–2,2′–dimethyldipyrromethane and 4,5-dimethyl-1,2-phenylenediamine, in methanol, in the presence of *p*-toluenesulfonic acid, followed by neutralisation with triethylamine afforded the macrocyclic ligand $H_4L^{Me}$, in an excellent yield as a yellow solid. The ligand requires rigorous drying, at 100 °C under reduced pressure to prevent the introduction of protic solvents e.g. water into the subsequent reactions. This was monitored by $^1$H NMR spectroscopy using the resonance due to the pyrrolic NH proton at 8.35 ppm, which is only visible when no protic solvents are present. The overall yield for $H_4L^{Me}$ is excellent, considering the number of steps involved.

### 2.1.2 Synthesis of $H_4L^{Et}$

In the case of the tetramethyl, tetraethyl macrocycle (R=Et), the corresponding 2,2′-diethyldipyrromethane, was synthesised.[5] An aqueous solution of pentan-3-one was acidified, pyrrole was added and the mixture boiled. The volatiles were removed under reduced pressure from the organic phase affording 2,2′–diethyldipyrromethane as a colourless crystalline powder in a good yield. A Vilsmeier-Haack reaction was carried out on 2,2′–diethyldipyrromethane with $POCl_3$ and DMF, to afford 5,5′-diformyl-2,2′-diethyldipyrromethane, in an excellent yield as a beige powder. The purity was confirmed by $^1$H NMR spectroscopy which showed the six resonances required for the six different environments (one NH, one CHO, two pyrrolic CH's, one $CH_2$ and one $CH_3$).

A mixture of 4,5-dimethyl-1,2-phenylenediamine and 5,5′–diformyl–2,2′–diethyldipyrromethane was stirred in methanol and *p*-toluenesulfonic acid added, the reaction then neutralised with triethylamine. This Schiff base condensation reaction, affords the ligand $H_4L^{Et}$, once dried under reduced pressure at 100 °C, in an excellent yield. The characteristic pyrrolic NH proton in this macrocycle is observed at 9.02 ppm. The formation of the [2+2] Schiff-base macrocycle is exclusive.

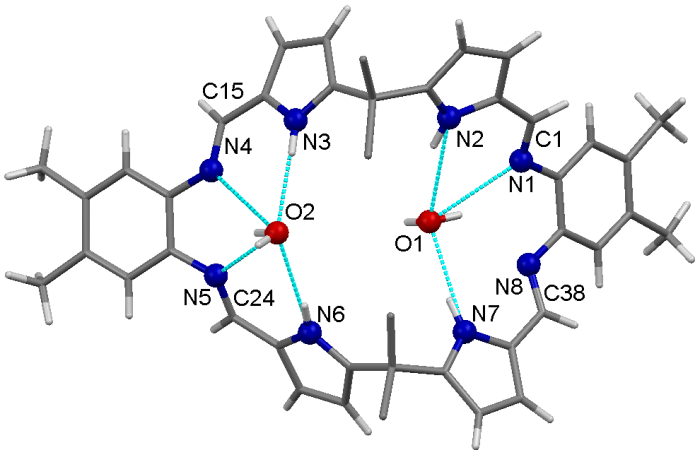


**Figure 2.1 – Ball and stick representations of the X-ray crystal structure of $H_4L^{Et}$, with the ethyl groups omitted for clarity, and hydrogen bonding shown in light blue.**

The X-ray structure from a single crystal of $H_4L^{Et}$ grown from a saturated THF solution shows a molecule of water being held by hydrogen bonding donor-acceptor interactions with the nitrogen atoms in each of the pockets formed when the molecule folds at the meso carbon between the pyrrole units, Figure 2.1. The hydrogen atoms on the water molecules were located from the difference Fourier map and refined using a riding model with restrained distances. One of the O-H bonds from the water points towards the centre of the two imine nitrogen atoms with the other pointing to THF molecules in the unit cell.

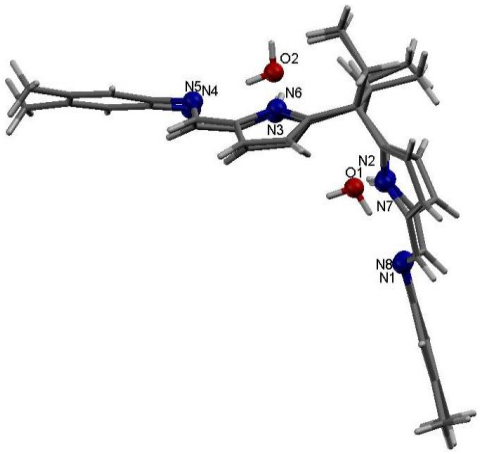


**Figure 2.2 – Top view of $H_4L^{Et}.(H_2O)_2$.**

As the view from the top, Figure 2.2, shows even when unbound to a metal atom, the ligand forms a folded shape with an angle of 106.35°.

| C=N | N(H)-O |
|---|---|
| C1–N1 1.281(3) | N2-O1 2.921 |
| C15-N4 1.277(4) | N7-O1 2.954 |
| C24-N5 1.280(4) | N3-O2 2.971 |
| C38-N8 1.283(3) | N6-O2 2.975 |

**Table 2.1 – Selected bond lengths in $H_4L^{Et}$.**

The imine bond lengths are consistent with the C=N assignment and the ligand shows no signs of tautomerisation, Table 2.1.

Previous single crystal structures of macrocyclic ligands within the group have also shown water binding.[6] The $H_4L$ macrocycle with *meso*-tetra-methylcyclohexyl substiution was crystallised from diethyl ether and the single crystal structure is shown in Figure 2.3.

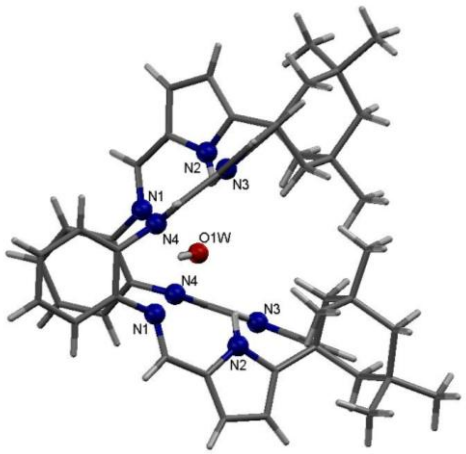


**Figure 2.3 – Structure of $H_4L^{CyMe}.(H_2O)$.**

As with $H_4L^{Et}$, the ligand forms a wedged shape due to the hydrogen bonding donor and acceptor interactions between the pyrrole and imine nitrogen atoms and the

molecule of water with the hydrogen atoms on the water molecule pointing to the middle of the imine nitrogen atoms in each of the binding pockets. In contrast, to $H_4L^{Et}$ , the macrocycle folds to form a Pacman shape rather than the 'bowl shape', leading to all nitrogen atoms pointing to the water in the centre of the cleft.

The binding of other solvent molecules has also been shown by the macrocyclic ligand, Figure 2.4. The polypyrrolic ligand derived from 1,2-diaminonaphthalene, $H_4L^{Nap}$ shows the binding of two ethanol molecules being held by hydrogen bonding donor-acceptor interactions with the nitrogen atoms in each of the pockets formed when the molecule folds at the meso carbon between the pyrrole units, just as in $H_4L^{Et}$ with the water molecules.

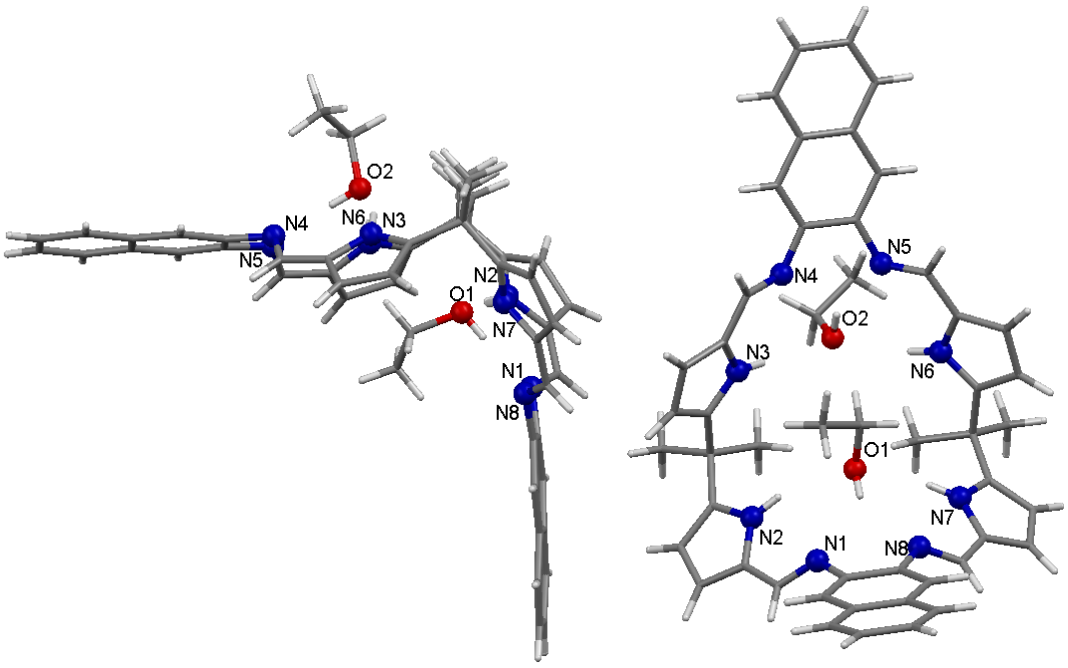


**Figure 2.4 – Structure of $H_4L^{Nap}.(EtOH)_2$.**

The shape formed by both $H_4L^{Et}$ and $H_4L^{Nap}$ in the presence of protic solvent can be described as 'bowl-shaped'. Like the water molecules in $H_4L^{Et}$, one of the ethanol molecules is in the cleft of the macrocycle and one on the outside of the macrocycle, both having hydrogen bonding interactions between the imine nitrogen atoms and the ethanolic hydroxide proton as well as the interaction between the pyrrole NH proton and the oxygen atom on the ethanol molecule. The $sp^2$ hybridised meso-carbon

between the pyrrole groups allows the folding of the macrocycle whereas in related porphyrin systems the meso-carbon is $sp^3$ hybridised which does not allow this folding.

## 2.2 Synthesis of Uranium Complexes

### 2.2.1 Synthesis of [U($L^{Et}$)]

The reaction between the uranium(III) tris(silylamide), [U{N($SiMe_3$)$_2$}$_3$], and $H_4L^{Et}$ in THF, formed exclusively the uranium(IV) complex [U($L^{Et}$)] in a 80% yield, Scheme 2.2.[7] The expected product [U{N($SiMe_3$)$_2$}($H_2L^{Et}$)] was never isolated but was observed by $^1$H NMR spectroscopy during the reaction between [U{N($SiMe_3$)$_2$}$_3$] and $H_4L^{Et}$ at room temperature. This spectrum was indicative of an unsymmetrical ligand environment with four different pyrrolic backbone resonances at 8.30, 7.07, 6.44 and 6.03 ppm and two imido proton environments at 11.28 and 9.64 ppm. However as the reaction progressed only one product observed with a symmetric ligand environment with resonances between +55 and -36 ppm, and was attributed to [U($L^{Et}$)]; this implies that the uranium(IV) complex is the thermodynamic sink.

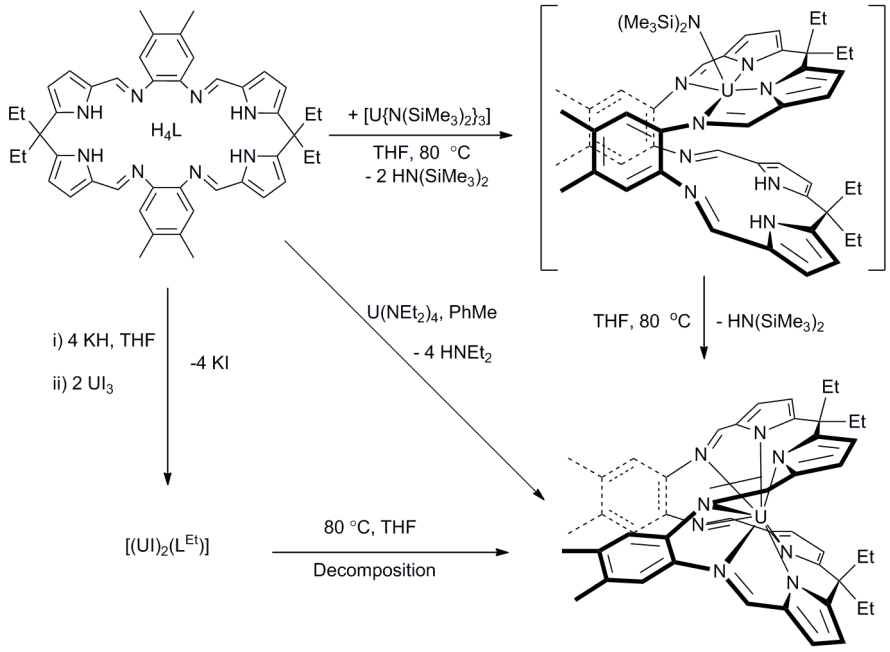


**Scheme 2.2 – Synthesis of [U($L^{Et}$)].**

The reaction to form [U($L^{Et}$)] *via* [U{N($SiMe_3$)$_2$}($H_2L^{Et}$)], is thought to proceed by transamination of the remaining silylamide group and the homolytic cleavage of the N-H bond by the uranium(III) cation, which in turn eliminates half a molecule of dihydrogen with the simultaneous single electron oxidation of the uranium cation to uranium(IV). This has previously been seen in another uranium(III) system by the Meyer group.[8] The uranium(III) complex [U{O($^{Ad}$Ar)}$_3$tacn], previously discussed in the introduction, was shown to react with 1*H*-indazole to produce a uranium(IV) indazolido complex, [({O($^{Ad}$Ar)}$_3$tacn)U($\eta^2$-Ind)] and half an equivalent of dihydrogen, see below.

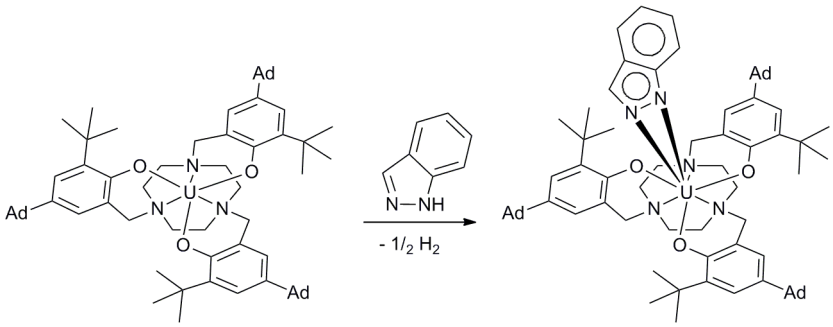


**Equation 2.1**

The uranium(IV) complex [U($L^{Et}$)], can also be synthesised directly from the reaction of [U($NEt_2$)$_4$], made in situ from $UI_4(OEt_2)_2$ and four equivalents of $LiNEt_2$, and $H_4L^{Et}$. The bimetallic uranium complex, [$(UI)_2L^{Et}$] (discussed in Chapter 3), was also shown to form [U($L^{Et}$)] at elevated temperatures by $^1$H NMR spectroscopy.

Single crystals of [U($L^{Et}$)] suitable for X-ray analysis were grown from a saturated $C_6D_6$ solution at room temperature, and an identical set were grown during an attempt to crystallise [$(UI)_2L^{Et}$] in THF, Figure 2.5.

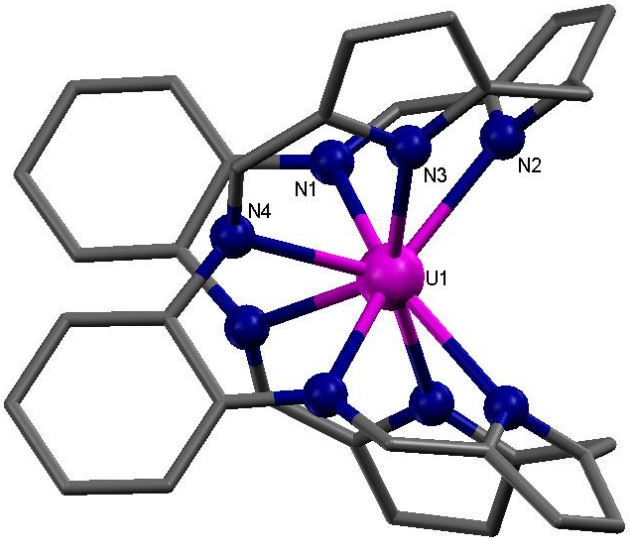


**Figure 2.5 – Ball and stick representations of the X-ray crystal structure of [U($L^{Et}$)] , the aryl backbone methyl groups and the ethyl groups from between the pyrrole groups, hydrogen atoms and solvents of crystallisation have been excluded for clarity.**

The structure shows that the uranium(IV) cation has been encapsulated by the macrocycle in an unprecedented binding mode, Figure 2.5. The uranium atom, U1, is eight coordinate with a distorted square-antiprismatic geometry, bonding to all eight nitrogen donors of the macrocycle. As such no donor solvent is required to complete the coordination sphere. The single crystal X-ray structure has a C2-symmetry, meaning that both halves of the molecule are identical.

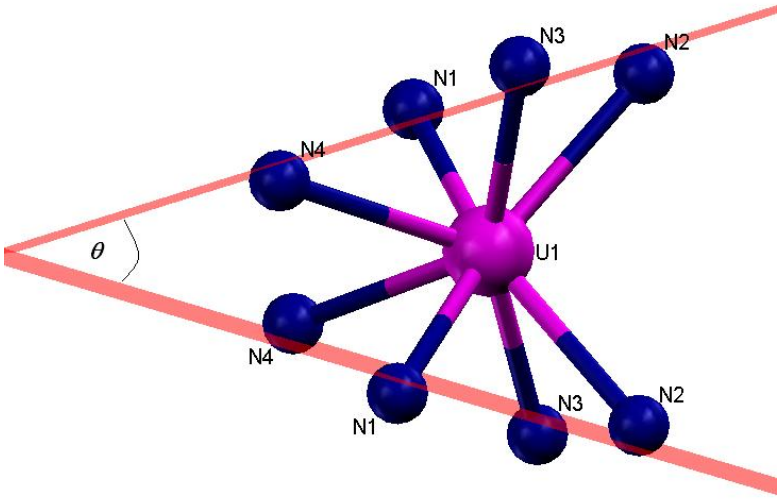


**Figure 2.6 –Coordination about the uranium atom in [U($L^{Et}$)].**

The bite angle, defined in Figure 2.7 formed between the two $N_4$ planes in [U($L^{Et}$)] is 34º and the twist angle formed in [U($L^{Et}$)] is 32°, which is the angle formed between the plane which is perpendicular to the $N_4$ plane and the aromatic backbone ring.

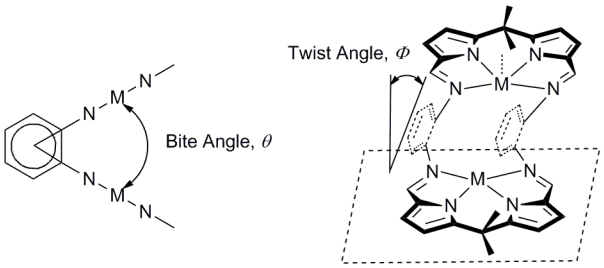


**Figure 2.7 - Definition of bite angle and twist angle.**

In related systems of the same ligand the aromatic hinges normally adapt a face-to-face π-stacking arrangement. However this face-to-face π-stacking is not possible in [U($L^{Et}$)] due to the incorporation of the large uranium atom, giving a twist from parallel between the aromatic hinges of 6.71°.

The U-N bond lengths are standard for related systems. The uranium(IV)-pyrrole distances (U1-N2, U1-N3) are 2.474(10) and 2.459(10) Å which lie in the range found for related porphyrin and polypyrrolic systems (2.35-2.59 Å).[9-13] From the limited examples of uranium(IV)-imine bonds, the bonds in [U($L^{Et}$)] (U1-N1, U1-

N4, 2.520(9), 2.533(8) respectively) fall within the literature range of 2.51-2.63 Å.[14-16]

| Imine | Pyrrole |
|---|---|
| U1-N1 2.533(8) | U1-N2 2.474(10) |
| U1-N4 2.520(9) | U1-N3 2.459(10) |

**Table 2.2 –Selected bond lengths in [U($L^{Et}$)] in Å.**

Related polypyrrolic and porphyrin systems are shown in Figure 2.8.

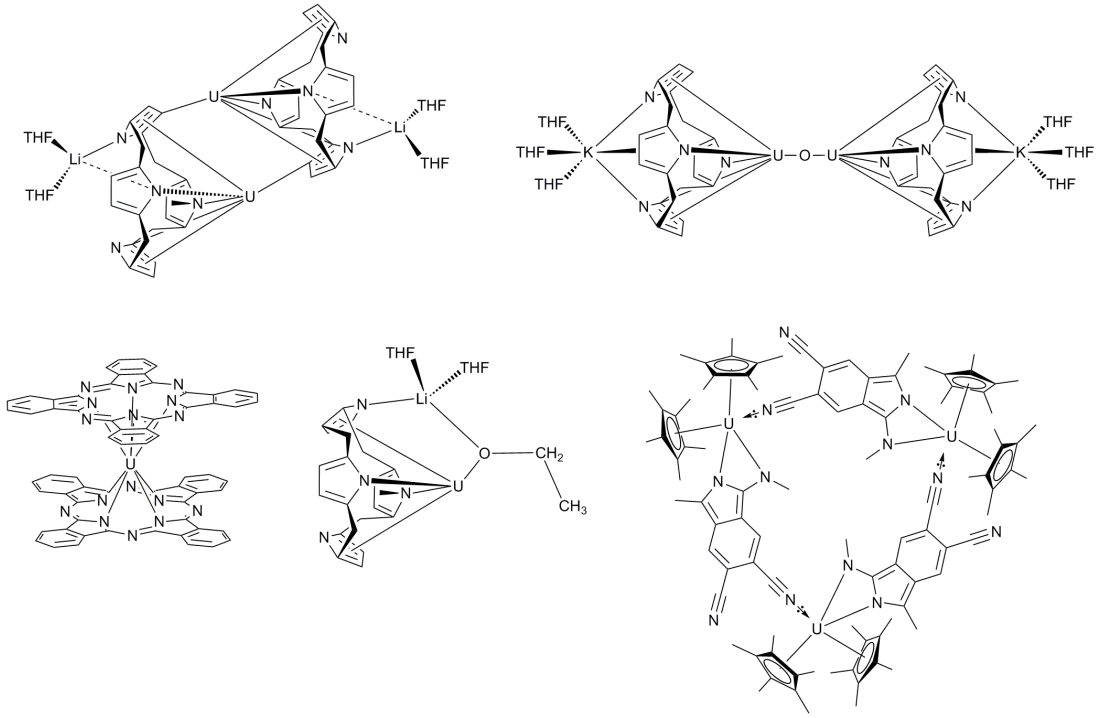


**Figure 2.8 – Examples of uranium(IV) related systems.**

The polypyrrolic structures synthesised by the Gambarotta group, as discussed in Chapter 1, highlight the unusual nature of the encapsulation of the uranium atom in [U($L^{Et}$)].[11] The bis(phthalocyaninato)-uranium(IV) complex shows that the phthalocyaninato ligands adopt a coplanar arrangement at the uranium centre.[17] The trinuclear uranium cyclic complex was isolated from the reaction of 1,2,4,5-

tetracyanobenzene with $[(Cp^*)_2U(CH_3)_2]$[10] and was formed by sequential nitrile-coupling and then self assembly.

The macrocyclic ligand $H_4L^{Et}$, has previously shown a range of binding modes as shown in Figure 2.9.

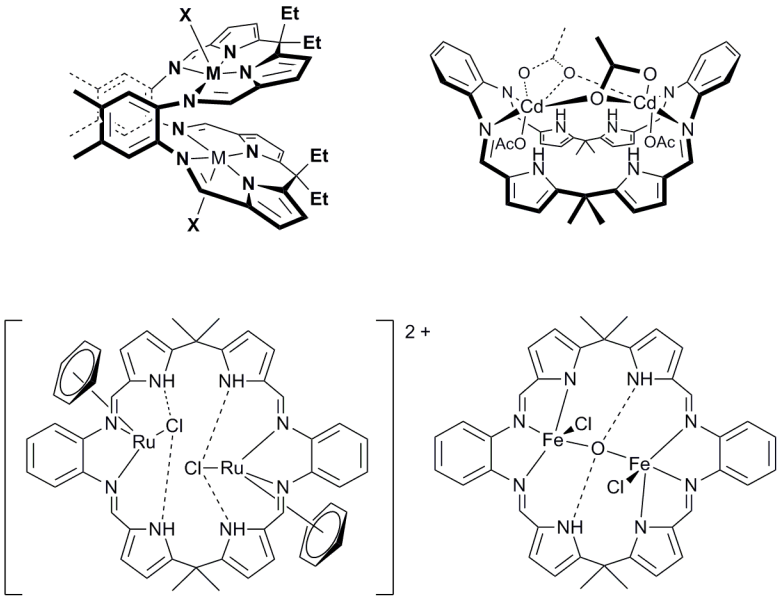


**Figure 2.9 – Examples of alternative binding modes of $H_4L$.**

The usual binding mode observed for bimetallic complexes of $H_4L$ ligands is the wedge-shaped "Pacman" motif, such as the $(MX)_2L^{Et}$ complex shown above. However, the ability of such ligands to adopt alternative binding modes is well documented. One example is the "bowl-shaped" conformation adopted by complexes such as $[\{Cd(OAc)_2\}_2(H_4L)]$ and $[\{RuCl(\eta^6\text{-}C_6H_6)\}_2(H_4L)]^{2+}$.[18] In both of these complexes complete deprotonation of all four pyrrolic NH groups is not achieved, allowing hydrogen bonding interactions between the NH groups and the metal centres to form. The Sessler group have also observed the flexibility of $H_4L$, from the reaction between iron mesityl and the HCl salt of the ligand which resulted in the formation of a complex where the iron atoms are bound to only one pyrrole and two imines to give another bowl-shaped structure.[19]

### 2.2.2 Synthesis of $[UO_2(Opy)(H_2L^{Et})]$

In an attempt to form a terminal uranium(VI) oxo, $[(UO)(L^{Et})]$, $[U(L^{Et})]$ was reacted with pyridine-n-oxide upon which the uranyl complex, $[UO_2(Opy)(H_2L^{Et})]$ was formed preferentially. This was confirmed by the diamagnetic $^1H$ NMR spectrum, which showed resonances corresponding to an asymmetric environment with a broad singlet for the pyrrolic NH hydrogen at 8.54 ppm. The resonances for the imino protons are found at 8.82 and 7.85 ppm with the ethyl $CH_2$ and $CH_3$ groups being inequivalent and slitting into eight resonances.

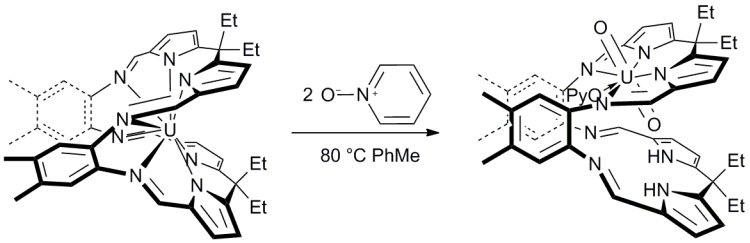


**Equation 2.2**

The reaction to form $[UO_2(Opy)(H_2L^{Et})]$ is an oxidation from uranium(IV) to (VI) with two equivalents of pyridine-n-oxide, one used as an oxidant and the other as a donor ligand. The remaining oxygen and the two hydrogen atoms are postulated to arise from traces of water.

The uranyl complexes of this type are usually synthesised by a transamination reaction between $H_4L$ and $[UO_2(THF)_2\{N(SiMe_3)_2\}_2]$ in THF, giving $[UO_2(THF)(H_2L)]$.[20] The pyridine adduct $[UO_2(py)(H_2L)]$ is also known for the macrocycle.[20] The synthesis of $[UO_2(Opy)(H_2L^{Et})]$ is the first of this ethyl substituted macrocycle. Single crystals of $[UO_2(Opy)(H_2L^{Et})]$ suitable for X-ray diffraction were grown from a toluene solution. The structure is shown in Figure 2.10 and selected bond lengths are given in Table 2.3.

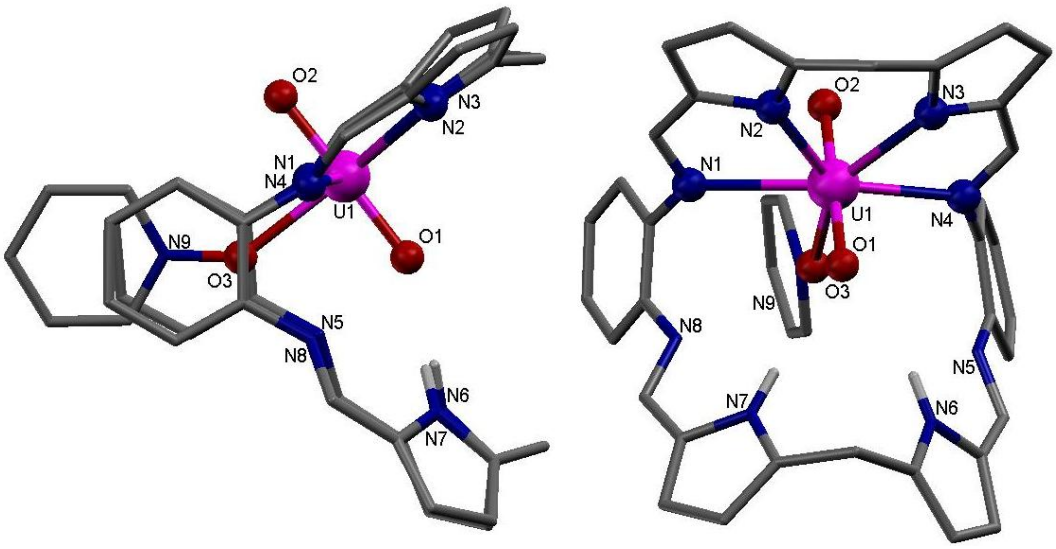


**Figure 2.10 – Ball and stick representations of the X-ray crystal structure of [$UO_2$(Opy)($H_2L^{Et}$)], the aryl backbone methyl groups and the ethyl groups from between the pyrrole groups, hydrogen atoms and solvents of crystallisation have been excluded for clarity.**

The structure shows that one of the binding pockets of the ligand is metal free and the uranium atom has moved into the top binding pocket from the centre of the ligand in [U($L^{Et}$)]. This is accompanied by the protonation of the pyrroles in the bottom pocket and the oxidation of the uranium(IV) to uranyl. The uranyl complex has very similar molecular topology to the previously reported complexes. The pyridine-n-oxide is sandwiched between the two aryl backbone rings. The distance between the aryl backbone rings from the centre of the $\pi$ system to the other is calculated as 6.700 Å. The uranium atom is seven coordinate with pentagonal bipyramidal geometry, with a *trans* uranyl and the four nitrogen atoms from the ligand and a pyridine-n-oxide in the equatorial positions, Figure 2.11. The uranium-oxygen bond lengths are standard for uranyl complexes with U1-O1, 1.803(2) and U1-O2, 1.794(2) Å which are slightly longer than those found in [$UO_2$(THF)($H_2L$)] (1.790(4) and 1.766(4) Å) but are still consistent with the hexavalent oxidation state of the uranium atom. The bond lengths also show slight enlongation of the *endo* oxygen (O1) compared to the *exo* oxygen (O2) (0.009(4)). The U1-O3 bond length for the equatorial pyridine-n-oxide is longer at 2.319(2) Å but is shorter than that of the bound THF in [$UO_2$(THF)($H_2L$)] which has a bond length of 2.442(5) Å and the

uranium-pyridine bond length in the pyridine adduct at 2.554(2) Å.[20] Other U-Opy bond lengths, where the pyridine is substituted in the *para* position, have a range of 2.337–2.377 Å.

| Pyrrole | Imine | U-O |
|---|---|---|
| U1-N2 2.452(3) | U1-N1 2.532(3) | U1-O1 1.803(2) |
| U1-N3 2.452(3) | U1-N4 2.520(3) | U1-O2 1.794(2) |
| | | U1-O3 2.319(2) |

**Table 2.3 – Selected bond lengths in $[UO_2(Opy)(H_2L^{Et})]$ in Å.**

The *endo* oxygen atom shows a hydrogen bonding interaction with the pyrrolic hydrogen atoms on N6 and N7. The O1-N separation is 3.185 and 3.199 Å for O1-N6 and O1-N7 respectively which are slightly longer than the interactions seen previously.[20] In a related system where R=Me and the coordinating solvent is pyridine the O1-N interactions are 3.146 and 3.112 Å and may relate to the lesser steric bulk at the 'mouth' of the Pacman (Me *vs* Et substituents).[20]

The uranyl O-U-O angle in $[UO_2(Opy)(H_2L^{Et})]$ is 179.38(10)° which is closer to linear than in the THF and pyridine adducts which have angles of 177.6(2)° and 176.99(3)° respectively.[20]

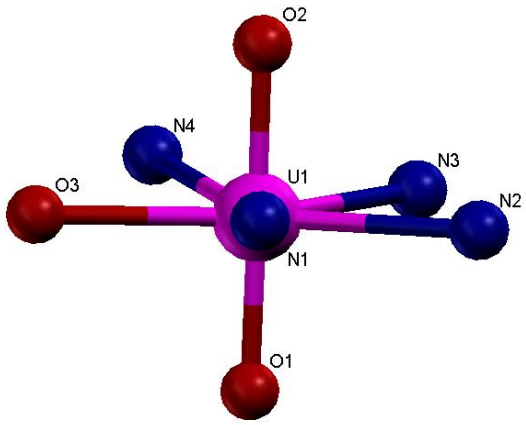


**Figure 2.11 – Geometry about the uranium atom in $[UO_2(Opy)(H_2L^{Et})]$.**

Interestingly whilst the pyridine n-oxide adduct is a very stable complex, reactions to replace the THF molecule in $[UO_2(THF)(H_2L)]$ with 2,2′-bipyridine or benzophenone, were unsuccessful.[20]

## 2.3 Synthesis of Cerium Complexes

### 2.3.1 Synthesis of $[Ce(HL^{Et})]_3$

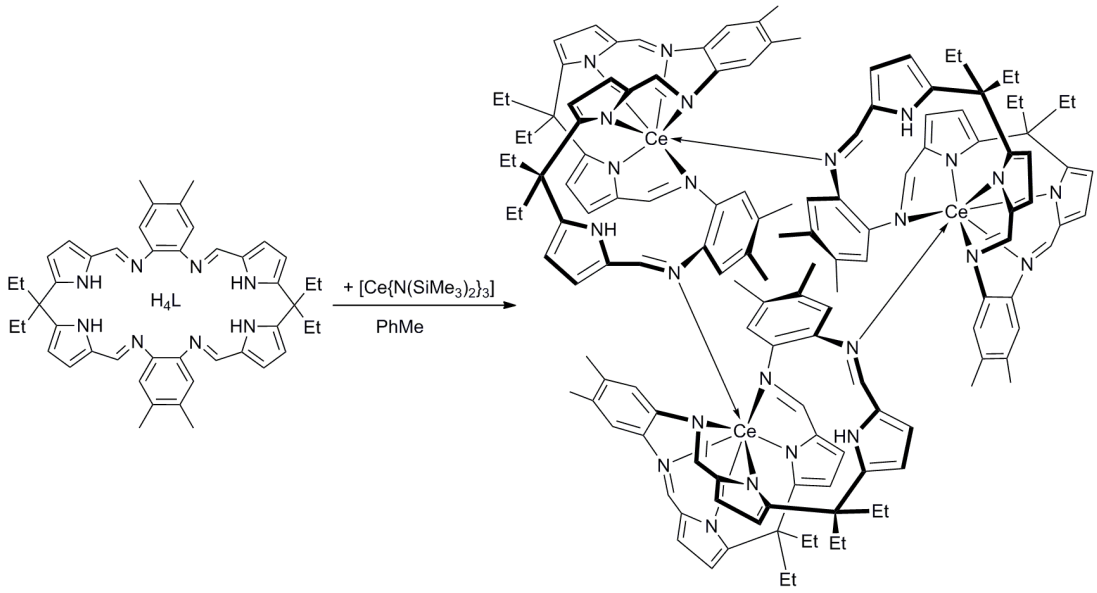


**Equation 2.3**

The reaction between the cerium tris(silylamide), $[Ce\{N(SiMe_3)_2\}_3]$ and the macrocycle, $H_4L^{Et}$ in toluene at room temperature results in the sole formation of $[Ce(HL^{Et})]_3$ that was isolated in high yield as an orange crystalline solid at -30 °C. As the cerium is in the +3 oxidation state not all of the pyrrolic protons have been eliminated in the protonolysis reaction. This leaves one of the pyrrolic protons unbound and free to twist away from the metal, which allows the adjacent imine to bond in an exocyclic manner to the next cerium cation, resulting in a trinuclear 'wheel' supramolecule.

This configuration has been confirmed both in the solid state, by single crystal X-ray studies, and in solution by $^1H$ NMR spectroscopy. Single crystals of $[Ce(HL^{Et})]_3$

were initially grown from a saturated $C_6D_6$ solution at room temperature, and subsequently on a larger scale in toluene at -30 °C.

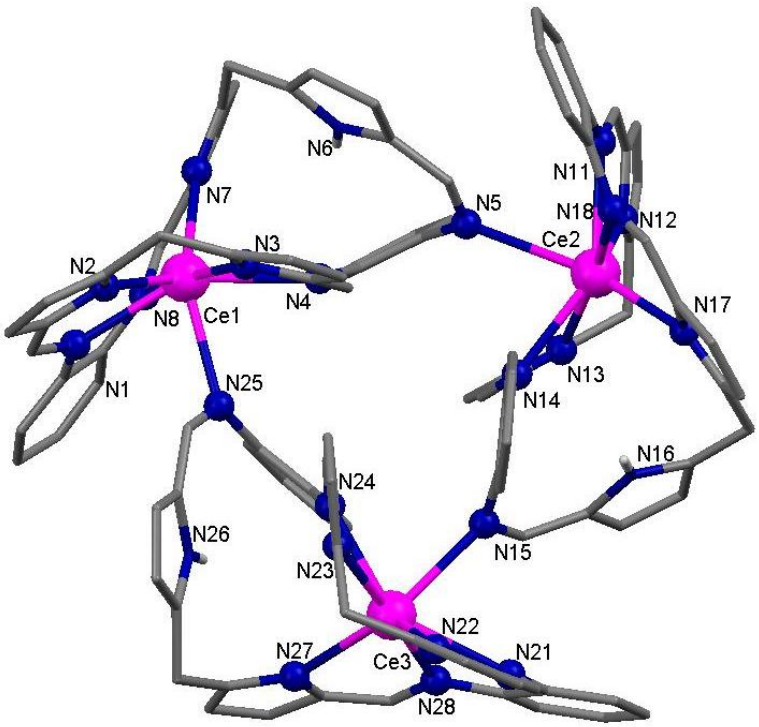


**Figure 2.12 – Ball and stick representations of the X-ray crystal structure of $[Ce(HL^{Et})]_3$ the aryl backbone methyl groups and the ethyl groups from between the pyrrole groups, hydrogen atoms and solvents of crystallisation have been excluded for clarity.**

The X-ray crystal structure shows the formation of a supramolecular wheel comprising three cerium atoms and three ligands. All the cerium cations are seven coordinate with distorted capped octahedral geometries. The structure shows hydrogen bonding between the unbound pyrrolic protons and their adjacent imine (N4-N6 3.017 Å, N14-N16 2.946 Å and N24-N26 3.017 Å), Figure 2.14.

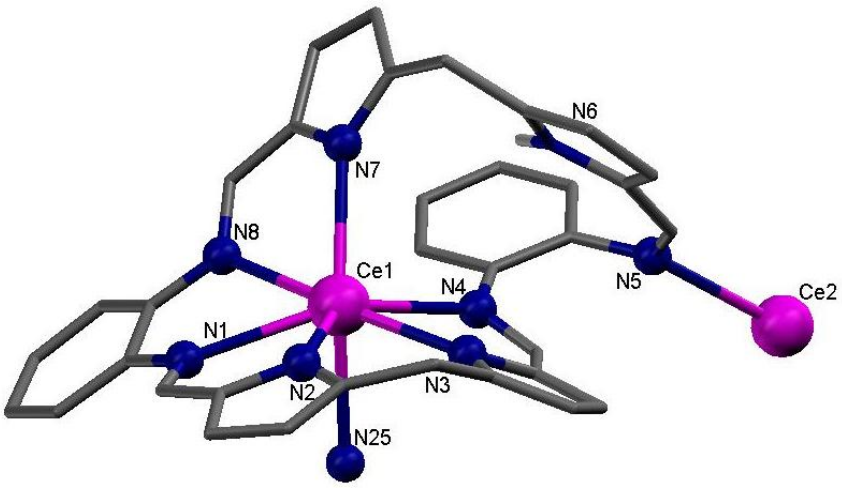


**Figure 2.13 – Coordination surrounding one cerium atom from $[Ce(HL^{Et})]_3$ linking from Ce1-N25 and N5-Ce2.**

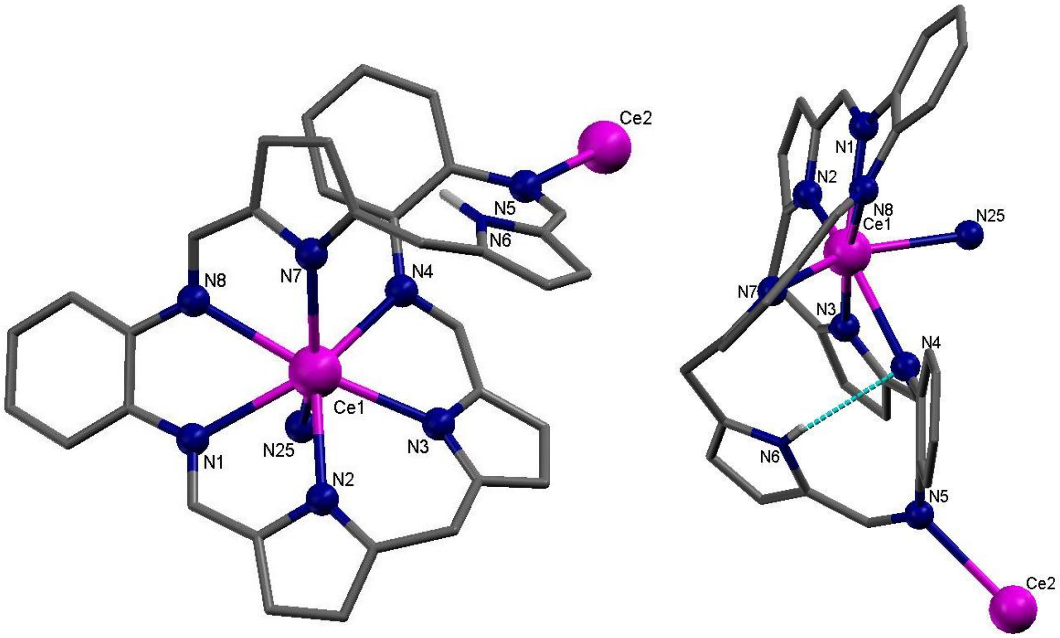


**Figure 2.14 - Coordination surrounding one cerium atom from $[Ce(HL^{Et})]_3$ from different angles, the right picture showing the hydrogen bonding present.**

The bond lengths between cerium and the Schiff-base nitrogen atoms in $[Ce(HL^{Et})]_3$ range from 2.597(4) to 2.664(4) Å and are similar to known complexes which range from 2.484 to 2.800 Å.[21-35] The Ce-N bonds formed by the interconnecting imines in $[Ce(HL^{Et})]_3$ which form the cyclic structure are a little longer than those which do not bridge at 2.658(4), 2.743(4) and 2.708(4) Å implying that the bond is relatively

weak; this can be shown by cleaving these bonds by coordinating solvents such as THF, see later. The cerium-pyrrole bond lengths in $[Ce(HL^{Et})]_3$ range from 2.504(4) to 2.699(4) Å which falls in the centre of known cerium-pyrrole bond lengths in cerium(III) porphyrin complexes (2.450 to 2.771 Å).[36-41]

| **Pyrrole** | **Imine** | **Interconnecting Imines** |
|---|---|---|
| Ce1-N3 2.505(4) | Ce1-N1 2.597(4) | Ce1-N25 2.658(4) |
| Ce1-N2 2.537(4) | Ce1-N8 2.617(4) | Ce2-N5 2.743(4) |
| Ce1-N7 2.641(4) | Ce1-N4 2.664(4) | Ce3-N15 2.708(4) |
| Ce2-N13 2.504(4) | Ce2-N11 2.599(4) | |
| Ce2-N12 2.511(4) | Ce2-N18 2.601(4) | |
| Ce2-N17 2.697(4) | Ce2-N14 2.645(4) | |
| Ce3-N23 2.510(4) | Ce3-N28 2.613(4) | |
| Ce3-N22 2.557(4) | Ce3-N24 2.616(4) | |
| Ce3-N27 2.699(4) | Ce3-N21 2.621(4) | |

**Table 2.4 – Selected $[Ce(HL^{Et})]_3$ bond distances in Å.**

The angles formed between the aromatic backbone rings in $[Ce(HL)]_3$ for each ligand are 29.42 °, 33.19 ° and 28.30 °. The angle formed between the planes of the pyrrolic nitrogen atoms is known as the bite angle and has a value of 67.55 °.

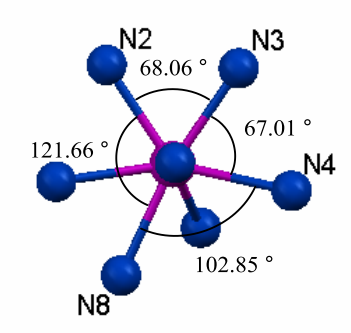


**Figure 2.15 –View down the Ce1–N25 axis showing the four nitrogen atoms in the equatorial plane.**

The equatorial plane contains the pyrrolic nitrogen atoms that are in the tetra coordinated half of the ligand (N2, N3), along with an imine from the doubly coordinated part of the ligand (N4) and one from the tetra coordinated half (N8). The axial ligands are a pyrrolic nitrogen in the doubly coordinated half of the ligand (N7) and an imine from the neighbouring ligand (N25). The remaining coordinating nitrogen is the other imine donor from the tetra coordinated half of the ligand (N1).

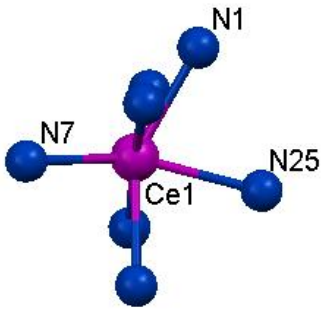


**Figure 2.16 – View along the Ce1 N2 N3 N4 N8 plane. Angle between < N7-Ce1-N25 146.17 °, < N7-Ce1-N1 111.51 ° and < N1-Ce1-N25 75. 55 °.**

The angles between Ce atoms are 60.68 °, 59.57 ° and 59.75 ° forming an equilateral triangle. This gives rise to an average Ce···Ce separation of 8.1 Å.

Elemental analysis supports the proposed formulation. The IR spectrum showed the NH stretch was present at 3408 $cm^{-1}$ compared to 3444 $cm^{-1}$ in the free ligand $H_4L^{Et}$ and also two stretches are found at 1603 and 1572 $cm^{-1}$, which correspond to unbound and metal-bound C=N stretches respectively.

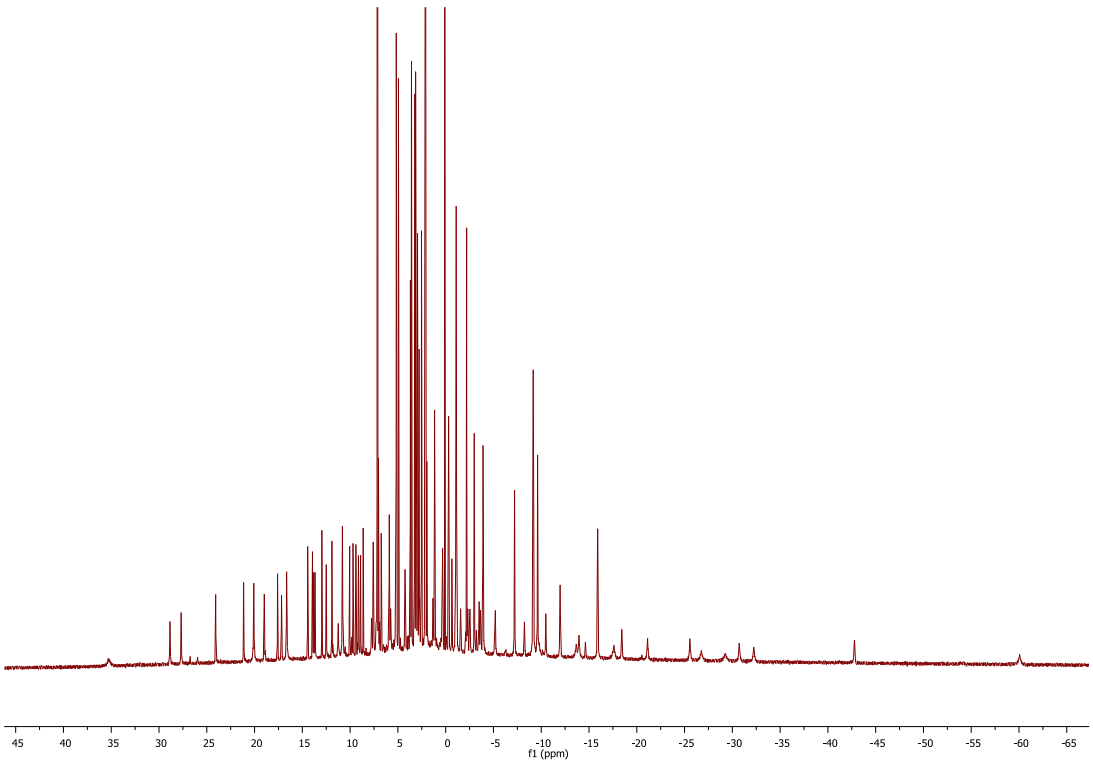


**Figure 2.17 - $^{1}$H NMR spectra of crystalline $[Ce(HL)]_3$ dissolved in $C_6D_6$.**

The $^{1}$H NMR spectrum of $[Ce(HL^{Et})]_3$ in $C_6D_6$, Figure 2.17, shows that the solid state structure is retained in solution. Three inequivalent ligand environments are observed, providing a total of 87 resonances. The resonances are spread from -40 to 40 ppm due to the effect of the paramagnetic cerium(III) centre, meaning that assignment of each resonance is extremely complex. Attempts of obtain further characterising NMR spectra e.g. 2D COSY and $^{13}$C NMR, were unsuccessful due to poor solubility and the paramagnetic nature of Ce(III).

Under both anaerobic and aerobic conditions, cerium(III) complexes of Schiff base ligands have been previously studied.

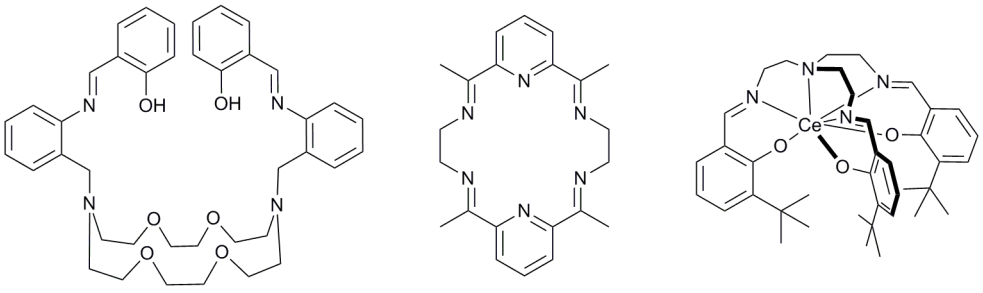


**Figure 2.18 – *N,N′*-bis(2-salicylaldiminobenzyl)-1,10-diaza-15-crown-5, tetramethylhexazatricyclotetracosadecaene, and the cerium complex of tris[4-(2-hydroxy-3-*tert*-butylphenol)-3-aza-3-butenyl]amine.**

*N,N′*-bis(2-salicylaldiminobenzyl)-1,10-diaza-15-crown-5 forms a cerium(III) complex in which the dianionic ligand has encapsulated the cerium cation resulting in a cryptand like structure, with a $ClO_4^-$ counter anion.[34] The metal is nine coordinate with the ligand forming $\pi$-$\pi$ interactions between the benzyl and the phenyl rings. The macrocyclic hexamine ligand, centre Figure 2.18, forms a complex with $Ce(NO_3)_3$ where the cerium cation is eleven coordinate, with coordination to the six ligand nitrogen atoms, two bidentate nitrates and a water molecule.[42] When bound to the cerium atom the ligand folds at the C-C bond (the carbon atoms between the imine nitrogen atoms) to a 59 ° angle. The cerium(III) complex of the tripodal ligand, tris[4-(2-hydroxy-3-*tert*-butylphenol)-3-aza-3-butenyl]amine, shows the full encapsulation of the metal centre.[43] The ligand exhibits a heptadentate binding site, with three imino groups, three phenolic hydroxyl groups and an apical nitrogen atom, to give pseudo-$C_3$ symmetry.

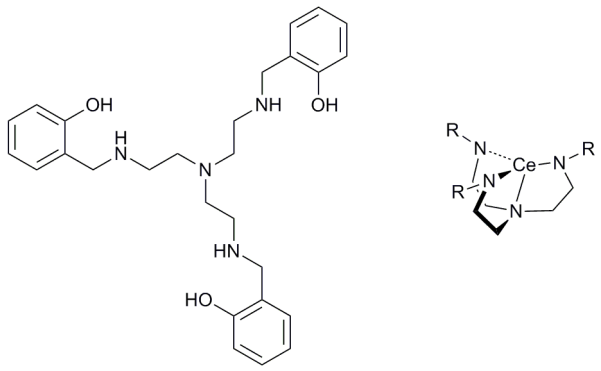


**Figure 2.19 – $H_6$TrenSal and [CeNN′$_3$].**

The reaction of [($H_6$TrenSal)Zn][$NO_3$] with cerium nitrate hexahydrate resulted in the formation of the complex [{($H_6$TrenSal)Ce}$_2$-$\mu^2$-$O_2$].[44] The oxidation states of the cerium atoms are postulated to be cerium(III) and (IV) with a bridging superoxo ligand. The triamidoamine ligand, [N($CH_2CH_2NSiMe_2t$-Bu)$_3$]$^{3-}$, (NN′$_3$), previously used to stabilise uranium, was also shown to bind to cerium(III) to give [CeNN′$_3$] which rapidly decomposes in air, Figure 2.19. This complex has shown to react with halides to give the resulting mixed valence bridging halide for bromine and chlorine and a terminal cerium(IV) complex for iodine.[45]

There are many examples of cerium porphyrin complexes. The majority of these are cerium(IV) with cerium(III) complexes mainly found as triple-decker molecules, Figure 2.20.

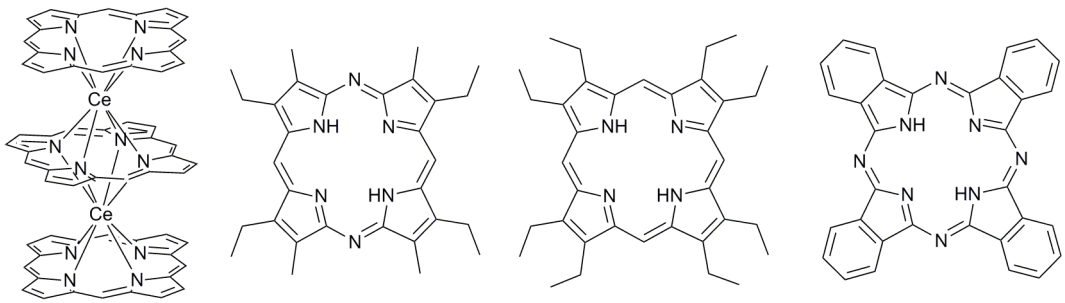


**Figure 2.20 – Structures of DAP, OEP and Pc.**

The ligands DAP, 2,8,12,18-tetraethyl-3,7,13,17-tetramethyl-5,15-diazaporphyrinate, OEP, octaethylporphyrin, Pc, phthalocyaninate and TPP, 5,10,15,20-tetraphenylporphyrin, have all been used to form these triple-decker complexes. In

the complex $[Ce_2(OEP)_3]$, the cerium atoms do not lie equidistant from the porphyrin ligands, with the cerium atoms lying closer to the external macrocycles with a distance of 1.394 Å compared to 1.876 Å for the internal porphyrin.[46] Mixed-ligand triple-decker complexes have also been synthesised with [(DAP)Ce(DAP)Ce(Pc)], [(TPP)Ce{$Pc(OMe)_8$}Ce(TPP)] and mixed-metal triple-decker complexes have also isolated, with the synthesis of the complex [(TPP)Ce(Pc)Gd(OEP)].[37, 38, 41] Again the metal atoms lie closer to the external macrocycle than the internal one.

Examples of exocyclic ligand bonding to more than one metal centre resulting in cyclic complexes is rare, with only the formation of silver supramolecular complexes to compare with $[Ce(HL)]_3$, Figure 2.21.[47-49]

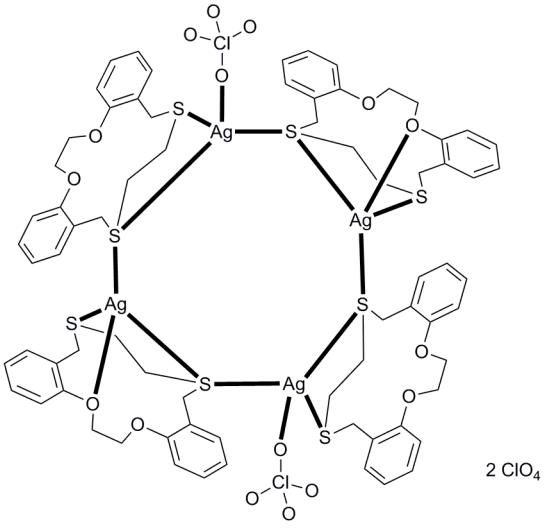


**Figure 2.21 – $[Ag(\kappa^2{:}\mu\text{-}S_2O_2)(ClO_4)_2][ClO_4]_2$.**

The reaction of AgX with $S_2O_2$, $S_3O_2$ or $S_2O$ macrocycles, where X is $PF_6$ or $ClO_4$ results in many supramolecular complexes including those with a cyclic structure.

There few examples of supramolecular chemistry with lanthanides all employ multiple ligands to enable the supramolecular structure to develop.[50] $[Ce(HL^{Et})]_3$ is a unique complex in that it has a ligand to metal ratio of only 1 to 1, and contains no other metals.

The cerium supramolecular structure with 1,3-benzeneditetrazol-5-yl, *m*-$BDTH_2$, is a three dimensional framework with a water cluster in the lattice, Figure 2.22.[51]

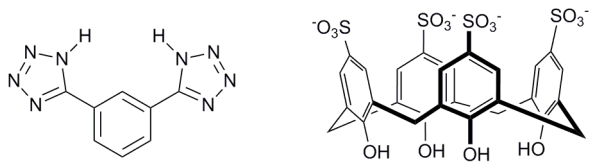

**Figure 2.22 – 1,3-benzeneditetrazol-5-yl and *p*-sulfonatocalix[4]arene.**

The cerium(III) cation is bound to eight water molecules and one nitrogen from a singly deprotonated *m*-$BDTH_2$ ligand with another *m*-$BDTH_2$ ligand doubly deprotonated but uncoordinated. The extended structure is formed by hydrogen bonding.

A two dimensional structure containing *p*-sulfonatocalix[4]arene and pentaaqua cerium(III) has been isolated.[52] The cerium atom is nine coordinate, binding to four oxygen atoms from four different calixarenes and the rest of the coordination sphere completed by water molecules. When the reaction is carried out in the presence of 18-crown-6 a new 'Ferris-wheel – molecular capsule' type structure is isolated, Figure 2.23

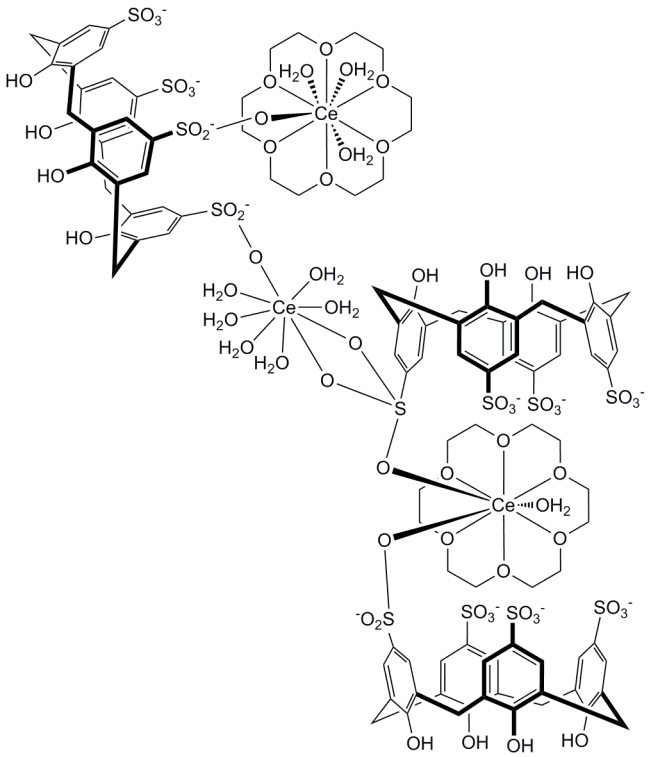

**Figure 2.23 – 'Ferris-wheel – molecular capsule' structure.**

The isolated product, [Ce($HL^{Et}$)] does not follow the trend exhibited by binuclear, trivalent transition metal complexes formed by the Love group.[18] When these metals are combined with the macrocyclic ligand, one metal is bound in each of the binding pockets, with the general formula [($M^{III}X)_2$(L)], where X is an anion. From the reaction to synthesise [$(VCl)_2$(L)], the complex [(VO)(VCl)(L)] was isolated after partial oxidation, Figure 2.24. This mixed V(III)/V(IV) complex, contains the vanadyl group *endo*, whilst the chloride is *exo*. The vanadium atoms have a distorted octahedral geometry with the vanadyl oxygen acting as a Lewis base towards the V(III) centre.

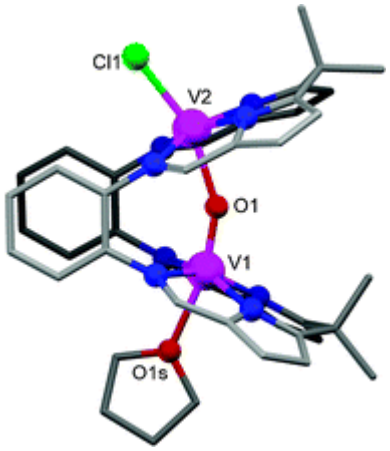


**Figure 2.24 – Structure of [(VO)(VCl)(L)].**

Other examples of metals in the +3 oxidation state within the macrocycle are cobalt and manganese. The dicolbalt(III) complex as discussed in Chapter 1, has a peroxide bridging the cobalt atoms, with the macrocycle being laterally twisted to bind the dioxygen molecule, Figure 2.25.[53]

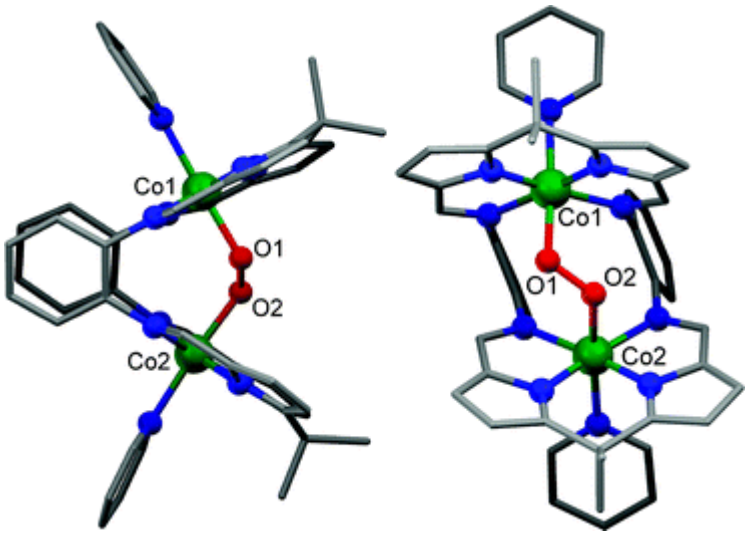


**Figure 2.25 - Structure of $[(Co)_2(\mu\text{-}O_2)(L)]$.**

During the synthesis of $[(Mn)_2(L)]$, adventitious oxygen incorporation resulted in the crystallisation of $[(Mn)_2(\mu\text{-}OH)(L)]$, Figure 2.26. This mixed-valence Mn(III)/Mn(II) complex contains a bridging hydroxo ligand, which is closer to Mn1 than Mn2, by 0.025 Å.[18]

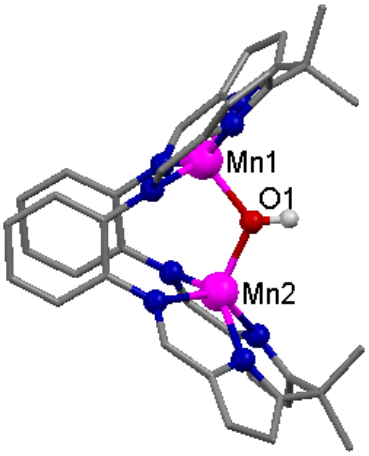


**Figure 2.26 – Structure of $[(Mn)_2(\mu\text{-}OH)(L)]$.**

This trend however does not seem to be exhibited with the larger elements of the Periodic Table. The cerium ion is large enough to be coordinated by both binding pockets, with the flexibility of the macrocyclic ligand allowing this new binding mode.

### 2.3.2 Synthesis of $[Ce(THF)_2(HL^{Et})]$

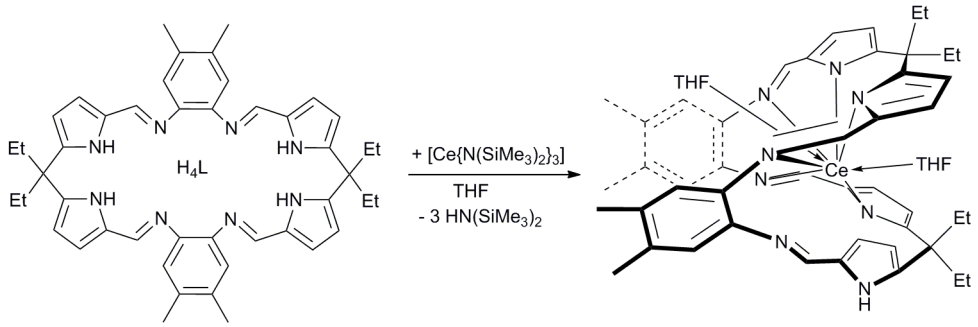


**Equation 2.4**

The transamination reaction between cerium tris(silylamide) and the macrocycle in THF at room temperature results in the sole formation of $[Ce(THF)_2(HL^{Et})]$ as a yellow crystalline solid in high yield. An alternative synthesis of $[Ce(THF)_2(HL^{Et})]$ is from the addition of THF to $[Ce(HL)]_3$, thus breaking the exocyclic bonding to give the mononuclear complex.

The THF adduct has a simpler $^1H$ NMR spectrum than that of $[Ce(HL)]_3$, with only 32 resonances present, although the resonances still range over 70 ppm, Figure 2.27. The number of resonances is consistent with a mononuclear THF adduct, and crude assignments based on the integrals were made. COSY experiments were unsuccessful due to the paramagnetic nature of the complex and the strong resonances of THF swamped the spectrum.

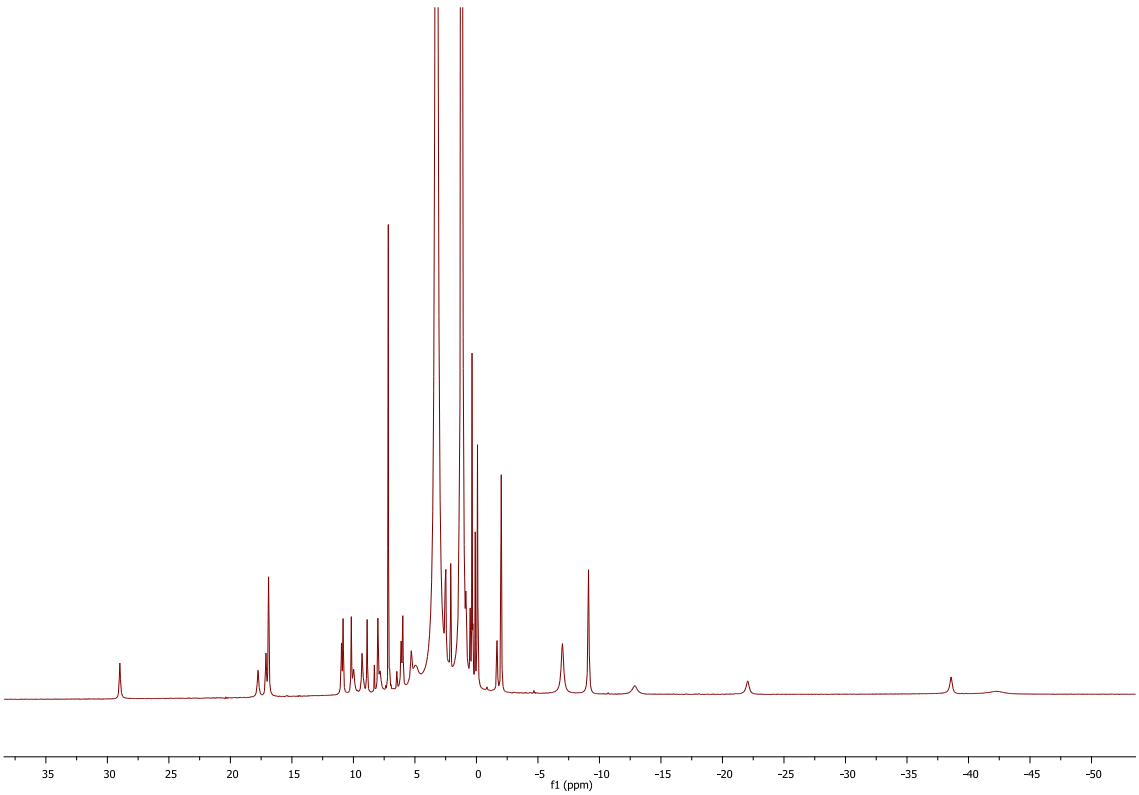


**Figure 2.27 - $^{1}$H NMR spectrum of [Ce(THF)$_2$(HL$^{Et}$)] in THF with a $C_6D_6$ capillary with solvent suppression.**

Crystals of [Ce(THF)$_2$(HL$^{Et}$)] suitable for X-ray crystallography were grown from a saturated THF solution. The solid state structure is shown in Figure 2.28, with selected bond lengths in Table 2.5.

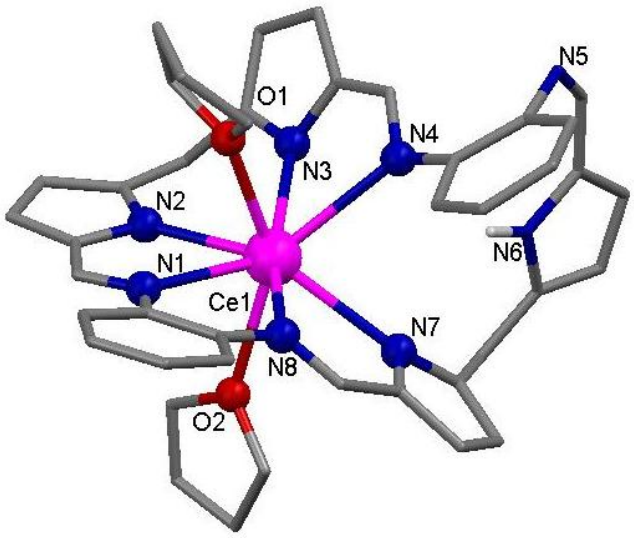


**Figure 2.28 – Ball and stick representations of the X-ray crystal structure of [Ce(THF)$_2$(HL$^{Et}$)], the aryl backbone methyl groups and the ethyl groups from between the pyrrole groups , hydrogen atoms and solvents of crystallisation have been excluded for clarity.**

In [Ce(THF)$_2$(HL$^{Et}$)], the cerium is 8-coordinate with a distorted square-antiprismatic geometry and lies in the centre of the two binding pockets of the macrocycle, Figure 2.29.

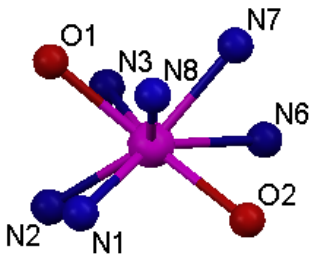


**Figure 2.29 – Cerium coordination in [Ce(THF)$_2$(HL$^{Et}$)].**

The macrocycle does not adopt the normal Pacman binding mode, with the unbound pyrrole N5 and imine N4 quadrant twisted away from the metal centre. The pyrrolic proton does not show any hydrogen bonding to any other part of the molecule. The adjacent imine donor N4 is now available for further supramolecular bonding as it has no interaction with the cerium ion and no short contacts in the crystal packing.

| Pyrrole | Imine | Bound THFs |
|---|---|---|
| Ce1-N2 2.5511(17) | Ce1-N1 2.6386(18) | Ce1-O1 2.5451(16) |
| Ce1-N3 2.5624(18) | Ce1-N8 2.5778(18) | Ce1-O2 2.6141(15) |
| Ce1-N7 2.6781(18) | Ce1-N4 2.7797(17) | |

**Table 2.5 – $[Ce(THF)_2(HL)]$ bond distances in Å.**

The cerium–pyrrole nitrogen bond lengths average to 2.5972(18) Å, which falls in the range for other known cerium(III) pyrrolic type complexes (2.450 to 2.771 Å).[36-41] The bond lengths between cerium and the Schiff-base imine nitrogen average to 2.6654(18) Å within the range of cerium(III)-Schiff base bond lengths already published (2.484-2.800 Å).[21-35] The bond lengths in $[Ce(THF)_2(HL^{Et})]$ are within the values reported for cerium in the +3 oxidation state for imine binding.

The two arene rings, 'hinges', are usually coplanar when metals are bound to form the Pacman structure, but due to the twisting of the macrocycle this is not the case in $[Ce(THF)_2(HL^{Et})]$.

The difference in the binding and the conformation of the THF adduct in comparison to the solvent free trinuclear complex is not seen in the IR spectrum where the stretching mode for N-H bond is 3408 $cm^{-1}$. As in $[Ce(HL^{Et})]_3$, there are two C=N stretching modes for the imine nitrogen atom bound to the Ce centre and unbound one, at 1598 and 1573 $cm^{-1}$ respectively.

### 2.3.3 Synthesis of [Ce($L^{Et}$)]

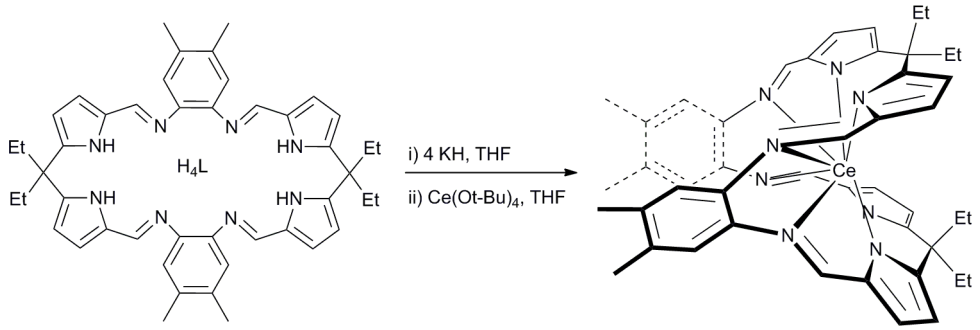


**Equation 2.5**

Cerium is the only lanthanide with a readily accessible +4 oxidation state in solution chemistry. As such, attempts to oxidise [$Ce(THF)_2(HL^{Et})$] were undertaken to form a Ce(IV) complex. A variety of reagents were tried including $I_2$, 1,4-benzoquinone, $AgBF_4$, AgCN, $TeCl_4$, $XeF_2$, $HgI_2$, but none gave isolable products. It was rationalised that since [$Ce(THF)_2(HL^{Et})$] was not able to be oxidised then [$Ce(L^{Et})$] could be synthesised from a cerium(IV) precursor.

The *in situ* synthesis of $K_4L^{Et}$, was followed by a salt elimination reaction with $Ce(O\textit{t}\text{-}Bu)_4$. After 12 hours, the by-product KO-*t*-Bu was washed away with hexane and solid [$Ce(L^{Et})$] isolated in high yield.

The $^1$H NMR resonances of [$Ce(L^{Et})$] are diamagnetic as expected for a cerium(IV) complex. The NMR spectrum also allowed the postulation that the structure is similar to that of [$U(L^{Et})$]. The pyrrolic protons resonances are found in two environments at 6.65 and 6.21 ppm, whereas the ethyl groups have been split into 4 different environments; 1.45, 1.33, 0.99 and 0.94 ppm which is characteristic of a Pacman geometry in solution. The elemental analysis supports the proposed formula of [$Ce(L^{Et})$], and does not appear to show any coordinated solvent, which is consistent with the $^1$H NMR data. The IR spectrum is also consistent with the binding of cerium(IV) in the macrocycle, with the absence of an N-H stretch and an imine stretch was present at 1590 $cm^{-1}$ (c.f. 1560 $cm^{-1}$ in [$U(L^{Et})$]). Reduction of this complex was not studied.

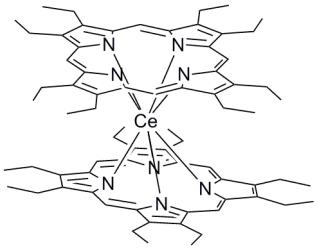


**Figure 2.30 – [Ce(OEP)$_2$].**

The cerium(IV) porphyrinate [Ce(OEP)$_2$], is one of a series of sandwich porphyrin complexes which contain cerium(IV). The [Ce(OEP)$_2$] is surrounded by eight nitrogen atoms in a distorted square antiprismatic geometry. The mean Ce-N bond distance is 2.475(1) Å, which reflects the higher oxidation state and therefore shorter bond distance compared to those in the cerium(III) triple decker complexes.

The cerium(III) and (IV) complexes of the macrocyclic ligand 6,8,15,17-tetramethyldibenzotetraaza[14]annulene have been synthesised.[54] The complex [Ce(tmtaa)(tmtaaH)] was synthesised from the reaction of [Ce{N(SiMe$_3$)$_2$}$_3$] and 3.14 equivalents of tmtaaH$_2$ at room temperature. Although crystals were grown from a toluene solution the crystals were twinned and the disorder could not be resolved. When heated [Ce(tmtaa)(tmtaaH)] forms the complex [Ce(tmtaa)$_2$] which has been structurally characterised by single crystal X-ray diffraction; however magnetic susceptibility studies show that this complex is not diamagnetic as expected but instead shows temperature-independent paramagnetism at 5K.

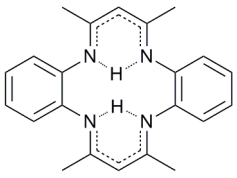


**Figure 2.31 – Structure of H$_2$tmtaa.**

### 2.3.4 Synthesis of [{Ce($L^{Et}$)}$_2$Zn]

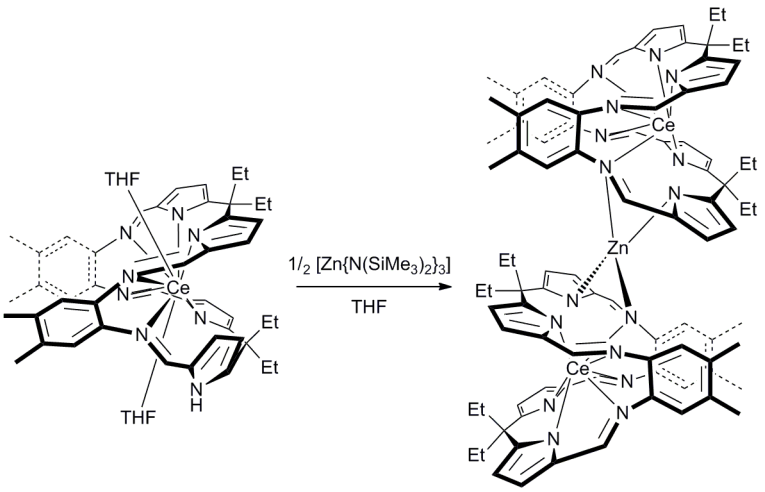


**Equation 2.6**

The reactivity of the THF-adduct, [Ce(THF)$_2$($HL^{Et}$)] with metal amides was studied, as it was thought that the remaining unbound pyrrole in [Ce(THF)$_2$($HL^{Et}$)] could go on to bind to another metal centre, so forming a supramolecular structure.

Zinc bis(silylamide) as a diamagnetic metal was attempted first. The reaction appears to have produced the complex [{Ce($L^{Et}$)}$_2$Zn], where two cerium macrocycles are joined via the pyrroles to a bridging zinc atom.

The elemental analysis implies that there is no coordinating solvent attached to either the cerium or the zinc atoms and supports the formula [{Ce($L^{Et}$)}$_2$Zn]. This could also imply that the coordination of a zinc atom has changed the coordination sphere of the cerium therefore no longer having space for coordinating solvent.

The IR spectrum shows a lack of an N-H absorption indicative of the ligand binding to the zinc atom. The imine absorption shows little change from the starting material with C=N stretches at 1598 and 1574 cm$^{-1}$.

The $^1$H NMR spectrum shows changes in the spectrum of [{Ce($L^{Et}$)}$_2$Zn] compared to that of [Ce(THF)$_2$($HL^{Et}$)] although there is not a clear disappearance of the NH resonance, Figure 2.32.

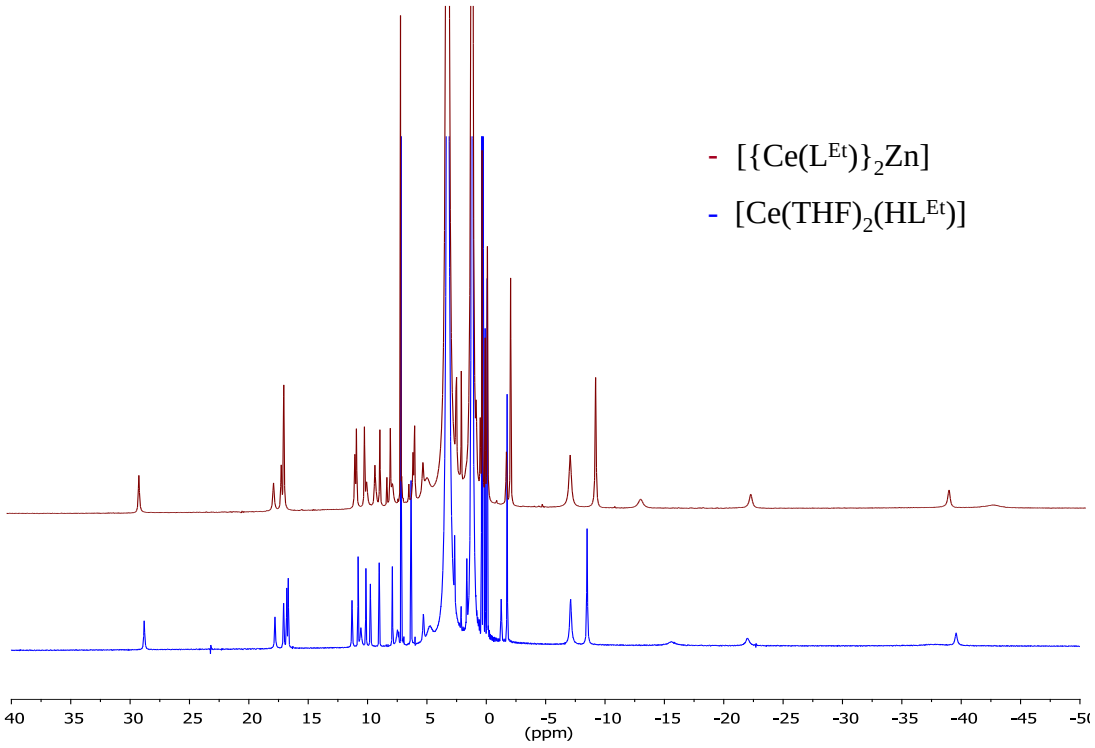


**Figure 2.32 – $^{1}$H NMR comparison of [{Ce(L$^{Et}$)}$_2$Zn] and [{Ce(THF)$_2$(HL$^{Et}$)].**

For further clarification by $^{1}$H NMR spectroscopy, the reaction could be repeated with a paramagnetic +2 metal centre so that the protons around the metal centre could be easily identified due to their paramagnetic shift.

Examples of cerium-zinc bimetallic complexes in the literature are scarce, with only seven in the Cambridge Crystallography Data Centre. Four of these are bridged by a carboxylate, and one is an anion-cation pair. The remaining two are shown in Figure 2.33.

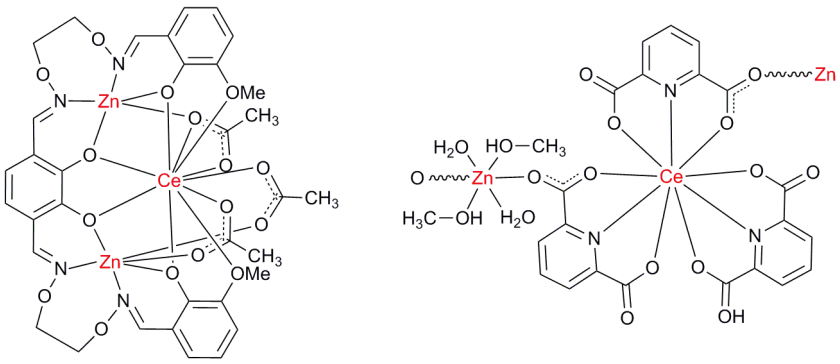


**Figure 2.33 – Examples of Ce-Zn systems.**

The bis(zinc)-cerium complex, $[Zn_2Ce(L)]$, involves a bis $N_2O_2$ binding site in which the zinc cations bind and then a guest recognition site where the cerium is located.[55] The cerium cation is nine coordinate with acetate molecules completing the coordination sphere. The metallohost-guest complex has a helical structure.

A chain polymeric structure of alternating cerium(IV) and zinc(II) can be isolated using dipicolinic acid as a ligand.[56] The metal centres are joined through the carboxylic acid group on the dipicolinic acid resulting in a polymeric chain.

## 2.4 Synthesis of Yttrium Complexes

### 2.4.1 Synthesis of $[Y(HL^{Et})]_3$

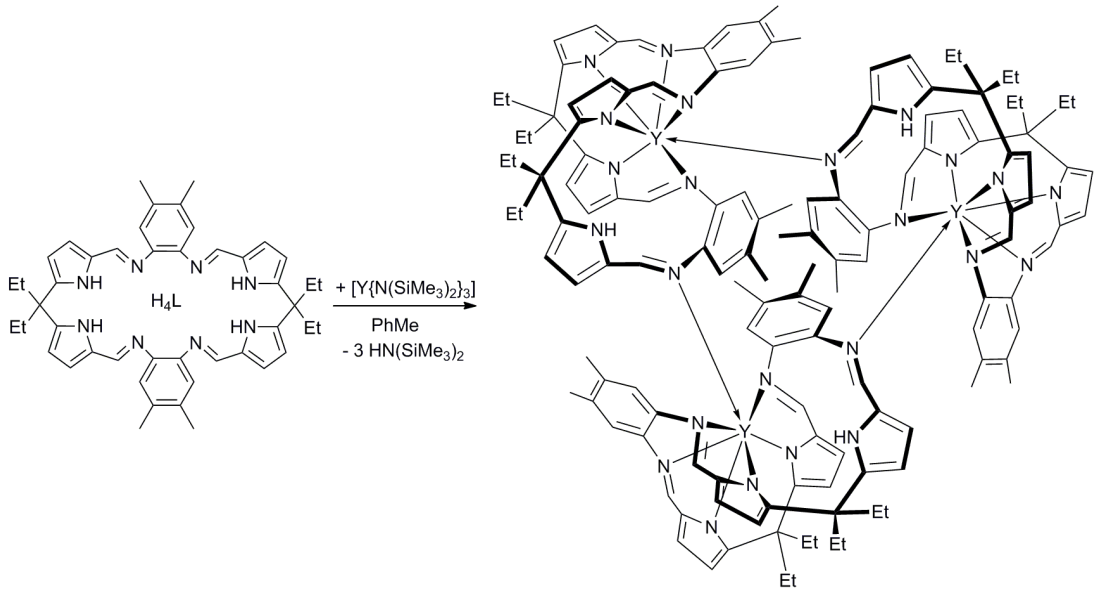


**Equation 2.7**

The protonolysis reaction between the yttrium amide, $[Y\{N(SiMe_3)_2\}_3]$ and $H_4L^{Et}$ in toluene at room temperature results in the sole formation of the trinuclear complex $[Y(HL^{Et})]_3$. The complex has been characterised by $^1H$ NMR, IR spectroscopy and by elemental analysis. Although diamagnetic, the $^1H$ NMR spectrum of $[Y(HL^{Et})]_3$ is difficult to assign due to the asymmetry of the complex which results in all the ligand environments being inequivalent. This generates 87 resonances over the range of 0–9.6 ppm, many of which overlap.

The infrared spectrum of $[Y(HL^{Et})]_3$ supports a remaining pyrrolic nitrogen hydrogen bond with stretches at 3442, 3408 and 3343 $cm^{-1}$ and has a similar wavenumber to the cerium analogue 3408 $cm^{-1}$ in cerium. The C=N stretches in the infrared spectrum are also similar to those seen in $[Ce(HL^{Et})]_3$ (1608, 1591 and 1575 $cm^{-1}$ in yttrium and 1602 and 1572 $cm^{-1}$ in cerium). The elemental analysis supports the ratio of 1:1 metal to ligand, although single crystal X-ray crystallography has yet to confirm the trimeric structure. The complex $[Y(HL^{Et})]_3$ is very sensitive to both air and moisture and decomposes rapidly. This might be an indication of the strained ligand

conformation to bind to the small yttrium centre. There was no observed reaction with $H_2$ gas even at elevated temperature.

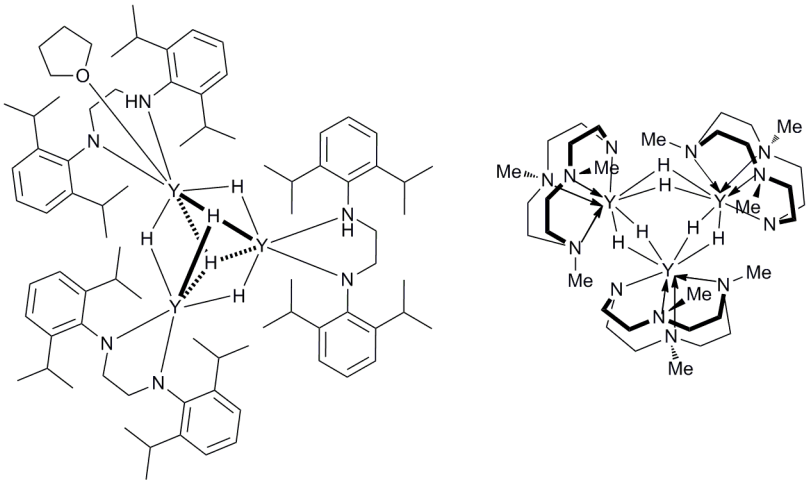

**Figure 2.34 –Examples of yttrium wheel structures.**

The formation of for example, yttrium hydride clusters supported by auxiliary ligands is not uncommon. From a reaction of molecular hydrogen and $[Y\{ArN(CH_2)_2NAr\}\{CH(SiMe_3)_2\}(THF)]$, the complex $[Y_3\{ArNH(CH_2)_2NAr\}_2\{ArN(CH_2)_2NAr\}(\mu\text{-}H)_3(\mu_3\text{-}H)_2(THF)]$ was isolated.[57] Another example is a cyclen-derived macrocycle which supports an yttrium hydrides cluster.[58] The latter reaction results in only one isomer isolated, and the trinuclear framework remains intact in solution.

Monoporphyrin complexes are the most common porphyrin complexes of yttrium that have been synthesised although bis- and double-decker porphyrin complexes have also been isolated.

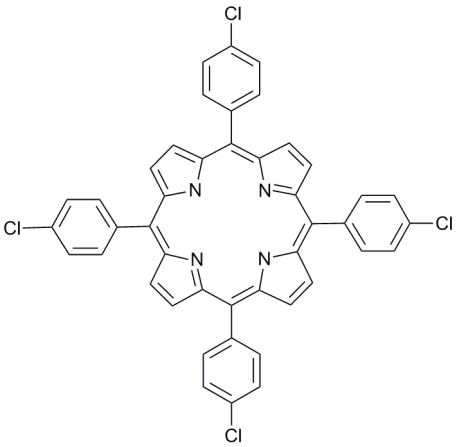

**Figure 2.35 – $TClPP^{2-}$.**

The double-decker complex, $[Y_2(Pc)(TClPP)_2]$,where Pc is phthalocyaninato, has the TClPP on the outside and the Pc ligand in the centre of the sandwich complex, Figure 2.35.[59] Each yttrium centre is octadentate to four nitrogen atoms of the pyrrole rings of the outer TClPP ligand and four nitrogen atoms of the isoindole rings of the Pc ligand, although the yttrium atom lies closer to the TClPP ligand.

### 2.4.2 Synthesis of $[Y(THF)_2(HL)]$

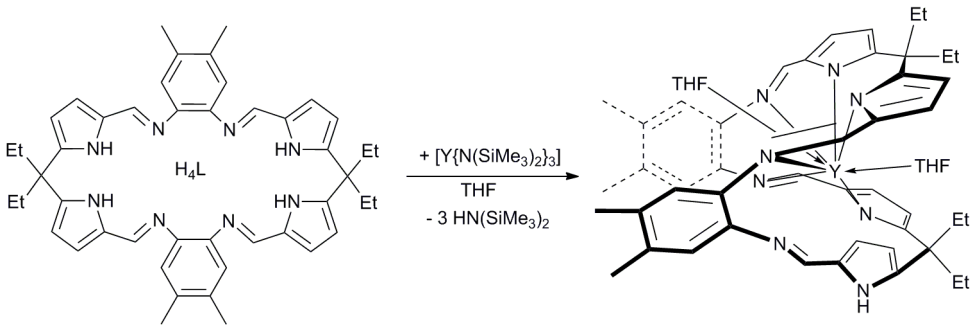


**Equation 2.8**

The transamination reaction between yttrium tris(silylamide), $[Y\{N(SiMe_3)_2\}_3]$ and $H_4L^{Et}$ in THF at room temperature results in the sole formation of $[Y(THF)_2(HL^{Et})]$, as a crystalline yellow solid, in high yield. This adduct can also be synthesised by the addition of THF to $[Y(HL^{Et})]_3$.

The adduct has a simpler $^{1}$H NMR spectrum than that of the trinuclear complex $[Y(HL^{Et})]_3$ as the trinuclear species has been broken up by the coordinating THF. The $^{1}$H NMR spectrum of the adduct complex is still complex however, with 32 resonances present over a narrow chemical shift range (0-9 ppm) but these are consistent with the asymmetric mononuclear complex with two bound THF molecules; assignments were difficult due to the large suppressed resonances of THF. The $[Y(THF)_2(HL^{Et})]$ complex has also been analysed by elemental analysis and supports the presence of two THF molecules.

The IR spectrum of $[Y(THF)_2(HL^{Et})]$ is consistent with one unbound pyrrole with an N-H stretch at 3439 $cm^{-1}$ and with the C=N stretches at 1613 and 1574 $cm^{-1}$ relating to free and metal-coordinated imines, respectively.

Crystals of $[Y(THF)_2(HL^{Et})]$ suitable for X-ray crystallography were grown from a saturated THF solution. The solid state structure is shown in Figure 2.36, with selected bond lengths in Table 2.6.

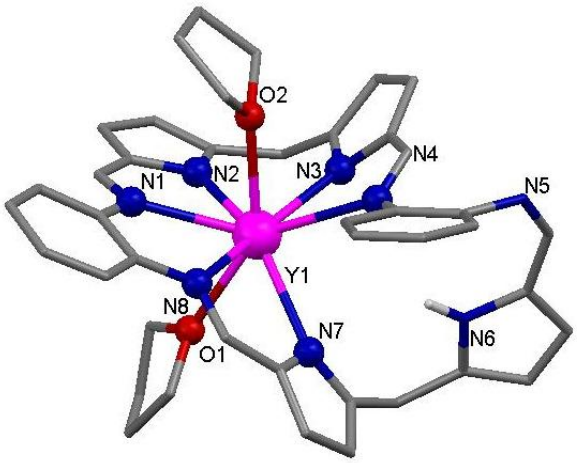


**Figure 2.36 – Ball and stick representations of the X-ray crystal structure of $[Y(THF)_2(HL^{Et})]$, the aryl backbone methyl groups and the ethyl groups from between the pyrrole groups, hydrogen atoms and solvents of crystallisation have been excluded for clarity.**

The yttrium centre is eight coordinate with a distorted square-antiprismatic geometry, Figure 2.37 and is isostructural to the cerium complex $[Ce(THF)_2(HL^{Et})]$.

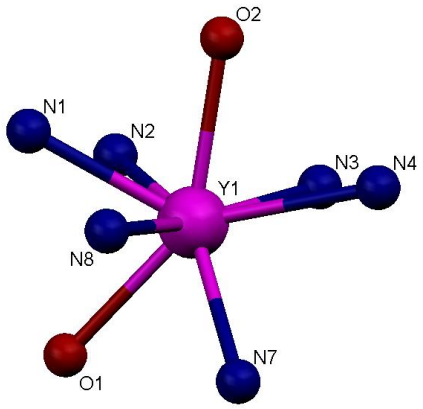


**Figure 2.37 – Coordination around the yttrium centre.**

The yttrium-pyrrole bond lengths in $[Y(THF)_2(HL^{Et})]$ average to 2.598(6) Å which are quite long by comparison to other yttrium-pyrrole nitrogen bond lengths in the literature which range from 2.269-2.469 Å with a mean average of 2.361(5) Å.[60-63] The Y-N imine bond length in the complex averages to 2.661 Å which lies at the longer end of the literature range (2.267-2.813 Å). The Y-O(THF) molecule bond lengths average to 3.591 Å and lie in the centre of the range quoted in the literature (range 2.214-2.733 Å).

| Pyrrole | Imine | Bound THFs |
|---|---|---|
| Y1-N2 2.542(6) | Y1-N1 2.612(7) | Y1-O1 2.586(5) |
| Y1-N3 2.567(6) | Y1-N8 2.612(6) | Y1-O2 2.595(6) |
| Y1-N7 2.685(6) | Y1-N4 2.759(6) | |

**Table 2.6 – Selected bond lengths in $[Y(THF)_2(HL^{Et})]$ in Å.**

The single crystal X-ray structure of $[Y(THF)_2(HL^{Et})]$ is isostructural with the cerium analogue, $[Ce(THF)_2(HL^{Et})]$. This can be seen below in Figure 2.38, where the structures have been overlaid with the yttrium complex in green and the cerium complex in orange. As it can be seen, there is only very minor deviation with the

main difference on the THF molecules, and a slight divergence on the arene backbone.

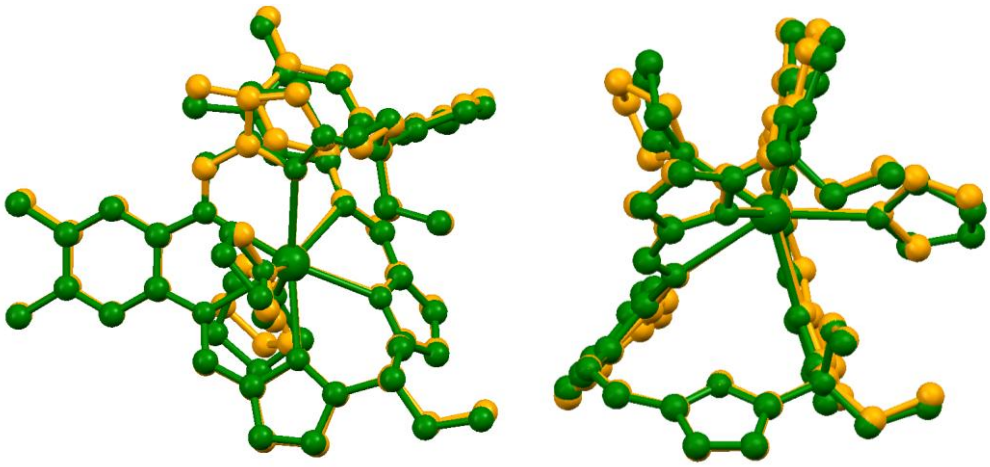

**Figure 2.38 – Overlay of [Y(THF)$_2$(HL$^{Et}$)] in green and [Ce(THF)$_2$(HL$^{Et}$)] in orange.**

The study of yttrium complexes in the literature is extensive. Much research has been carried out on this element due to its lanthanide-like properties, whilst being diamagnetic in nature. Below are examples of Schiff-base, polypyrrolic and porphyrin yttrium complexes.

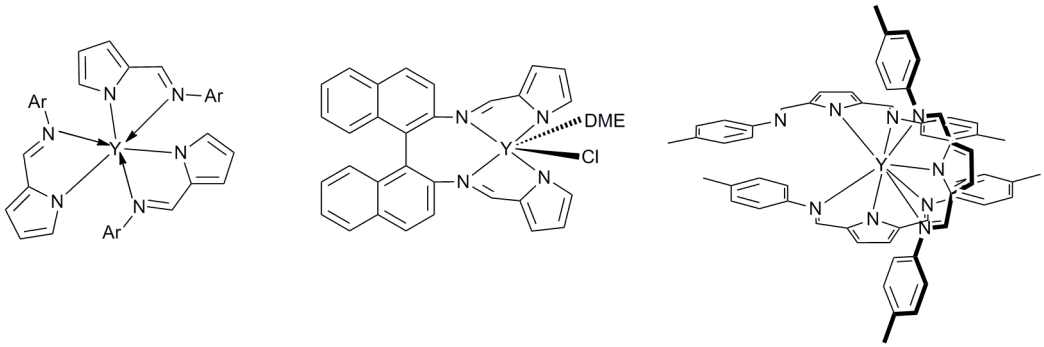


**Figure 2.39 –Examples of yttrium imido complexes.**

The homoleptic tris($\eta^1$:$\kappa^1$-pyrrolylaldiminato)yttrium complex was isolated from a protonolysis reaction of the protonated ligand and the tris(alkyl) yttrium precursor Y(CH$_2$SiMe$_3$)$_3$(THF)$_2$, Figure 2.39.[62] The three bidentate ligands saturate the coordination sphere leading to no room for any molecules of coordinating solvent.

When the ligand (*R*)-bis-(pyrrole-2-ylmethyleneamino)-1,1′-binaphthyl was treated with an excess of NaH and then $YCl_3$, the complex [YCl(L)(DME)] was isolated, Figure 2.39.[64] The chloride can be replaced with amides for further reactivity, including the cyclisation of aminoalkenes.

The homoleptic tris(bis(aryliminomethyl)pyrrolyl) yttrium complex was isolated and shown to be eight coordinate with an uncoordinated imine, which is thought to be because of the steric congestion at the metal centre, Figure 2.39.[65]

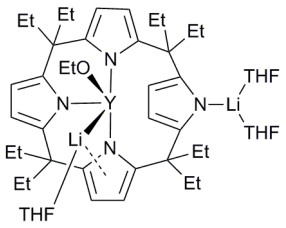


**Figure 2.40 – [{Li(THF)$_2$}{OEPg)Y($\mu$-OEt)Li(THF)}].**

The porphyrin precursor octethylporphyrinogen, OEPg, has been shown to bind to yttrium *via* the cleavage of THF to give the complex [{Li(THF)$_2$}{OEPg)Y($\mu$-OEt)Li(THF)}] and ethylene.[66] The bis(porphyrin) complex, [Y(OEP)$_2$], contains an $(OEP)^{2-}$ ion and an $(OEP^{\bullet})^{-}$ $\pi$-radical ion with an yttrium +3 ion in the centre, Figure 2.41.[36, 67]

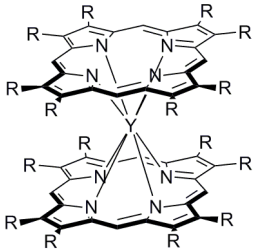


**Figure 2.41 – [Y(OEP)$_2$].**

The complex [Y(OEP)$_2$] shows 'internal charge-transfer' bands in the near IR spectrum and the magnetic moment in the solid state reflects the radical nature of the complex with a $\mu_{eff}$ = 1.5 B.M. between 5 and 100 K.

When $[Y(HL^{Et})]_3$ is dissolved in pyridine as new pyridine adduct is formed with the proposed formula $[Y(py)_2(HL^{Et})]$. The complex was studied by $^1H$ NMR spectroscopy showed the pyrrolic NH proton at 10.95 ppm and the imino protons were at 8.43, 8.40, 8.22 and 8.20 ppm. The pyridine adduct in the $^1H$ NMR spectroscopy appears to have a similar structure to that of the THF adduct.

### 2.4.3 Synthesis of $[\{Y(OH_2)(H_2L^{Et})\}_2(\mu\text{-}OH)_2]$

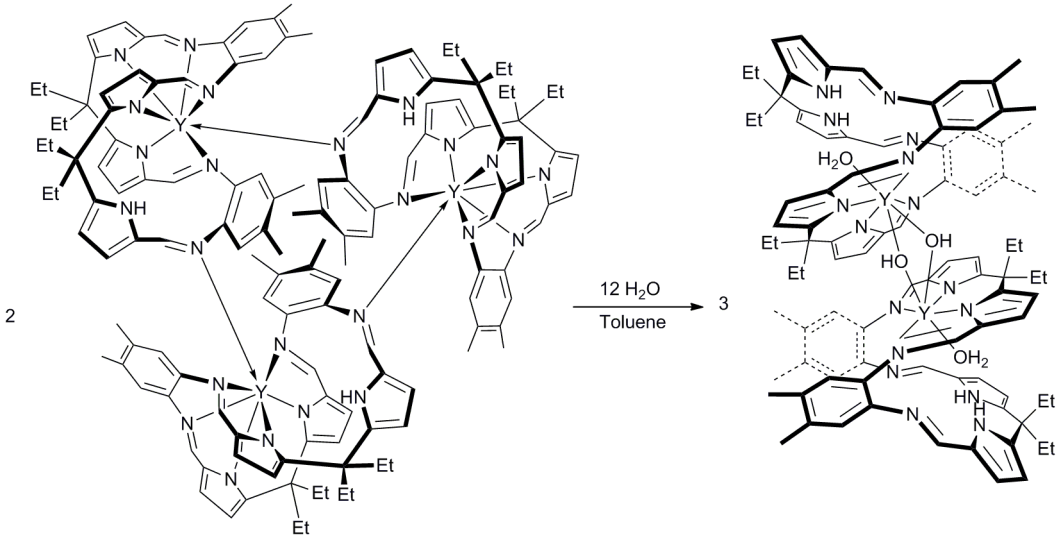


**Equation 2.9**

In an attempt to crystallise $[Y(HL^{Et})]_3$ from a saturated toluene solution, partial hydrolysis instead resulted in the formation of crystals of $[\{Y(OH_2)(H_2L^{Et})\}_2(\mu\text{-}OH)_2]$. This complex can be synthesised rationally by the careful addition of degassed water to a toluene solution of $[Y(HL^{Et})]_3$, and its formation is supported by elemental analysis.

The $^1H$ NMR spectrum in both $C_6D_6$ and $CDCl_3$ shows only the free ligand resonances of $H_4L^{Et}$ implying that in solution the structure may be fluxional.

The IR spectrum was also consistent with the formation of $[\{Y(OH_2)(H_2L^{Et})\}_2(\mu\text{-}OH)_2]$ showing an N-H absorption at 3440, a YO-H adsorption at 3097 and imine absorptions at 1614 and 1557 $cm^{-1}$.

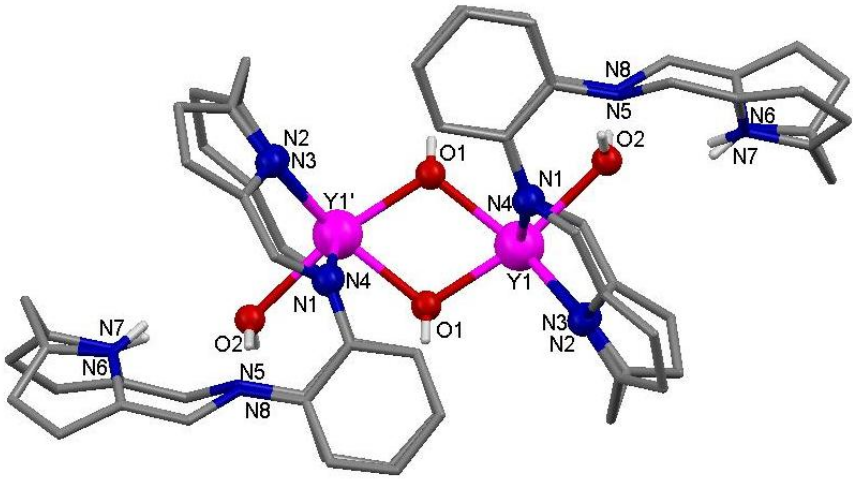


**Figure 2.42 –Ball and stick representations of the X-ray crystal structure of side view of [{Y(OH$_2$)(H$_2$L$^{Et}$)}$_2$($\mu$-OH)$_2$], the aryl backbone methyl groups and the ethyl groups from between the pyrrole groups, hydrogen atoms and solvents of crystallisation have been excluded for clarity.**

The single crystal X-ray structure shows an inversion centre between the yttrium atoms to create the dimer which is bridged by two hydroxyl groups. The yttrium atom lies in one of the $N_4$ pockets with a molecule of water in the cleft with the coordination sphere of the yttrium completed by the two bridging hydroxides.

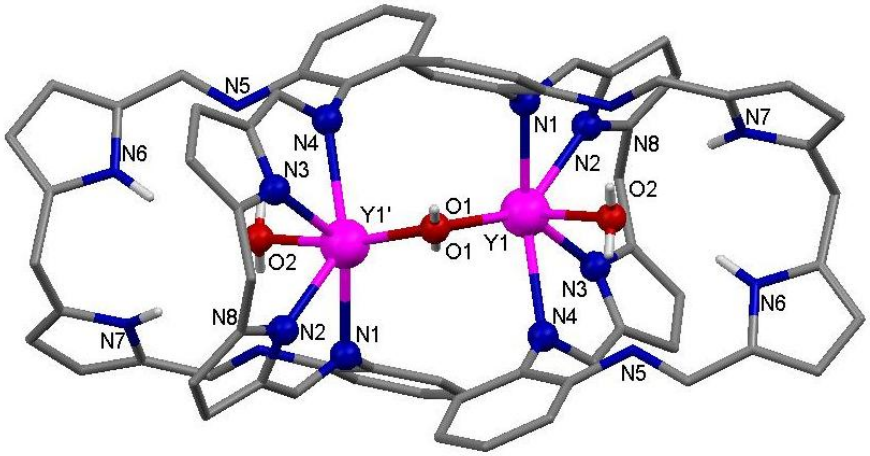


**Figure 2.43 – Top view of [{Y(OH$_2$)(H$_2$L$^{Et}$)}$_2$($\mu$-OH)$_2$].**

The yttrium centre is seven coordinate with approximately pentagonal bipyramidal geometry. The bite angle, the angle between the $N_4$ planes is 47.39°, which is within the normal range seen for homobimetallic complexes of $H_2L$ (45-62°), and the aryl hinge groups are seen to splay away from each other with an angle of 43.27° as seen in other monometallic Pacman complexes such as $[SnMe_2Fe(THF)(L)]$ and $[UO_2(THF)(H_2L)]$.[20, 68] The molecule of water in the centre of the ligand cleft shows hydrogen-bonding towards both imine nitrogen atoms in the unbound part of the ligand (O2-N6 3.158 Å and O2-N7 3.225 Å).

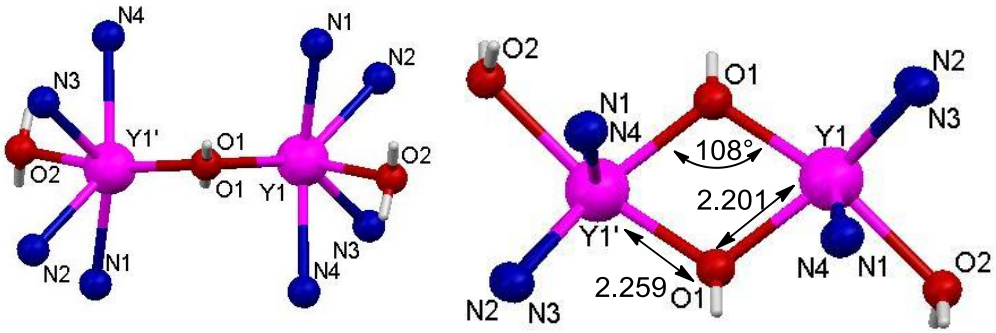


**Figure 2.44 – Coordination around the yttrium atoms in $[\{Y(OH_2)(H_2L^{Et})\}_2(\mu\text{-}OH)_2]$ in Å and °.**

The yttrium-yttrium distance is 3.616 Å, which is within the large range seen the literature (3.291-3.951 Å). Selected bond distances for $[\{Y(OH_2)(H_2L^{Et})\}_2(\mu\text{-}OH)_2]$ are shown in Table 2.7. The bond distances for Y-O in hydroxyl bridged complexes range from 2.202–2.428 Å with a mean average of 2.29(1) Å, whilst those shown in $[\{Y(OH_2)(H_2L^{Et})\}_2(\mu\text{-}OH)_2]$ are the short end of this range at 2.201(5) and 2.259(6) Å. Other complexes containing a yttrium hydroxide bridge have shown a Y-O(H)-Y angle range from 90.471–137.175°, with a mean of 107.377(2.48)° whereas the angle in $[\{Y(OH_2)(H_2L^{Et})\}_2(\mu\text{-}OH)_2]$ is 108.33°. The Y-N bond lengths are shorter than those found in $[Y(THF)(HL^{Et})]$.

| Pyrrole | Imine | Y-O |
|---|---|---|
| Y1-N2 2.392(9) | Y1-N1 2.539(8) | Y1-O1 2.201(5) |
| Y1-N3 2.408(8) | Y1-N4 2.531(9) | Y1-O2 2.393(5) |
| | | O1-Y1' 2.259(6) |

**Table 2.7 – Selected bond lengths in $[\{Y(OH_2)(H_2L^{Et})\}_2(\mu\text{-}OH)_2]$ in Å.**

Binuclear yttrium complexes with bridging hydroxide ligands are fairly common in the literature. Below there are examples of a few containing nitrogen donor supporting ligands.

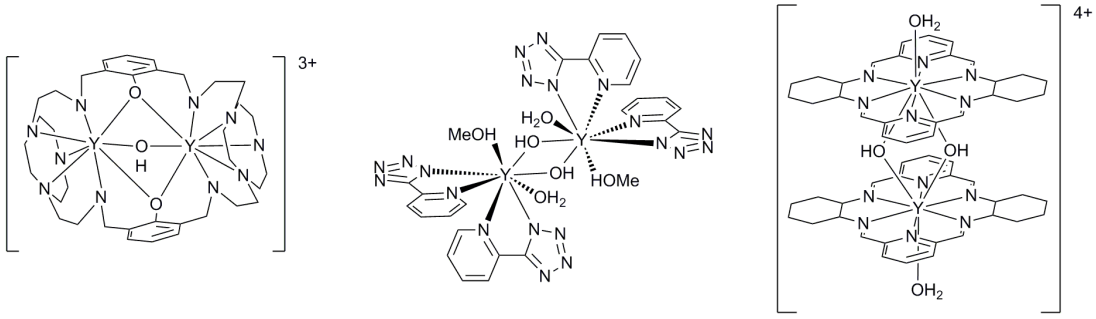


**Figure 2.45 – Examples of (bis)yttrium hydroxyl complexes.**

A binucleating macrocycle utilising [9]ane$N_3$ has been shown to encapsulate two yttrium atoms with a bridging hydroxide.[69] The yttrium atoms are 3.4295(19) Å apart with each atom having an eight coordinate geometry.

$[Y_2(pytz)_4(\mu\text{-}OH)_2(MeOH)_2]$ was isolated from the reaction between $YCl_3$, Hpytz and $NEt_3$ in methanol.[70] The yttrium atoms lay 3.687(2) Å apart, with each being eight coordinate.

The dimeric yttrium complex, $[YL(OH)(H_2O)_2](NO_3)_4$, where L is a 18-membered hexaazamacrocycle, has been shown to degrade double-stranded DNA.[61] The yttrium atoms are coordinated to six nitrogen atoms on the macrocycle in an equatorial position, two hydroxide bridging units and one water molecule in an axial position, making it nonadentate. The monomeric yttrium analogue does not show the same

affinity to cleave DNA. The yttrium hydroxyl-bridged dimer is capable of hydrolysing double-stranded DNA with 90-95% efficiency for supercoiled, closed, circular form of plasmid DNA.

## 2.5 Conclusions

In this chapter, the synthesis and characterisation of the monometallic complexes [M(L)] or [M(HL)], where M = Y, La, Ce, U, and Th, of the octadentate Schiff-base pyrrole macrocycle $H_4L$ has been described. The solid state structure of [Ce(HL)] was found to be a unique trinuclear supramolecular wheel.

The reactions of the mononuclear structures with hydrolysis, oxygen sources and other metal reagents were investigated.

The investigation of synthesis of bimetallic complexes was then explored as explained in Chapter 3.

## 2.6 References


1. G. Givaja, A. J. Blake, C. Wilson, M. Schroeder and J. B. Love, *Chem. Commun.*, 2003, 2508-2509.
2. J. L. Sessler, W.-S. Cho, S. P. Dudek, L. Hicks, V. M. Lynch and M. T. Huggins, *J.Porphyrins Phthalocyanines* 2003, **7**, 97-104.
3. B. J. Littler, M. A. Miller, C. H. Hung, R. W. Wagner, D. F. O'Shea, P. D. Boyle and J. S. Lindsey, *J. Org. Chem.*, 1999, **64**, 1391-1396.
4. J. B. Love, P. A. Salyer, A. S. Bailey, C. Wilson, A. J. Blake, E. S. Davies and D. J. Evans, *Chem. Commun.*, 2003, 1390-1391.
5. A. J. F. N. Sobral, N. G. C. L. Rebanda, M. da Silva, S. H. Lampreia, M. Ramos Silva, A. M. Beja, J. A. Paixao and A. M. d. Rocha Gonsalves, *Tetrahedron Lett.*, 2003, **44**, 3971-3973.
6. G. Givaja, M. Volpe, J. W. Leeland, M. A. Edwards, T. K. Young, S. B. Darby, S. D. Reid, A. J. Blake, C. Wilson, J. Wolowska, E. J. L. McInnes, M. Schroder and J. B. Love, *Chem. Eur. J.* , 2007, **13**, 3707-3723.

7. P. L. Arnold, N. A. Potter, C. D. Carmichael, A. M. Z. Slawin, P. Roussel and J. B. Love, *Chem. Commun.*, 2010, **46**, 1833-1835.
8. O. P. Lam, P. L. Feng, F. W. Heinemann, J. M. O'Connor and K. Meyer, *J. Am. Chem. Soc.*, 2008, **130**, 2806-2816.
9. G. S. Girolami, S. N. Milam and K. S. Suslick, *Inorg. Chem.*, 1987, **26**, 343-344.
10. J. L. Kiplinger, J. A. Pool, E. J. Schelter, J. D. Thompson, B. L. Scott and D. E. Morris, *Angew. Chem., Int. Ed. Engl.*, 2006, **45**, 2036-2041.
11. I. Korobkov, S. Gambarotta and G. P. A. Yap, *Organometallics*, 2001, **20**, 2552-2559.
12. I. Korobkov, S. Gambarotta and G. P. A. Yap, *Angew. Chem., Int. Ed.*, 2002, **41**, 3433-3436.
13. K. Meyer, D. J. Mindiola, T. A. Baker, W. M. Davis and C. C. Cummins, *Angew. Chem., Int. Ed.*, 2000, **39**, 3063-3066.
14. L. Salmon, P. Thuery and M. Ephritikhine, *Dalton Trans.*, 2004, 1635-1643.
15. L. Salmon, P. Thuery and M. Ephritikhine, *Polyhedron*, 2006, **25**, 1537-1542.
16. L. Salmon, P. Thuery, E. Riviere, S. Miyamoto, T. Yamato and M. Ephritikhine, *New J. Chem.*, 2006, **30**, 1220-1227.
17. I.S.Kirin, A.B.Kolyadin and A.A.Lychev, *Zh.Strukt.Khim.*, 1974, **15**, 486.
18. J. B. Love, *Chem. Commun.*, 2009, 3154-3165.
19. J. M. Veauthier, W. S. Cho, V. M. Lynch and J. L. Sessler, *Inorg. Chem.*, 2004, **43**, 1220-1228.
20. P. L. Arnold, A. J. Blake, C. Wilson and J. B. Love, *Inorg. Chem.*, 2004, **43**, 8206-8208.
21. X.-L. Zheng, Y. Liu, M. Pan, X.-Q. Lü, J.-Y. Zhang, C.-Y. Zhao, Y.-X. Tong and C.-Y. Su, *Angew. Chem., Int. Ed. Engl.*, 2007, **46**, 7399-7403.
22. S. Kano, H. Nakano, M. Kojima, N. Baba and K. Nakajima, *Inorg. Chim. Acta*, 2003, **349**, 6-16.
23. M. G. B. Drew, M. R. S. Foreman, M. J. Hudson and K. F. Kennedy, *Inorg. Chim. Acta*, 2004, **357**, 4102-4112.
24. J. Magull and A. Simon, *Z. Anorg. Allg. Chem.*, 1992, **615**, 77-80.

25. P. V. Bernhardt, B. M. Flanagan and M. J. Riley, *Aust. J. Chem.*, 2001, **54**, 229.
26. Z. Lijuan, Z. Yunshan and J. Fei, *J. Chem. Crystallogr.*, 2008, **38**, 595-599.
27. T. B. Jensen, R. Scopelliti and J.-C. G. Bunzli, *Inorg. Chem.*, 2006, **45**, 7806-7814.
28. J. Mazurek and J. Lisowski, *Polyhedron*, 2003, **22**, 2877-2883.
29. Cheng-Yong Su, Bei-Sheng Kang, Xiao-Qin Mu, Jie Sun, Ye-Xiang Tong and Z.-N. Chen, *Aust. J. Chem.*, 1998, **51**, 565.
30. D. J. Berg, C. Zhou, T. Barclay, X. Fei, S. Feng, K. A. Ogilvie, R. A. Gossage, B. Twamley and M. Wood, *Can. J. Chem*, 2005, **83**, 449-459.
31. G. M. de-Oliveira, R. Bortolotto, D. G. Ribas, E. Faoro, E. S. Lang and R. A. Burrow, *Z. Anorg. Allg. Chem.*, 2009, **635**, 484-487.
32. W.-K. Wong, L. Zhang, W.-T. Wong, F. Xue and T. C. W. Mak, *J. Chem. Soc., Dalton Trans.*, 1999, 615 - 622.
33. C. Platas, F. Avecilla, A. d. Blas, T. Rodriguez-Blas, R. Bastida, A. Macias, A. Rodriguez and H. Adams, *J. Chem. Soc., Dalton Trans.*, 2001, 1699-1705.
34. M. Gonzalez-Lorenzo, C. Platas-Iglesias, F. Avecilla, C. F. G. C. Geraldes, D. Imbert, J.-C. G. Bunzli, A. de Blas and T. Rodriguez-Blas, *Inorg. Chem.*, 2003, **42**, 6946-6954.
35. A. M. Arif, J. D. J. Backer-Dirks, C. J. Gray, F. A. Hart and M. B. Hursthouse, *J. Chem. Soc., Dalton Trans.*, 1987, 1665 - 1673.
36. J. W. Buchler and B. Scharbert, *J. Am. Chem. Soc.*, 1988, **110**, 4272-4276.
37. D. Chabach, M. Lachkar, A. D. Cian, J. Fischer and R. Weiss, *New J. Chem.*, 1992, **16**, 431-433
38. D. Chabach, A. D. Cian, J. Fischer, R. Weiss and M. E. M. Bibout, *Angew. Chem., Int. Ed. Engl.*, 1996, **35**, 898-899.
39. H. Hückstädt, A. Tutaß, M. Göldner, U. Cornelissen and H. Homborg, *Z. Anorg. Allg. Chem.*, 2001, **627**, 485-497.
40. Y. Bian, J. Jiang, Y. Tao, M. T. M. Choi, R. Li, A. C. H. Ng, P. Zhu, N. Pan, X. Sun, D. P. Arnold, Z.-Y. Zhou, H.-W. Li, T. C. W. Mak and D. K. P. Ng, *J. Am. Chem. Soc.*, 2003, **125**, 12257-12267.

41. N. Pan, Y. Bian, M. Yokoyama, R. Li, T. Fukuda, S. Neya, J. Jiang and N. Kobayashi, *Eur. J. Inorg. Chem.*, 2008, **2008**, 5519-5523.
42. A. M. Arif, J. D. J. Backer-Dirks, C. J. Gray, F. A. Hart and M. B. Hursthouse, *J. Chem. Soc., Dalton Trans.*, , 1987, 1665 - 1673.
43. S. Mizukami, H. Houjou, M. Kanesato and K. Hiratani, *Chem.-Eur. J.*, 2003, **9**, 1521-1528.
44. A. Mustapha, J. Reglinski and A. R. Kennedy, *Inorg. Chim. Acta*, 2009, **362**, 1267-1274.
45. P. Roussel, P. B. Hitchcock, N. Tinker and P. Scott, *Chem. Commun. (Cambridge) FIELD Full Journal Title:Chemical Communications (Cambridge)*, 1996, 2053-2054.
46. J. W. Buchler, A. De Cian, J. Fischer, M. Kihn-Botulinski, H. Paulus and R. Weiss, *J. Am. Chem. Soc.*, 1986, **108**, 3652-3659.
47. J. Seo, M. R. Song, J.-E. Lee, S. Y. Lee, I. Yoon, K.-M. Park, J. Kim, J. H. Jung, S. B. Park and S. S. Lee, *Inorg. Chem.*, 2006, **45**, 952-954.
48. S. Y. Lee, J. Seo, I. Yoon, C.-S. Kim, K. S. Choi, J. S. Kim and S. S. Lee, *Eur. J. Inorg. Chem.*, 2006, 3525-3531.
49. H. J. Kim, I. Yoon, S. Y. Lee, K. S. Choi and S. S. Lee, *New J. Chem.*, 2008, **32**, 258-263.
50. I. Beletskaya, V. S. Tyurin, A. Y. Tsivadze, R. Guilard and C. Stern, *Chemical Reviews*, 2009, **109**, 1659-1713.
51. G. E. Kostakis, G. Abbas, C. E. Anson and A. K. Powell, *CrystEngComm*, 2009, **11**, 82-86.
52. J. L. Atwood, L. J. Barbour, S. Dalgarno, C. L. Raston and H. R. Webb, *J. Chem. Soc., Dalton Trans.*, 2002, 4351-4356.
53. M. Volpe, H. Hartnett, J. W. Leeland, K. Wills, M. Ogunshun, B. J. Duncombe, C. Wilson, A. J. Blake, J. McMaster and J. B. Love, *Inorg. Chem.*, 2009, **48**, 5195-5207.
54. M. D. Walter, R. Fandos and R. A. Andersen, *New J. Chem.*, 2006, **30**, 1065-1070.
55. S. Akine, T. Taniguchi and T. Nabeshima, *J. Am. Chem. Soc.*, 2006, **128**, 15765-15774.

56. T. K. Prasad and M. V. Rajasekharan, *Cryst. Growth Des.*, 2008, **8**, 1346-1352.
57. A. G. Avent, F. G. N. Cloke, B. R. Elvidge and P. B. Hitchcock, *Dalton Trans.*, 2004, 1083-1096.
58. M. Ohashi, M. Konkol, I. Del Rosal, R. Poteau, L. Maron and J. Okuda, *J. Am. Chem. Soc.*, 2008, **130**, 6920-6921.
59. X. Sun, R. Li, D. Wang, J. Dou, P. Zhu, F. Lu, C. Ma, C.-F. Choi, D. Y. Y Cheng, D. K. P. Ng, N. Kobayashi and J. Jiang, *Eur. J. Inorg. Chem.*, 2004, **2004**, 3806-3813.
60. L. Lavanant, T.-Y. Chou, Y. Chi, C. W. Lehmann, L. Toupet and J.-F. o. Carpentier, *Organometallics*, 2004, **23**, 5450-5458.
61. S. W. A. Bligh, N. Choi, E. G. Evagorou, M. McPartlin and K. N. White, *J. Chem. Soc., Dalton Trans.*, 2001, 3169-3172.
62. Y. Yang, S. Li, D. Cui, X. Chen and X. Jing, *Organometallics*, 2007, **26**, 671-678.
63. W. J. Evans, J. M. Olofson and J. W. Ziller, *J. Am. Chem. Soc.*, 1990, **112**, 2308-2314.
64. L. Xiang, Q. Wang, H. Song and G. Zi, *Organometallics*, 2007, **26**, 5323-5329.
65. Y. Matsuo, K. Mashima and K. Tani, *Organometallics*, 2001, **20**, 3510-3518.
66. J. Jubb, S. Gambarotta, R. Duchateau and J. H. Teuben, *Chem. Commun.*, 1994, 2641 - 2642.
67. J. W. Buchler, J. Huettermann and J. Loeffler, *Bull. Chem. Soc. Jpn.*, 1988, **61**, 71-77.
68. J. W. Leeland, A. M. Z. Slawin and J. B. Love, *Organometallics*, 2010, **29**, 714-716.
69. L. Tei, A. J. Blake, F. A. Devillanova, A. Garau, V. Lippolis, C. Wilson and M. Schroder, *Chem. Commun.*, 2001, 2582-2583.
70. P. C. Andrews, T. Beck, B. H. Fraser, P. C. Junk and M. Massi, *Polyhedron*, 2007, **26**, 5406-5413.

# Chapter 3: Bimetallic Complexes

Bimetallic actinide complexes could provide information to help the understanding of the fundamental properties of the f-elements. In particular, studies of the magnetic properties of complexes involving f-block elements are immensely interesting as they can lead to an increased understanding of the 5f electrons. The magnetism of the lanthanides has been of great interest recently with many advances especially in the area of molecular magnets.[1, 2] However due to the more challenging synthetic procedures the study of magnetic communication between actinide elements has been slower to grow.[3, 4] The close relationship between the electronic structure and magnetic properties in actinide complexes causes difficulty in the modelling of these systems. The 5f electrons can behave differently within the actinide series with the electrons forming bands or being localised. The 5f bands are formed by either hybridisation with s, p or d electrons or 5f-5f wavefuntion overlap.[5, 6]

## 3.1 Direct uranium–metal bonds

Most uranium-metal bonds are formed by salt elimination or alkane elimination. A review of uranium-metal bonds has recently been published by Liddle.[7] Porchia synthesised the first structurally characterised uranium-metal bond with a uranium–tin complex with a U-Sn bond distance of 3.166(1) Å, reported from the reaction of $[Cp_3U(NEt_3)]$ and $HSnPh_3$, Figure 3.1.[8, 9] Arnold and co-workers have been instrumental in the investigation of metal-metal bonds. The isolation of $[U(\eta^5\text{-}C_5H_4SiMe_3)_3(AlCp)]$ was the first actinide-group 13 bond complex, Figure 3.1. It is an unsupported uranium–aluminium bond had a 3.117(3) Å distance and was formed from the reaction of $[U(\eta^5\text{-}C_5H_4SiMe_3)_3]$ and $[(AlCp)_4]$.[8 200, 10] Further research afforded the gallium analogue, containing a U-Ga distance of 3.0648(12) Å.

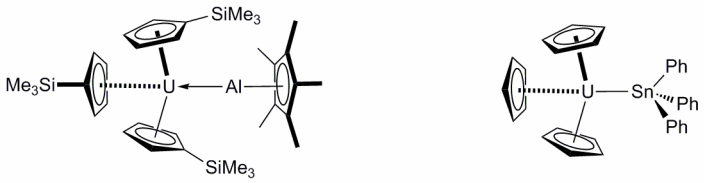


**Figure 3.1 – Examples of CpU-M interactions**

Marks reported in 1987 the synthesis of $[U(Cp)_3\{FeCp(CO)_2\}]$ and $[U(Cp)_3\{RuCp(CO)_2\}]$.[11] These complexes were not structurally characterised by single crystal X-ray diffraction analysis, but the IR data and NMR data support their formation. In 2000, Ephritikhine isolated the complex $[Li_2(py)_3U(1,1'\text{-ferrocenylene})_3]$, Figure 3.2, which contains a U-Fe bond.[12] The X-ray structure revealed a propeller type structure with three ferrocenylene units in the equatorial plane with the lithium atoms in axial positions. The average U-Fe bond length is 3.14(2) Å which is less than the sum of the atomic radii of the elements (3.28 Å), suggesting a direct interaction.

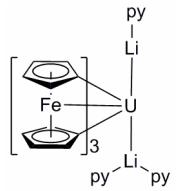


**Figure 3.2 – Tris(1,1'-ferrocenylene) uranium complex**

Another uranium-iron interaction was reported for the complex $[U\{Fc(NSiMe_2t\text{-}Bu)_2\}_2]$-$[BPh_4]$, which contained an average U-Fe distance of 2.962(1) Å.[13]

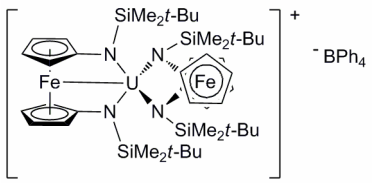


**Figure 3.3 – $[U\{fc(NSiMe_2t\text{-}Bu)_2\}_2][BPh_4]$**

More recently, the Liddle group has been exploring metal-metal interactions of the f-elements, Scheme 3.4. The stabilisation of complexes containing a uranium-gallium interaction in $[(N_3N^{TMS})UGa(NArCH)_2(THF)]$ and a uranium-rhenium bond in $[(N_3N^{TMS})URe(Cp)_2]$, have been facilitated using the tren type, $N_3N^{TMS}$ ligand, and using simple salt elimination methodology.[14, 15]

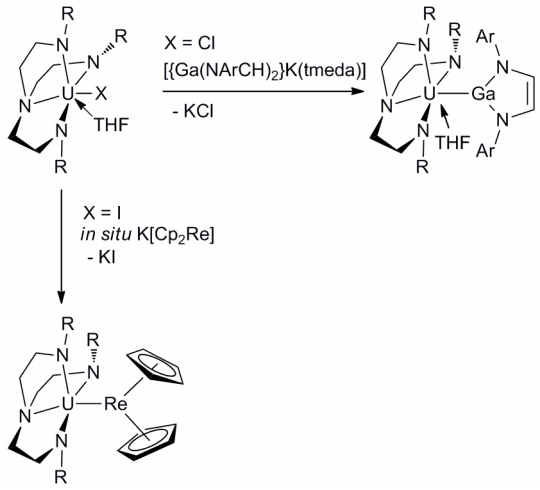


**Scheme 3.4 – Reactivity of [($N_3N^{TMS}$)UX]**

The U-Ga bond length is reported as 2.2115(8) Å and 2.2983(9) Å for the two molecules present in the asymmetric unit cell. The shorter bond length is much smaller than the sum of the covalent radii (3.18 Å), although the unusual, but not unheard-of, variation in the bond lengths could be due to the 'elasticity' of f-elements.[16, 17] The U-Re bond length is 3.0475(4) Å which is also shorter than the sum of the covalent radii by 0.42 Å, and was shown by computational studies to have both σ and π components.

## 3.2 Multinuclear uranium complexes

As of yet, no uranium–uranium bonds have been observed. The shortest uranium–uranium distance reported is 3.3549(6) Å, which was found in the bridging dinitride complex [{K(DME)(calix[4]tetrapyrrole)U]$_2$($\mu$-NK)$_2$][K(DME)$_4$] by Gambarotta, Figure 3.5.[18]

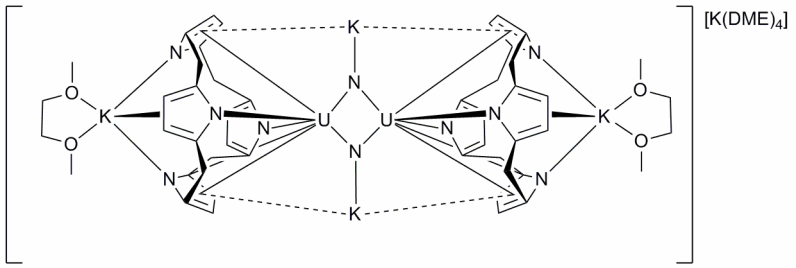


**Figure 3.5 - [{K(DME)(calix[4]tetrapyrrole)U]$_2$($\mu$-NK)$_2$][K(DME)$_4$]**

The closest uranium–uranium distance, without a bridging ligand directly between the uranium centres, has been stabilised by one ligand in [[Li(THF)$_2$]($\mu$-Cl)$_2${U$_2$[{(Cy)$_4$-calix[4]tetrapyrrole}Cl$_2$], Figure 3.6.[19] The intermetallic distance between the +3 uranium centres is 3.365(6) Å, but the complex shows only small antiferromagnetic coupling in its magnetism at 2 K.

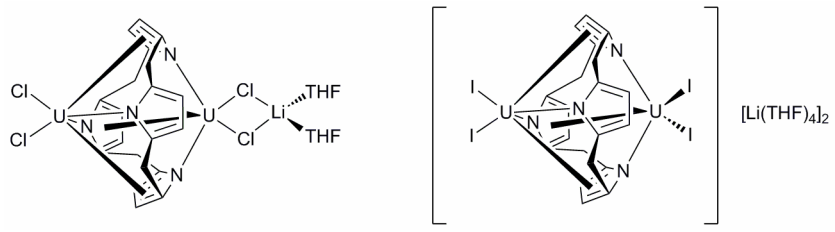


**Figure 3.6 – Lithium adducts of uranium calix[4]tetrapyrrole complexes**

The reaction of UI$_3$(THF)$_4$ and the tetralithium salt of the calix[4]tetrapyrrole results in the isolation of the diuranium(III) complex, [[Li(THF)$_4$]$_2$[U$_2$I$_4${(Cy)$_4$-calix[4]tetrapyrrole}].[19] Each uranium centre coordinates to two iodides, two pyrrolic nitrogen atoms and also to the other two pyrrole rings in a $\eta^5$ mode. Two lithium counter ions are present but are discrete and solvated by THF. This complex displays the uranium(III)-uranium(III) distance at 3.4560(8) Å and exhibits intramolecular antiferromagnetic coupling at 2 K.

The use of S, Se or Te, as a bridging ligand between two UCp′$_3$ units did not yield any magnetic coupling to 5 K.[20] A stronger coupling between uranium centres is found in the bimetallic imido bridged complex, [(Cp′$_3$U)$_2$(μ-1,4-N$_2$C$_6$H$_4$)], Figure 3.7. When 1,4-diazidobenzene is used as a bridging ligand, antiferromagnetic coupling is observed at ~20 K between the uranium(V) centres.[21] The uranium atoms are connected by the diimido unit which can form a conjugated ring, which allows the uranium centres to communicate.

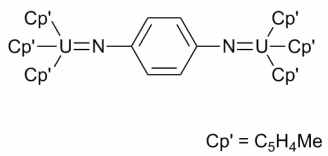


**Figure 3.7 – [(UCp′$_3$)$_2$(μ-1,4-N$_2$C$_6$H$_4$)]**

The uranium(IV) coordination polymers, $[U(TCNE)_2I_2(THF)_2]_n$ and $[U(TCNQ)_2I_2(THF)_2]_n$ were synthesised from $UI_3(THF)_4$ and TCNE or TCNQ in THF, by Kiplinger and co-workers.[22] The insoluble polymers formed show no magnetic ordering but have magnetic behaviour which is consistent with a uranium(IV) ion. No structural characterisation by singe crystal X-ray diffraction was obtained due to the insolubility of the complexes.

The reaction of $[U(N\text{-}t\text{-}Bu)_2(I)_2(t\text{-}Bu_2bpy)]$ and two equivalents of NaCp* form the uranium(V) dimer $[\{U(N\text{-}t\text{-}Bu)_2(I)(t\text{-}Bu_2bpy)\}_2]$, Figure 3.8, instead of the expected uranium(VI) Cp* complex via salt elimination.[23] The solid state structure shows a cation-cation interaction between the $[U(N\text{-}t\text{-}Bu)_2]^+$ moieties with two bridging U=N-*t*-Bu-U units and two U=N-*t*-Bu units. The dimer shows an antiferromagnetic interaction at 13 K, between the $5f^1$ centres indicated in the magnetic susceptibility ($\chi$) versus temperature (T) data. The $1/\chi$ versus T gives an effective magnetic moment of 2.53 $\mu_B$ per mol of uranium.

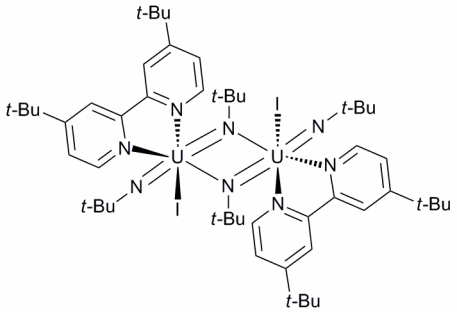


**Figure 3.8 - $[\{U(N\text{-}t\text{-}Bu)_2(I)(t\text{-}Bu_2bpy)\}_2]$**

The multimetallic complex, $[Cp^*_2An\{N{=}C(Bn)(tpy\text{-}UCp^{\ddagger}_2)\}_2]$, where An is Th or U was synthesised from the $[Cp^*_2An\{N{=}C(Bn)(tpy)_2]$, $[UCp^{\ddagger}_2I(THF)]$ and a slight excess of potassium in a one-pot reaction.[24] When An is uranium, there is evidence for magnetic coupling between the uranium(IV) and uranium(III) centres. The magnetic studies allowed the assignment of the formally uranium(III) centres coordinated to the singly-reduced terpyridyl-ketimide coordinated to the uranium(IV) centre. The terpyridyl-ketimide group has a single unpaired electron. The magnetism attributed to the uranium(IV) centre was assigned by studying the thorium analogue and verified by electrochemical data. Cyclic and square-wave voltammetry experiments were

carried out showing three waves, the oxidation of $tpy^{\bullet-}$ to the neutral ligand, the reduction of $tpy^{\bullet-}$ to $tpy^{2-}$, and the oxidation of the metal centre uranium(IV) to uranium(III). For non interacting metal centres the two redox waves for the ligand redox processes should have irresolvable voltametric waves, where as there is significant splitting shown between each pair of waves in the complexes.

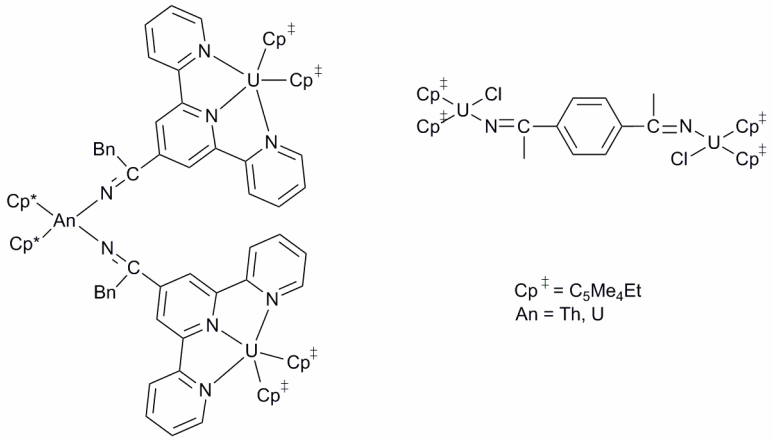


**Figure 3.9 – Imido bridged uranium complexes**

The isolation of the diuranium(IV) 1,4-phenylenediketimide bridged complex, $[\{(Cp^{‡})_2(Cl)U\}_2(\mu\text{-}\{N{=}C\text{-}(CH_3)\text{-}C_6H_4\text{-}(CH_3)C{=}N\})]$, Figure 3.9, was obtained from the addition of 1,4-dicyanobenzene to $[\{(Cp^{‡})_2(Cl)U(CH_3)]$ by Kiplinger and coworkers.[25] The complex exhibits electronic communication between the uranium(IV) centres through the π system of the bridging ligand. Additionally the thorium analogue was synthesised which allows the direct comparison of a $5f^0$ and a $5f^2$ system.

The uranium(IV) cluster $Cs[U_4(\mu_4\text{-}N)(\mu\text{-}1,1\text{-}N_3)_8(CH_3CN)_8I_6]$, Figure 3.10, was formed from the unstable complex '$Cs_3[U(N_3)_7]$' and $UI_3(THF)_4$.[26] Structural characterisation shows that the complex forms a 1D polymeric chain with uranium clusters connected through cesium ions. The cluster contains four uranium cations which are interconnected by eight 1,1-end on bridged azido units with a four coordinate nitrido ligand in the centre. While the uranium-uranium separations are short and range from 3.55-3.90 Å no magnetic coupling was detected to 6K.

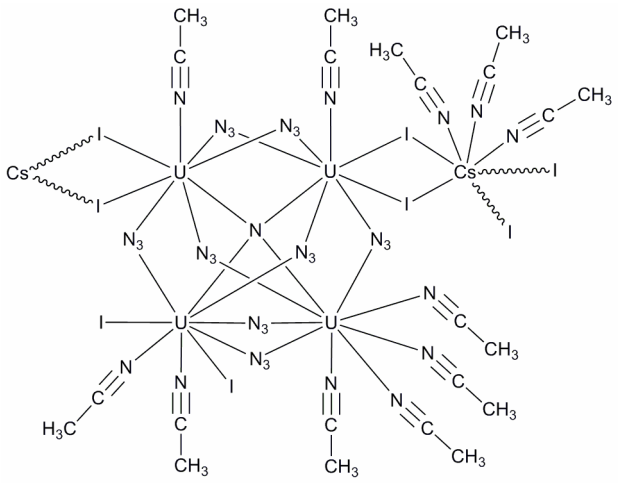

**Figure 3.10 –Uranium(IV) cluster**

Recently the di- and trinuclear complexes of uranium(IV) with bridging aryl acetylide ligands have been studied.[27] The uranium centres are encapsulated in $[N(CH_2CH_2NSiMe_2\text{-}t\text{-}Bu)_3]^{3-}$, $(NN'_3)$. The complexes are formed from the reaction of $[U(bit\text{-}NN'_3)]$, where $(bit\text{-}NN'_3)$, is $[N(CH_2CH_2NSiMe_2\text{-}t\text{-}Bu)_2(CH_2CH_2NSi\text{-}t\text{-}BuMeCH_2)]$ the uranium has bitten into the ligand, and the appropriate equivalents of the bis- or tris(ethynyl)benzenes, Figure 3.11. Using 1,3- and 1,4-diethynylbenzene and 1,3,5-triethynylbenzene supramolecular structures are formed. The metal centres show weak ferromagnetic coupling in all three complexes.

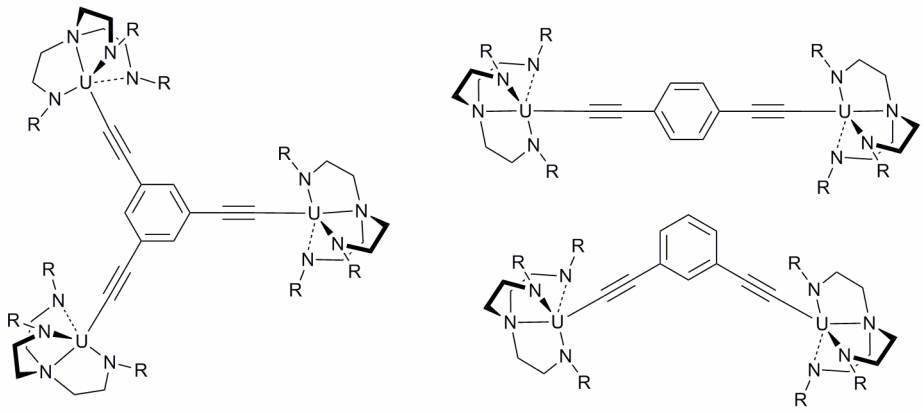

**Figure 3.11 – Ethynylbenzene uranium complexes**

## 3.3 Synthesis of Starting Materials

### 3.3.1 Preparation of [$K_4L^{Et}$]

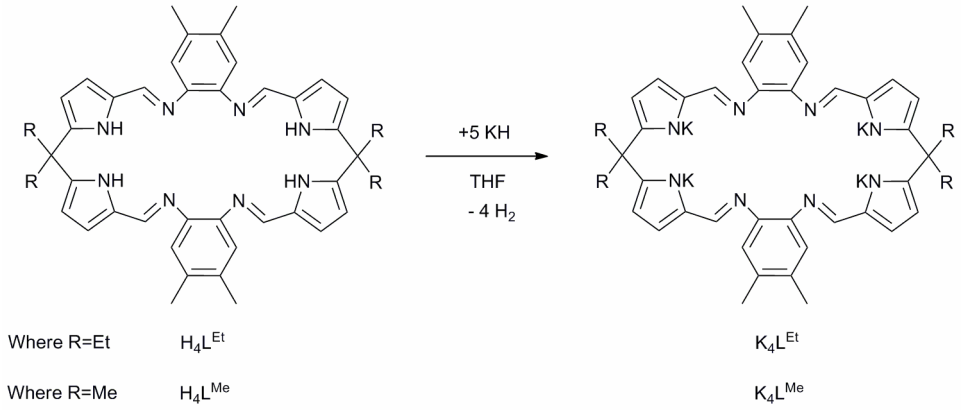


**Equation 3.1**

The macrocycle was deprotonated using a five-fold excess of potassium hydride in THF, thus making the potassium salt of the ligand, $K_4L$, Equation 3.1. This complex was usually made *in situ* and not isolated. The R substituents used in the preparation were either methyl or ethyl groups, forming $K_4L^{Me}$ and $K_4L^{Et}$ respectively. Potassium salts of the macrocyclic ligand bearing different substituent patterns have been isolated previously and their solid state structures determined.[28] For example, when R is a methyl group and the methyl groups on the aryl backbone are not present, the crystal structure exhibits a 1D polymeric chain structure with the polymer growing from a potassium atom coordinating $\eta^5$ to a pyrrole on another molecule.

The potassium salt $K_4L^{Et}$ was characterised by elemental analysis, $^1H$ and $^{13}C$ NMR spectroscopy and IR spectroscopy. The elemental analysis supports the formation of $K_4L^{Et}$. The $^1H$ NMR spectrum shows the characteristic four resonances corresponding to the $CH_3$ groups of the ethyl group environments that become dissimilar upon complexation (2.11, two overlapping signals at 1.24 and 0.90 ppm). Accompanying this is the pyrrolic backbone protons become shifted downfield upon complexation to 6.96 and 6.56 ppm. The infrared spectrum of $K_4L^{Et}$ shows the absence of the N-H absorbance and strong C=N stretches at 1589 and 1567 $cm^{-1}$.

### 3.3.2 Preparation of $UI_3(THF)_4$

Freshly cleaned oxide-free uranium turnings were amalgamated with $HgI_2$ in THF. These amalgamated turnings were then reacted with iodine at -10 °C, and kept cool until a blue precipitate started to appear. The key to the smooth running of the synthesis of $UI_3(THF)_4$ is maintaining the reaction temperature at or below 10 °C.[29] At higher temperatures than this the reaction accelerates too quickly, resulting in an oily green product, a uranium(IV) 4-iodobutoxide complex, due to the ring opening of THF. The complex $UI_3(THF)_4$, was isolated as dark blue precipitate in a fair yield.

Alternatively $UI_3$ was made via combination of the elements of uranium and iodide in diethyl ether it was then extracted into THF, and the volatiles removed to yield $UI_3(THF)_4$ quantitatively.[22]

## 3.4 Synthesis of Bimetallic Complexes

### 3.4.1 Synthesis of $[(UI)_2(L^{Me})]$ and $[(UI)_2(L^{Et})]$

Previously the unmethylated analogue of $[(UI)_2(L)]$ has been synthesised by Prof. Polly Arnold, where the aryl backbone is not methylated and R=H.[30]

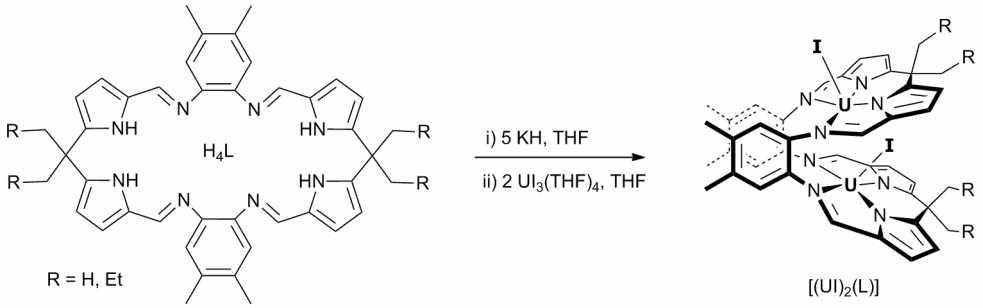


**Equation 3.2**

The bimetallic uranium complexes $[(UI)_2(L)]$ (L = $L^{Me}$, $L^{Et}$) were synthesised using a salt elimination methodology.[30] The potassium salt of the ligand, $K_4L$, was synthesised *in situ* and then combined with half an equivalent of $UI_3$ in THF at -78 °C, Equation 3.2. The resulting green slurry was allowed to warm to room temperature overnight and the volatiles then removed from the dark red solution under reduced

pressure, to yield a dark red solid. For the synthesis of $[(UI)_2(L^{Me})]$, the product was isolated from the THF solution, whereas the product for the synthesis of $[(UI)_2(L^{Et})]$ was extracted into toluene and then isolated. The yields for $[(UI)_2(L^{Me})]$ and $[(UI)_2(L^{Et})]$ dark red complexes are 50% and 90% respectively. The resulting complexes have been studied using a range of techniques. Elemental analysis of $[(UI)_2(L^{Me})]$ and $[(UI)_2(L^{Et})]$ supported the stoichiometery of the complexes. The IR spectra showed no difference between the complexes as would be expected. The UV-vis spectrum of $[(UI)_2(L^{Et})]$ confirmed the oxidation state of uranium as +3 with an absorption seen at $\lambda_{max}$ 1179 nm ($\varepsilon$ = 1315.6 $dm^3$ $mol^{-1}$ $cm^{-1}$ ) in THF. Other data were not extracted due to the strong absorption of the ligand in this range. An assignable $^1H$ NMR spectrum was obtained for $[(UI)_2(L^{Et})]$ in THF with a $C_6D_6$ internal standard, however none could be obtained for $[(UI)_2(L^{Me})]$. In $[(UI)_2(L^{Et})]$ the $^1H$ NMR spectrum ranges from 36 to -43 ppm with 9 resonances corresponding to a symmetric environment. The polymeric nature of the complexes led to the isolation of only polycrystalline solids and never single crystals suitable for X-ray diffraction. Many different crystallisation techniques were attempted, utilising the methods of interface, single solvent, diffusion and Soxhlet extraction, see the experimental section (Chapter 5) for full listings. Higher temperature attempts to crystallise the bimetallic complexes with the use of vapour phase sublimination, resulted in decomposition (including the decomposition to $[U(L^{Et})]$, see Chapter 2).

The structural information for these complexes is very interesting as there is a possibility that the two uranium atoms can undergo magnetic superexchange coupling. For this to occur, a bridging iodide would have to be present. The magnetic susceptibility at various temperatures 2 to 300K and in an applied field of 1 and 7 T were recorded.

The variable temperature solid state magnetic susceptibility of $[(UI)_2(L^{Et})]$ was measured on a Superconducting Quantum Interference Device (SQUID) susceptometer. The magnetism studies experimental data for $[(UI)_2(L^{Et})]$ are shown in Figures 3.12 and 3.13.

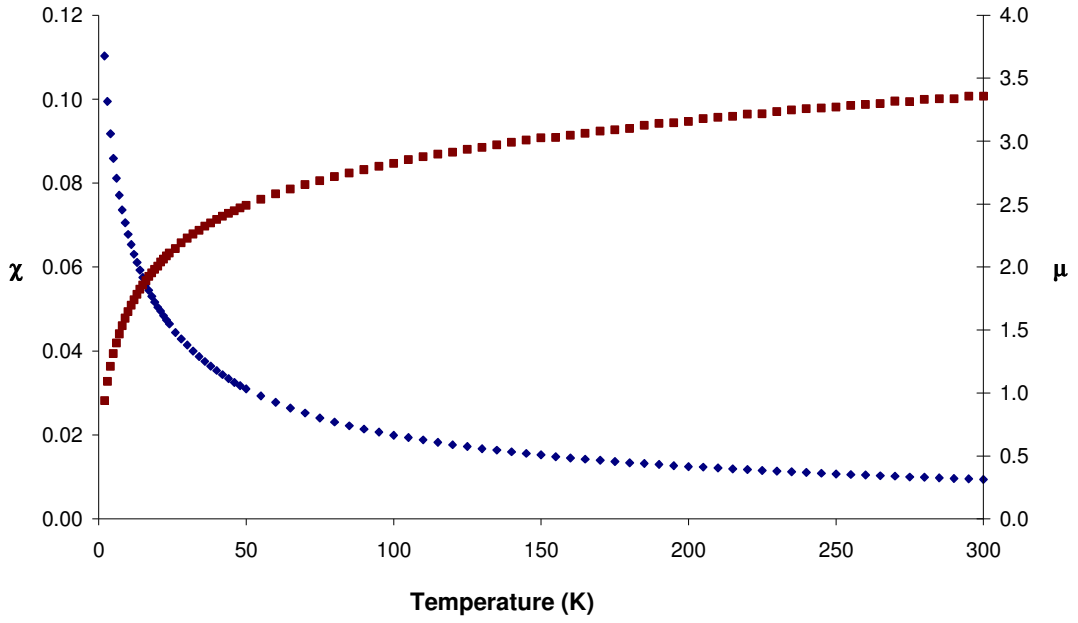


**Figure 3.12 – Magnetic susceptibility $\chi$ (red) and effective magnetic moment $\mu$ (blue) in B.M. for 300 K – 2 K at 1 T**

A 29.1 mg sample of $[(UI)_2(L^{Et})]$ was used for the magnetism studies and the diamagnetic correction of -741 x $10^{-6}$ emu/mol was applied. The data shows the magnetic susceptibility and the effective magnetic moment with respect to temperature. The effective magnetic moment shows at high temperature a linear dependence with decreasing temperature and in the low temperature region shows temperature independent paramagnetism. The experimental effective magnetic moment was calculated as 2.45 ± 0.03 $\mu_B$. This effective magnetic moment is significantly reduced with respect to the free ion value for uranium(III) (3.7 $\mu_B$). In solution the $\mu_{eff}$ for $[(UI)_2(L^{Me})]$ was 3.02 $\mu_B$ in a $C_5D_5N$ solution, calculated by Evans' method.[31]

The magnetic susceptibility shows an overall increase with decreasing temperature. Below 50 K the magnetic susceptibility rapidly increases. When the reciprocal of magnetic susceptibility is plotted, Figure 3.13, it displays Curie Weiss paramagnetic behaviour.

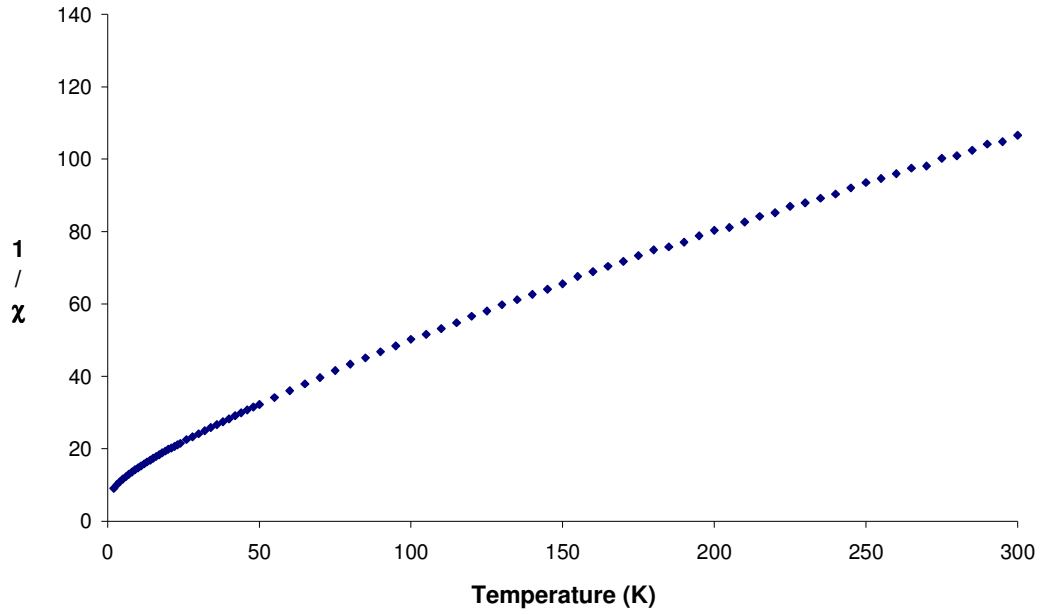


**Figure 3.13 – 1/χ plotted against temperature for 300 K – 2 K at 1 T**

Possible structures for the complexes $[(UI)_2(L)]$ are shown in Figure 3.14. Although there are more possibilities; π-heterocyclic or arene fragment from part of another ligand coordinating to another metal was disregarded due to the interaction between the metal and halide being stronger and the halide bridge has been observed in previously characterised complexes e.g. $[(VO)(VCl)(L)]$ and $[Zn_2Cl(L)BF_4]$.[28, 32]

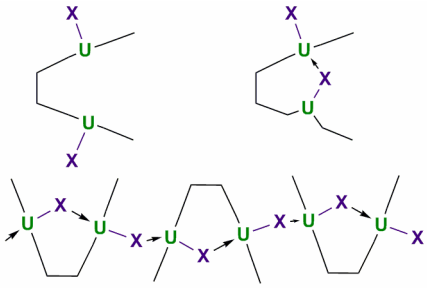


**Figure 3.14 – Possible structural conformations where X=I or $BH_4$**

If the uranium atoms are isolated magnetically and there are no bridging ligands to connect them, the magnetism would be dominated by the ligand field over the entire temperature range. This model compared to the experimental data is shown in Figure 3.15, with the magnetically isolated model shown in purple.

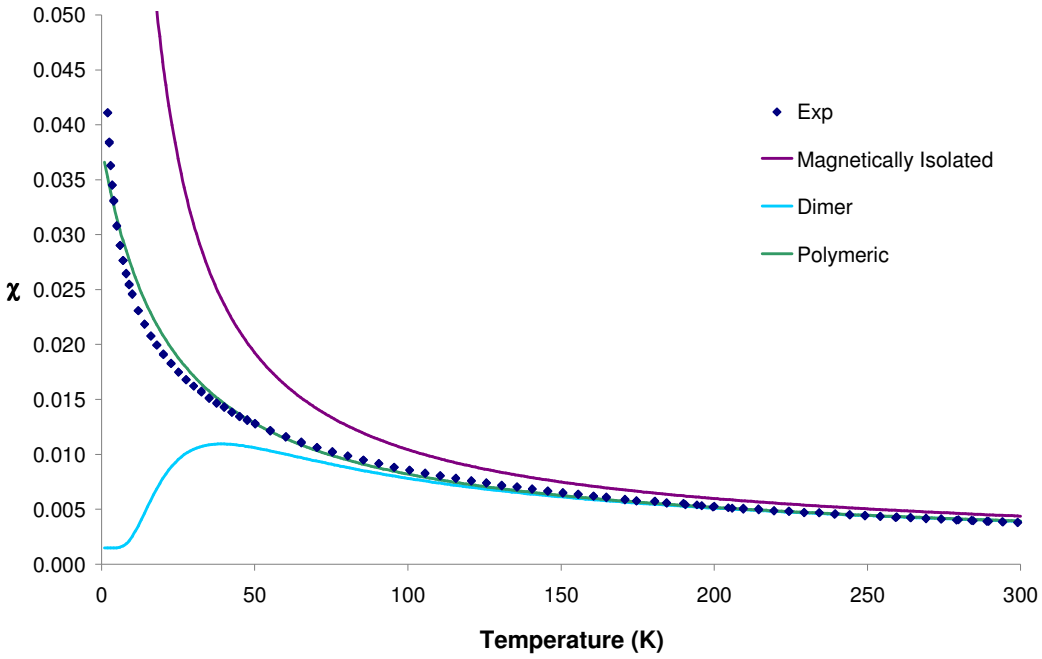


**Figure 3.15 – Comparison of models to experimental data of [(UI)$_2$(L$^{Et}$)] between 300 – 2 K at 1 T**

In Figure 3.15, the effective magnetic moment was plotted against absolute temperature and shows the comparison between the experimental data and the modelled plots for magnetically isolated, dimeric and polymeric structures.

Dimers with different magnetic ground states were also considered, but as a tetrameric structure would exhibit behaviour similar to a single dimer, only the single dimer was studied. The model for the dimeric system was modelled using the largest possible impurity contribution and also assuming that the magnetic susceptibility at 2 K is totally due to the impurity. Antiferromagnetic exchange is required to fit the high temperature 1/$\chi$ values. As seen in Figure 3.15, the dimer model, shown in light blue does not fit the experimental data well, with large deviations from 20 K and below. The best fitting model for the experimental magnetism data is the polymeric structure where a mean-field approach was used as it could not be constricted by a finite dimensionality. The excellent agreement between the model and the experimental data is shown in Figure 3.15, in green. The solid-state structure of [(UI)$_2$(L$^{Et}$)] is therefore suggested to be polymeric based on the strong evidence from the magnetism studies

conducted on this complex, showing a relatively strong antiferromagnetic coupling between the uranium centres. For modelling information see Chapter 5.

Many substitution reactions to replace the iodide were undertaken to synthesise a more crystalline variant of the diuranium complex, including substitution by Cp, Cp*, Bn, $O(C_6H_3t\text{-}Bu_2)$, $OC(CH_3)_2(CH_2CH_3)$ and $N(SiMe_3)_2$. All were synthesised for crystallisation purposes, and no further characterisation was carried out. Despite the numerous attempts, no single crystals suitable for X-ray diffraction studies were grown. The substitution reaction attempted between $[(UI)_2(L^{Et})]$ and KH did not produce the desired $[(UH)_2(L^{Et})]$, but instead reacted with the ligand leading to decomposition.

In another attempt to synthesise a more crystalline version of the biuranium complex, a fluorenyl-substituted ligand at the *meso*-position carbons was used, as shown in Figure 3.16.

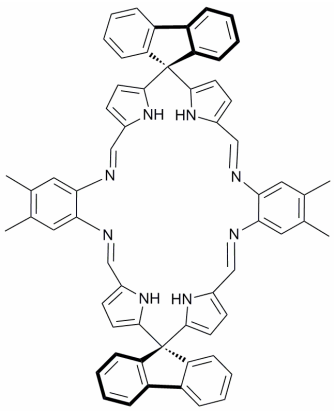


**Figure 3.16 – $H_4L^{Flu}$, fluorenyl substituted ligand**

While elemental analysis supported the formation of the new complex $[(UI)_2(L^{Flu})]$, crystallisation attempts did not produce any single crystals suitable for X-ray diffraction studies.

### 3.4.2 Preparation of $[(UBH_4)_2(L^{Et})]$

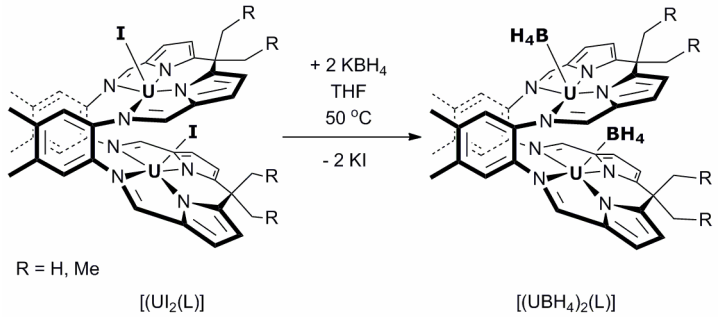


**Equation 3.3**

In an attempt to form a precursor suited to hydride formation through $BH_3$ elimination, $[(UI)_2(L^{Et})]$ was reacted with potassium borohydride to create a diuranium borohydride complex, $[(UBH_4)_2(L)^{Et}]$, Equation 3.3. In an ampoule, $[(UI)_2(L^{Et})]$ was combined with two equivalents of $KBH_4$ in THF and heated to 50 °C overnight and the precipitation of KI was observed. The red solution was isolated from the KI and the filtrate dried under vacuum resulting in $[(UBH_4)_2(L)^{Et}]$ as a dark red solid in good yield of 79 %. The complex was studied by elemental analysis which supported the replacement of the iodide with borohydride. The UV-vis spectrum of $[(UBH_4)_2(L)^{Et}]$ suggested that the uranium oxidation state was maintained as +3 with a $\lambda_{max}$ of 1178 nm ($\varepsilon$ = 1001 $dm^3$ $mol^{-1}$ $cm^{-1}$ ) in THF. The IR spectra of $[(UBH_4)_2(L)^{Et}]$ showed bands for the $BH_4$ groups that shifted in wavenumber from the $KBH_4$ starting material. The IR spectrum exhibits a BH stretching mode at 2449 $cm^{-1}$ and a doublet at 2211 $cm^{-1}$ (compared to $KBH_4$ 2378, 2274, 2209 and 1115 $cm^{-1}$). A strong band is seen at 1187 $cm^{-1}$ which is due to the bridging deformation, indicates that the $BH_4$ group is bound in a $\mu^3$ configuration. [33]

As described in Part 1.7, uranium borohydrides are well studied complexes, the majority of them in the tetravalent state. The study of trivalent uranium borohydrides within a macrocyclic environment has not been attempted before, making it difficult to draw comparisons.

A magnetic study carried out on $[(UBH_4)_2(L)^{Et}]$ showed similar results to those from the $[(UI)_2(L^{Et})]$ complex, Figures 3.17 and 3.18. The structure is thought to be poly-

meric, similar to $[(UI)_2(L^{Et})]$. The Figure 3.17 shows the magnetic susceptibility against temperature in blue and the effective magnetic moment versus absolute temperature in red. The effective magnetic moment shows at high temperature a linear dependence with decreasing temperature and in the low temperature region shows temperature independent paramagnetism. The magnetic susceptibility shows an overall increase with decreasing temperature. Below 50 K the magnetic susceptibility rapidly increases. When the reciprocal of magnetic susceptibility is plotted, Figure 3.18, it displays Curie Weiss paramagnetic behaviour

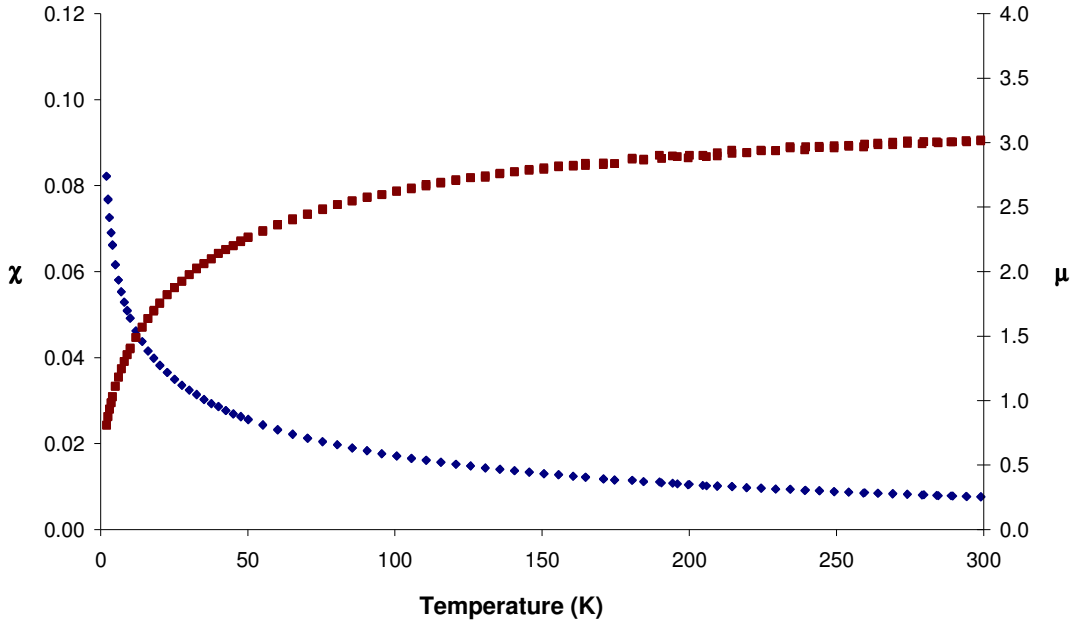


**Figure 3.17 - Magnetic susceptibility *χ* (red) and effective magnetic moment *μ* (red) for 300 K – 2 K at 1 T**

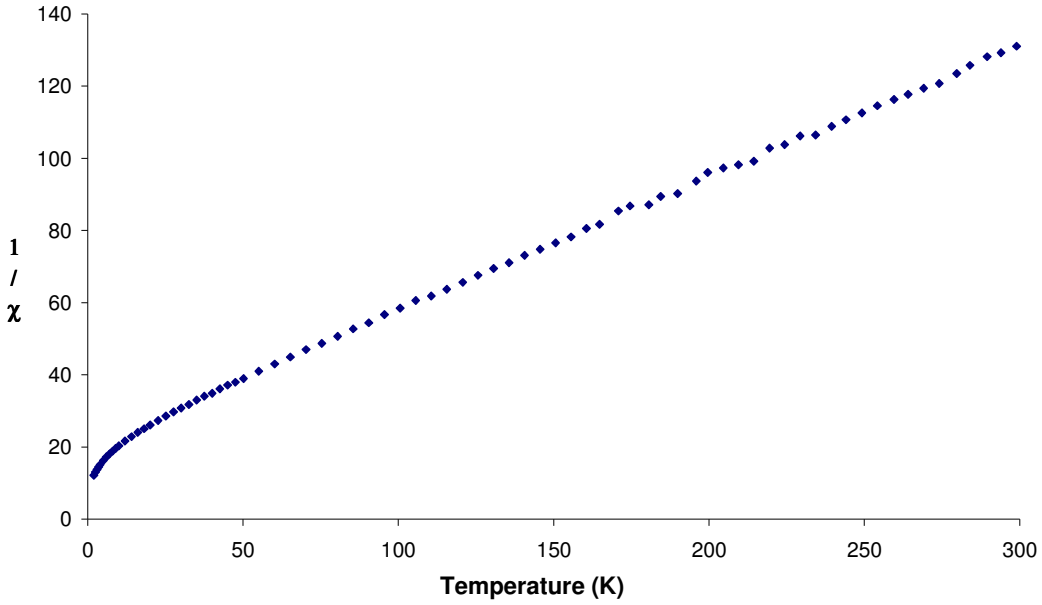


**Figure 3.18 - 1/χ plotted against temperature for 300 K – 2 K at 1 T**

The effective magnetic moment calculated from the experimental data was 2.15 ± 0.05 $\mu_B$. This effective magnetic moment is significantly reduced with respect to the free ion value for uranium(III) (3.7 $\mu_B$) and can be attributed to the magnetic coupling between the uranium ions.

In Figure 3.19, the effective magnetic moment was plotted against absolute temperature and shows the comparison between the experimental data and the modelled plots for magnetically isolated, dimeric and polymeric structures.

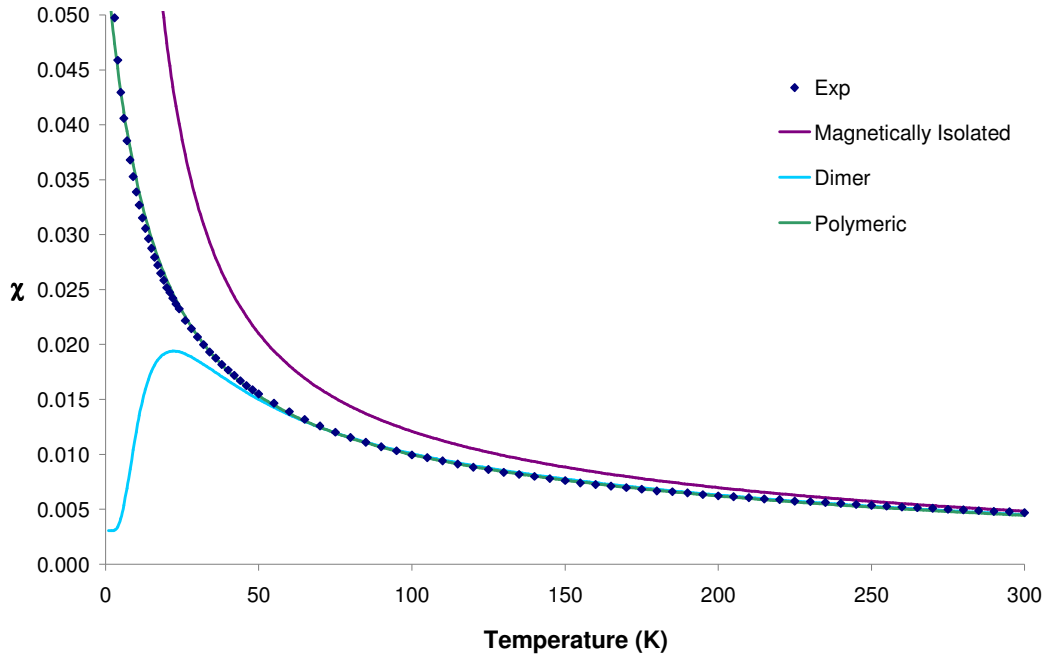


**Figure 3.19 - Comparison of models to experimental data of $[(UBH_4)_2(L^{Et})]$ between 300 – 2 K at 1 T**

As can be seen from Figure 3.19, the magnetic calculation for a polymeric chain model is the best fit for the experimental data. When a dimer is modelled the model fails at low temperatures but is in good agreement at higher temperatures. The dimer model does not have a good fit with the experimental at any temperatures.

Other boron groups $KBEt_3H$ and $KBPh_4$, were used in attempts to replace the iodides in $[(UI)_2(L^{Et})]$, in particular to produce a more crystalline form. White precipitate, presumably KI was observed in both cases, although no single crystals suitable for X-ray diffraction studies were grown. No further characterisation was carried out.

### 3.4.3 Preparation of $[(UH)_2(L^{Et})]$

Using a phosphorus donor, it was postulated that the $BH_3$ unit could be removed from $[(UBH_4)_2(L^{Et})]$ to generate a uranium hydride. Metal hydrides have been generated previously in this way, see Chapter 1.4.[34]

An excess of a 0.02 M solution of $PMe_3$ in toluene was added to a solution of $[(UBH_4)_2(L^{Et})]$ in toluene. The resultant mixture was heated to 80 °C for 16 hours

after which the volatiles were removed and the solid washed in cold toluene yielding a brown/yellow solid. The infrared spectrum showed a lack of B-H stretches, but new U-H stretching modes were not identified. An IR spectrum was recorded in hexachloro-1,3-butadiene to be able to observe the regions usually covered by nujol at 1465-1450 and 1380-1370 $cm^{-1}$, as a U-H stretch might reside in these regions. The spectrum did show stretches in this region however it was unclear which may be attributed to the desired product $[(UH)_2(L^{Et})]$.

The reaction to remove the BH3 group using t-butyl isocyanide was also investigated; however, two equivalents of *t*-BuNC did not appear to remove the $BH_3$ units by IR analysis.

### 3.4.4 Preparation of $[(UCl_2)_2(L^{Et})]$

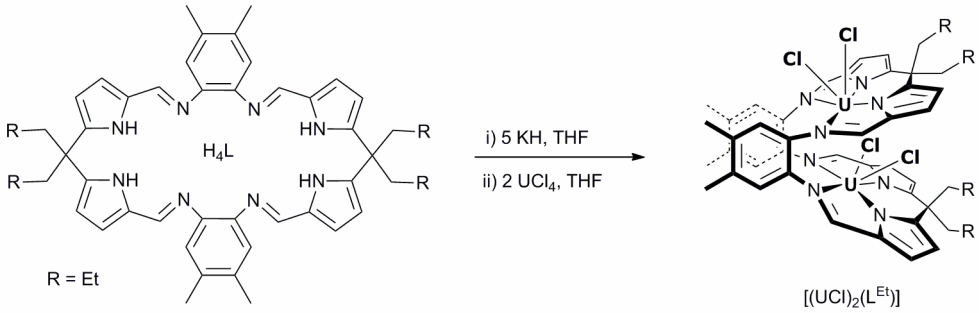


**Equation 3.4**

The preparation of the tetravalent diuranium complex, $[(UCl_2)_2(L^{Et})]$, was undertaken using the same methodology as that for $[(UI)_2(L^{Et})]$, Equation 3.4. The polypyrrolic ligand was first deprotonated using a slight excess of KH, producing the potassium salt quantitatively. The potassium salt in THF was then added to $UCl_4$ at -78 ºC, and allowed to warm to room temperature overnight. The resulting red solution was isolated from KCl by filtration, concentrated and layered with hexane and cooled to -78 ºC. The resulting yellow solid of $[(UCl_2)_2(L^{Et})]$ was isolated in an 81%yield.

The elemental analysis results supported the isolation of the $[(UCl_2)_2(L^{Et})]$ complex. No traces of $[U(L^{Et})]$ were found by $^1H$ NMR spectroscopy. The oxidation state of uranium(IV) was confirmed by the weak absorption shown in the UV-vis spectrum in THF where the $\lambda_{max}$ is 1180 nm and ε is 370.7 $dm^3$ $mol^{-1}$ $cm^{-1}$. The infrared spec-

trum shows a slight difference to that of the trivalent diuranium complexes but indicates that complexation of two uranium atoms has occurred as no N-H stretches were observed and the C=N stretches were found at 1575 $cm^{-1}$ compared to 1572 $cm^{-1}$ in $[(UI)_2(L^{Et})]$. No single crystals suitable for X-ray diffraction studies were grown. Although no magnetic data was obtained for $[(UCl_2)_2(L^{Et})]$, it could be postulated that it has a polymeric structure similar to that of $[(UI)_2(L^{Et})]$.

### 3.4.5 Synthesis of $[(CeI)_2(L^{Et})]$

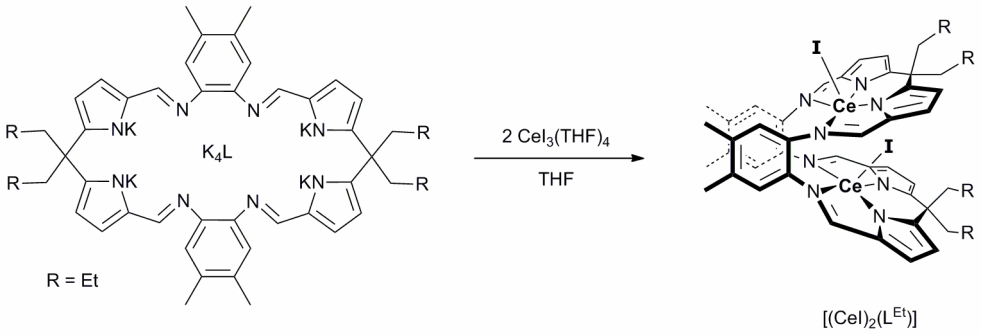


**Equation 3.5**

The reaction between $K_4L^{Et}$ and $CeI_3(THF)_4$ in THF at 70°C for 16 hours afforded $[(CeI)_2(L^{Et})]$ as a the dark yellow solid in an 66% yield, Equation 3.5. The $^1H$ NMR spectrum of the complex is observed over the range of 13 to -21 ppm and therefore indicates that the complex is paramagnetic and still cerium(III); these data are characteristic of a symmetric complex with 13 resonances and the $^{13}C\{^1H\}$ NMR spectrum also suggests a symmetric complex with 14 resonances (166 – 6 ppm). The elemental analysis suggests the proposed formula although the nitrogen value was low, which may be a result of poor combustion. No single crystals suitable for X-ray diffraction studies were grown, suggesting that the complex may be polymeric similar to the uranium analogue. Studies on the magnetic properties of this Ce complex would be interesting to carry out to compare to the uranium(III) analogue.

## 3.5 Neptunium Chemistry

Neptunium is the first transuranic element and is not found naturally in the environment. The element was first isolated in 1940 by McMillan and Abelson at Berkeley,

USA, who bombarded uranium with neutrons produced from a cyclotron. The electronic structure is $[Rn]5f^4 6d^1 7s^2$. Neptunium can exist in the oxidation states of +2 to +7, but +5 is the most common. There are seventeen isotopes of neptunium, with the most long lived being $^{236}Np$ ($1.55 \times 10^5$ years) and $^{237}Np$ ($2.14 \times 10^6$ years),[35] the latter being used in chemistry. Neptunium undergoes α, and β decay and so great care must be taken when handling these elements.

All work undertaken with Neptunium was carried out at the ITU (The Institute of Transuranium Elements) under strict control. The work was carried out under collaboration with Prof. Roberto Caciuffo and his colleagues; Dr Christos Apostolidis, Dr Nicola Magnani, Dr Eric Colineau and Dr Jean-Christophe Griveau. The Institute of Transuranium Elements (ITU) is one of the seven institutions of the Joint Research Commission of the European Union. It focuses its research on the Actinides, from basic properties to safety in the nuclear fuel cycle. Entrance and exit for all personnel to the ITU is through a metal and radiation detector. Everyone entering the ITU has had security checks and a full medical examination. Before embarking on research a body and lung count is undertaken to establish a normal radiation level for you and these experiments are conducted in a sealed room to prevent interference by background radiation. The body and lung count are carried out again at the end of the time at ITU to ensure no contamination has occurred. At the entrance to the contamination zone, there is a full body contamination monitor to prevent radiation contamination being transported out of the 'hot' zone (where these radioactive elements are handled). All materials going in and out must be monitored. Inside the contamination zone all personnel must wear all white and these clothes must be left on site for professional cleaning. Everyone must also wear a quartz fibre dosimeter and a film badge dosimeter for personal radiation monitoring.

**Figure 3.20 – The ITU**

All transuranic materials must be handled in a reduced pressure glove box which has constant radiation monitoring, as seen in Figure 3.21. All material leaving the glove box must be double-bagged and monitored for contamination.

**Figure 3.21 – Glove box at ITU**

The combination of the restrictions due to the radiation of the elements and the air and moisture sensitivity of the complexes formed make this a difficult area of research.

Infrared and far-infrared (FIR) samples were made by dilution of the appropriate Np complex in KBr (IR) or polyethylene powder (FIR) and compression into a tablet for data collection. Samples for solid state NIR spectra were made by dilution of a small amount of the Np complex in polyethylene powder and compression into a tablet.

### 3.5.1 Synthesis of $[(NpI)_2(L^{Et})]$

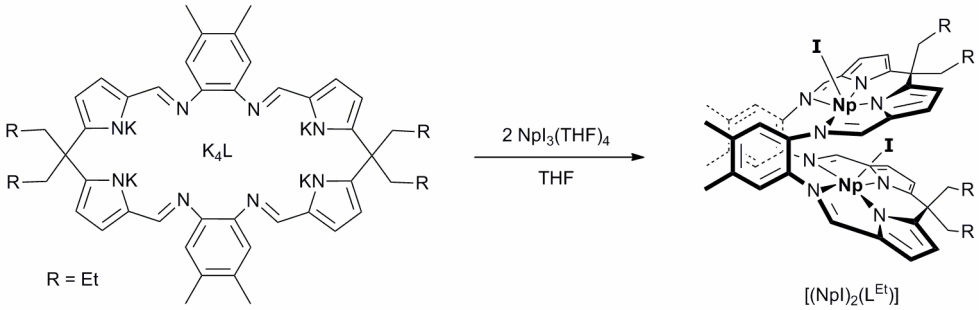


**Equation 3.6**

The starting material $NpI_3(THF)_4$, was synthesised using the route published by Clark and co-workers in 1994.[29] The reaction between $K_4L$ and 2 equivalents of $NpI_3(THF)_4$ in THF at room temperature yielded the complex $[(NpI)_2(L^{Et})]$ as a dark red microcrystalline solid with a yield of 98 %, Equation 3.6. The synthesis is similar to the uranium analogue with the reaction between the neptunium metal and stoichiometric amounts iodine in THF forming the terracotta coloured solid of $NpI_3(THF)_4$. The preparation is much less temperature controlled compared to the synthesis of $UI_3(THF)_4$, with the reaction being carried out at room temperature.

This is the first low valent bi-metallic neptunium complex reported in the literature. Variable temperature magnetic susceptibility studies using a 57mg sample showed that there may be magnetic superexchange between the 5*f* centres.

Figure 3.22 shows the magnetic susceptibility and the effective magnetic moment with respect to temperature. The effective magnetic moment shows at high

temperature a linear dependence with decreasing temperature and in the low temperature region shows temperature independent paramagnetism. The effective magnetic moment calculated from the experimental data was 2.43 $\mu_B$ which is reduced compared to the free ion moment of 2.68 $\mu_B$.[36]

The magnetic susceptibility shows an overall increase with decreasing temperature. Below 50 K the magnetic susceptibility rapidly increases.

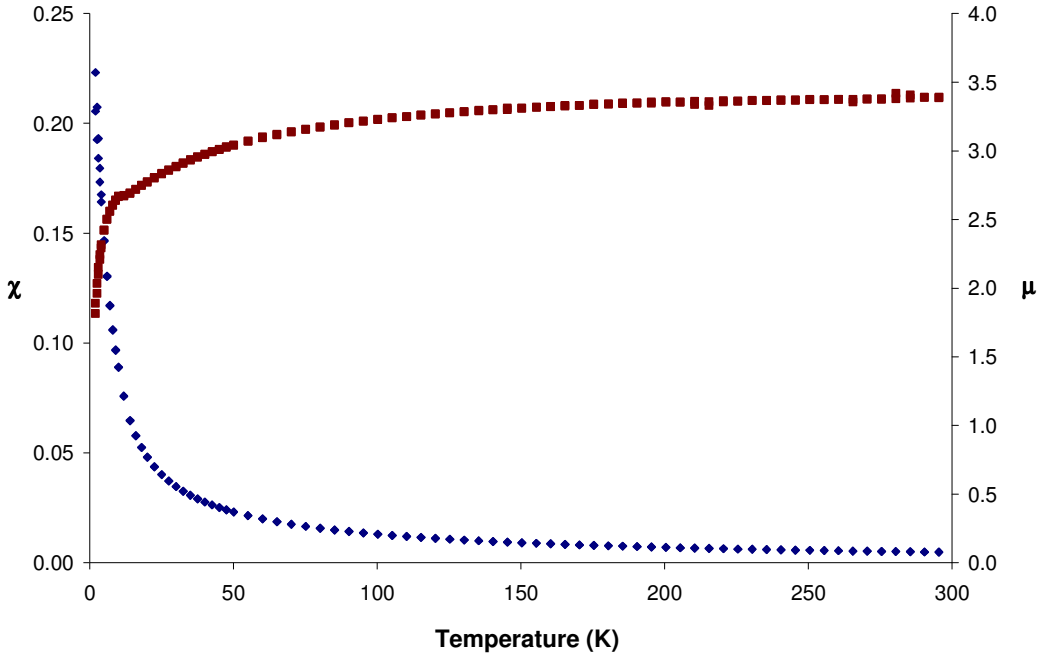


**Figure 3.22 - Magnetic susceptibility *χ* (red) and effective magnetic moment *μ* (blue) in B.M. for 300 K – 2 K at 1 T**

When the reciprocal of magnetic susceptibility is plotted, Figure 3.23, it displays Curie Weiss paramagnetic behaviour.

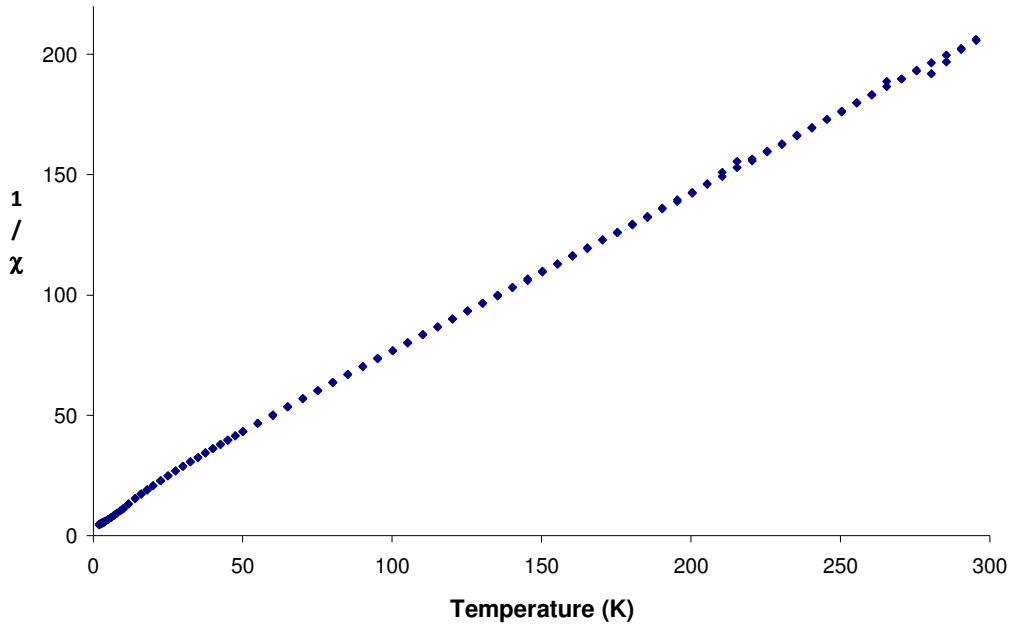


**Figure 3.23 - 1/χ plotted against temperature for 300 K – 2 K at 1 T**

In Figure 3.24, the effective magnetic moment was plotted against absolute temperature and shows the comparison between the experimental data and the modelled plots for ground state doublet and ground state level separated by 206 K from the first excited state structures.

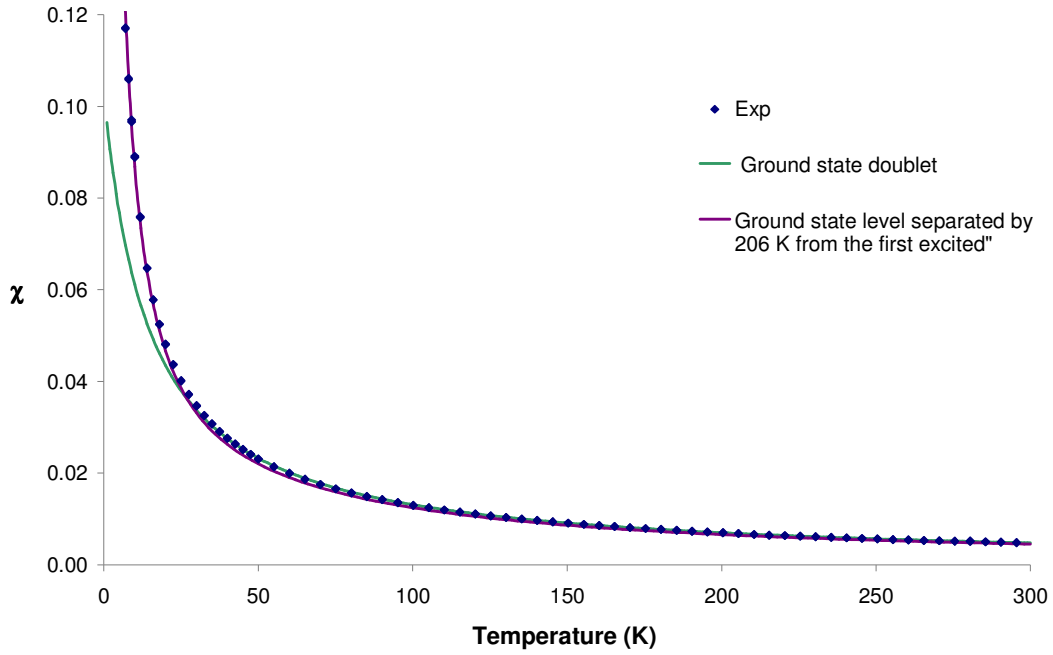


**Figure 3.24 - Comparison of models to experimental data of [(NpI)$_2$(L$^{Et}$)] between 300 – 2 K at 1 T**

The experimental data was modelled using the ligand-field interaction derived from the free ion. The first model was based on a $|J_z = \pm 4\rangle$ a ground state doublet, which gave a good fit at high temperature but failed at low temperatures. The model was then altered to a $|J_z = \pm 3\rangle$ ground state separated by 206 K to the first excited state of $|J_z = \pm 2\rangle$. The latter model was a better fit at low temperatures although a slight discrepancy still exists below 5 K which could be due to coupling between the Np centres; however it is a least one order of magnitude smaller than that shown in the uranium complexes. This suggests that the complex [(NpI)$_2$(L$^{Et}$)] is polymeric and is similar to the structures of the uranium complexes. The smaller superexchange coupling could be due to the smaller radial extension of the neptunium atom compared to the uranium atoms.

As elemental analysis was unavailable other methods were used to determine the Np content in [(NpI)$_2$(L$^{Et}$)]. Radiometric analysis (α from $^{237}$Np and γ from $^{237}$Np and its $^{233}$Pa daughter) and gravimetric analysis were carried out, giving 33.22 % and 32.5 % respectively which supported the percentage of neptunium calculated for [(NpI)$_2$(L$^{Et}$)] of 32.90 %.

Infrared studies on $[(NpI)_2(L^{Et})]$ showed similar characteristics to that of $[(UI)_2(L^{Et})]$, showing strong C=N stretches at 1575 and 1513 $cm^{-1}$.

Neptunium coordination complexes are sparse in the literature, as it is a relatively new field of research. Despite the first preparation of neptunium(III) halides in 1972, the research in this area has been held up by the problems that the handling of neptunium poses.[37] With the ease of synthesis of $NpI_3(THF)_4$ and $Np\{N(SiMe_3)_2\}_3$, the low valent chemistry of neptunium has been opened up.[29, 38]

Neptunium(III) is more stable towards oxidation than uranium(III) in the absence of oxygen, in aqueous solutions.[39] $Np(COT)_2$ was synthesised from $NpCl_4$ and two equivalents of $K_2COT$ in THF, and shows similar structural characteristics as the uranium analogue.[40] Later the neptunium(III) $[(K)Np(COT)_2]$ complex was isolated from the reaction of $NpBr_3$ with two equivalents of $K_2COT$ in THF and magnetism studies showed two temperature dependent paramagnetism regions, the lower temperature one having a $\mu_{eff}$ of 1.04 BM at 5.5 K.[41]

Recently magnetic studies of neptunium clusters were carried out in collaboration between the University of Manchester and the ITU.

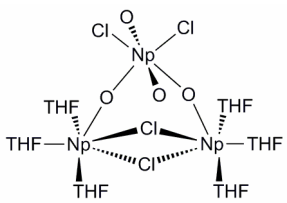


**Figure 3.25 - $[\{Np^{VI}O_2Cl_2\}\{Np^{V}O_2Cl(THF)_3\}_2]$**

The first polymetallic transuranic complex was synthesised and found to show superexchange coupling between the neptunium ions. The complex $[\{Np^{VI}O_2Cl_2\}\{Np^{V}O_2Cl(THF)_3\}_2]$ was synthesised by the partial oxidation of $\{NpO_2Cl_2(THF)\}_n$ in THF. The mixed valence trinuclear neptunium complex has been shown to contain two $5f^2$ ions and one $5f^1$ ion by variable temperature SQUID measurements. These ions have been shown to display slow relaxation magnetism and effective superexchange interactions.

Previous Schiff-base complexes of neptunium are restricted to one described by Sessler.[42] An expanded porphyrin allowed the incorporation of neptunyl into its cavity, see Figure 3.26.

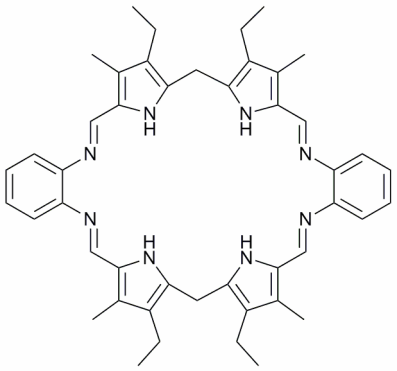

**Figure 3.26 – The expanded porphyrin shown to enclose neptunyl**

When a source of neptunyl(VI) is used, an immediate colour change from yellow to blue was observed. This was postulated to be due to the reduction of the neptunyl to its pentavalent state and the accompanying oxidation of the ligand forming an extended π system. This was supported by the use of a neptunyl(V) source which showed much slower reaction times as there is no built in oxidant and the ligand is oxidised by $O_2$ slowly over time.

The oxidised form of hexaphyrin(1.0.1.0.0.0) was also found to complex neptunyl. A single crystal X-ray diffraction study showed the neptunium was coordinated in the centre of the expanded porphyrin, Figure 3.27.

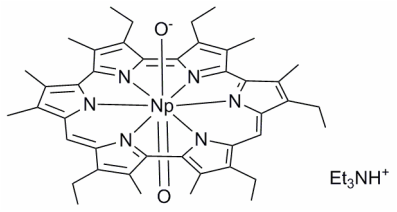


**Figure 3.27 – [24]hexphyrin(1.0.1.0.0.0) neptunyl complex**

The complex was synthesised from neptunyl(V) chloride and oxidised macrocycle in the presence of a base.

## 3.6 Conclusions

Although no single crystal X-ray diffraction studies have been carried out on these complexes, the data obtained from the study of their magnetic properties have given an indication of possible solid state structures. The use of other techniques to form a model of the structure is not common. The characteristics of $[(UI)_2(L^{Me})]$, $[(UI)_2(L^{Et})]$, $[(UBH_4)_2(L^{Et})]$, $[(UCl_2)_2(L^{Et})]$ and $[(NpI)_2(L^{Et})]$ have been studied and thought to be of a polymeric structure. $[(UBH_4)_2(L^{Et})]$ has been reacted with $PMe_3$ in an attempt to form $[(UH)_2(L^{Et})]$ with inconclusive results.

## 3.7 References


1. R. Sessoli and A. K. Powell, *Coord. Chem. Rev.*, 2009, **253**, 2328-2341.
2. G. Karotsis, M. Evangelisti, S. J. Dalgarno and E. K. Brechin, *Angew. Chem. Int. Ed.*, 2009, **48**, 9928.
3. K. T. Moore and G. van der Laan, *Reviews of Modern Physics*, 2009, **81**, 235-298.
4. N. M. Edelstein and G. H. L. Lander, in *The Chemistry of the Actinide and Transactinide Elements*, eds. J.J. Katz, L.R Morss, J.Fuger and N.Edelstein, Springer, 2006, pp. 2225-2306.
5. T. Durakiewicz, J. J. Joyce, G. H. Lander, C. G. Olson, M. T. Butterfield, E. Guziewicz, C. D. Batista, A. J. Arko, L. Morales, K. Mattenberger and O. Vogt, *Physica B: Condensed Matter*, 2006, **378-380**, 1033-1034.
6. M. B. Brodsky, *Rep. Prog. Phys.*, 1978, **41**, 1547.
7. S. T. Liddle and D. P. Mills, *Dalton Trans.*, 2009, 5592-5605.
8. S. G. Minasian, J. L. Krinsky, V. A. Williams and J. Arnold, *J. Am. Chem. Soc.*, 2008, **130**, 10086-10087.
9. M. Porchia, U. Casellato, F. Ossola, G. Rossetto, P. Zanella and R. Graziani, *Chem. Commun.*, 1986, 1034-1035.
10. S. G. Minasian, J. L. Krinsky, J. D. Rinehart, R. Copping, T. Tyliszczak, M. Janousch, D. K. Shuh and J. Arnold, *J. Am. Chem. Soc.*, 2009, **131**, 13767-13783.
11. R. S. Sternal and T. J. Marks, *Organometallics*, 1987, **6**, 2621-2623.

12. A. Bucaille, T. Le Borgne, M. Ephritikhine and J.-C. Daran, *Organometallics*, 2000, **19**, 4912-4914.
13. M. J. Monreal, C. T. Carver and P. L. Diaconescu, *Inorg. Chem.*, 2007, **46**, 7226-7228.
14. S. T. Liddle, J. McMaster, D. P. Mills, A. J. Blake, C. Jones and W. D. Woodul, *Angew. Chem., Int. Ed. Engl.*, 2009, **48**, 1077-1080.
15. B. M. Gardner, J. McMaster, W. Lewis and S. T. Liddle, *Chem. Commun.*, 2009, 2851-2853.
16. W. J. Evans, *Inorg. Chem.*, 2007, **46**, 3435-3449.
17. M. Kaupp, B. Metz and H. Stoll, *Angew. Chem., Int. Ed.*, 2000, **39**, 4607-4609.
18. I. Korobkov, S. Gambarotta and G. P. A. Yap., *Angew. Chem. Int. Ed.*, 2002, **41**, 3433-3436.
19. I. Korobkov, S. Gambarotta, G. P. A. Yap, L. Thompson and P. J. Hay, *Organometallics*, 2001, **20**, 5440-5445.
20. J. G. Brennan, R. A. Andersen and A. Zalkin, *Inorg. Chem.*, 1986, **25**, 1761-1765.
21. R. K. Rosen, R. A. Andersen and N. M. Edelstein, *J. Am. Chem. Soc.*, 1990, **112**, 4588-4590.
22. E. J. Schelter, D. E. Morris, B. L. Scott, J. D. Thompson and J. L. Kiplinger, *Inorg. Chem.*, 2007, **46**, 5528-5536.
23. L. P. Spencer, E. J. Schelter, P. Yang, R. L. Gdula, B. L. Scott, J. D. Thompson, J. L. Kiplinger, E. R. Batista and J. M. Boncella, *Angew. Chem.-Int. Ed.*, 2009, **48**, 3795-3798.
24. E. J. Schelter, R. L. Wu, B. L. Scott, J. D. Thompson, D. E. Morris and J. L. Kiplinger, *Angew. Chem. Int. Ed.*, 2008, **47**, 2993-2996.
25. E. J. Schelter, J. M. Veauthier, C. R. Graves, K. D. John, B. L. Scott, J. D. Thompson, J. A. Pool-Davis-Tournear, D. E. Morris and J. L. Kiplinger, *Chem. Eur. J.*, 2008, **14**, 7782-7790.
26. G. Nocton, J. Pecaut and M. Mazzanti, *Angew. Chem. Int. Ed. Engl.*, 2008, **47**, 3040-3042.

27. B. S. Newell, A. K. Rappè and M. P. Shores, *Inorg. Chem.*, 2010, **49**, 1595-1606.
28. M. Volpe, S. D. Reid, A. J. Blake, C. Wilson and J. B. Love, *Inorg. Chim. Acta*, 2007, **360**, 273-280.
29. L. R. Avens, S. G. Bott, D. L. Clark, A. P. Sattelberger, J. G. Watkin and B. D. Zwick, *Inorg. Chem.*, 1994, **33**, 2248-2256.
30. P. L. Arnold, N. A. Potter, N. Magnani, C. Apostolidis, J.-C. Griveau, E. Colineau, A. Morgenstern, R. Caciuffo and J. B. Love, *Inorg. Chem.*, 2010, **49**, 5341-5343.
31. D. F. Evans, *J. Chem. Soc.*, 1959, 2003-2005.
32. A. Devoille and J. Love, *manuscript in preparation*, 2011.
33. T. J. Marks, W. J. Kennelly, J. R. Kolb and L. A. Shimp, *Inorg. Chem.*, 1972, **11**, 2540-2546.
34. D. Baudry, P. Charpin, M. Ephritikhine, M. Lance, M. Nierlich and J. Vigner, *Chem. Commun.*, 1987, 739-740.
35. S. Cotton, *Lanthanide and actinide chemistry*, Wiley, 2006.
36. E. Colineau, F. Wastin, J. P. Sanchez and J. Rebizant, *J. Phys.: Condens. Matter*, 2008, 075207.
37. D. Brown and J. Edwards, *J. Chem. Soc., Dalton Trans.*, 1972, 1757-1762.
38. D. G. Karraker, *Inorg. Chim. Acta*, 1987, **139**, 189-191.
39. J. I. Bullock and M. E. King, *J. Chem. Soc., Dalton Trans.*, 1975, 1360.
40. D. G. Karraker, J. A. Stone, E. R. Jones and N. Edelstein, *J. Am. Chem. Soc.*, 1970, **92**, 4841.
41. D. G. Karraker and J. A. Stone, *J. Am. Chem. Soc.*, 1974, **96**, 6885-6888.
42. J. L. Sessler, P. J. Melfi, E. Tomat, W. Callaway, M. T. Huggins, P. L. Gordon, D. W. Keogh, R. W. Date, D. W. Bruce and B. Donnio, *J. Alloys Compd.*, 2006, **418**, 171-177.

# Chapter 4: Adducts of Uranium Halides

Following the attempts to substitute the iodide ligand in $[(UI)_2(L)]$, a methodology to substitute the iodide before complexation with the Schiff base polypyrrolic macrocycle was developed. During this research the synthesis of the starting material $UI_3$ was also investigated as was the use of oxygen and nitrogen donor macrocycles to stabilise $UI_3$ rather than coordinating solvents.

## 4.1 Uranium halides

### 4.1.1 Uranium trihalide

To date, the chemistry of uranium(IV) has been more heavily investigated than its uranium(III) counterpart. One barrier to uranium(III) chemistry was the lack of soluble, easy to synthesise starting materials. This all changed when the synthesis of $UI_3(THF)_4$ was developed.[1-3]

$UCl_3(THF)_x$ which is made *in situ*, from $UCl_4$ and a reductant (e.g. sodium amalgam) in THF, is a poorly understood material, limiting its use in organometallic chemistry.[4-6] Unsolvated uranium trichloride is polymeric and insoluble in all organic solvents, restricting its use. However, while the THF imparts solubility to the metal centre, the presence of THF can restrict low valent uranium chemistry. For example, uranium is known to ring-open THF, Equation 4.1, and as such the synthesis of $UI_3(THF)_4$ is carried out below 10 ºC to minimize the formation of ring-opened products.[2, 7, 8]

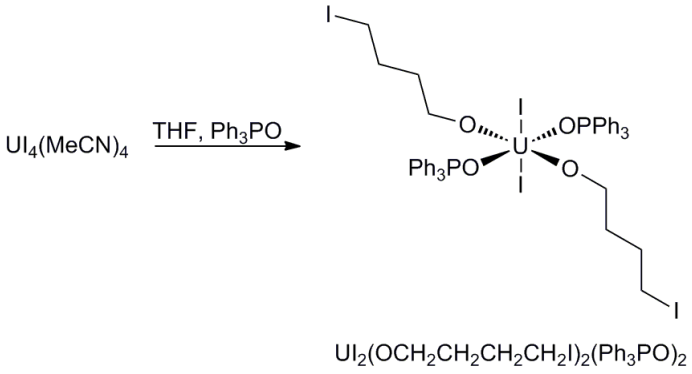


**Equation 4.1**

Therefore, the isolation of an unsolvated uranium(III) starting material is of great importance. Unsolvated $UI_3$ has been prepared but not by a convenient route. The original route to this starting material was the reduction of $UI_4$ using Zn at 870 K.[9, 10] Cloke and co-workers has recently optimised the solid state synthesis of $UI_3$ which was first reported by Corbett in 1983. The method involves the reaction of uranium metal and mercuric iodide at 320°C in a sealed ampoule.[11, 12] Evans and co-workers has recently published a gentler synthesis, in which $UI_3$ is made from uranium and iodide in stoichiometric quantities. The process is mercury-free, in grease free environment and involves heating with a Bunsen flame using reaction vessels attached by tubing.[13]

The use of unsolvated $UI_3$ has permitted the synthesis of complexes unobtainable in the presence of strong donor solvents. For example, Cloke and co-workers have used $UI_3$ in the synthesis of an unsolvated pentalene complex activating dinitrogen, and a tri-metallic system activating diethyl ether. [12, 14] The Evans' group has used $UI_3$ in developing new syntheses for various tetramethylcyclopentadienyl uranium halides.[13]

The characterisation of $UI_3$ is somewhat difficult, due to the formation of adducts in solution. The use of NMR spectroscopy is restricted by the lack of carbon and hydrogen atoms. The U-I stretch is not within the normal KBr-accessible IR region, therefore IR spectroscopy for $UI_3$ cannot be used as a characterising handle. One of the only traditional means of characterising $UI_3$ is the elemental analysis of the percentage of uranium and iodine in the solid.

The route commonly used in organometallic laboratories is the synthesis of $UI_3(THF)_4$ was developed by Clark and co-workers. The method uses a slight excess of amalgamated uranium turnings and elemental iodine in THF, using low temperatures (at or below 10 °C) to prevent any ring-opening reactions. The reaction is then stirred for 24 hours and forms $UI_3(THF)_4$ cleanly and can be carried out on a large scale.

### 4.1.2 Uranium tetrahalide

Uranium tetrahalide chemistry is dominated by $UCl_4$, which can be synthesised in high yields and relatively safely.[15] The original synthesis for $UCl_4$ involved the heating of $UO_3.2H_2O$ and hexachloropropene to high temperatures in a 'one-pot' reaction, which can lead to increased pressure inside the vessel which has the potential to cause accidents.[16] This procedure was modified in 2002 where the $UO_3.2H_2O$ is added in portions to the hot hexachloropropene allowing more control over the radical initiated reaction.[15] Uranium tetraiodide is thermally unstable at room temperature, and decomposes slowly to uranium triiodide and iodine.[1] The simplest method of synthesising $UI_4$ is using a vessel that consists simply of two sections of glass tubing joined through a constriction.[17] Iodine, in 50% excess, is placed with uranium metal turnings in one section and the whole of the vessel evacuated. The empty section is heated to 140 °C and the iodine-uranium mixture is then gradually heated to 530 °C by means of a second furnace, and maintained at this temperature for several hours. On simultaneous cooling of the two sections the excess of iodine is quantitatively sublimed out of the section containing uranium tetraiodide. Recently $UI_4(NCMe)_4$ and $UI_4(NCPh)_4$ have been synthesised, thereby stabilising $UI_4$ with nitrile ligands.[18]

The complexes $UI_4(tppo)_2$ (tppo = triphenylphosphine oxide), $UI_4(tdpo)_2$ (tdpo= tris(dimethylamino)phosphine oxide) and $UI_4(tpyrpo)_2$ (tpyrpo= tris(pyrrolidinyl)phosphine oxide) have been prepared and IR and electronic spectra of both the solid and solutions are reported for them, but no solid state structure was ever recorded.[19]

## 4.2 New Preparation of $UI_3$ and $UI_4(OEt_2)_2$

A convenient method to the synthesis of unsolvated $UI_3$ is much needed. Recently, Evans and co-workers published a new method but this has proved problematic to replicate in our laboratory.[13]

The preparation of unsolvated plutonium triiodide by Neu and co-workers led us to try to develop an analogous reaction with uranium.[20] As such, uranium turnings were found to react with elemental iodine in ether at room temperature, with sonication and/or stirring, over a period of days to afford $UI_3$ or $UI_4(OEt_2)_2$ in the case of diethyl ether or $UI_4(OBu_2)$ in the case of dibutyl ether and depending on the stoichiometry or ether solvent. This is the first room temperature, thus safe and convenient synthesis of $UI_3$.

Aspects of the work in this section were carried out in collaboration with Dr. Christopher D. Carmichael.[21]

### 4.2.1 Synthesis of $UI_3$

$$U + I_2 \xrightarrow{\text{Diethyl Ether}} UI_3$$

**Equation 4.2**

The reaction between cleaned uranium turnings and iodine was undertaken in diethyl ether. After several days of stirring and sonication, the uranium turnings were no longer visible and a dark purple black solid formed, the red diethyl ether solution was filtered away and the solid washed with diethyl ether and dried (N.B. $UI_3$ sparingly soluble in diethyl ether). The reaction time is highly dependent on the efficiency of the stirring. Although the isolated solid was in a quantitative yield, a small amount of impurities were present. These trace impurities can be isolated by the extraction of the $UI_3$ by coordinated solvents, e.g. THF, pyridine and DME, leaving the black insoluble residue in 1-2% by weight. This impurity is thought to be the reaction product of the cleavage of ether by the uranium(III) centre, which has been seen recently by Cloke and co-workers with possibly some residual metallic impurities.[14] The elemental analysis supports this theory as carbon and hydrogen were present in

trace amounts as well as the uranium and iodide being approximately 3% below expected values. The use of amalgamated uranium turnings instead of cleaned turnings in the reaction lead to significantly lower yields of $UI_3$ and the increased quantity of $UI_4(OEt_2)_2$ remaining in the solution. It is postulated that the presence of mercury disfavours the reduction of $UI_4(OEt_2)_2$ to $UI_3$ at the surface of the uranium metal.

To verify that the compound formed in the above reaction contained uranium(III) and not uranium(IV), the reaction of the $UI_3$ with three and four equivalents of sodium-2,4,6-tri-*tert*-butyl-phenolate was undertaken in a NMR tube and monitored by $^1H$ NMR spectroscopy.

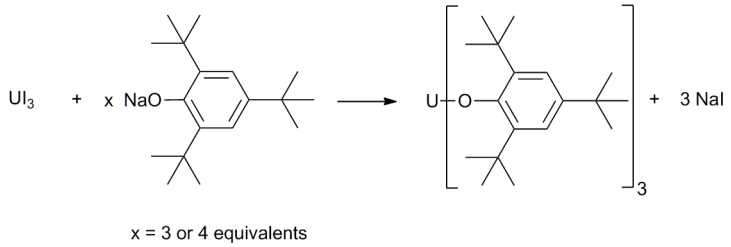


**Equation 4.3**

The reaction of $UI_3$ with three equivalents of sodium-2,4,6-tri-*tert*-butyl-phenolate formed exclusively $[U(OC_6H_2{}^tBu_3)_3]$. The reaction of four equivalents of sodium-2,4,6-tri-*tert*-butyl-phenolate with $UI_3$ produced $[U(OC_6H_2{}^tBu_3)_3]$ with one equivalent of sodium-2,4,6-tri-*tert*-butyl-phenolate left unreacted. The $[U(OC_6H_2{}^tBu_3)_3]$ produced was characterised by $^1H$ NMR spectroscopy with three resonances at 16.40, 4.96 and -1.44 ppm which corresponded to the three environments for the paramagnetic complex.

The electronic absorption spectrum of $UI_3$ in THF confirmed the formation of $UI_3(THF)_4$. This is in excellent agreement with that previously reported with absorptions in the region of 800-1400 nm, see Figure 4.1.[2] The IR spectrum of $UI_3(THF)_4$ shows only the coordinated THF molecules, as the U-I stretch does not fall within the normal KBr-accessible IR region.[1]

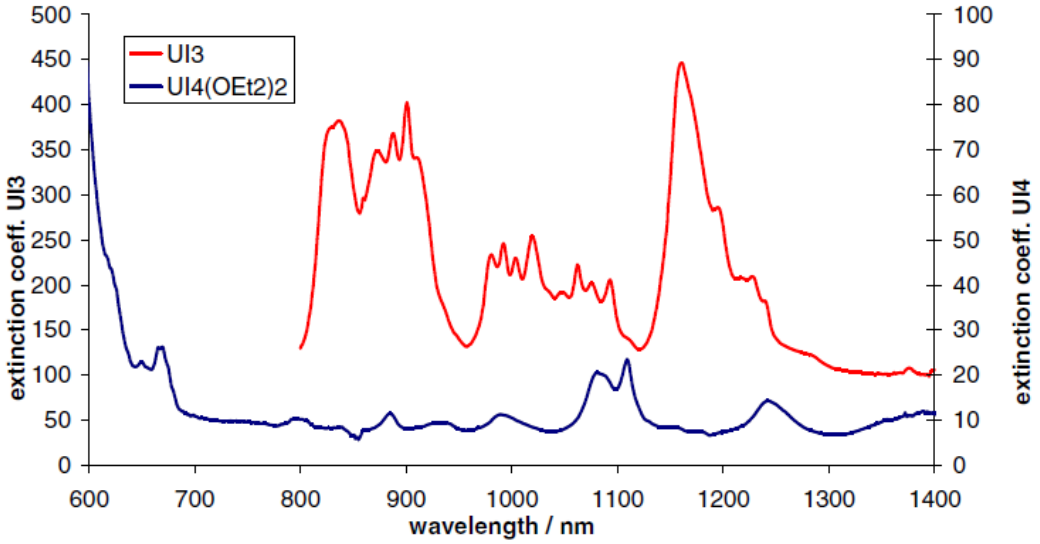


**Figure 4.1 –NIR-UV-vis spectrum of $UI_3$ (in THF) and $UI_4(OEt_2)_2$ (in $Et_2O$).**

To further confirm that the synthesis of $UI_3$ by our revised route had been successful, the synthesis of $[U\{(NSiMe_3)_2\}_3]$ was carried out, on a small scale in a 63% yield.

### 4.2.2 Synthesis of $UI_4(OEt_2)_2$

During the synthesis of $UI_3$, a bright red solution was observed which was thought to be an intermediate of the reaction. This proceeded to react with more uranium turnings to afford the insoluble $UI_3$. A dark red, octahedral crystal isolated from the intermediate solution was studied by X-ray crystallography, and showed that this intermediate was the U(IV) complex $UI_4(OEt_2)_2$.

The intermediacy of $UI_4(OEt_2)_2$ in the synthesis of $UI_3$ is supported further by the fact that the reaction of $UI_4(OEt_2)_2$ and uranium turnings which leads to $UI_3$ in a 93% yield, Scheme 4.1.

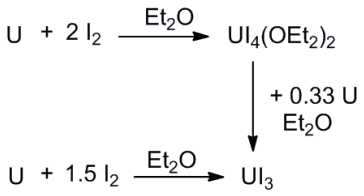


**Scheme 4.1 – Reactivity of uranium with iodine.**

$UI_4(OEt_2)_2$ was synthesised from the reaction of uranium turnings and two equivalents of iodine in diethyl ether, with vigorous stirring and sonication over 48 h. The bright red microcrystalline solid was isolated by filtration from a concentrated solution in a 77 % yield. $UI_4(OEt_2)_2$ is sensitive to the loss of diethyl ether, and is thermally unstable and unstable to long periods in solution (except diethyl ether), changing from red to black. Elemental analysis supported the stoichiometry of the bulk material. In solution the $^1H$ NMR spectrum in $C_6D_6$ shows two paramagnetically-shifted broad resonances at -10.45 and -22.54 ppm and are assigned to the methyl and methylene protons of the coordinated diethyl ether. The electronic absorption spectrum obtained in diethyl ether shows several weak and broad absorptions typical of a six-coordinate uranium(IV) species, see Figure 4.1.[19] A value of 2.15 $\mu_B$ was calculated using the solution Evans' method. This value is significantly lower than that calculated for a $^3H_4$ ground state of free uranium(IV) (3.58 $\mu_B$), but the magnetic moments reported for other uranium(IV) coordination complexes are normally lower, and usually in the range 2.5-2.8 $\mu_B$; the reduced values are attributed to the quenching of spin-orbit coupling.[22]

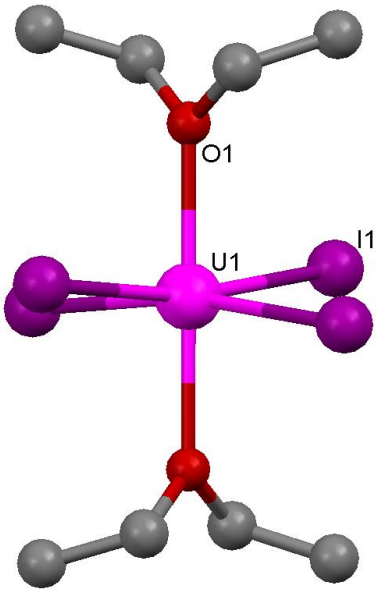


**Figure 4.2 – Ball and stick representations of the X-ray crystal structure of $UI_4(OEt_2)_2$, hydrogen atoms have been excluded for clarity.**

The solid state single crystal structure shows that the uranium centre adopts a distorted octahedral geometry with the diethyl ether ligands in a trans-orientation. $UI_4(OEt_2)_2$ crystallises in the space group *I*4/*acd*, which has high symmetry, meaning that the asymmetric unit cell only contains $U_{0.25}IOC_2H_5$. Due to diethyl ether being a weak donor, the uranium–iodide bond lengths (2.9614(6) Å), are short for uranium(IV) iodide complexes (2.9558(4) Å–3.0438(4) Å).[18, 19, 23] Interestingly, the iodides are distorted from the equatorial plane by 5° (all due to the symmetry operator). The U-O bond length is 2.366(8) Å and is similar to other uranium(IV) etherate complexes.[24-26] The coordination of diethyl ether to uranium complexes is uncommon with only three structurally characterised examples in the literature, $U(BH_4)_4(Et_2O)$, $[Fc(NSi\textit{t}BuMe_2)_2U(CH_2Ph)(OEt_2)][BPh_4]$ and the oxygen-bridged dimer $U_2Cl_2O_2$(1,2,3,4-tetramethyl-5-(2-pyridyl)-cyclopentadienide)$_2(Et_2O)_2$.[24-26]

The formation of both $UI_3$ and $UI_4(OEt_2)_2$ is heavily dependent on agitation. Reactions that do not use both sonication and vigorous stirring can take up five times longer than those using both agitation methods. This is thought to be due to the formation of the $UI_3$ at the surface of the uranium turnings preventing further reaction until the reaction surface is cleaned.

The use of $UI_4(OEt_2)_2$ as a source of $UI_4$ was shown by the synthesis of $UCp_3I$ in 71 % yield from the reaction of $UI_4(OEt_2)_2$ and 3 equivalents of NaCp.[27, 28]

Whilst our synthetic route was in press in Inorganic Chemistry, the Hayton Group published the synthesis of $UI_4(OEt_2)_2$ albeit *via* a different synthetic route in Dalton Transactions.[29] Identical characterisations of $UI_4(OEt_2)_2$ were reported.

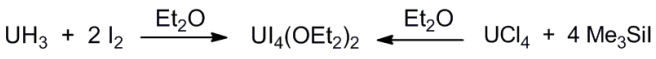


**Scheme 4.4 – Alternative synthesis of $UI_4(OEt_2)_2$.**

Hayton and co-workers report the formation of $UI_4(OEt_2)_2$ in a 78 % yield from the reaction of uranium hydride and 2 equivalents of iodine in diethyl ether, Scheme 4.4. The reaction is quick (4.5 h) and vigorous gas evolution is observed. An alternative synthesis was also reported from the reaction of $UCl_4$ with four equivalents of

trimethyliodosilane in diethyl ether. Again the reaction time is vastly reduced (3 h) compared with our synthetic method and an 86% yield. Although both methods are complete in shorter reaction times, the precursors must be synthesised. The group also investigated the synthesis $UI_4(OEt_2)_2$ from uranium metal and elemental iodine in diethyl ether. The reaction product was isolated after 24 hours as an oily red solid. The $^1H$ NMR spectrum contained resonances attributed to $UI_4(OEt_2)_2$ but also other unassigned resonances, and the method is not elaborated on. The solid state structure reported by Hayton for $UI_4(OEt_2)_2$, exhibited slight differences in bond lengths, possibly due to the data collected were from a larger crystal, (0.20 × 0.20 × 0.10 *c.f.* 0.12 × 0.07 × 0.04) resulting in better data and a better fit to the model. The differences in U-O bond lengths are marginal, with the difference being 0.008 Å (2.374(11) Å *c.f.* 2.366(8) Å) and an even smaller difference in the U-I bond lengths 0.0025 Å (2.9639(10) Å *c.f.* 2.9614(6) Å). Hayton has also investigated the reactivity of the U-I bonds within $UI_4(OEt_2)_2$.[30]

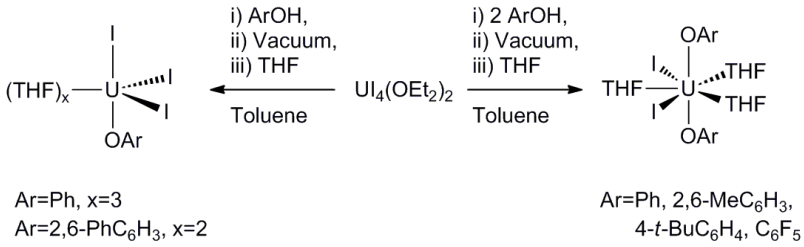


**Scheme 4.2 – Reactivity of $UI_4(OEt_2)_2$.**

The reactivity of $UI_4(OEt_2)_2$ with phenols was described with the isolation of the mono and di-substituted complexes, Scheme 4.2. The reaction results in the elimination of HI, which is removed under dynamic vacuum. The complexes were isolated from THF solutions in moderate yields. The aryloxide uranium(IV) complexes all have U-I bond lengths similar to other uranium(IV) iodides. Attempts to make the tri and tetra aryloxide complexes yielded only the mono and di-substituted uranium complexes. The use of $NEt_3$ negated the requirement for a dynamic vacuum, however this did lead to the product contamination with $[NEt_3H]I$.

When solutions of $UI_4(OEt_2)_2$ in diethyl ether were left at room temperature in glass vials, $[UI_5(OEt_2)][H(OEt_2)_2]$ was isolated. This was the result of the addition of HI to

$UI_4(OEt_2)_2$. The uranium atom has an octahedral coordination, and U-I bond lengths are characteristic of uranium(IV), thus ruling out the formation of a pentavalent $UI_5$ complex, Equation 4.5.

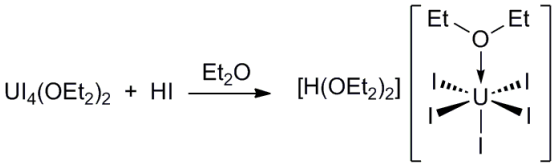


**Equation 4.5**

The origin of the protonation agent was investigated and found to be an OH group on the walls of the glass reaction vessel. This leads to the cleavage of a U-I bond and the formation of HI, which then reacts with another $UI_4(OEt_2)_2$ molecule, giving $[UI_5(OEt_2)][H(OEt_2)_2]$.

### 4.2.3 Synthesis of $UI_4(OBu_2)$

The analogous reaction to the synthesis of $UI_4(OEt_2)_2$ was carried out in dibutyl ether. The reaction between uranium turnings and elemental iodine in dibutyl ether formed the complex $UI_4(OBu_2)$ in 85 % yield as an insoluble green solid. The stoichiometry is supported by elemental analysis and $^1H$ NMR experiments with an internal standard of 1,3,5-tri-*tert*-butylbenzene. The solid state structure has not been confirmed as single crystals were not grown due to the insolubility of the complex.

## 4.3 Preparation of $UI_3$ adducts

### 4.3.1 Synthesis of $[U(OPPh_3)_2(THF)_2I_3]$

The reaction between $UI_3$ and triphenylphosphine oxide, $Ph_3P{=}O$, in THF, formed the complex $[U(OPPh_3)_2(THF)_2I_3]$ in a 45% yield as a purple microcrystalline solid, Equation 4.6.

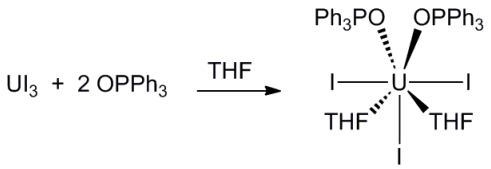


**Equation 4.6**

Single crystals suitable 4.for X-ray diffraction were grown from a THF solution of $[(UI)_2(L^{Et})]$ with $OPPh_3$ added as a crystallisation aid but have since been synthesised systematically.[31]

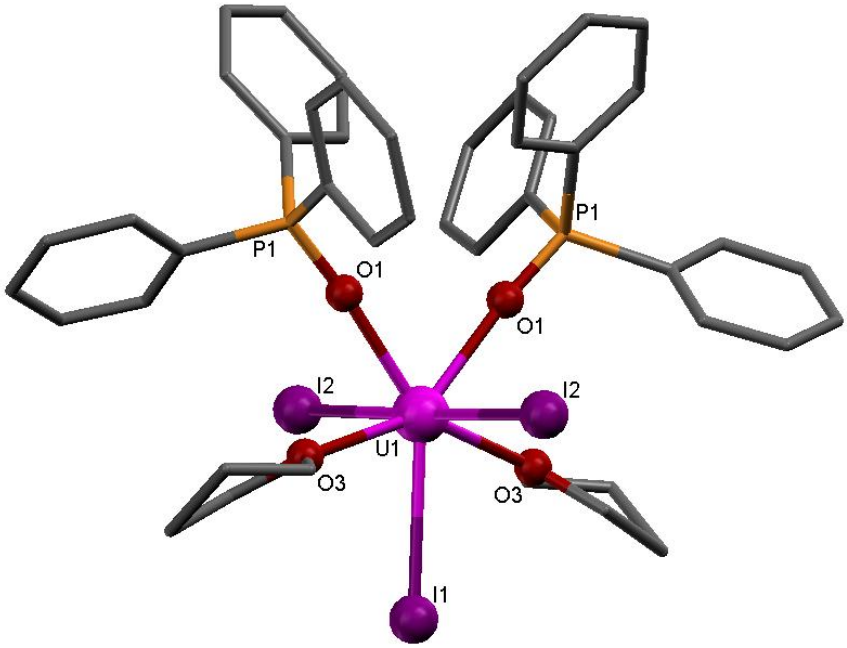


**Figure 4.3 – Ball and stick representations of the X-ray crystal structure of $U(OPPh_3)_2(THF)_2I_3$, hydrogen atoms have been excluded for clarity**

The molecule crystallises with a two fold rotational axis along U1-I1 vector, and in the extended structure there is a glide plane.

The uranium atom is seven coordinate, with a pentagonal-bipyramidal geometry and with I2 as the axial ligands, Figure 4.4.

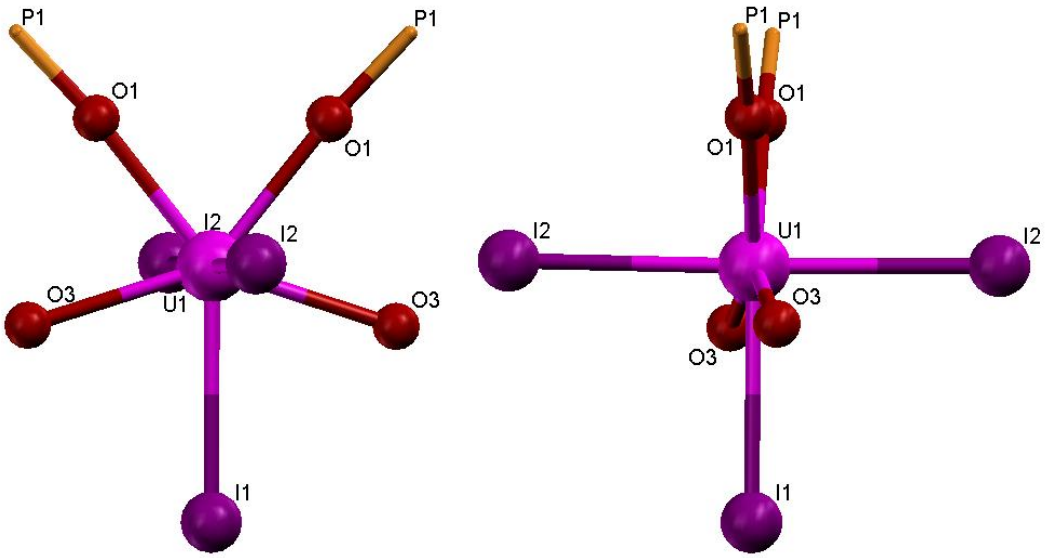


**Figure 4.4 –Coordination of the uranium atom.**

The U-I bond lengths, see Table 4.1, are within the normal range for uranium(IV) complexes (2.933-3.263 Å). The uranium-oxygen bond lengths in both the triphenylphosphine oxide and THF fall within the expected range for uranium(III) complexes. The oxygen-phosphorus bond length shows the P=O remains intact and the oxygen is acting as a Lewis base.

| **U-I** | **U-O** | **O-P** |
|---|---|---|
| U1-I1 3.2702(12)<br><br>U1-I2 3.1442(10) | U1-O1 2.405(9)<br><br>U1-O3 2.539(10) | O1-P1 1.504(9) |

**Table 4.1 – Selected bond lengths in $[U(OPPh_3)_2(THF)_2I_3]$ in Å.**

The uranium triiodide triphenylphosphine oxide adduct, $[UI_2(OPPh_3)_4][I]$, has been previously isolated by Ephritikhine and co-workers. The anion cation pairs are discrete and is shown in Figure 4.5.[32]

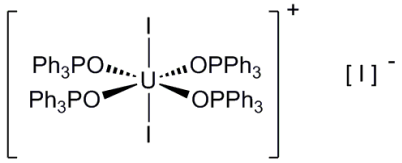


**Figure 4.5 – Structure of $[UI_2(OPPh_3)_4][I]$.**

Single crystals suitable for X-ray diffraction were grown from the reaction of $UI_3$ and an excess of $OPPh_3$ in pyridine. The U-I bond lengths average to 2.37(2) Å and U-O to 3.151(7) Å. The triflate analogue $[U(OTf)_2(OPPh_3)_4][OTf]$ was also isolated.[33]

There are many examples of triphenylphosphine oxide coordinated to uranium. Other uranium(III) examples include $[U(MeC_5H_4)_3(OPPh_3)]$ and $[Tp^{iPr2}UI_2(OPPh_3)]$, where $Tp^{iPr2}$ is a homoscorpionate.[34, 35] Uranium(IV) tetrahalides have also been shown to coordinate triphenylphosphine oxide with the isolation of $[UBr_4(OPPh_3)_2]$ and $[UCl_4(OPPh_3)_2]$.[36, 37]

### 4.3.2 Synthesis of [U(18-crown-6)$I_3$]

While much research has gone into the interactions of trivalent rare earth metal with crown ethers significantly less has been reported for the actinides. Of those reported for the actinides they are predominately involving the uranyl dication. [38,39]

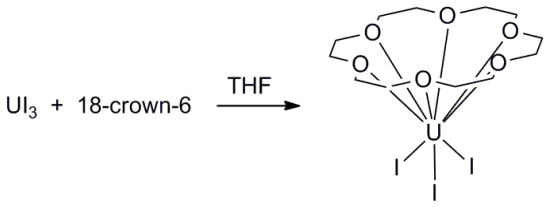


**Equation 4.7**

The addition of 18-crown-6 to $UI_3$ in THF results in the precipitation of a dark pink solid after 2 hours, the blue colour from the solution is lost as the $UI_3(THF)_4$ is consumed. An excess of 18-crown-6 yielded no further product. The [U(18-crown-6)$I_3$] complex was found to be soluble in pyridine but not in DME, THF, toluene or hexane.

The $^{1}$H NMR of [U(18-crown-6)$I_3$] shows one broad resonance at 11.67 ppm which integrates for 24 protons corresponding to 18-crown-6 (free 18-crown-6 has a chemical shift of 3.52 ppm). The elemental analysis supports the proposed formula for the complex.

Reactions were attempted to substitute the iodides in [U(18-crown-6)$I_3$] including reactions with KH, NaOAr (Ar=2,6-di-*t*-butylphenyl and 2,4,6-tri-*t*-butylphenyl), LiMe, LDA (lithium diisoproylamine), KBn, KN($SiMe_3$)$_2$, Li$^{n}$Bu, KO$^{t}$Bu and $Me_2Mg$. All of these reactions failed to produce any isolable product. Reactions to make a more soluble variant of [U(18-crown-6)$I_3$] were unsuccessful, as the reaction with dibenzo-18-crown-6, did not yield a more soluble product although did seem to produce a uranium complex.

There are a few examples of uranium complexes coordinated to crown ethers. [U(18-crown-6)$Cl_4$] has been synthesised previously but not yet crystallised.[40] Other crown-ether uranium chloride complexes in +4 oxidation state are shown in Figure 4.6.[41] The $UCl_6$ unit in the example below is stabilised by two ammonium molecules coordinated by 18-crown-6 units.[42] In another example the uranium trichloride is coordinated directly to the crown ether with all six oxygen atoms coordinated with a $UCl_6$ counter ion.[43]

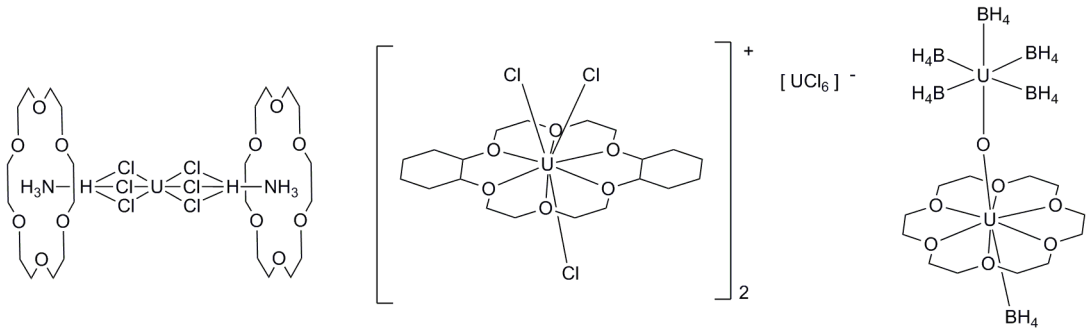


**Figure 4.6 – Examples of uranium complexes of 18-crown-6.**

The uranium(IV) borohydride 18-crown-6 complex above shows an unusual asymmetric structure.[44] One uranium atom is bound to the crown ether and a terminal $BH_4$ group and a bridging oxygen atom connects to a U($BH_4$)$_5$ unit.

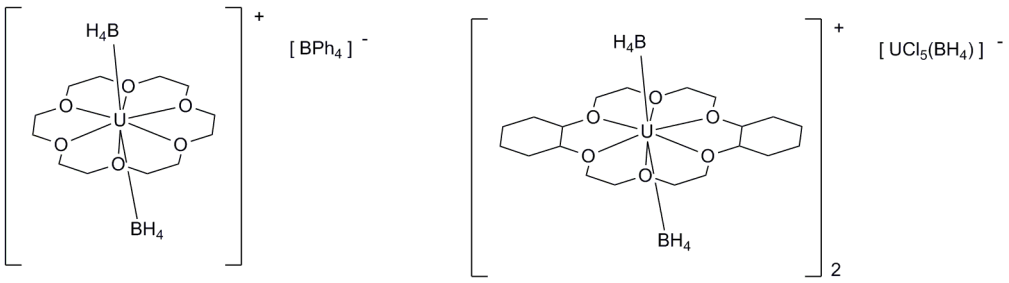


**Figure 4.7 – Other uranium(III) crown ether complexes.**

The $[U(crown)(BH_4)_2]^+$ unit has been isolated in two uranium(III) crown ether examples with either a $BPh_4$ or $[UCl_5(BH_4)]$ counter ion.[45, 46] The $[U(18\text{-crown-}6)(BH_4)_2][BPh_4]$ complex was synthesised by the addition of the crown ether to the $[U(BH_4)_2(THF)_5][BPh_4]$ in THF. The uranium(III) complex $[U(dicyclohexyl\text{-}18\text{-crown-}6)(BH_4)_2]_2[UCl_5(BH_4)]$ was isolated as a result of partial oxidation of $[U_3(dicyclohexyl\text{-}18\text{-crown-}6)_2(BH_4)_9]$ in dichloromethane.

Recently, Schreckenbach has studied the crown ether uranium complexes theoretically and it was shown that pentavalent uranyl has increased stability with respect to hexavalent uranyl in crown ether systems due to the effect of solvation and not due to ion size.[47]

### 4.3.3 Synthesis of $[U(OAr)_4][Na(py)_2(18\text{-crown-}6)]$

The reaction between $UI_3$ and the sodium salt of 2,4,6-tri-*t*-butylphenol (NaOAr) in pyridine formed the new complex $[U(OAr)_4][Na(py)_2(18\text{-crown-}6)]$ in 79 % yield as a red solid.

The initial synthesis of $[U(OAr)_4][Na(py)_2(18\text{-crown-}6)]$, occurred from an attempt to substitute the iodides of $[UI_3.18\text{-crown-}6]$ with aryloxide groups *via* salt elimination. Instead of the isolation of the desired $[U(18\text{-crown-}6)(OAr)_3.]$, the anion-cation complex $[U(OAr)_4][Na(py)_2(18\text{-crown-}6)]$ was produced, Equation 4.8.

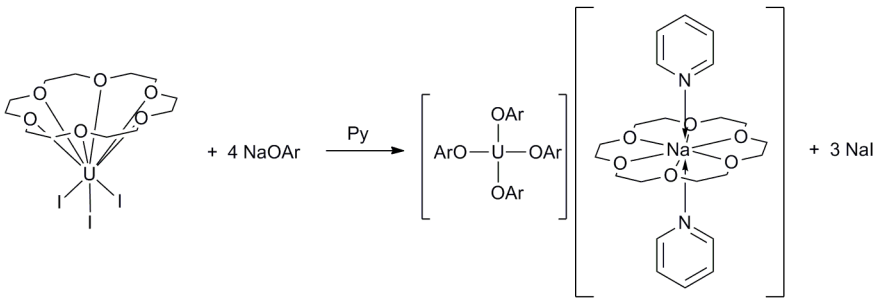


**Equation 4.8**

Single crystals suitable for X-ray diffraction were grown from a saturated pyridine solution at -20 °C. The crystal structure show the uranium atom has a tetrahedral geometry with four aryloxide groups coordinated. The sodium counter ion is encapsulated within the crown ether and its position in the unit cell is split over two positions, one of which has two pyridine molecules coordinated while the other has none, Figure 4.8.

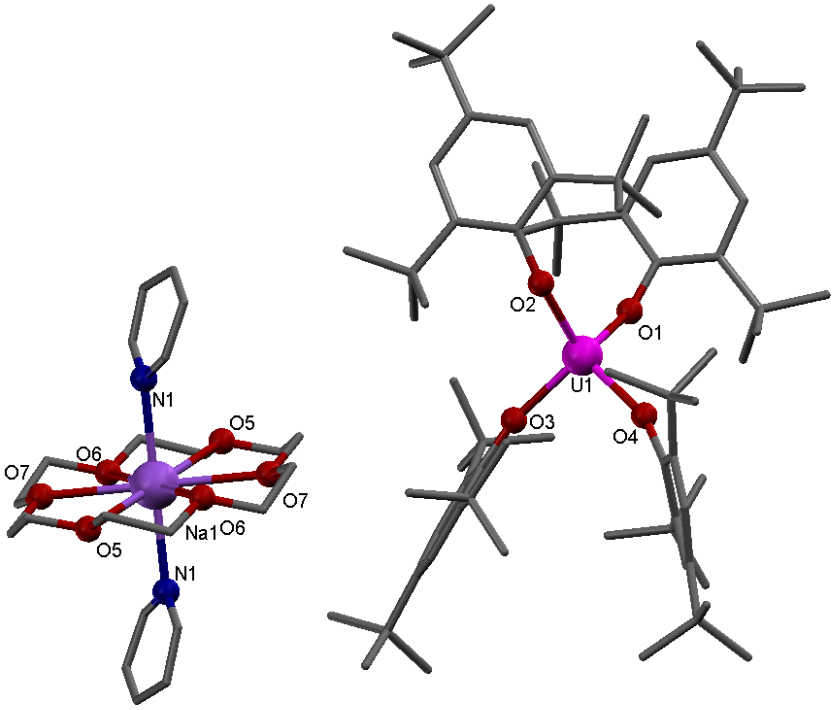


**Figure 4.8 –Ball and stick representations of the X-ray crystal structure of $[U(OAr)_4][Na(py)_2(18\text{-crown-}6)]$, hydrogen atoms and solvents of crystallisation have been excluded for clarity.**

The uranium atom has a tetrahedral environment with the largest deviation from the idealised geometry about the O3-U1-O4 angle at 99.77(12)°. The average U-O-C angle of 155.2(3)° with U1-O1-C1 and U1-O2-C19 approximately 146.5° and U1-O3-C37 and U1-O4-C55 approximately 164.0°.

Four coordinate uranium complexes are not uncommon despite the large size of the uranium atom. The uranium-oxygen bond lengths are similar to those found in other uranium aryloxide complexes (2.073–2.582 Å). The bond lengths in the crown-ether-solvated sodium cation are all standard.

| **U-O** | **Na-O** | **Na-N** |
|---|---|---|
| U1-O1 2.279(3)<br>U1-O2 2.279(3)<br>U1-O3 2.220(3)<br>U1-O4 2.234(3) | Na1-O5 2.773(4)<br>Na1-O6 2.806(4)<br>Na1-O7 2.627(4) | Na1-N1 2.475(7) |

**Table 4.2 – Selected bond lengths in [U(OAr)4][Na(py)2(18-crown-6)] in Å.**

The packing in the crystal is shown in Figure 4.9.

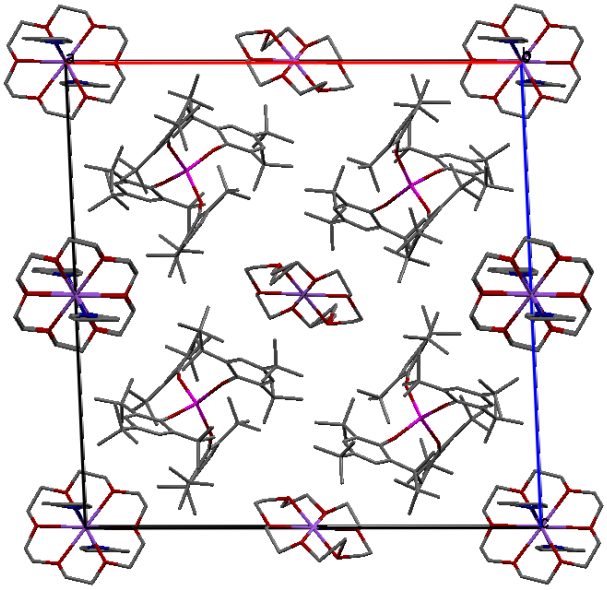

**Figure 4.9 – Packing in the structure of $[U(OAr)_4][Na(py)_2(18\text{-crown-6})]$.**

It is postulated that the reactions previously attempted with salts to displace the iodide ligands are producing similar products where the alkali metal becomes bound in the 18-crown-6.

This is the first uranium complex containing 2,4,6-tri-*t*-butylphenol which has been structurally characterised. Homoleptic complexes of Mn and Fe have been previously published, and display two aryloxides bridging the two metal centres and two terminal.[48]

The interest in uranium aryloxides began in the Manhattan project, where their volatility was studied. Since then many complexes have been synthesised, for examples see Figure 4.10. The octahedral complex $[U(OC_6F_5)_6][Li(DME)_3]_2$ was synthesised from $[U(O\textit{t}Bu)_6][Li(THF)_2]_2$ and ten equivalents of $HOC_6F_5$, which in turn was made from $LiO\textit{t}Bu$ and $UCl_4$.[49-51] $[U(OC_6F_5)_6][Li(DME)_3]_2$ can be successively oxidised with AgOTf to yield uranium(V) complexes.

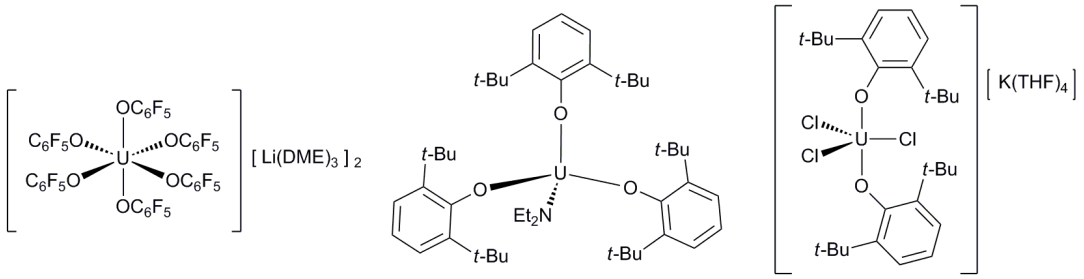


**Figure 4.10 – High valence uranium aryloxides.**

$[U(NEt_2)(OAr)_3]$ is formed when an excess of 2,6-di-*t*-butylphenol is reacted with $[U(NEt_2)_4]_2$ in *n*-pentane, failing to produce the homoleptic tetraaryloxide complex; instead only triple substitution is possible.[52] The uranium is tetrahedral with an average U-O bond distance of 2.143(4) Å and a U-O-C angle of 154°. The Lappert group continued the research into uranium phenolates and isolated $[Li(THF)_4][U(OAr)_5]$.[53] The anion-cation pair of $[UCl_3(OAr)_2][K(THF)_4]$, was synthesised from $UCl_4$ and two equivalents of KOAr, in which the uranium centre has a trigonal bipyramidal geometry with two of the chloride atoms bridging to the potassium ion and forming an infinite-chain structure.[54]

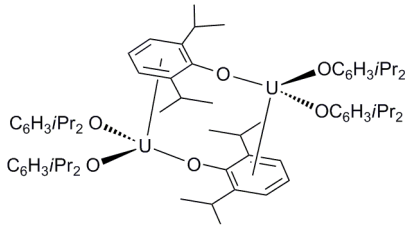


**Figure 4.11 – Example of a uranium(III) aryloxide complex.**

The first homoleptic uranium(III) aryloxide complex was synthesised in 1988 by Sattelberger and co-workers.[55] The dimeric complex $[U(O\text{-}2,6\text{-}i\text{-}PrC_6H_3)_3]$ was synthesised by the transamination reaction between $[U\{N(SiMe_3)_2\}_3]$ and just over three equivalents of 2,6-di-*iso*-propylphenol in hexane. The uranium centres adopt piano-stool geometries with coordination to three terminal aryloxide groups and a $\pi$ arene interaction to an aryloxide ligand from the other uranium atom. The U-U distance is 5.34 Å and the U-O bonds are shorter than the uranium(IV) analogues

with the average distance of 2.132(8) Å for the terminal aryloxides and increases to 2.214(7) Å for the bridging ligands. One electron oxidation of $[U(O\text{-}2,6\text{-}i\text{-}PrC_6H_3)_3]$ has since been carried out to form a myriad of uranium(IV) complexes.[56]

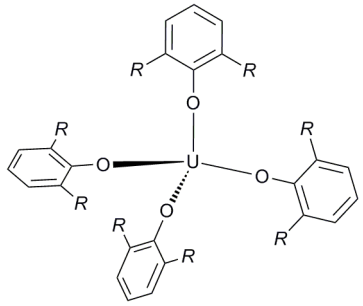


**Figure 4.12 – $[U(OAr)_4]$ where R=*i*-Pr or *t*-Bu.**

The homoleptic tetraaryloxide uranium(IV) complexes of 2,6-*iso*-propylphenol and 2,6-*tert*-butylphenol have been synthesised.[57, 58] The complexes are synthesised from the uranium(IV) metallacycle $[\{N(SiMe_3)_2\}_2U(CH_2SiMe_3NSiMe_3)]$ and four equivalents of the corresponding alcohol in refluxing toluene. The X-ray crystal structure of $[U(OAr)_4]$ where R=*t*-Bu shows that the uranium centre displays a tetrahedral geometry with U-O bond lengths of 2.135(4) Å and a U-O-C angle off 154.0(6)°. The $[U(OPh)_4(dmpe)_2]$ complex has also been synthesised with the uranium atom having a coordination number of eight.[59] It was synthesised from $UCl_4$ and four equivalents of LiOPh in the presence of dmpe.

### 4.3.4 Synthesis of $U(BH_4)_3(THF)_x$

The reaction between $UI_3$ and a slight excess of potassium borohydride (3.2 equivalents) in THF forms the complex $U(BH_4)_3(THF)_x$ in a 87% yield as a microcrystalline red solid. The presence of the coordinating solvent is paramount in the synthesis of the uranium(III) borohydride. The reaction between $UI_3$ and a slight excess of potassium borohydride in toluene results in the isolation of the starting materials, as they are too insoluble to react. The reaction when carried out in THF, changes from a blue solution to a red solution on warming to room temperature. The red solution is isolated from the white precipitate of KI (which was weighed and

corresponded to three equivalents of KI) and the volatile removed to give the microcrystalline red solid.

$^1$H NMR spectroscopy was used to study the proton environments in the complex, and showed resonances corresponding to bound THF which were paramagnetically shifted up field to 5.60 and 3.28 ppm and a resonance at 110.5 ppm corresponding to the $BH_4$ groups was identified. The IR spectrum in nujol mull, shows that the borohyride is bound in a tridentate ($\mu^3$) fashion with stretches at 2455, 2212 and 1165 $cm^{-1}$. The stretch at 2212 $cm^{-1}$ has a triplet appearance. No suitable single crystals were grown for further characterisation by X-ray diffractometery to study the solid state structure.

As discussed in Chapter 1.3.3. trivalent uranium borohydrides are less well studied that their uranium(IV) counterparts. The uranium(III) borohydride, $U(BH_4)_3(THF)_x$, was formed from *in situ* synthesised $UCl_3(THF)_x$ and an excess of $NaBH_4$ in THF at room temperature.[4] $U(BH_4)_3$ has also been synthesised from the decomposition of $U(BH_4)_4$ in toluene by a cycle of heating to 127 °C, cooling, and pumping to remove the diborane and hydrogen evolved.[60]

The molecular structure of $[U(BH_4)_3(THF)_3]$ was calculated from the single crystal X-ray study by Nöth in 1986.[61] The uranium atom displays a distorted facial octahedral geometry coordinated to three borohydrides and three THF molecules. $[U(BH_4)_3(THF)_3]$ was synthesised from a reaction of $UH_3$ with diborane in THF.

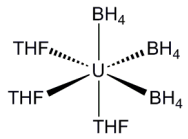


**Figure 4.13 –Structure of $[U(BH_4)_3(THF)_3]$.**

### 4.3.5 Synthesis of $[U(Cyclam)I_3]$

Cyclam (1,4,8,11-tetraazacyclotetradecane) is a fourteen membered tetraamine macrocycle with the ability to bind to a wide range of metal ions.

A reaction between $UI_3$ and cyclam at -20 °C in pyridine, forms the new complex [U(Cyclam)$I_3$] in a 74% yield as a pink solid, Equation 4.9. The $^1$H NMR spectrum indicated the complexation of the uranium atom to the cyclam by the paramagnetically shifted resonances corresponding to the cyclam and supporting an asymmetric arrangement ranging from 27 to -35 ppm.

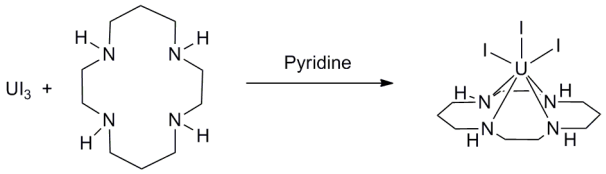


**Equation 4.9**

[U(Cyclam)$I_3$] was found to be only partially soluble in pyridine and so substituted cyclam ligands were investigated to increase solubility.

Complexes of cyclam have been shown to be affective for the treatment of AIDS and for cell stem mobilization. The use of cyclam is wide spread due to its high thermodynamic and kinetic stability with respect to metal dissociation.[62] The number of substituted cyclam macrocycles is vast with some examples shown in Figure 4.14.

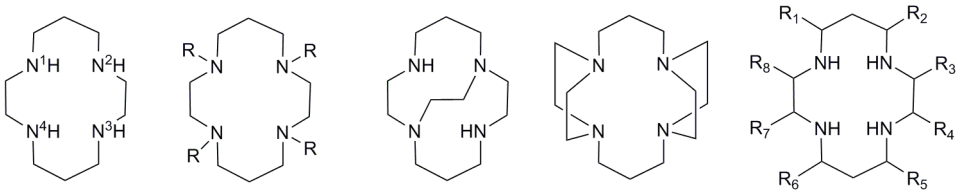

**Figure 4.14 – Cyclam and derivatives.**

Many studies have involved *N*-substituted derivatives, which the majority are tetra substituted but can also be mono, di and tri substituted. Examples of R groups include R=Me, Et, *i*-Pr, *i*-Bu, $CH_2COOH$, $CH_2CH_2OH$, $CH_2(CH_2)_2OH$, $CH_2PO_3H_2$, $CH_2P(O)(C_6H_5)OH$, $CH_2Ph$, $CH_2(C_5H_4N)$, $CH_2PPh_2$, $CH_2CH_2SO_2Ph$, $CH_2CONR_2$ to terpyridyl fragments.[60-71] Some of these groups can then be deprotonated and bind to the metal centre.

Disubstituted cyclam molecules are formed by the protection of the other two nitrogen atoms first. When the nitrogen atoms to be protected are $N^1$ and $N^4$ diethyl oxalate is used.[72]

Cross-bridged cyclam ligands add a constraining bridge to the macrocycle and it has been shown to strengthen the metal ligand bonding. The addition of these bridges can be across the macrocycle in a diagonal fashion or in a vertical way. Additional groups can also be added upon the formation of the bridge and sulphur atoms have been added to increase the available atoms for coordination.[66]

While the coordination of uranium into a cyclam is unprecedented, it is present in complexes where cyclam is coordinated into another metal atom, so forming a superstructure.

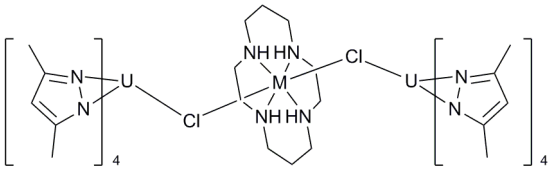


**Figure 4.15 – Linear chloride-bridged cluster where M=Zn, Cu, Ni, Co.**

The chloride-bridged complex, Figure 4.15, was synthesised via a reaction between the metal chloride cyclam complex with the uranium(IV) tetrapyrazolate complex in dichloromethane. The trinuclear centres exhibit magnetic exchange coupling; when M=Co, ferromagnetic coupling was observed at 5K and when M=Ni a weak ferromagnetic coupling was present.[76, 77]

### 4.3.6 Synthesis of $^{TMS}$Cyclam

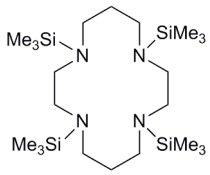


**Figure 4.16 – $^{TMS}$Cyclam.**

The synthesis of tetrakis(trimethylsilyl)cyclam was adapted from the synthesis of tetrakis(trimethylsilyl)cyclen, $^{TMS}$Cyclam where cyclen is 1,4,7,10-tetraazacyclododecane published by Richman in 1977.[78] Cyclen is an aza analogue of the crown ether 12-crown-4.

The reaction between cyclam and four and a half equivalents of trimethylsilyl chloride was performed in THF at -78°C, in the presence of the base DABCO. The reaction was stirred at room temperature for 16 hours and the solution isolated and the volatiles removed. The yield was low, but not optimised. The $^{TMS}$Cyclam was analysised by $^{1}$H and $^{13}$C{$^{1}$H} NMR spectroscopy which supported the loss of the NH and the formation of the NSi(CH$_3$)$_3$ groups. The $^{1}$H NMR spectrum showed four distinct environments three for the protons on the cyclam backbones (2.90, 2.77 and 1.77 ppm) and one for the NSi(CH$_3$)$_3$ groups at 0.14 ppm. The $^{13}$C{$^{1}$H} NMR spectrum showed four different carbon environments with resonances at 48.76, 46.75, 31.20 and 0.42 ppm.

### 4.3.7 Attempted Synthesis of [U($^{TMS}$Cyclam)I$_3$]

In an attempt to coordinate UI$_3$ to a cyclam and form a soluble product, the tetratrimethylsilylcyclam was synthesised. The reaction between UI$_3$ and $^{TMS}$Cyclam in THF did not produce the desired product, [U($^{TMS}$Cyclam)I$_3$] and only the starting materials were isolated. The $^{1}$H NMR spectrum only showed the resonances associated with free uncoordinated $^{TMS}$Cyclam. It is unclear as to why the $^{TMS}$Cyclam does not bind to the UI$_3$.

### 4.3.8 Synthesis of [U($^{Bn}$Cyclam)I$_3$]

In an attempt to coordinate UI$_3$ to a cyclam and form a soluble product, the tetrabenzylcyclam, $^{Bn}$Cyclam was also synthesised. The reaction between UI$_3$ and $^{Bn}$Cyclam in THF formed the desired product, [U($^{Bn}$Cyclam)I$_3$]. Unfortunately the new complex, [U($^{Bn}$Cyclam)I$_3$] like [U(Cyclam)I$_3$] also showed low solubility. The addition of the benzyl groups to the cyclam did not increase the solubility of the complex. The complex [U($^{Bn}$Cyclam)I$_3$] was found to be only soluble in pyridine. Due to its lack of solubility, no further studies were performed on [U($^{Bn}$Cyclam)I$_3$].

The synthesis of $^{Bn}$Cyclam was adapted from research done by the Tsukube group, where the cyclam is reacted with benzyl chloride in basic conditions.[64]

## 4.4 Conclusions

In this chapter, the new synthesis of $UI_3$ has been described in addition to the full characterisation of the new uranium tetraiodide complex, $UI_4(OEt)_2$. The study of adducts of $UI_3$ with neutral donors, triphenylphosphine oxide, 18-crown-6 and cyclam, was also investigated. The substitution of the iodide groups on the new complex, [U(18-crown-6)$I_3$] was also explored with an array of reagents.

Further study on the complexation of substituted cyclam macrocycles to uranium(III) was also investigated with the formation of poorly soluble complexes.

## 4.5 References


1. D. L. Clark, A. P. Sattelberger, S. G. Bott and R. N. Vrtis, *Inorg. Chem.*, 1989, **28**, 1771-1773.
2. L. R. Avens, S. G. Bott, D. L. Clark, A. P. Sattelberger, J. G. Watkin and B. D. Zwick, *Inorg. Chem.*, 1994, **33**, 2248-2256.
3. D. L. Clark and A. P. Sattelberger, *Inorg. Synth.*, 1997, **31**, 307-315.
4. D. C. Moody and J. D. Odom, *J. Inorg. Nucl. Chem.* , 1979, **41**, 533-535.
5. R. A. Andersen, *Inorg. Chem.*, 1979, **18**, 1507-1509.
6. W. G. Van der Sluys, C. J. Burns and A. P. Sattelberger, *Organometallics*, 1989, **8**, 855-857.
7. C. Boisson, J. C. Berthet, M. Lance, M. Nierlich and M. Ephritikhine, *Chem. Commun.*, 1996, 2129-2130.
8. W. J. Evans, S. A. Kozimor and J. W. Ziller, *J. Am. Chem. Soc.*, 2003, **125**, 14264-14265.
9. J. H. Levy, J. C. Taylor and P. W. Wilson, *Acta Crystallogr., Sect. B* 1975, **B31**, 880-882.
10. W. Zachariasen, *Acta Crystallogr.*, 1948, **1**, 265-268.
11. J. D. Corbett, *Inorg. Synth.*, 1983, **22**, 31-36.

12. F. G. N. Cloke and P. B. Hitchcock, *J. Am. Chem. Soc.*, 2002, **124**, 9352-9353.
13. W. J. Evans, S. A. Kozimor, J. W. Ziller, A. A. Fagin and M. N. Bochkarev, *Inorg. Chem.*, 2005, **44**, 3993-4000.
14. C. P. Larch, F. G. N. Cloke and P. B. Hitchcock, *Chem. Commun.*, 2008, 82-84.
15. J. L. Kiplinger, D. E. Morris, B. L. Scott and C. J. Burns, *Organometallics*, 2002, **21**, 5978-5982.
16. J. A. Hermann, J. F. Suttle and H. R. Hoekstra, in *Inorg. Synth.*, ed. M. Therald, 2007, pp. 143-145.
17. K. W. Bagnall, D. Brown, P. J. Jones and J. G. H. Du Preez, *J. Chem. Soc.*, 1965, 350-353.
18. J.-C. Berthet, P. Thuery and M. Ephritikhine, *Inorg. Chem.*, 2005, **44**, 1142-1146.
19. J. G. H. Du Preez, B. Zeelie, U. Casellato and R. Graziani, *Inorg. Chim. Acta*, 1987, **129**, 289-296.
20. A. J. Gaunt, A. E. Enriquez, S. D. Reilly, B. L. Scott and M. P. Neu, *Inorg. Chem.*, 2008, **47**, 26-28.
21. C. D. Carmichael, N. A. Jones and P. L. Arnold, *Inorg. Chem.*, 2008, **47**, 8577-8579.
22. O. P. Lam, C. Anthon, F. W. Heinemann, J. M. O'Connor and K. Meyer, *J. Am. Chem. Soc.*, 2008, **130**, 6567-6576.
23. A. E. Enriquez, B. L. Scott and M. P. Neu, *Inorg. Chem.*, 2005, **44**, 7403-7413.
24. R. R. Rietz, N. M. Edelstein, H. W. Ruben, D. H. Templeton and A. Zalkin, *Inorg. Chem.*, 1978, **17**, 658-660.
25. T. Le Borgne, P. Thuery and M. Ephritikhine, *Acta Crystallogr., Sect. C: Cryst. Struct. Commun.*, 2002, **C58**, m8-m9.
26. M. J. Monreal and P. L. Diaconescu, *Organometallics*, 2008, **27**, 1702-1706.
27. N. K. Sung-Yu, F. F. Hsu, C. C. Chang, G. R. Her and C. T. Chang, *Inorg. Chem.*, 1981, **20**, 2727-2728.

28. R. D. Fischer, R. Von Ammon and B. Kanellakopulos, *J. Organometal. Chem.* , 1970, **25**, 123-137.
29. D. D. Schnaars, G. Wu and T. W. Hayton, *Dalton Trans.*, 2008, 6121-6126.
30. D. D. Schnaars, G. Wu and T. W. Hayton, *Dalton Trans.*, 2009, 3681-3687.
31. M. C. Etter and P. W. Baures, *J. Am. Chem. Soc.*, 1988, **110**, 639-640.
32. J.-C. Berthet, M. Nierlich and M. Ephritikhine, *Polyhedron*, 2003, **22**, 3475-3482.
33. J. C. Berthet, M. Lance, M. Nierlich and M. Ephritikhine, *Eur. J. Inorg. Chem.*, 1999, 2005-2007.
34. J. G. Brennan, R. A. Andersen and A. Zalkin, *Inorg. Chem.*, 1986, **25**, 1761-1765.
35. L. Maria, A. Domingos, A. Galvao, J. Ascenso and I. Santos, *Inorg. Chem.*, 2004, **43**, 6426-6434.
36. G. Bombieri, F. Benetollo, K. W. Bagnall, M. J. Plews and D. Brown, *J. Chem. Soc., Dalton Trans.*, 1983, 343 - 348.
37. G. Bombieri, D. Brown and R. Graziani, *J. Chem. Soc., Dalton Trans.*, 1975, 1873 - 1876.
38. J.-C. G. Bünzli and D. Wessner, *Coord. Chem. Rev.*, 1984, **60**, 191-253.
39. V. K. Belsky and B. M. Bulychev, *Russ. Chem. Rev. (Engl. Transl.)*, 1999, **68**, 119.
40. R. M. Costes, G. Folcher, P. Plurien and P. Rigny, *Inorg. Nucl. Chem. Lett.*, 1976, **12**, 13-21.
41. R. D. Rogers, L. K. Kurihara and M. M. Benning, *Inorg. Chem.*, 1987, **26**, 4346-4352.
42. R. D. Rogers and M. M. Benning, *Acta Crystallogr., Sect. C*, 1988, **44**, 1397-1399.
43. G. C. de Villardi, P.Charpin, R.-M. Costes, G. Folcher, P. Plurien, P. Rigny and C. de Rango, *J. Chem. Soc., Chem. Commun.*, , 1978, 90 - 92.
44. C. Villiers, P. Thuery and M. Ephritikhine, *Acta Crystallogr., Sect. C*, 2006, **62**, m243-m245.
45. T. Arliguie, L. Belkhiri, S.-E. Bouaoud, P. Thuery, C. Villiers, A. Boucekkine and M. Ephritikhine, *Inorg. Chem.*, 2008, **48**, 221-230.

46. A. Dejean, P. Charpin, G. Folcher, P. Rigny, A. Navaza and G. Tsoucaris, *Polyhedron*, 1987, **6**, 189-195.
47. G. Schreckenbach and G. A. Shamov, *Acc. Chem. Res.*, 2010, **43**, 19-29.
48. R. A. Bartlett, J. J. Ellison, P. P. Power and S. C. Shoner, *Inorg. Chem.*, 1991, **30**, 2888-2894.
49. S. Fortier, G. Wu and T. W. Hayton, *Inorg. Chem.*, 2008, **47**, 4752-4761.
50. S. Fortier, G. Wu and T. W. Hayton, *Dalton Trans.*, 2010, **39**, 352-354.
51. S. Fortier, G. Wu and T. W. Hayton, *Inorg. Chem.*, 2009, **48**, 3000-3011.
52. P. B. Hitchcock, M. F. Lappert, A. Singh, R. G. Taylor and D. Brown, *Chem. Commun.*, 1983, 561-563.
53. P. C. Blake, M. F. Lappert, R. G. Taylor, J. L. Atwood and H. Zhang, *Inorg. Chim. Acta*, 1987, **139**, 13-20.
54. S. D. McKee, C. J. Burns and L. R. Avens, *Inorg. Chem.*, 1998, **37**, 4040-4045.
55. W. G. Van der Sluys, C. J. Burns, J. C. Huffman and A. P. Sattelberger, *J. Am. Chem. Soc.*, 1988, **110**, 5924-5925.
56. L. R. Avens, D. M. Barnhart, C. J. Burns, S. D. McKee and W. H. Smith, *Inorg. Chem.*, 1994, **33**, 4245-4254.
57. J. M. Berg, D. L. Clark, J. C. Huffman, D. E. Morris, A. P. Sattelberger, W. E. Streib, W. G. Van der Sluys and J. G. Watkin, *J. Am. Chem. Soc.*, 1992, **114**, 10811-10821.
58. W. G. Van Der Sluys, A. P. Sattelberger, W. E. Streib and J. C. Huffman, *Polyhedron*, 1989, **8**, 1247-1249.
59. P. G. Edwards, R. A. Andersen and A. Zalkin, *J. Am. Chem. Soc.*, 1981, **103**, 7792-7794.
60. G. V. Fazakerley, G. Folcher and H. Marquet-Ellis, *Polyhedron*, 1984, **3**, 457-461.
61. D. Männig and H. Nöth, *Z. Anorg. Allg. Chem.*, 1986, **543**, 66-72.
62. X. Liang and P. J. Sadler, *Chem. Soc. Rev.*, 2004, **33**, 246-266.
63. X. Liang and P. Sadler, *Chem. Soc. Rev.*, 2004, 246-266.
64. G. Royal, V. Dahaoui-Gindrey, S. Dahaoui, A. Tabard, R. Guilard, P. Pullumbi and C. Lecomte, *Eur. J. Org. Chem.*, 1998, **1998**, 1971-1975.

65. J. S. Bradshaw, K. E. Krakowiak, R. M. Izatt and D. J. Zamecka-Krakowiak, *Tetrahedron Lett.*, 1990, **31**, 1077-1080.
66. J. W. Sibert, A. H. Cory and J. G. Cory, *Chem. Commun.*, 2002, 154-155.
67. H. Tsukube, K. Takagi, T. Higashiyama, T. Iwachido and N. Hayama, *J. Chem. Soc., Perkin Trans. 1*, 1986, 1033-1037.
68. J. Narayanan, M. E. Sosa-Torres and R. A. Toscano, *J. Chem. Crystallogr.*, 2001, **31**, 129-133.
69. S. Subramanian, T. M. Barclay, K. R. Coulter and A. McAuley, *Coord. Chem. Rev.*, 2003, **245**, 65-71.
70. H. Hope, M. Viggiano, B. Moezzi and P. P. Power, *Inorg. Chem.*, 1984, **23**, 2550-2552.
71. A. de Castries, A. Escande, H. Fensterbank, E. Magnier, J. Marrot and C. Larpent, *Tetrahedron*, 2007, **63**, 10330-10336.
72. F. Cuenot, M. Meyer, E. Espinosa and R. Guilard, *Inorg. Chem.*, 2005, **44**, 7895-7910.
73. E. P.-T. Miguel, L. José Manuel, M.-M. Ramón, B. Angel, S. Juan, P. Teresa, A. M. Miguel and M. D. Marcos, *Eur. J. Inorg. Chem.*, 2000, 741-748.
74. M. R. Spirlet, J. Rebizant, M. F. Loncin and J. F. Desreux, *Inorg. Chem.*, 1984, **23**, 4278-4283.
75. F. Bellouard, F. Chuburu, N. Kervarec, L. Toupet, S.Triki, Y. Le Mest and H. Handel, *J. Chem. Soc., Perkin Trans. 1*, 1999, 3499 - 3505.
76. J. D. Rinehart, B. M. Bartlett, S. A. Kozimor and J. R. Long, *Inorg. Chim. Acta*, 2008, **361**, 3534-3538.
77. S. A. Kozimor, B. M. Bartlett, J. D. Rinehart and J. R. Long, *J. Am. Chem. Soc.*, 2007, **129**, 10672-10674.
78. J. E. Richman, *Tetrahedron Lett.*, 1977, **18**, 559-562.
79. P. Comba, H. Pritzkow and W. Schiek, *Angew. Chem., Int. Ed. Engl.*, 2001, **40**, 2465-2468.

# Chapter 5: Conclusions and Experimental details

In terms of the general objectives for the thesis (see Chapter 1) it has not yet proven possible to isolate molecular uranium hydride complexes of 'Pac-man' ligands. However, the multidentate polypyrrolic macrocyclic ligand has been shown to be very effective in forming stable complexes of uranium in lower oxidation states and other f-block cations and allowed the isolation and study of a range of unusual compounds.

Unprecedented structures with the 'Pac-man' ligand have been characterised for complexes of the f-block elements, for example with uranium(IV) encapsulated within the ligand in [U(L)]. A supramolecular structure is formed by cerium(III) in the absence of donor solvents giving a trinuclear wheel arrangement $[Ce(HL)]_3$. Yttrium(III) shows similar chemistry with the macrocycle forming an extended structure in non-donor solvents. The "cerium wheel" is an unusual structure for lanthanide macrocycle complexes.

Extending this work to other lanthanide and actinide metals could provide very interesting comparisons with the systems already studied. An X-ray structure determination of [Ce(L)] would allow comparison with [U(L)] and provide information for on how bonding differs between 4f and 5f valence shells.

We have shown in chapter 2 that two f-block metal centres can be introduced into the 'Pac-man' macrocycle, giving novel complexes such as $[(UI)_2(L)]$, and an attempt to incorporate hydride ligands into this resulted in the synthesis of $[\{U(BH_4)\}_2(L)]$. The synthetic methodology developed for the binuclear uranium complex allowed us to isolate the first example of a dinuclear neptunium(III) complex, $[(NpI)_2(L)]$ and opens the possibility of exploring the coordination chemistry of this element in controlled environments.

One of the challenges faced in characterising new complexes of the types made in this thesis is that only a limited number of techniques can be applied, especially as they are both polymeric and paramagnetic. This led us to establish a collaboration

with the ITU who developed a model for predicting the solid state structure using the magnetic measurements obtained from SQUID data.

Having had mixed success in substitution of the iodide group from [$(UI)_2$(L)], we decided to synthesise other uranium trihydrides which could directly incorporate a UH moiety into the 'Pac-man' ligand.

Attempts to use neutral macrocycles to solubilise the polymeric $UH_3$ are discussed. However the only reagents with which $UH_3$ demonstrated reactivity in our hands are acids, in agreement with other literature reports. Adducts of $UI_3$ with neutral macrocycles were also targeted as trihydride precursors. During this, high yielding routes to $UI_3$ and $UI_4(OEt)_2$ were developed which should find application generally for the preparation of complexes of uranium in a range of oxidation states.

# Experimental details

Unless otherwise stated, all reactions were carried out using standard Schlenk techniques under an atmosphere of nitrogen or in a nitrogen filled glove-box. Solvents were dried (hexane, toluene, $Et_2O$ and THF were passed through activated alumina towers, dichloromethane was distilled from $CaH_2$, pyridine was refluxed over K), and stored over 4 Å molecular sieves.[1] Deuterated benzene and pyridine were dried over potassium and then distilled under reduced pressure.

$^{1}H$ and $^{13}C\{^{1}H\}$ NMR spectra were recorded either on a Bruker DPX-360 spectrometer operating at 360.75 MHz and 90.55 MHz respectively, or a Bruker ARX-250 spectrometer operating at 250.13 MHz, or a Bruker AVA-600 spectrometer operating at 599.81 MHz, or a Bruker AVA-400 spectrometer operating at 400.25 MHz and resonances was reported relative to tetramethylsilane ($\delta$ = 0 ppm). $^{31}P\ \{^{1}H\}$ NMR spectra were recorded on a Bruker AVA-400 spectrometer operating at 161.92 MHz and resonances was reported relative to 85% phosphoric acid as an external standard ($\delta$ = 0 ppm). Coupling constants are quoted in Hertz and chemical shifts in $\delta$ (ppm).

Elemental analyses were carried out by Mr. Stephen Boyer at the London Metropolitan University. Uranium analyses were performed on a Perkin Elmer Optima 5300 DV ICP-OES instrument and iodide analyses were performed on an Agilent 7500ce ICP-MS instrument, both by Ms. Lorna Eades at the University of Edinburgh.

Infrared spectra were recorded in the range 400 - 4000 $cm^{-1}$ on a Jasco 410 FT-IR spectrophotometer as Nujol mulls between KBr discs, unless otherwise stated. Far infrared were recorded on a Perkin-Elmer FT-IR-spectrophotometer Far IR 1700x in the range of 10 - 400 $cm^{-1}$ as a polyethylene pellet at the Institute of Transuranium Elements, Karlsruhe with the help of Dr Christos Apostolidis. UV-vis-nIR measurements were recorded on a Perkin Elmer Lambda 900 UV-vis-nIR spectrometer, and the solutions were made in the glovebox and recorded in a Teflon tapped 10 mm quartz cell.

DC-magnetization measurements were carried out on a Quantum Design-SQUID magnetometer (MPMS-7) in magnetic fields up to 7 T on samples encapsulated in sealed plexiglas tubes whose magnetic contribution was preliminarily measured in order to be subtracted. Measurements were carried out at the Institute of Transuranium Elements, Karlsruhe with the help of Dr Eric Colineau and Dr Jean-Christophe Griveau, with the data modelled by Dr Nicola Magnani, and Prof. Roberto Caciuffo.

The compounds 5,5'-dimethyldipyrromethane,[2] 5,5'-diformyl-2,2'-dimethyldipyrromethane,[3] $H_4L^{Me}$,[4] diethyl-2,2'-dipyrromethane,[5] $UI_3(THF)_4$,[6] $UCl_4$,[7] $[U\{N(SiMe_3)_2\}_3]$,[8] $[Ln\{N(SiMe_3)_2\}_3]$,[9] 1,3-bis-(2,4,6-trimethylphenyl)imidazolin-2-ylidene,[10] 1,4,8,11-tetrabenzyl-1,4,8,11-tetraazacyclotetradecane [11] and were prepared using literature methods. $Ce(O\text{-}t\text{-}Bu)_4(THF)_2$ was kindly donated by Dr. Ian J. Casely. Potassium hydride was purchased from Aldrich as a dispersion in oil, and was washed with hexane before use. All crown ethers were sublimed prior to use. All other compounds were used as purchased without further purification.

## 5.1 Chapter 2: Preparation of $H_4L^{Et}$ and $H_4L^{Me}$ Macrocycles

### 5.1.1 Preparation of 5,5'-diformyl-2,2'-diethyldipyrromethane

To a stirred, cooled (0 °C) solution of diethyl 2,2'-dipyrromethane (40.0 g, 0.197 mol) in DMF (400 mL), $POCl_3$ (40.4 mL, 0.433 mol) was added dropwise. The cherry red reaction mixture was stirred at 0 °C for 1 h and was then allowed to warm to room temperature. The mixture was quenched with $H_2O$ (400 mL) and 2 M KOH (1 L), resulting in a pale pink precipitate. The suspension was heated to 70 °C for 50 minutes, and allowed to cool to room temperature; the solids filtered and washed with $H_2O$ until the washings were pH neutral. The solid was dried under reduced pressure to afford a cream powder. Yield: 40.0 g (78 %).

$^1$H NMR ($CDCl_3$, 250 MHz, 293 K) δ: 10.36 (2H, s, NH), 9.05 (2H, s, CHO), 6.76 and 6.19 (4H, d, $^3$J = 4.0 Hz, pyrrolic CH), 1.98 (4H, q, $^3$J= 7.4 Hz, $CH_2$), 0.65 (6H, t, $^3$J= 7.4 Hz, $CH_3$) ppm.

$^{13}C\{^{1}H\}$ NMR ($CDCl_3$, 360 MHz, 293 K) δ: 179.2 (CHO), 146.6 (Q), 132.6 (Q), 122.4 (CH), 111.1 (CH), 45.3 (Q), 29.6 ($CH_2$), 8.7 ($CH_3$) ppm.

Analysis. Found: C, 69.72; H, 7.04; N, 10.75 %; $C_{15}H_{18}N_2O_2$ requires: C, 69.74; H, 7.02; N, 10.84 %.

### 5.1.2 Preparation of $H_4L^{Et}$

A mixture of 4,5-dimethyl-1,2-phenylenediamine (21.0 g, 0.155 mol) and 5,5'-diformyl-2,2'-diethyldipyrromethane (40.0 g, 0.155 mol) was warmed in MeOH (900 mL) until complete dissolution. A solution of *p*-toluenesulfonic acid monohydrate (65.0 g, 0.342 mol) in MeOH (90 mL) was added dropwise and the resulting deep red solution was stirred for 45 minutes, after which time a bright orange precipitate formed. The solid was collected by filtration and washed with MeOH (3 × 10 mL). It was then suspended in MeOH (1000 mL) and $NEt_3$ was added dropwise until the conversion to a yellow solid was complete. The solid was collected, washed with cold (0 °C) MeOH (3 × 10 mL) and hexane (3 × 10 mL) and dried under reduced pressure at 100 °C to afford 39.0 g, 70 %, of $H_4L^{Et}$, as a yellow solid.

$^{1}H$ NMR ($CDCl_3$, 250 MHz, 293 K) δ: 9.02 (4H, s, NH), 8.06 (4H, s, imino), 6.81 (4H, s, aromatic), 6.41 and 6.06 (8H, m, pyrrolic CH), 2.21 (12H, s, aromatic $CH_3$), 1.99 (8H, q, $^{3}J$=7.4 Hz, $CH_2$), 0.675 (12H, t, $^{3}J$= 7.4 Hz, $CH_3$) ppm.

$^{13}C\{^{1}H\}$ NMR ($CDCl_3$, 360 MHz, 293 K) δ: 148.9 (CHN), 143.3 (q), 134.7 (Q), 131.1 (Q), 119.9 (aromatic, Q), 116.8 (CH), 108.0 (CH), 44.0 (Q), 27.7 ($CH_2$), 19.8 (aromatic $CH_2$), 8.7 ($CH_3$) ppm.

Analysis. Found: C, 76.85; H, 7.20; N, 15.50 %; $C_{46}H_{52}N_8$ requires: C, 77.00; H, 7.30; N, 15.60 %.

IR (Nujol, KBr): 3442 (m, N-H), 1614 (s), 1557 (m), 1423 (w), 1331 (m), 1281 (m), 1246 (m), 1199 (s), 1175 (s), 1117 (m), 1080 (m), 1045 (m), 1000 (w), 951 (w), 881 (m), 771 (m) $cm^{-1}$.

EI-MS: m/z 717 (100%, $[M]^+$).

## 5.2 Chapter 2: Preparation of Monometallic Complexes

### 5.2.1 Synthesis of [U($L^{Et}$)]

a) To a high pressure ampoule charged with $H_4L^{Et}$ (100 mg, 0.139 mmol) and [U{N($SiMe_3$)$_2$}$_3$] (100 mg, 0.139 mmol) was added THF (20 mL) and the resultant brown solution heated to 80 °C overnight, during which time a red solution formed. Removal of the solvents under vacuum afforded [U($L^{Et}$)] as a red solid which was washed with hexane (2 × 5 mL), in a yield of 105 mg, 80 %.

Two separate batches of crystals suitable for X-ray diffraction were grown: (i) from a $C_6D_6$ solution of [(UI)$_2$(L)], which had been heated to 80 °C, and (ii) from a $C_6D_6$ solution of [(UN")($H_2$L)], which had been heated to 80 °C.

b) To a -78 °C toluene solution of [$UI_4(OEt_2)_2$] (198 mg, 0.222 mmol), $LiNEt_2$ was added slowly in a toluene solution (70 mg, 0.886 mmol), and was allowed to warm to room temperature over 4 hours. The resulting suspension was filtered, and the solution combined with $H_4L^{Et}$ (159 mg, 0.222 mmol). After 16 hours of stirring, the volatiles were removed and the resulting solid washed with hexane (2 × 15 mL). [U($L^{Et}$)] was isolated in a 90% yield (190 mg).

$^1$H NMR ($C_6D_6$, 360 MHz, 298 K) δ: 55.14, 39.38, 26.55. 25.35, 14.15, 13.29, -2.14, -12.31, -16.76, -35.84 ppm.

Analysis. Found: C, 57.93; H, 4.94; N, 11.84 %; $C_{60}H_{52}N_8U$ requires : C, 58.10; H, 5.09; N, 11.78 %.

IR (Nujol, KBr): 1560 (s, C=N), 1512 (w), 1251 (s), 1181 (m), 1052 (s), 1016 (w), 929 (w), 842 (w), 762 (m) $cm^{-1}$.

UV-vis (THF) $\lambda_{max}$ = 1112 nm ($\varepsilon$ = 78.27 $dm^3mol^{-1}cm^{-1}$)

$\mu_{eff}$ = 2.296 $\mu_B$ in a $C_6D_6$ solution.

EI-MS: m/z 950 (30 %, $[U(L)]^+$-2H), 921 (100% $[U(L)]^+$-Et), 892 (8 %, $[U(L)]^+$-2Et$]^+$), 720 (95 %, $[U(L)]^+$-4Et -U]).

$^1$H NMR of [U{N($SiMe_3$)$_2$}($H_2L^{Et}$)]: ($C_6D_6$, 360 MHz, 298 K) δ: 11.28 (2H, s, imino), 9.64 (2H, s, imino), 9.18 (2H, br s, NH), 8.30 (2H, s, pyrrolic CH), 7.16 (2H, s, aromatic), 7.07 (2H, s, pyrrolic CH), 6.44 (2H, s, pyrrolic CH), 6.03 (2H, s, pyrrolic CH), 2.25 (12H, s, aromatic $CH_3$), 2.07 (3H, s, $CH_3$), 1.42 (3H, s, $CH_3$), 0.50

(3H, s, $CH_3$), 0.30 (2H, s, $CH_2$), 0.13 (2H, s, $CH_2$), -2.82 (3H, s, $CH_3$),-2.91 (2H, s, $CH_2$), -3.16 (2H, s, $CH_2$), -13.07 (s, 18H, $N(SiMe_3)_2$) ppm.

### 5.2.2 Synthesis of $[UO_2(OPy)(L^{Et})]$

To a solution of $[U(L^{Et})]$ (200 mg, 0.21 mmol) in toluene (10 mL), pyridine N-oxide (46 mg, 0.42 mmol) in toluene (5 mL) was added. The resulting solution was stirred over 16 hours at 80 °C and the volatiles removed. The resulting dark brown solids (178 mg ) were washed with hexane and dried, with 86 % yield.

$^1$H NMR ($C_6D_6$, 298 K, 360 MHz) δ: 8.82 (2H, s, imino), 8.54 (2H, s, NH), 7.85 (2H, s, imino), 7.66 (2H, m, pyrrolic CH), 7.35 (2H, m, pyrrolic CH), 6.88 (2H, m, pyrrolic CH), 6.81 (2H, m, pyrrolic CH), 6.28 (2H, s, OPy), 6.16 (2H, s, aromatic), 5.87 (2H, s, aromatic), 5.74 (3H, s, OPy), 2.68 (2H, m, $CH_2$), 2.65 (2H, m, $CH_2$), 1.86 (12H, s, aromatic $CH_3$), 1.36 (2H, m, $CH_2$), 1.16 (3H, m, $CH_3$), 0.95 (2H, m, $CH_2$), 0.72 (3H, m, $CH_3$), 0.35 (3H, m, $CH_3$), 0.29 (3H, m, $CH_3$) ppm.

Analysis. Found: C, 56.87; H, 5.05; N, 11.44 %; $C_{52}H_{57}N_9UO_3$ requires: C, 57.08; H, 5.25; N, 11.52 %.

IR (Nujol, KBr): 3362 (m, NH), 1602 (s), 1584 (s, C=N), 1514 (w), 1282 (s), 1259 (s), 1182 (m), 1048 (s), 1014 (m), 895 (m, U=O), 840 (m), 800 (w), 765 (w), 718 (w), 673 (w) $cm^{-1}$.

### 5.2.3 Synthesis of $[UN_3(L^{Et})]$

To a solution of $[U(L^{Et})]$ (270 mg, 0.284 mmol) in toluene (10 mL), an excess of trimethylsilylazide in toluene (5 mL) was added at -78 °C. The resulting solution was allowed to warm to room temperature and stirred over 16 hours and the volatiles removed. The resulting dark brown solids were washed with hexane and dried, in a 64 % yield (182 mg).

$^1$H NMR ($C_6D_6$, 298 K, 360 MHz) δ: 56.72, 55.42, 19.86, 2.03, -1.71, -3.57, -5.58, -7.86, -8.23, -11.40, -12.68, -16.52, -20.22, -20.80, -23.90, -25.69, -30.65, -33.38 ppm.

IR (Nujol, KBr): 2080 (s, $N_3$), 1574 (s, C=N), 1251 (s), 1180 (m), 1100 (w), 1049 (s), 923 (w), 885 (m), 841 (m), 769 (s) $cm^{-1}$.

### 5.2.4 Synthesis of [{(Ce(HL$^{Et}$)}$_3$]

To a stirred solution of $H_4L$ (250 mg, 0.349 mmol) in toluene (5 mL) was added dropwise a solution of [Ce{N(SiMe$_3$)$_2$}$_3$] (217 mg, 0.349 mmol) in toluene (5 mL) at room temperature. The resulting orange mixture was stirred for 4 h, after which the solvent was removed under vacuum. The resulting orange solid was washed with cold hexanes (0 ºC, 10 mL) and dried under vacuum to yield 208 mg, 70% of [Ce(HL$^{Et}$)]$_3$. Single crystals of [{Ce(HL$^{Et}$)}$_3$] were grown from a saturated $C_6D_6$ solution.

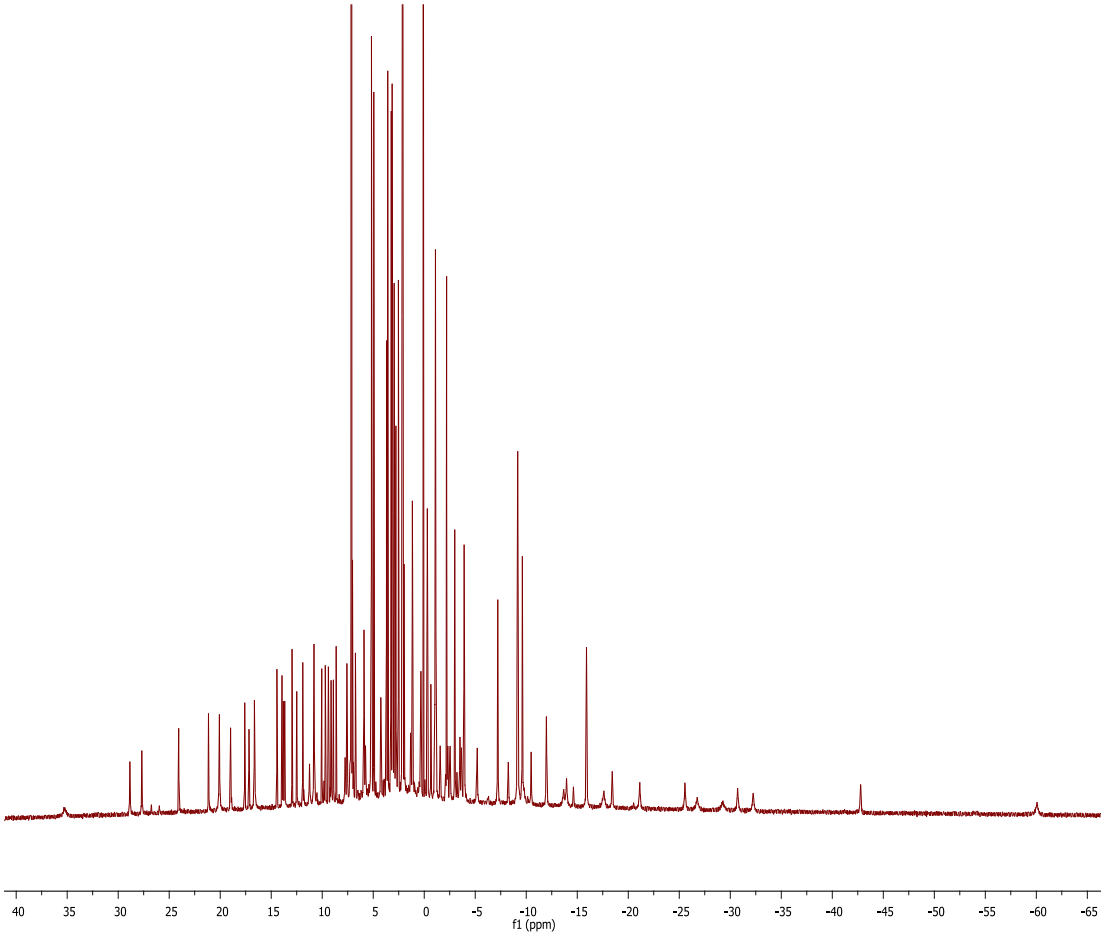


**Figure 1: $^1$H NMR spectrum of [{Ce(HL$^{Et}$)}$_3$]**

$^1$H NMR ($C_6D_6$, 298 K, 360 MHz) δ: 35.00 (1H), 28.83 (1H), 27.67 (1H), 24.06 (1H), 21.13 (1H), 20.06 (2 × 1H), 18.97 (1H), 17.58 (1H), 17.17 (1H), 16.63 (2 × 1H), 14.43 (1H), 13.93 (1H), 13.80 (1H), 13.66 (1H), 12.95 (1H), 12.49 (1H), 11.90 (1H), 11.23 (1H), 10.79 (3 × 1H), 10.03 (1H), 9.68 (1H), 9.38 (1H), 9.11 (1H), 8.89 (1H), 8.62 (1H), 7.57 (1H), 7.52 (1H), 6.73 (1H), 5.89 (2 × 1H), 5.75 (1H), 5.16 (2 ×

3H), 4.93 (3H), 4.24 (2H), 3.68 (3H), 3.56 (3H), 3.22 (3H), 3.13 (3H), 3.06 (3H), 2.93 (3H), 2.76 (3H), 2.51 (3H), 2.17 (3H), 1.96 (3H), 1.29 (2H), 1.15 (3H), 0.31 (2H), 0.09 (2 × 2H), -0.32 (3H), -0.67 (2H), -1.56 (2H), -2.20 (3H), -2.30 (1H), -3.00 (3H), -3.22 (1H), -3.52 (2H), -3.66 (2H), -3.92 (3H), -5.20 (2H), -7.22 (2 × 3H), -8.26 (2H), -9.18 (2 × 3H), -9.64 (3H), -10.50 (1H), -11.99 (2H), -13.69 (1H), -13.96 (1H), -14.64 (1H), -15.92 (3H), -17.64 (1H), -18.45 (1H), -21.14 (1H), -25.58 (1H), -26.78 (1H), -29.27 (1H), -30.73 (1H), -32.29 (1H), -42.79 (1H), -60.08 (1H) ppm.

Analysis. Calculated $C_{138}H_{147}N_{24}Ce_3$: C, 64.69; H, 5.86; N, 13.12 %. Found: C, 64.77; H, 5.86; N, 13.02 %.

IR (Nujol, KBr): 3408 (w, N-H), 1602 (s, C=N), 1572 (s, C=N), 1282 (s), 1252 (s), 1204 (w), 1184 (m), 1051 (s), 1001 (m), 894 (w), 863 (w), 845 (w), 832 (w), 758 (m) $cm^{-1}$.

### 5.2.5 Synthesis of $[Ce(THF)_2(HL^{Et})]$

To a stirred solution of $H_4L$ (250 mg, 0.349 mmol) in THF (5 mL) was added dropwise a solution of $[Ce\{N(SiMe_3)_2\}_3]$ (217 mg, 0.349 mmol) in THF (5 mL) at room temperature. The resulting orange mixture was stirred for 4 h, after which the solvent was removed under vacuum. The resulting orange solid was washed with cold hexanes (0 ºC, 10 mL) and dried under vacuum to yield 251 mg, 72% $[Ce(THF)_2(HL^{Et})]$. The THF adduct can also be synthesised by the addition of THF to a toluene solution of $[\{Ce(HL^{Et})\}_3]$.

Single crystals of $[Ce(THF)_2(HL^{Et})]$were grown from a saturated THF solution at -20 °C.

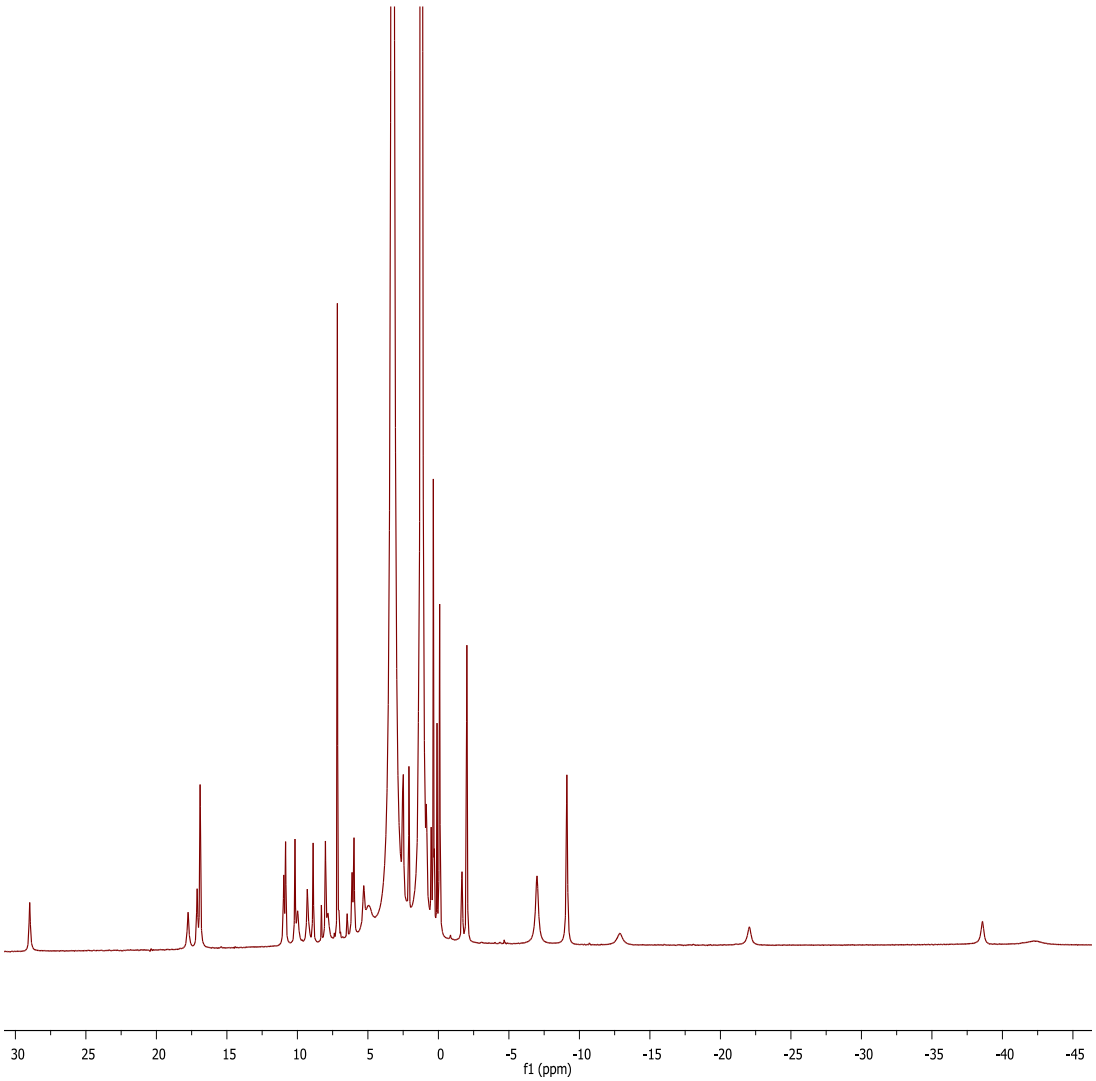


**Figure 2: $^{1}$H NMR of [Ce(THF)$_2$(HL$^{Et}$)]**

$^{1}$H NMR ($C_4D_8O$, 298 K, 360 MHz) δ: 29.14 (1H), 16.99 (1H), 16.79 (1H), 16.71 (1H), 16.56 (1H), 11.11 (1H), 10.72 (1H), 9.93 (1H), 9.56 (1H), 8.83 (1H), 8.66 (1H), 8.12 (2H), 7.83 (1H), 5.89 (2H), 5.66 (1H), 5.09 (2H), 4.78 (2H), 2.76 (1H), 2.67 (1H), 1.33 (3H), 1.24 (3H), 0.96 (2H), 0.53 (3H), 0.05 (1H), -0.31 (3H), -1.68 (2H), -2.14 (3H), -7.22 (2 × 3H), -9.47 (3H), -12.25 (2H), -22.86 (2H), -38.15 (2H) ppm.

Analysis. Calculated $C_{55}H_{68}N_8O_2Ce$: C, 65.34; H, 7.05; N, 10.69 %. Found: C, 65.20; H, 6.94; N, 10.85 %.

IR (Nujol, KBr): 3412 (w, N-H), 1598 (s, C=N) 1573 (s, C=N) 1282 (s), 1257 (s), 1184 (m), 1050 (s), 885 (w), 793 (w), 758 (m) cm$^{-1}$.

### 5.2.6 Synthesis of [Ce($L^{Et}$)]

A stirred solution of $K_4L^{Et}$ (453 mg, 0.521 mmol) (preparation in 1.3.1) in THF (25 mL) was added to a solution of $Ce(O^tBu)_4(THF)_2$ (300 mg, 0.521 mmol) in THF (20 mL) at -78 °C. The mixture was allowed to warm to room temperature and stirred for 12 h after which the volatiles were removed under reduced pressure to give an orange solid which was washed with hexane (3 × 20 mL) to remove the $KO^tBu$ to yield 365 mg, 82 % of [Ce($L^{Et}$)].

$^1$H NMR ($C_6D_6$, THF double presaturation, 360 MHz, 298 K) δ: 8.22 (4H, s, imino), 6.86 (4H, s, aromatic), 6.65 (4H, m, pyrrolic CH), 6.21 (4H, m, pyrrolic CH), 2.57 (2H, m, $CH_2$), 2.40 (2H, m, $CH_2$), 2.06 (12H, s, aromatic $CH_3$), 1.78 (2H, m, $CH_2$), 1.45 (3H, m, $CH_3$), 1.33 (3H, m, $CH_3$), 1.28 (2H, m, $CH_2$), 0.99 (3H, m, $CH_3$), 0.94 (3H, m, $CH_3$) ppm.

Analysis. Calculated $C_{46}H_{48}N_8Ce$: C, 64.77; H, 5.67; N, 13.14 %. Found: C, 64.82; H, 5.73; N, 13.08 %.

IR (Nujol, KBr): 1590 (s, C=N), 1566 (s, C=N), 1284 (s), 1173 (m), 1037 (s), 999 (w), 964 (w), 887 (w), 788 (w), 748 (m), 728 (m) $cm^{-1}$.

### 5.2.7 Synthesis of [{Ce($L^{Et}$)}$_2$Zn]

Toluene was added to a mixture of [Ce($HL^{Et}$)] (240 mg, 0.233 mmol) and $[Zn\{N(SiMe_3)_2\}_2]$ (43 mg, 0.116 mmol) at -78 °C, and the resulting solution was allowed to warm to room temperature over 16 hours. The volatiles were removed under vacuum and the remaining orange solid washed with hexane and dried under vacuum. The orange solid of [{Ce($L^{Et}$)}$_2$Zn] was obtained in a 92 % yield (380 mg).

$^1$H NMR ($C_6D_6$, THF double presaturation, 360 MHz, 298 K) δ: 29.08 (1H), 16.94 (1H), 16.74 (2 × 1H), 16.52 (1H), 11.07 (1H), 10.68 (1H), 9.89 (1H), 9.54 (1H), 8.78 (1H), 8.62 (1H), 8.10 (1H), 7.76 (1H), 5.84 (1H), 5.62 (1H), 5.06 (1H) 2.71 (3H), 1.67 (3H), 1.28 (3H), 1.20 (3H), 0.93 (3H), -1.72 (3H), -2.07 (3H), -7.25 (2H), -9.51 (3H), -12.24 (2H), -22.87 (2H), -38.15 (2H) ppm.

Analysis. $C_{92}H_{96}N_{16}Ce_2Zn$: C, 62.38; H, 5.46; N, 12.65 %. Found: C, 62.43; H, 5.72; N, 12.44 %.

IR (Nujol, KBr): 1598 (s, C=N), 1574 (s, C=N), 1256 (s), 1183 (m), 1052 (s), 1016 (w), 930 (w), 884 (w), 841 (w), 800 (w), 758 (w), 722 (w) $cm^{-1}$.

### 5.2.8 Synthesis of [{(Y(HL$^{Et}$)}$_3$]

To a stirred solution of $H_4L$ (250 mg, 0.349 mmol) in toluene (5 mL) was added a solution of [Y{N(SiMe$_3$)$_2$}$_3$] (217 mg, 0.349 mmol) in toluene (5 mL) at room temperature. After 4 h the solvent was removed under vacuum and the orange solid residues were washed with cold hexane and dried under vacuum to yield 184 g, 66 % [{Y(HL)}$_3$] as an orange solid.

$^1$H NMR ($C_6D_6$, 360 MHz, 298 K) δ: 9.46 (1H, s), 8.56 (1H, s), 8.28 (3 × 1H, s), 8.03 (1H, s), 8.01 (1H, d), 7.99 (1H, s), 7.91 (1H, d), 7.77 (1H, s), 7.43 (1H, d), 7.38 (1H, s), 7.32 (1H, s), 7.05 (1H, d), 6.98 (1H, d), 6.96 (1H, s), 6.94 (2 × 1H, d), 6.85 (2 × 1H, s), 6.79 (2 × 1H, d),6.67 (1H, d), 6.63 (1H, d), 6.54 (1H, d), 6.47 (1H, d), 6.41 (2 × 1H, d), 6.39 (2 × 1H, d), 6.27 (1H, s), 6.26 (1H, s), 6.24 (2 × 1H, d), 6.20 (2 × 1H, d), 6.17 (1H, s), 6.16 (1H, s), 6.10 (2 × 1H, s), 6.04 (1H, s), 6.03 (1H, s), 6.02 (1H, s), 6.01 (1H, s), 5.98 (1H, s), 5.97 (1H, s), 5.86 (1H, s), 5.73 (2 × 1H, d), 5.33 (1H, s), 2.60 (2H, m), 2.52 (2H, m), 2.40 (2H, m), 2.22 (2H, m), 2.06 (6 × 3H, s), 2.04 (3H, s), 1.99 (3H, s), 1.97 (3H, s), 1.91 (3H, s), 1.79 (3H, m), 1.69 (3H, m), 1.67 (3H, m), 1.58 (3H, m), 1.45 (3H, m), 1.40 (2H, s), 1.36 (3H, s), 1.29 (3H, m), 1.19 (3H, m), 1.18 (3H, s), 1.17 (3H, m), 1.11 (3H, s), 1.05 (2H, s), 0.97 (2H, s), 0.95 (2H, s), 0.87 (3H, m), 0.85 (2H, s), 0.75 (3H, m), 0.52 (3H, m), 0.47 (3H, m), 0.28 (3H, m), 0.22 (3H, m) ppm.

Analysis. Calculated $C_{138}H_{147}N_{24}Y_3$: C, 68.82; H, 6.15; N, 13.96 %. Found: C, 68.73; H, 6.26; N, 13.40 %.

IR (Nujol, KBr): 3442 (m, N-H), 3408 (m, N-H), 3343 (w, N-H), 1608 (s, C=N), 1591 (s, C=N), 1575 (s, C=N), 1456 (s), 1396 (w), 1377 (m), 1330 (w), 1274 (s), 1249 (s), 1177 (m), 981 (s), 864 (m), 832 (m), 772 (m), 730 (w) cm$^{-1}$.

EI-MS: m/z 802 (15%, [Y(HL)]$^+$), 773 (100 %, [Y(HL)-Et]$^+$),741 (57%[Y(HL)-3Et+Na]$^+$), 717 (59 %, [Y(HL)-3Et]$^+$), 688 (95 %, [Y(HL)-4Et]$^+$).

### 5.2.9 Synthesis of [(Y(THF)$_2$(HL$^{Et}$)]

A solution of [Y{N(SiMe$_3$)$_2$}$_3$] (217 mg, 0.349 mmol) in THF (5 mL) was added to a solution of $H_4L^{Et}$ (250 mg, 0.349 mmol) in THF (5 mL) at room temperature. After 4 hours the solvent was removed under vacuum and the orange solid residues were

washed with cold hexane and dried under vacuum to yield a yellow solid of 49 % of $[Y(THF)_2(HL^{Et})]$.

$[Y(THF)_2(HL^{Et})]$ can also be synthesised by the addition of THF to $[\{Y(HL)\}_3]$.

Single crystals of $[Y(THF)_2(HL^{Et})]$were grown from a saturated $C_6D_6$ solution.

$^1$H NMR ($C_6D_6$, THF double presaturation, 360 MHz, 298 K) δ: 9.75 (1H, s), 9.33 (1H, s), 8.57 (1H, s), 8.19 (1H, s), 8.17 (1H, s), 8.11 (1H, s), 8.10 (1H, s), 7.55 (1H, s), 7.37 (1H, s), 7.04 (1H, s), 6.80 (1H, d) 6.79 (1H, d), 6.55 (1H, s), 6.50 (1H, d), 6.42 (1H, s), 6.32 (1H, d), 6.27 (1H, t), 6.16 (1H, d), 6.10 (1H, d), 6.03 (1H, s), 5.87 (1H, t), 2.44 (2H, m), 2.01 (2H, m), 1.86 (2H, m), 1.07 (3H, t), 0.82 (3H, t), 0.72 (3H, t), 0.62 (2H, m), 0.46 (3H, t) ppm.

Analysis. Calculated $C_{50}H_{57}N_8OY$: C, 68.64; H, 6.57; N, 12.81 %. Found: C, 68.75; H, 6.70; N, 12.71 %.

IR (Nujol, KBr): 3439 (m, N-H), 1613 (s, C=N), 1574 (s, C=N), 1249 (s), 1176 (s), 1047 (s), 981 (s), 932 (w), 833 (m), 772 (w) $cm^{-1}$

EI-MS: m/z 802 (6%, $[Y(HL)]^+$), 773 (46 %, $[Y(HL)-Et]^+$), 740 (46%, $[Y(HL)-3Et+ Na]^+$), 718 (100 %, $[Y(HL)-3Et]^+$), 687 (100 %, $[Y(HL)-4Et]^+$).

$[\{Y(HL^{Et})\}_3]$ was dissolved in $d_5$-pyridine, to give the pyridine adduct, $[(Y(Pyr)_2(HL^{Et})]$.

$^1$H NMR ($C_5D_5N$, 250 MHz, 298 K) δ: 10.95 (1H, s, NH), 10.00 (1H, s, pyr), 8.63 (2H, s, pyr), 8.43 (1H, s, imino), 8.40 (1H, s, imino), 8.32 (2H, s, pyr), 8.22 (1H, s, imino), 8.20 (1H, s, imino), 7.70 (1H, s, aromatic), 7.18 (1H, s, aromatic), 7.16 (1H, d, pyrrolic CH), 7.08 (1H, s, aromatic), 6.97 (1H, d, pyrrolic CH), 6.87 (1H, s, aromatic), 6.78 (1H, d, pyrrolic CH), 6.58 (1H, d, pyrrolic CH), 6.56 (1H, d, pyrrolic CH), 6.43 (1H, d, pyrrolic CH), 6.33 (1H, d, pyrrolic CH), 6.28 (1H, d, pyrrolic CH), 3.01 (2H, m, $CH_2$), 2.51 (2H, m, $CH_2$), 2.43 (3H, s, aromatic $CH_3$), 2.37 (2H, m, $CH_2$), 2.29 (3H, s, aromatic $CH_3$), 2.16 (3H, s, aromatic $CH_3$), 1.89 (3H, s, aromatic $CH_3$), 1.26 (3H, m, $CH_3$), 0.92 (3H, m, $CH_3$), 0.76 (3H, m, $CH_3$), 0.43 (3H, m, $CH_3$), 0.38 (2H, m, $CH_2$) ppm.

### 5.2.10 Synthesis of [{Y(OH$_2$)(H$_2$L$^{Et}$)}$_2$(μ-OH)$_2$]

To a stirred solution of [{Y(HL$^{Et}$)}$_3$] (50 mg, 0.0207 mmol) in toluene (5 mL), degassed water (2.2 mL, 0.124 mmol) was added dropwise. An immediate colour change occurred from orange to yellow. The solvent was removed to yield a yellow solid (45 mg, 85 %).

Analysis. Calculated $C_{47}H_{56}N_8O_2Y$: C, 66.11; H, 6.61; N, 13.12 %. Found: C, 65.71; H, 6.47; N, 13.19 %.

IR (Nujol, KBr): 3440 (m, N-H), 3097 (m, b, OH), 1614 (s, C=N), 1557 (s, C=N), 1331 (m), 1282 (m), 1249 (m), 1199 (s), 1176 (s), 1117 (m), 1081 (m), 1045 (s), 1000 (s), 952 (w), 881 (m), 771 (s) cm$^{-1}$

## 5.3 Chapter 3: Preparation of Bimetallic Complexes

### 5.3.1 Preparation of tetrapotassium salt, [K$_4$(L$^{Et}$)]

THF (20 mL) was added to a stirred mixture of H$_4$L$^{Et}$ (600 mg, 0.84 mmol) and an excess of KH (170 mg), causing rapid effervescence. After 2 h, the resulting slurry was allowed to settle, the yellow supernatant liquors was decanted, and evaporated under vacuum to yield 489 mg, 67% of [K$_4$(L$^{Et}$)], as an orange powder.

$^1$H NMR ($C_6D_6$, 360 MHz, 293 K) δ: 8.36 (4H, s, imino), 7.16 (4H, s, aromatic), 6.96 and 6.56 (2 × 4H, m, pyrrolic CH), 2.62 (2 × 2H, m, $CH_2$), 2.26 (12H, s, aromatic $CH_3$), 2.11 (3H, m, $CH_3$), 1.24 (2 × 3H, m, $CH_3$), 0.90 (1 × 3H, 1 × 2H, m, $CH_3$, $CH_2$), 0.23 (2H, m, $CH_2$) ppm.

$^{13}$C{$^1$H} NMR ($C_6D_6$, 360 MHz, 293 K) δ: 158.99, 151.02, 138.23, 131.89, 128.151, 127.93, 120.77, 118.06, 108.40, 47.38, 19.79, 1.42 ppm.

Analysis. Found: C, 76.85; H, 7.20; N, 15.50 %. $C_{46}H_{48}N_8K_4$ requires: C, 77.0, H, 7.30; N, 15.60 %.

IR (Nujol mull, KBr): 1589 (s), 1567 (s), 1462 (s), 1377 (m), 1284(m), 1175 (w), 1038 (s), 968 (w), 889 (w), 792 (w), 750 (w) cm$^{-1}$.

### 5.3.2 Preparation of [(UI)$_2$(L$^{Me}$)]

To a mixture of H$_4$L$^{Me}$ (240 mg, 0.36 mmol) and an excess of KH (78 mg, 1.94 mmol), THF (20 mL) was added and the slurry was stirred for 2 h. The resulting

yellow solution was transferred, away from remaining KH, to a slurry of $UI_3(THF)_4$ (662 mg, 0.73 mmol) in THF (10 mL) at -78 ºC. On addition the solution turned green. After warming to room temperature overnight the red solution is filtered from the KI precipitate and the KI washed with THF (2 × 5 mL). The volatiles were removed and the product extracted into warm toluene. The solution was isolated and the volatiles removed to give a red precipitate. Drying under reduced pressure afforded $[(UI)_2(L^{Me})]$ as a red solid. Yield: 249 mg (50 %).

Solubility: in THF 15mg/mL.

No assignable NMR spectrum could be observed.

Analysis. Calculated $C_{42}H_{40}N_8I_2U_2$: C, 36.38; H, 2.91; N, 8.08 %. Found C, 36.42; H, 2.97; N, 7.97 %.

IR (Nujol, KBr): 1572 (s), 1512 (w), 1277 (s), 1210 (m), 1048 (s), 1017 (m), 951 (w), 896 (w), 796 (m), 769(m), 728(m).

$\mu_{eff}$ = 3.02 $\mu_B$ in a $C_5D_5N$ solution.

### 5.3.3 Preparation of $[(UI)_2L^{Et}]$

To a mixture of $H_4L^{Et}$ (240 mg, 0.36 mmol) and an excess of KH (78 mg, 1.94 mmol), THF (20 mL) was added and the slurry was stirred for 2 h. The resulting yellow solution was decanted off the remaining KH onto a slurry of $UI_3$ (451 mg, 0.73 mmol) in THF (10 mL) at -78 ºC. On addition the solution turned green. After warming to room temperature overnight the red solution was filtered from the KI precipitate and the KI washed with THF (2 × 5 mL). The volatiles were removed under reduced pressure and the product extracted into warm toluene. The solution was isolated and dried to a red precipitate characterised as $[(UI)_2L^{Et}]$. Yield 214 mg (90 %).

Solubility: in toluene 10mg/mL; in THF > 20mg/mL.

$^1$H NMR ($C_6D_6$, THF double presaturation, 298 K, 300 MHz) δ: 35.9, (3H, s, aromatic $CH_3$), 24.6, (1H, s, aromatic CH), 12.8, (1H, s, NCHCN), -0.86, (3H, s, $CH_2CH_3$), -3.2, (1H, s, THF), -4.6, (2H, s, $CH_2CH_3$) , -10.7, (1H, s, THF), -17.1, (1H, s, pyrrolic CH) -42.5, (1H, s, pyrrolic CH) ppm.

Analysis. Calculated $C_{46}H_{48}N_8I_2U_2$: C, 38.29; H, 3.35; N, 7.71 %. Found: C, 38.39; H, 3.44; N, 7.67 %.

IR (Nujol mull, KBr): 1572 (s), 1512 (w), 1277 (s), 1210 (m), 1048 (s), 1017 (m), 951 (w), 896 (w), 796 (m), 769 (m), 728 (m) $cm^{-1}$.

UV-vis (THF) $\lambda_{max}$ = 1179 nm ($\varepsilon$ = 1315.6 $dm^3$ $mol^{-1}$ $cm^{-1}$ ).

The following crystallisation strategies were tried for complexes $[(UI)_2L^{Et}]$ and $[(UI)_2L^{Me}]$ in addition to room temperature crystallisation attempts. Vapour phase crystal growth was not possible since sublimation results in decomposition.

Soxhlet extraction using toluene, toluene/hexane (50:50) and benzene solution.

**Single solvent:** THF at RT, at -30 °C and at -80 °C.

Toluene at RT, at -30 °C and at -80 °C.

Pyridine at RT, at -30 °C and at -80 °C.

Benzene at RT.

**Slow diffusion:** THF/hexane (50:50) at RT and at -20 °C.

Toluene/hexane (50:50) at RT and at -20 °C.

Pyridine/hexane (50:50) at RT and at -20 °C.

THF/diethyl ether (50:50) at RT and at -20 °C.

THF/toluene (50:50) at RT, at -20 °C.

Benzene/hexane (50:50) at RT.

Benzene/hexane (80:20) at RT.

**Interface:** THF/hexane (50:50) at RT, at -20 °C and at -80 °C.

Toluene/hexane (50:50) at RT, at -20 °C and at -80 °C.

Pyridine/hexane (50:50) at RT and at -20 °C.

THF/diethyl ether (50:50) at RT and at -80 °C.

THF/toluene (50:50) at RT, at -20 °C and at -80 °C.

THF/toluene (20:80) at -80 °C.

Benzene/hexane (50:50) at RT.

Benzene/hexane (80:20) at RT.

### 5.3.4 Substitution reactions of $[(UI)_2L]$

General synthetic procedure:

To the diuranium complexes either $[(UI)_2(L^{Et})]$, or $[(UI)_2(L^{Me})]$, two equivalents of the potassium or sodium salt of the reagent was added. The mixture was then cooled to -78 °C. THF was added and the reaction solution was allowed to warm to room

temperature overnight. The resulting solution was filtered from the KI or NaI precipitate and the precipitate washed with THF (2 × 5 mL). The volatiles were removed.

$[(UCp)_2(L^{Et})]$: $[(UI)_2(L^{Et})]$ (50 mg, 0.034 mmol) and NaCp (9.0 mg, 0.069 mmol). The solid was then redissolved in toluene (10 mL), and refiltered ensuring all NaI was removed. The toluene solution was concentrated to 3 mL, layered with hexane and cooled to -30 °C to give a red precipitate, $[(UCp)_2(L^{Et})]$.

$[(UCp^*)_2(L^{Et})]$: $[(UI)_2(L^{Et})]$ (100 mg, 0.0720 mmol) and KCp* (25.0 mg, 0.144 mmol).

$[(UCH_2Ph)_2(L^{Et})]$: $[(UI)_2(L^{Et})]$ (50 mg, 0.036 mmol) and $KCH_2Ph$ (9.4 mg, 0.072 mmol).

$[(U\{N(SiMe_3)_2\})_2(L^{Me})]$: $[(UI)_2(L^{Me})]$ (75 mg, 0.054 mmol) and $K\{N(SiMe_3)_2\}$ (21.0 mg, 0.108 mmol). The red solid was redissolved in toluene (5 mL), layered with hexane and then cooled to -30 °C.

$[\{UO(C_6H_3\text{-}t\text{-}Bu_2)\}_2(L^{Me})]$: $[(UI)_2(L^{Me})]$ (64 mg, 0.046 mmol) and $NaO(C_6H_3\text{-}t\text{-}Bu_2)$ (21 mg, 0.092 mmol)

$[\{UOC(CH_3)_2(CH_2CH_3)\}_2(L^{Et})]$: $[(UI)_2(L^{Et})]$ (250 mg, 0.173 mmol) and $KOC(CH_3)_2(CH_2CH_3)$ (44 mg, 0.035 mmol).

A mixture of $[(UI)_2(L^{Et})]$ (50 mg, 0.036 mmol) and KH (2.9 mg, 0.072 mmol) was cooled to -78 °C. THF (10 mL) was added and the reaction solution was allowed to warm to room temperature overnight. The resulting red solution was filtered from the KI precipitate and the KI washed with THF (2 × 5 mL). The volatiles were removed and the product extracted into warm toluene. The solution was isolated and the volatiles removed to give a red precipitate.

### 5.3.5 Preparation of $[(UBH_4)_2(L^{Et})]$

A high pressure ampoule was charged with $[(UI)_2(L^{Et})]$ (56.0 mg, 0.0403 mmol) and $KBH_4$ (4.40 mg, 0.0803 mmol) and THF (10 mL) was added. The reaction solution was heated at 50 °C overnight. The resulting red solution was filtered from the KI precipitate and the KI washed with THF (2 × 5 mL). The combined filtrate and washings were dried to afford $[(UBH_4)_2(L^{Et})]$ as a dark red solid. Yield 44 mg (79 %).

Solubility: in THF > 20 mg/ml.

Analysis. Calculated $C_{46}H_{56}N_8B_2U_2$: C, 45.34; H, 4.63; N, 9.19 %. Found: C, 45.30; H, 4.71; N, 9.03 %.

IR (Nujol mull, KBr): 2451 (m, B-H stretch), 2211 (m, B-H stretch), 1575 (s), 1511 (w), 1260 (s), 1187 (w, B-H bridging deformation), 1093 (s), 1019 (s), 862 (m), 799 (s), 704 (w) $cm^{-1}$.

UV-vis (THF) $\lambda_{max}$ = 1178 nm ($\varepsilon$ = 1001.2 $dm^3mol^{-1}cm^{-1}$).

### 5.3.6 Substitution reactions of [(UI)$_2$(L)] by Boron groups

A solution of $KBEt_3H$ (10.40 mL, 0.208 mmol, 0.02 M solution in THF) was added to a -78 °C solution of [$(UI)_2(L^{Me})$] (150 mg, 0.104 mmol) in THF (10 mL). After warming to room temperature overnight, the red solution was filtered away from the KI, and washed with THF (2 × 5 mL). The volatiles were removed under reduced pressure and the product extracted into toluene and cooled to -30 °C.

THF (10 mL) was added to [$(UI)_2(L^{Me})$] (50 mg, 0.036 mmol) and $KBPh_4$ (25.8 mg, 0.072 mmol) at -78 °C. After warming to room temperature overnight, the red solution was filtered away from the KI, and washed with THF (2 × 5 mL). The solution was concentrated under reduced pressure which was then cooled to -30 °C.

### 5.3.7 Attempted Preparation of [(UH)$_2$(L)]

Attempts to remove the $BH_3$ group from [$(UBH_4)_2(L^{Et})$] were performed with $PMe_3$ and *t*-BuNC.

In a high pressure ampoule, an excess of $PMe_3$ (25.7 mL, 0.514 mmol, 0.02 M solution in toluene) was added to a solution of [$(UBH_4)_2(L^{Et})$] (252 mg, 0.206 mmol) in toluene (10 mL). The resultant mixture was heated to 80 °C for 16 h after which time the volatiles were removed and the solid washed in cold toluene yielding a brown-yellow solid (180 mg, 73 %).

IR (Nujol, KBr): 1576 (m), 1260 (m), 1168 (m), 1087 (m), 1036 (m), 993 (m), 800 (s), 721 (w) $cm^{-1}$.

IR (hexachloro-1,3-butadiene mull, KBr): 1514 (w), 1459 (m), 1214 (w), 1183 (m), 1095 (m) $cm^{-1}$.

To a solution of $[(UBH_4)_2(L^{Et})]$ (80 mg, 0.123 mmol) in THF (10 mL), *t*-BuNC (12 mg, 0.245 mmol) was added. The solution was stirred at room temperature for 16 h and then the volatiles were removed to give a brown solid (90 mg, 67 %).

### 5.3.8 Preparation of $[(UCl_2)_2(L^{Et})]$

To $H_4L^{Et}$ (240 mg, 0.36 mmol) an excess of KH (78 mg, 1.94 mmol) and THF (20 mL) were added and the slurry was stirred for 2 h. The resulting yellow solution was transferred, away from remaining KH, to a slurry of $UCl_4$ (255 mg, 0.67 mmol) in THF (10 mL) at -78 ºC. After warming to room temperature overnight the red solution was filtered from the KCl precipitate and the KCl washed with THF (2 × 5 mL). The THF solution was concentrated to 3 mL and layered with hexane at -78 °C, which resulted in a yellow precipitate. This was dried under reduced pressure to afford $[(UCl_2)_2(L^{Et})]$, as a yellow solid, yield of 81 % (347 mg).

No assignable $^1$H NMR was obtained.

Analysis. Calculated $C_{46}H_{48}N_8Cl_4U_2$: C, 41.52; H, 3.64; N, 8.42 %. Found: C, 42.35; H, 3.93; N, 8.38 %.

IR (Nujol, KBr,): 1575 (s), 1504 (w), 1260 (s), 1056 (s), 1016 (s), 898 (m), 791 (w), 766 (m), 721 (m) $cm^{-1}$.

UV-vis (THF) $\lambda_{max}$ = 1180 nm ($\varepsilon$ = 370.7 $dm^3mol^{-1}cm^{-1}$).

### 5.3.9 Preparation of $[(CeI)_2(L^{Et})]$

To $K_4L^{Et}$ (306 mg, 0.35 mmol) in THF (20 mL) a slurry of $CeI_3(THF)_4$ (570 mg, 0.70 mmol) in THF (10 mL). The reaction was then heated to 70 °C overnight and the brown solution was filtered from the KI precipitate and the KI washed with THF (2 × 5 mL). The THF solution was dried under reduced pressure to afford $[(CeI)_2(L^{Et})]$, as a dark yellow solid, yield of 66 % (290 mg).

$^1$H NMR ($C_6D_6$, 360 MHz, 298 K) δ: 12.19, 10.44, 7.50, 5.09, 1.13, 0.62, -2.79, -4.48, -9.08, -12.94, -20.90 ppm.

$^{13}C\{^1H\}$ NMR ($C_6D_6$, 500 MHz, 300 K) δ: 165.47, 153.32, 151.91, 131.24, 130.97, 124.30, 123.37, 117.71, 55.09, 48.24, 37.13, 18.92, 17.57, 6.18 ppm.

Analysis. Calculated $C_{46}H_{48}N_8Cl_4Ce_2$: C, 44.31; H, 3.88; N, 8.99 %. Found: C, 44.45; H, 3.84; N, 7.89 %.

### 5.3.10 Preparation of $[(NpI)_2(L^{Et})]$

Solid $K_4L^{Et}$ (250 mg, 0.286 mmol) was added in portions to a solution of $NpI_3(THF)_4$ (519 mg, 0.573 mmol) in THF (20 mL) at room temperature causing an immediate colour change from terracotta to dark brown. The solution was stirred for 3 days at room temperature. The solids were filtered using a frit, washed with a small quantity of pentane and the combined filtrate and washings evaporated to dryness under vacuum. The solids were dried for 2 h at 90 ºC under vacuum to yield $[(NpI)_2(L^{Et})]$ as a microcrystalline dark brown solid (405 mg, 98 %).

Solubility: in toluene, 2.0 mg/ml; in THF > 17.0 mg/ml.

Analysis. Calculated. for $[(NpI)_2(L^{Et})]$: Np, 32.90 %. Found: gravimetric Np, 32.5. radiometric (α-,γ-spectroscopy) Np, 33.22.

[Starting material, Analysis. Calculated. for $NpI_3(THF)_4$ Calculated. 26.15 %, Found: 26.39 (radiometric)].

FTIR $\nu_{max}$ ($cm^{-1}$): 3397 (w, br), 3278 (w, br), 2966 (vs), 2932 (vs), 2873 (vs), 1648 (vs), 1619 (sh), 1596 (vs), 1575 (vs), 1513 (s), 1475 (sh), 1452 (s), 1396 (w), 1327 (sh), 1264 (vs), 1184 (s), 1122 (w), 1106 (w), 1050 (vs), 1015 (s), 898 (s), 862 (s), 769(s), 719 (w), 682 (w), 564 (sh), 522 (s).

FIR $\nu_{max}$ ($cm^{-1}$): 562 (sh), 525 (vs), 396 (vs), 180 (w), 117 (w).

UV/vis/nir-IR (THF) $\lambda_{max}$ nm, (ε, $M^{-1}$ $cm^{-1}$): 746 (sh), 771 (63), 785 (sh), 796 (sh), 812 (sh), 852 (44), 941 (46), 980 (sh), 1012 (42), 1034 (sh), 1079 (32), 1308 (5, br), 1690 (17, br), charge transfer 369 (30500), 456 (sh).

UV/vis/nir-IR (toluene) $\lambda_{max}$ nm, (ε, $M^{-1}$ $cm^{-1}$): 732 (75), 748 (70), 767 (66), 827 (49), 867 (56), 917 (sh), 946 (sh), 990 (38), 1229 (14, br), 1366 (14,br) 1617 (14, br), charge transfer 344 (34600).

UV/vis/nir-IR (solid) $\lambda_{max}$ nm: 721, 749, 763, 826, 852, 997, 1147, 1184, 1268, 1369, 1407, 1591, 1791, 1883.

## 5.4 Chapter 4: Adducts of Uranium Halides

### 5.4.1 Uranium Turnings

Uranium turnings, stored under oil, were prepared by washing with concentrated $HNO_3$ (16 M) until a shiny metallic surface was exposed, washed with distilled $H_2O$,

then acetone and then dried under vacuum. Turnings prepared in this way, of diameters between 0.5 and 1.0 mm, were stored in a sealed container, under a nitrogen atmosphere (<0.1 ppm $O_2$) at –35 ºC, and were viable for up to a year after cleaning.

### 5.4.2 Synthesis of $UI_3$

Diethyl ether (100 mL) was added to a mixture of uranium turnings (2.00 g, 8.40 mmol) and iodine (3.18 g, 12.5 mmol). The resulting mixture was vigorously stirred, and sonicated twice daily for 30 mins, for five days during which time the brown solution turned red then faded to a pale purple as a dark purple solid was deposited. The mixture was filtered and the residue washed with diethyl ether (2 × 10 mL). Drying of the solid under vacuum gave $UI_3$ as a dark purple-black powder in a 96 % yield (4.98 g).

Analysis. Calculated $UI_3$: U, 38.47; I, 61.53 %. Found: U, 35.41; I, 59.21; C, 1.13; H, 0.50 %.

UV-vis (THF) $\lambda_{max}$ = 1178 nm ($\varepsilon$ = 197.0 $dm^3mol^{-1}cm^{-1}$).

### 5.4.3 Synthesis of $UI_4(OEt_2)_2$,

Diethyl ether (50 mL) was added to a mixture of uranium turnings (0.30 g, 1.26 mmol) and iodine (0.64 g, 2.52 mmol). The resulting mixture was sonicated for 1 h and then vigorously stirred for 16 h, sonicated for a further 30 minutes, then stirred for a further 4 h, during which time the brown solution turned pale red, and a dark red microcrystalline solid was deposited. The mixture was concentrated to ~10 mL volume and filtered. Drying of the solid under vacuum gave $UI_4(OEt_2)_2$ as a microcrystalline red solid in a 71 % yield (0.80 g). X-ray quality crystals of $UI_4(OEt_2)_2$ were grown from a saturated diethyl ether solution.

$^1$H NMR (360 MHz, $C_6D_6$, 298 K) δ: -10.45 (12H, s, C*H*$_3$), -22.54 (8H, s, C*H*$_2$) ppm.

Analysis. Calculated $UI_4(OEt_2)_2$: U, 26.63; I, 56.79; C, 10.75; H, 2.26 %. Found: U, 27.15; I, 59.3; C, 10.68; H, 2.19 %. $UI_4(Et_2O)_{1.5}$ requires: I, 59.24 %.

UV-vis (Diethyl ether): $\lambda_{max}$ = 1077 nm ($\varepsilon$ = 19.6 $dm^3mol^{-1}cm^{-1}$).

$\mu_{eff}$ = 2.15 $\mu_B$ in a $C_6D_6$ solution.

### 5.4.4 Reaction of $UI_4(OEt_2)_2$ with uranium turnings to give $UI_3$

Diethyl ether (50 mL) was added to a mixture of uranium turnings (44.1 mg, 0.19 mmol) and $UI_4(OEt_2)_2$ (500 mg, 0.56 mmol). The resulting mixture was vigorously stirred, and sonicated twice daily for 30 mins, for 5 days, during which time the red colour dissipated and a dark purple-black solid was deposited. The mixture was filtered and the solid washed with ether (2 × 10 mL). Drying of the solid under vacuum gave $UI_3$ as a dark violet-black powder in a 93 % yield (0.43 g).
Analysis. Calculated $UI_3$: U, 38.47; I, 61.53 %. Found: U, 35.30; I, 59.18 %.

### 5.4.5 Synthesis of $UI_4(OBu_2)$

Dibutyl ether (30 mL) was added to a mixture of uranium turnings (0.22 g, 0.93 mmol) and iodine (0.47 g, 1.86 mmol). The resulting mixture was vigorously stirred, and sonicated twice daily for 30 mins, for seven days during which time the brown solution faded and turned green, and a green powder was deposited. The mixture was concentrated to ~10 mL volume and filtered. Drying of the solid under vacuum gave $UI_4(OBu_2)$ as a finely divided green solid in a 85% yield (0.69 g).
Analysis. Calculated $UI_4(OBu_2)$: C, 10.97; H, 2.07 %. Found: C, 10.68; H, 2.34 %.

### 5.4.6 Synthesis of $[U\{N(SiMe_3)_2\}_3]$ from $UI_3$

Toluene (10 mL) was added to a mixture of $UI_3$ (100 mg, 0.162 mmol) and $K\{N(SiMe_3)_2\}$ (96.7 mg, 0.485 mmol). The resulting dark purple solution was stirred for 24 h during which time the solution took on a distinct reddish colour. The solution was filtered to remove KI, and the solvent evaporated to yield the crude product as a purple-red solid that was collected and dried under vacuum and isolated in a 63 % yield (72.6 mg).
$^1H$ NMR ($C_6D_6$, 250 MHz, 298 K) δ: -11.20 (46H, s, $CH_3$) ppm; this agrees with the literature value.[8]

### 5.4.7 Synthesis of $U(Cp)_3I$ from $UI_4(OEt_2)$

To a cold (-78 °C) mixture of $UI_4(OEt_2)_2$ (400 mg, 0.51 mmol) and NaCp (135 mg, 134 mmol) was added cold THF (40 ml, -78 °C). The resulting mixture was allowed to warm to room temperature overnight, upon which the colour changed from red to

brown, and a colourless precipitate formed. The solution was filtered to remove NaI, and the solvent evaporated to yield the crude product as a brown solid that was collected and dried under vacuum and was isolated in a 63 % yield (71 mg).

$^{1}$H NMR ($C_6D_6$, 250 MHz, 298 K) δ: -4.26 (15H, s, Cp) ppm; this agrees with the literature value.[12, 13]

### 5.4.8 Synthesis of $[U(OC_6H_2{}^tBu_3)_3]$

In a Young's tap NMR tube, $UI_3$ (10.0 mg, 0.0323 mmol) and sodium-2,4,6-tri-tert-butyl-phenolate (14.0 mg, 0.0969 mmol) were mixed in $C_6D_6$ (4 $cm^3$). Immediate formation of $[U(OC_6H_2$-*t*-$Bu_3)_3]$ resulted at room temperature.

$^{1}$H NMR ($C_6D_6$, 250 MHz, 293 K) δ: 16.40 (2H, s, ArH), 4.96 (9H, s, *para t*-Bu), -1.44 (18H, b s, *ortho t*-Bu) ppm.

### 5.4.9 Synthesis of $UI_3(Ph_3PO)_2(THF)_2$

THF (15 mL) was added to a mixture of $UI_3$ (200 mg, 0.323 mmol) and $OPPh_3$ (180mg, 0.646 mmol) at room temperature. Stirred overnight and the volatiles removed under reduced pressure. A purple microcrystalline solid was isolated in a yield of 45 % (192mg).

$^{1}$H NMR ($C_6D_6$, THF double presaturation, 250 MHz, 293 K) δ: 47.38 (1H, s), 26.47 (6H, s), 21.96 (1H, s), 10.99 (6H, s), 10.51 (3H, s) ppm.

$^{31}$P {$^{1}$H} NMR ($C_6D_6$, 400 MHz, 298 K) δ: 48.42 ppm.

### 5.4.10 Synthesis of $U(BH_4)_3(THF)_x$

THF (15 mL) was added to a mixture of $UI_3$ (1 g, 1.616 mmol) and $KBH_4$ (300 mg, an excess) at -30 °C. The resulting mixture was stirred overnight and the resultant red solution isolated from the white precipitate. The volatiles were removed and a red solid isolated in a yield of 87 % (600 mg).

$^{1}$H NMR ($C_6D_6$, 360 MHz, 293 K) δ: 110.50, (br, s, $UBH_4$), 5.60 (4H, br, s, bound THF), 3.28 (4H, br, s, bound THF) ppm.

IR (Nujol mull, KBr): 2455 ($BH_4$), 2212 (t, $BH_4$), 1165 ($BH_4$) $cm^{-1}$.

### 5.4.11 Synthesis of [U(18-crown-6)$I_3$]

To a stirred solution of $UI_3$ (1.80 g, 2.72 mmol) in THF (15 mL), 18-crown-6 (720 mg, 2.72 mmol) in THF (5 mL) was added. The resulting mixture was stirred for 2 hours and a pink precipitate formed. The solid was filtered and washed with THF (2 × 5 mL). The solid was isolated and dried under reduced pressure to yield [U(18-crown-6)$I_3$] (1.47 g, 61 %) as a pink solid.

$^1$H NMR ($C_5D_5N$, 600 MHz, 300 K) δ: 11.67 (24H, br s, 18-crown-6) ppm.

Analysis. Calculated $UI_3O_6C_{12}H_{24}$: C, 16.32; H, 2.74 %. Found: C, 16.20; H, 2.66 %.

### 5.4.12 Synthesis of [Na(18-crown-6)(py)][U($OC_6H_2$-*t*-$Bu_3)_4$]

Toluene (15 mL) was added to a mixture of [U(18-crown-6)$I_3$] (200 mg, 0.226 mmol) and $NaOC_6H_2$-*t*-$Bu_3$ (256 mg, 0.904 mmol) at room temperature and stirred for 16 hours. The resulting red solution was concentrated, and cooled to -30 °C. The [Na(18-crown-6)(py)][U($OC_6H_2$-*t*-$Bu_3)_4$] was isolated in 295 mg, 79 % yield as a red solid.

Suitable single crystals for X-ray diffraction were obtained from a toluene solution at -30 °C. The complex crystallised with free 18-crown-6 in the unit cell.

$^1$H NMR ($C_6D_6$, 600 MHz, 298 K) δ: 11.50 (8H, s, Ar-H), 7.56 (1H, br s, py), 6.51 (2H, br s, py), 6.07 (2H, br s, py), 3.11 (free 18-crown-6), 1.88 (24H, s, Na{18-crown-6}), 1.82 (36H, br s, *p*-*t*-Bu), -0.77 (72H, br s, *o*-*t*-Bu) ppm.

Analysis. Calculated $C_{96}H_{164}O_{16}NaU$ ([Na(18-crown-6)(py)][U($OC_6H_2$*t*-$Bu_3)_4$]. 18-crown-6): C, 62.82; H, 9.01 %. Found: C, 61.55; H, 8.82 %.

### 5.4.13 Synthesis of [$^{TMS}$Cyclam]

Modification of the procedure for the synthesis of $^{TMS}$Cyclen.[14]

THF (20 mL) was added at -78 °C to a mixture of cyclam (250 mg, 1.24 mmol), DABCO (630 mg, 5.62 mmol) and trimethylsilyl chloride (0.71 mL, 5.62 mmol). The resulting solution was allowed to warm to room temperature over 16 hours. The solution was isolated and the volatiles removed under reduced pressure to yield $^{TMS}$Cyclam 223 mg, 37% as a white solid. (Unoptimised yield)

$^1$H NMR ($C_6D_6$, 360 MHz, 298 K) δ: 2.90 (2H, t, $CH_2N$), 2.77 (2H, t, $NCH_2CH_2N$), 1.77 (1H, m, $CH_2CH_2$), 0.14 (9H, s, $Si(CH_3)_3$) ppm.

$^{13}C\{^{1}H\}$ NMR ($C_6D_6$, 360 MHz, 298 K) δ: 48.76, 46.75, 31.20, 0.42 ($Si(CH_3)_3$) ppm.

### 5.4.14 Synthesis of [U(Cyclam)$I_3$]

Pyridine (15 mL) was added to a mixture of $UI_3$ (370 mg, 0.600 mmol) and cyclam (120 mg, 0.600 mmol) at -20 °C. The mixture was stirred and allowed to warm to room temperature for 16 hours and the volatiles removed under reduced pressure. The pink solid was isolated as [$UI_3$Cyclam] in yield 364 mg, 74 %.
$^{1}H$ NMR ($C_6D_6$, 360 MHz, 298 K) δ: 26.26 (2H), 20.94 (2H), 13.06 (2H), 10.47 (2 × 2H), 4.12 (2H), -3.69 (4H), -24.76 (2H), -30.64 (2H), -34.78 (2H) ppm.

### 5.4.15 Attempted Synthesis of [U($^{TMS}$Cyclam)$I_3$]

$UI_3$ (266 mg, 0.429 mmol) and $^{TMS}$Cyclam (210 mg, 0.429 mmol) were combined at -78 °C in THF and allowed to warm to room temperature over 16 hours. Volatiles were removed, but only starting materials were present by $^{1}H$ NMR spectroscopy.

### 5.4.16 Attempted Synthesis of [U($^{Bn}$Cyclam)$I_3$]

$UI_3$ (11 mg, 0.0017 mmol) and $^{Bn}$Cyclam (10 mg, 0.0017 mmol) were combined at room temperature in THF in a Youngs Tap NMR tube. The resulting solid was only soluble in pyridine.

## 5.5 SQUID magnetic studies

Variable temperature magnetic studies were carried out with a Quantum Design SQUID magnetometer in the temperature range 2 to 300 K, in an applied field of 1 and 7 tesla. [$(UI)_2(L^{Et})$] sample mass of 29.1 mg, diamagnetic correction of -741 × $10^{-6}$ emu/mol; [$(UBH_4)_2(L^{Et})$] sample mass of 33.43 mg, diamagnetic correction of -647 × $10^{-6}$ emu/mol; [$(Np_2(L^{Et})$] sample mass of 57.00 mg, diamagnetic correction of –523 × $10^{-6}$ emu/mol.
The susceptibility curves resulting from measurements in an external field of 7 tesla are not distinguishable from the low-field ones, but in the low temperature range below ~20 K slightly smaller values are obtained.

### 5.5.1 Ligand field analysis

The simplest ligand field Hamiltonian for the $U^{(III)}$ ions would be obtained assuming a four-fold symmetry axis. However, the presence of distortions lowering the point symmetry is likely and the presence of rhombic terms cannot be excluded *a priori*. Therefore,

$$H_{LF} = \sum_{k=1}^{3} \sum_{q=0}^{k} B_{2k}^{2q} O_{2k}^{2q}$$

where $O_{2k}^{2q}$ are Stevens operator equivalents and $B_{2k}^{2q}$ the ligand field coefficients to be determined.

Evidence for a strong ligand field potential is given by the value of the effective paramagnetic moment $\mu_{eff}$ that can be immediately extracted from the slope of the reciprocal susceptibility $1/\chi$ at high temperature. The experimental values, $\mu_{eff} = 2.45 \pm 0.03\ \mu_B$ and $\mu_{eff} = 2.15 \pm 0.05\ \mu_B$ for $[(UI)_2(L^{Et})]$ and $[(UBH_4)_2(L^{Et})]$ respectively, are indeed significantly reduced with respect to the free ion value for $U^{(III)}$ (3.7 $\mu_B$). The most straightforward way to reproduce quantitatively the resulting slope of the $1/\chi$ curve is to assume a dominant axial contribution to $H_{LF}$ which would isolate either (i) a $|J_z = \pm 9/2\rangle$ doublet or (ii) a $|J_z = \pm 1/2, \pm 3/2\rangle$ pseudo-quartet ground state. The high temperature $1/\chi$ *vs.* T data can be fitted best by either (i) or (ii), but the lower temperature part is better fitted by (ii). This means that $H_{LF}$ can be simplified to $H'_{LF} = \tilde{B}_2^0 O_2^0 + \tilde{B}_2^2 O_2^2$ as the other contributions have zero matrix elements. It should be noted that the rhombic term $\tilde{B}_2^2$ does not affect the susceptibility values in the assumed energy level scheme, and cannot therefore be determined by magnetic measurements.

## 5.6 References


1. A. B. Pangborn, M. A. Giardello, R. H. Grubbs, R. K. Rosen and F. J. Timmers, *Organometallics* 1996, **15**, 1518-1520.

2. B. J. Littler, M. A. Miller, C. H. Hung, R. W. Wagner, D. F. O'Shea, P. D. Boyle and J. S. Lindsey, *J. Org. Chem.*, 1999, **64**, 1391-1396.

3. J. B. Love, A. J. Blake, C. Wilson, S. D. Reid, A. Novak and P. B. Hitchcock, *Chem. Commun.*, 2003, 1682-1683.

4. G. Givaja, A. J. Blake, C. Wilson, M. Schroder and J. B. Love, *Chem. Commun.*, 2003, 2508-2509.

5. A. J. F. N. Sobral, N. G. C. L. Rebanda, M. da Silva, S. H. Lampreia, M. R. Silva, A. M. Beja, J. A. Paixao and A. M. d. Rocha Gonsalves, *Tet. Lett.*, 2003, **44**, 3971-3973.

6. D. L. Clark and A. P. Sattelberger, *Inorganic Synthesis*, 1997, 307-315.

7. J. L. Kiplinger, D. E. Morris, B. L. Scott and C. J. Burns, *Organometallics*, 2002, **21**, 5978-5982.

8. R. A. Andersen, *Inorg. Chem.*, 1979, **18**, 1507-1509.

9. D. C. Bradley, J. S. Ghotra and F. A. Hart, *J. Chem. Soc., Chem. Commun.*, 1972, 349-350.

10. H. Tsukube, K. Takagi, T. Higashiyama, H. A. Craig and N. Hayama, *Tetrahedron*, 1999, 1033-1037.

11. H. Tsukube, K. Takagi, T. Higashiyama, T. Iwachido and N. Hayama, *J. Chem. Soc., Perkin Trans. 1*, 1986, 1033-1037.

12. N. K. Sung-Yu, F. F. Hsu, C. C. Chang, G. R. Her and C. T. Chang, *Inorg. Chem.*, 1981, **20**, 2727-2728.

13. J. Rebizant, M. R. Spirlet, C. Apostolidis and B. Kanellakopulos, *Acta Crystallogr., Sect. C: Cryst. Struct. Commun.*, 1991, **C47**, 854-856.

14. J. E. Richman, *Tetrahedron Lett.*, 1977, **18**, 559-562.

15. L. J. Farrugia, *J. Appl. Crystallogr.*, 1999, **32**, 837.

## 5.7 Appendixes

### 5.7.1 X-ray details

X-ray crystallographic data were collected at 150 K on a Bruker SMART APEX CCD diffractometer using graphite monochromated Mo-Kα radiation (λ = 0.71073 Å), 170 K on an Oxford Diffraction Excalibur diffractometer using graphite monochromated Mo-Kα radiation, or 100 K on an Oxford Diffraction Excalibur diffractometer using mirror monochromated Cu- Kα radiation (λ = 1.5418 Å). Using the WinGX suite of programs, all structures were solved using direct methods and refined using a full matrix least square refinement on $|F|^2$ using SHELXL-97.[15] Unless otherwise stated, all non-hydrogen atoms were refined with anisotropic displacement parameters and hydrogen atoms placed using a riding model.

| Compound reference | $H_4L^{Et}$ | $[U(L^{Et})]$ | $[UO_2(Opy)(H_2L^{Et})]$ | $[Ce(HL^{Et})]_3$ | $[Ce(THF)_2(HL^{Et})]$ |
|---|---|---|---|---|---|
| **Chemical formula** | $C_{46}H_{52}N_8$•$2(H_2O_1)$• $2(C_4H_8O_1)$ | $C_{184}H_{192}N_{32}U_4$ | $C_{51}H_{55}N_9O_3U$• $3(C_7H_8)$ | $C_{138}H_{147}Ce_3N_{24}$• $C_{60}H_{60}$ | $C_{54}H_{65}CeN_8O_2$ |
| **Formula Mass** | 897.20 | 3803.82 | 1356.51 | 3343.24 | 998.26 |
| **Crystal system** | Orthorhombic | Monoclinic | Monoclinic | Triclinic | Monoclinic |
| ***a*/Å** | 13.042 | 15.1086(15) | 14.48880(10) | 19.2737(5) | 23.4691(5) |
| ***b*/Å** | 18.746 | 33.751(4) | 14.4713(2) | 20.1203(6) | 12.2848(2) |
| ***c*/Å** | 20.385 | 8.3453(8) | 29.7820(3) | 22.5956(6) | 23.6793(5) |
| ***α*/°** | 90.00 | 90.00 | 90.00 | 75.830(2) | 90.00 |
| ***β*/°** | 90.00 | 100.747(6) | 93.5490(10) | 86.608(2) | 117.8990(10) |
| ***γ*/°** | 90.00 | 90.00 | 90.00 | 83.598(2) | 90.00 |
| **Unit cell volume/Å$^3$** | 4983.8 | 4180.8(7) | 6232.47(11) | 8438.2(4) | 6033.6(2) |
| **Temperature/K** | 150(2) | 93.2(2) | 100(2) | 150(2) | 150(2) |
| **Space group** | *P*212121 | *C*2/*c* | *P*21/*c* | *P*1 | *P*2(1)/*n* |
| **No. of formula units per unit cell, *Z*** | 4 | 1 | 4 | 2 | 4 |
| **Radiation type** | MoKα | MoKα | CuKα | MoKα | MoKα |
| **Absorption coefficient, *μ*/mm$^{-1}$** | 0.076 | 3.924 | 7.702 | 0.857 | 0.794 |
| **No. of reflections measured** | 45692 | 20447 | 60445 | 131909 | 69526 |
| **No. of independent reflections** | 10175 | 4285 | 12333 | 46587 | 16459 |
| $R_{int}$ | 0.0425 | 0.0997 | 0.0455 | 0.0687 | 0.0544 |
| **Final $R_1$ values ($I > 2\sigma(I)$)** | 0.0564 | 0.0828 | 0.0282 | 0.0748 | 0.0405 |
| **Final $wR(F^2)$ values ($I > 2\sigma(I)$)** | 0.1410 | 0.1679 | 0.0721 | 0.1472 | 0.0939 |
| **Final $R_1$ values (all data)** | 0.0649 | 0.1030 | 0.0350 | 0.1020 | 0.0545 |
| **Final $wR(F^2)$ values (all data)** | 0.1469 | 0.1793 | 0.0747 | 0.1609 | 0.0990 |
| **Goodness of fit on $F^2$** | 0.948 | 1.154 | 1.006 | 1.202 | 1.019 |
| **CCDC number** | - | 727811 | - | 727812 | 727813 |

| **Compound reference** | **$[Y(THF)_2(HL^{Et})]$** | **$[\{Y(OH_2)(H_2L^{Et})\}_2(\mu\text{-}OH)_2]$** | **$UI_4(Et_2O)_2$** | **$[U(OPPh_3)_2(THF)_2I_3]$** | **$[U(OAr)_4][Na(py)_2(18\text{-crown-}6)]$** |
|---|---|---|---|---|---|
| **Chemical formula** | $C_{58}H_{64}N_8O_2Y$ | $C_{92}H_{106}N_{16}O_4Y_2 \bullet 2(C_7H_8)$ | $C_8H_{20}I_4O_2U$ | $C_{44}H_{46}I_3O_4P_2U$ | $2(C_{72}H_{116}O_4U) \bullet C_{22}H_{34}N_2NaO_6 \bullet C_{12}H_{24}NaO_6$ |
| **Formula Mass** | 947.05 | 1862.02 | 893.87 | 1319.08 | 3168.00 |
| **Crystal system** | Triclinic | Triclinic | Tetragonal | Monoclinic | Monoclinic |
| ***a*/Å** | 9.7010(3) | 12.5092(6) | 12.9006(3) | 13.043 | 25.4722(11) |
| ***b*/Å** | 11.9016(4) | 13.9890(7) | 12.9006(3) | 20.774 | 15.7949(7) |
| ***c*/Å** | 22.6420(7) | 15.7958(8) | 22.9677(7) | 16.531 | 26.0287(11) |
| ***α*/°** | 102.300(2) | 107.544(3) | 90.00 | 90.00 | 90.00 |
| ***β*/°** | 97.701(2) | 92.141(3) | 90.00 | 103.30 | 92.366(2) |
| ***γ*/°** | 91.911(2) | 112.612(3) | 90.00 | 90.00 | 90.00 |
| **Unit cell volume/Å$^3$** | 2525.97(14) | 2395.8(2) | 3822.41(17) | 4359.1 | 10463.2(8) |
| **Temperature/K** | 150(2) | 150(2) | 120(2) | 150(2) | 150(2) |
| **Space group** | *P*1 | *P*1 | *I*41/*acd* | *C*2/*c* | *P*21/*c* |
| **No. of formula units per unit cell, *Z*** | 2 | 1 | 8 | 4 | 2 |
| **Radiation type** | MoKα | MoKα | MoKα | MoKα | MoKα |
| **Absorption coefficient, *μ*/mm$^{-1}$** | 1.202 | 1.266 | 14.941 | 5.962 | 1.598 |
| **No. of reflections measured** | 42927 | 28397 | 25046 | 15705 | 173759 |
| **No. of independent reflections** | 10286 | 9824 | 1108 | 4326 | 21744 |
| **$R_{int}$** | 0.0505 | 0.0573 | 0.1124 | 0.0600 | 0.0717 |
| **Final $R_1$ values ($I > 2\sigma(I)$)** | 0.0817 | 0.0786 | 0.0429 | 0.0646 | 0.0637 |
| **Final $wR(F^2)$ values ($I > 2\sigma(I)$)** | 0.2494 | 0.1690 | 0.0674 | 0.1885 | 0.2000 |
| **Final $R_1$ values (all data)** | 0.0911 | 0.1044 | 0.0616 | 0.1075 | 0.0882 |
| **Final $wR(F^2)$ values (all data)** | 0.2608 | 0.1807 | 0.0733 | 0.2360 | 0.2185 |
| **Goodness of fit on $F^2$** | 1.152 | 1.098 | 1.164 | 1.035 | 1.110 |
| **CCDC number** | - | - | 691375 | - | - |